TSINGHUA-PRINCETON-COMBUSTION INSTITUTE

2026 SUMMER SCHOOL ON COMBUSTION

Combustion Chemistry: From Fundamentals to Kinetic Modelling for Low-Carbon Technologies

Alison Tomlin

University of Leeds, UK

July 06-10, 2026

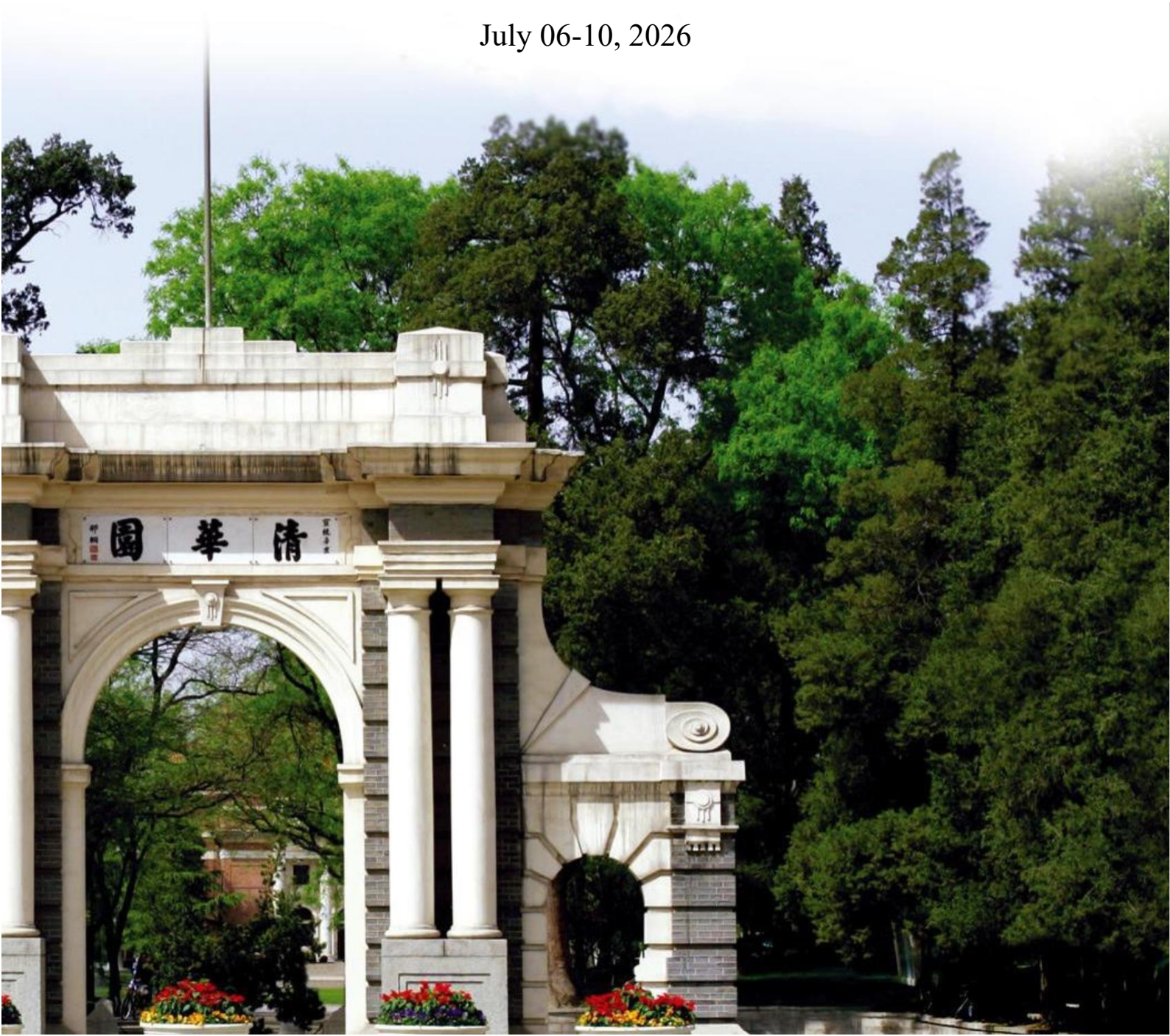

TSINGHUA-PRINCETON-COMBUSTION INSTITUTE

2026 SUMMER SCHOOL ON COMBUSTION

Key Activities / 重要活动			
July 5 (Sunday) /7 月 5 日 （周日）	10:00-17:30	Registration 注册	Northeast Gate, Lee Shau Kee Sci. and Tech. Building 李兆基科技大楼东北门
	18:30	Welcome Reception 开班仪式	A-278, Multifunction Room, Lee Shau Kee Sci. and Tech. Building 李兆基科技大楼多功能厅
Class Schedule / 课程安排			
Schedule 时间	Location 地点	Morning 上午 (9:00-9:50/10:00-10:50/11:00-11:50)	Afternoon 下午 (14:00-14:50/15:00-15:50/16:00-16:50)
July 6-10 (Monday-Friday) /7 月 6-10 日 （周一至周五）	Zone A, 6th Teaching Building 第六教学楼 A 区	**Theoretical and Numerical Combustion** **classroom: 6A018 (0th floor)** Thierry Poinsot	**Combustion Chemistry: From Fundamentals to Kinetic Modelling for Low-Carbon Technologies** **classroom: 6A018 (0th floor)** Alison Tomlin
July 6-7 (Monday-Tuesday) /7 月 6-7 日 （周一至周二）	Zone A, 6th Teaching Building 第六教学楼 A 区	**Spectroscopic Diagnostics for Combustion Chemistry** **classroom: 6A203 (2nd floor)** Pascale Desgroux	**Quantum Mechanics, Statistical Mechanics,and Machine Learning for Molecular Simulations** **classroom: 6A203 (2nd floor)** Alexandre Tkatchenko
July 8-10 (Wednesday-Friday) /7 月 8-10 日 （周三至周五）	Zone A, 6th Teaching Building 第六教学楼 A 区	**Introduction to Plasma-assisted Combustion** **classroom: 6A203 (2nd floor)** Deanna Lacoste	**AI for Combustion** **classroom: 6A016 (0th floor)** Matthias Ihme
Special Activities / 特殊活动			
July 5 (Sunday) /7 月 5 日 （周日）	13:30-17:30	Art Museum Visit / 艺术博物馆参观	Tsinghua University Art Museum 清华大学艺术博物馆
July 7 (Tuesday) /7 月 7 日 （周二）	17:00-18:00	Campus Tour / 校园游览	Tsinghua University 清华大学

July 8 (Wednesday) /7 月 8 日 （周三）	17:00-17:30	Group Picture Taking / 暑期学校合影	Mong Man Wai Concert Hall 蒙民伟音乐厅
July 8 (Wednesday) /7 月 8 日 （周三）	18:30-19:30 19:30-21:00	Poster Presentation / 海报展示 Career Panel / 职业发展论坛	B-518, Lee Shau Kee Sci. and Tech. Building 李兆基科技大楼 B-518 会议室
July 9 (Thursday) /7 月 9 日 （周四）	18:00	Farewell Reception / 欢送会	Guan Chou Yuan Restaurant 观畴园餐厅
July 10 (Friday) /7 月 10 日 （周五）	8:00-18:00	Program Certificate Distribution / 学习证书发放	6th Teaching Building 第六教学楼
July 11 (Saturday) /7 月 11 日 （周六）	9:30-11:30	CCE Laboratory Tour / 燃烧能源中心实验室参观	Northeast Gate, Lee Shau Kee Sci. and Tech. Building 李兆基科技大楼东北门

Electronic version of all lecture materials are available at the summer school website

UNIVERSITY OF LEEDS

Reaction Kinetics and Modelling Chemical Processes in Combustion

Professor Alison Tomlin

University of Leeds
School of Chemical and Process Engineering

Acknowledgements

- Thanks to the following people for input to slides and advice.
  - Professor Mike Pilling, Professor Bill Green, Dr. Scott Wisemann, Prof. Mike Burke, Prof. Brandon Rotavera, Professor Stephen Klippenstein, Dr. Christian Michelbach.

Lets start with the obvious problem…

Existing evidence of climate change is already quite strong, IPPC report, AR5, 2014

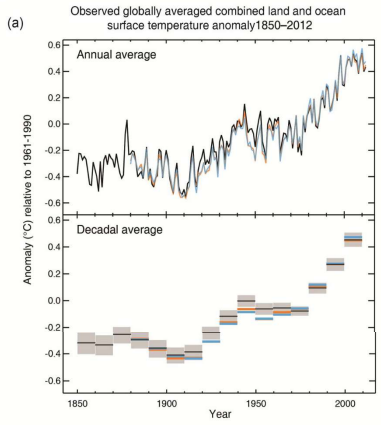

Mean datasets (lines) + uncertainty (grey)

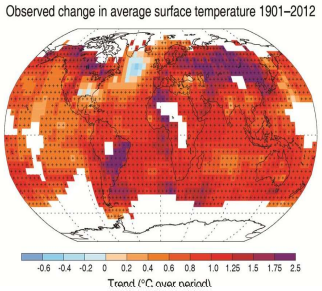

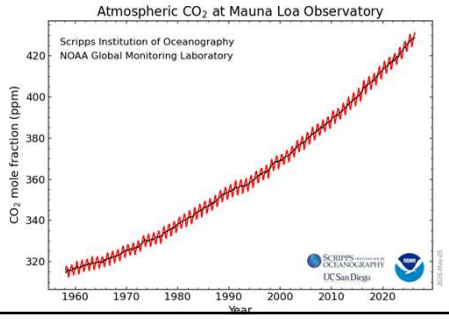

How to achieve net zero?

- **Fossil fuel (FF) combustion** and **deforestation** are the two main causes of increases in atmospheric CO_2.
- We need to transition away from FF use.
- There are a range of schools of thought on how to achieve the energy transition ranging from "**Electrify everything**" to the use of **carbon free fuels**, to the continued use of carbonaceous fuels with Carbon Dioxide Removal (CDR) and **Carbon Capture and Storage (CCS)** methods.
- In reality, a wide range of technologies will be required as well as naturally based CDR approaches.
- The power generation sector (electricity production) has proven the easiest to decarbonise so far.
- Other sectors such as domestic heating, ground based transport, aviation, marine, industrial sectors such as glass, steel, concrete, pharmaceuticals will be much more challenging and progress has been slower.

We need to get from here:

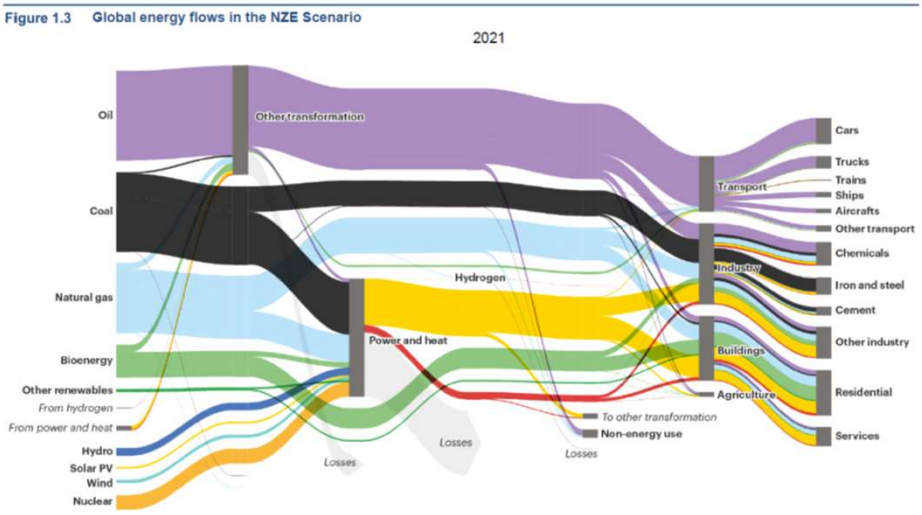

Figure 1.3 Global energy flows in the NZE Scenario

Note *the losses here due to inefficiencies in combustion technologies.*

Energy Technology Perspectives, IEA, 2023

To here…

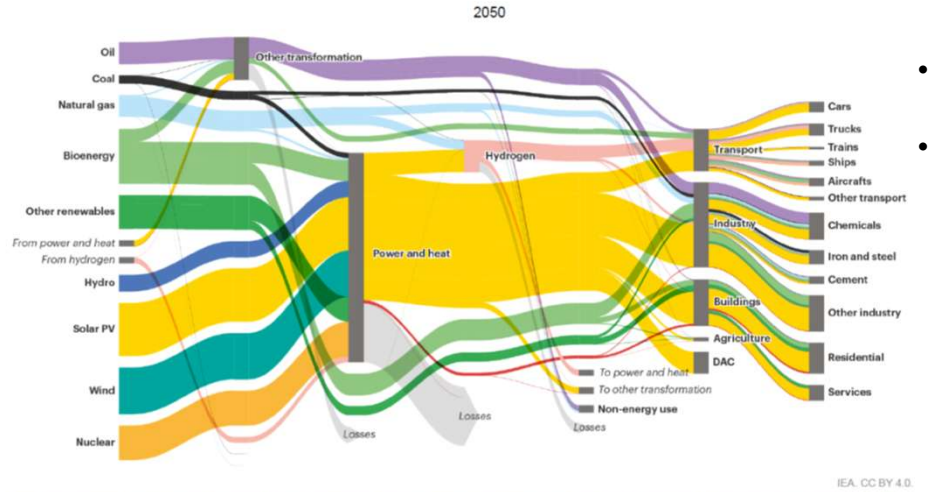

Notes: Some electricity is used to generate hydrogen from water electrolysis, while some hydrogen (and hydrogen-based fuels such as ammonia) is in turn used for power generation in 2050. Losses include fuel, heat and power distribution losses, as well as transformation process conversion losses and own use.

Electricity becomes the largest energy vector in the NZE Scenario, with demand more than doubling between 2021 and 2050.

- *Most primary sources are non FF.*
- *Electricity main energy vector.*
- *Still some direct air capture (DAC of carbon).*

In the electrify most things scenario:

- Heat provided by electrically driven heat pumps with small amount of bioenergy.
- Ground based vehicles are electric.
- Electrification of industrial processes OR use of green hydrogen.
- Still come tricky sectors:

➢ Marine and aviation – use of low carbon fuels such as hydrogen, methanol, ammonia.

➢ We are unlikely to have removed the need for plastics which has oil demand.

- We can expect to see a large increase in electricity demand as we transition away from FFs but we will need to store it.

Time-scales are short! So we need to get a move on to continue to be relevant.

IPCC, 2018

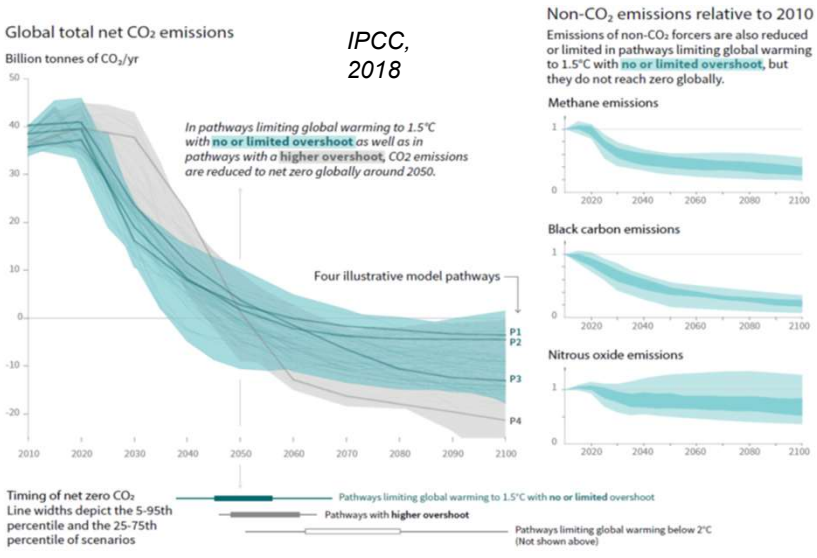

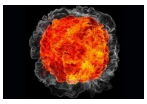

The Future World

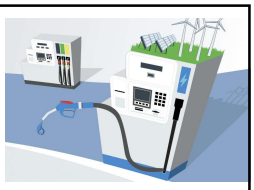

- It is clear that the world is changing rapidly.
- The energy status quo **cannot/should not** be maintained.
- In a low carbon future what role should combustion science and research play?
  - Development of strategies for utilising low carbon fuels.
    - Hydrogen, E-fuels, biofuels, ammonia, biomass and use of CCS?
    - What are the potential broader environmental impacts of their use?
    - In what sectors does combustion have a role to play? Heat? Heavy duty trucks? Shipping? Aviation? Energy Storage and Power Generation?
  - What are the fire and explosion risks of low carbon energy vectors and strategies.
    - Batteries, electrification, hydrogen storage and transport, biofuel storage.
    - Fire risk from energy efficiency measures.
    - Hydrogen safety in nuclear plant and potentially gas turbines.
  - What additional risks will climate change pose?
    - Wild fires, air quality threats.

Future challenges

- Use of low carbon fuels likely to require re-designing many devices.
  - Additional challenges posed by blending or using pure hydrogen in gas turbines, industrial heat applications.
  - Design of heavy duty engine and gas turbine operation on biofuels, ammonia, E-fuels and blends.
  - Can we design effective devices based on ammonia or metal combustion without impacting on air quality?
- Assessing fire risks involves understanding the combustion of complex materials.
  - Batteries, polymers used in insulation, complex biomass sources in fuel storage and wild fires, interactions with atmospheric flows.

Many questions which could be assisted by modelling combustion processes which requires the coupling of flow and chemical processes.

What is the purpose of a model?

- A model is an ***interpretation*** and an ***approximation*** of physical reality.
- A construction which helps us to understand the governing principles behind physical/chemical phenomena we are trying to describe.
- We also need it to make predictions about physical behaviour.
  - means telling us ***things we do not yet know or have not yet measured – extrapolation/predictive.***
  - **potentially saving time and money performing experiments**.
  - **assisting the design of sustainable processes.**
- A model needs to be **general enough to predict** across a wide range of conditions (temperatures, pressures, equivalence ratios).
- Not easy to achieve when data sets used in **model evaluation** are time consuming and expensive to obtain.
- There is only one physical reality, but can be a **large number of models** representing it.
- We might expect that the more fundamental the model, the closer it might become to reality. **Is this true?**

Historical development of combustion models

(Blurock & Battin-LeClerc, Cleaner Combustion, 2013)

- The more complex the model, the larger number of parameters it contains; a lot of work has to be done to quantify them.
- In combustion, tendency for models to become increasingly complex as understanding of fundamental processes improves.
- Semenov's theory of chain mechanisms and thermal explosions (Semenov 1935, 1958) was really the start of the modern science of combustion including **detailed reaction chemistry**.
- Nowadays a mechanism describing a complex bio-fuel may have 10 thousand reactions.
- To model a real combustion device **chemical kinetics** needs to be **coupled** to descriptions of **laminar or turbulent flows**.

Lu & Law (2009)

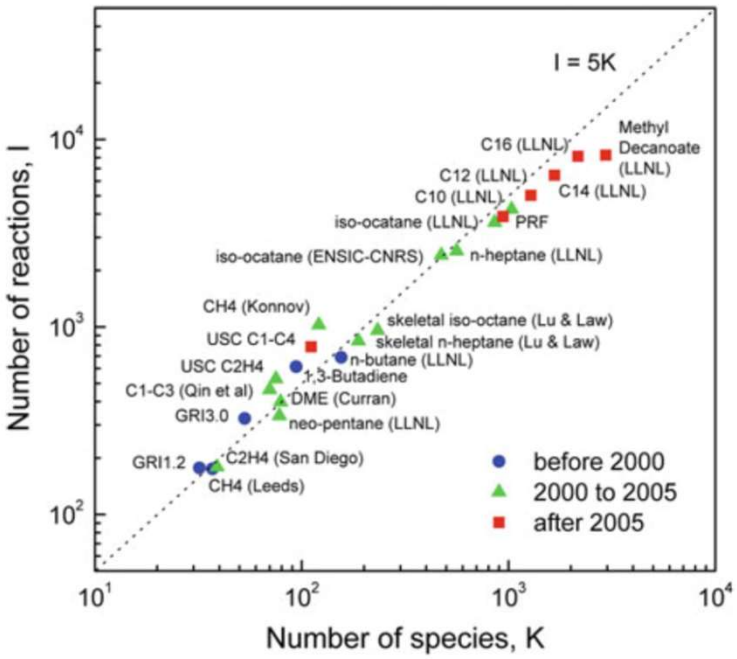

What is the difference between a model and a digital twin?

- **Model**
  - A simplified representation of a real system used to understand, explain, or predict behaviour.
  - Usually static or run for specific scenarios.
  - Based on assumptions and input data chosen by the user.
  - Does not automatically update unless you rerun it.
- **Digital twin**
  - A model that is continuously linked to a real, physical system.
  - Receives real-time or near-real-time data from sensors.
  - Updates automatically as the real system changes.
  - Not just to predict, but to monitor, diagnose, and optimise performance.

Many different models for same chemistry

- **Perfect Fidelity model:** Very large number of species & elementary step reactions, **true** thermo & rate coefficients. We think this would exactly predict the true chemistry in full detail. **Humans never achieve this.**
- **"Detailed Chemistry":** Human attempt at high fidelity: many (but not all) species & elementary step reactions, best known thermo & rate parameters.
- **"Reduced Model":** Often an approximation to "Detailed Chemistry" with fewer species and reactions. Often the rate expressions are not mass-action-law (e.g. maybe derived from steady state approximations).
- **"Empirical models"**: Small models focused on a (small number) of experimental observables. Try to keep number of parameters small so they can be determined from limited experimental data.

Often **multiple models have been created for the same system**, with different numbers of species and reactions, and different thermo & rate parameters.

Narrative of lectures…in reverse…

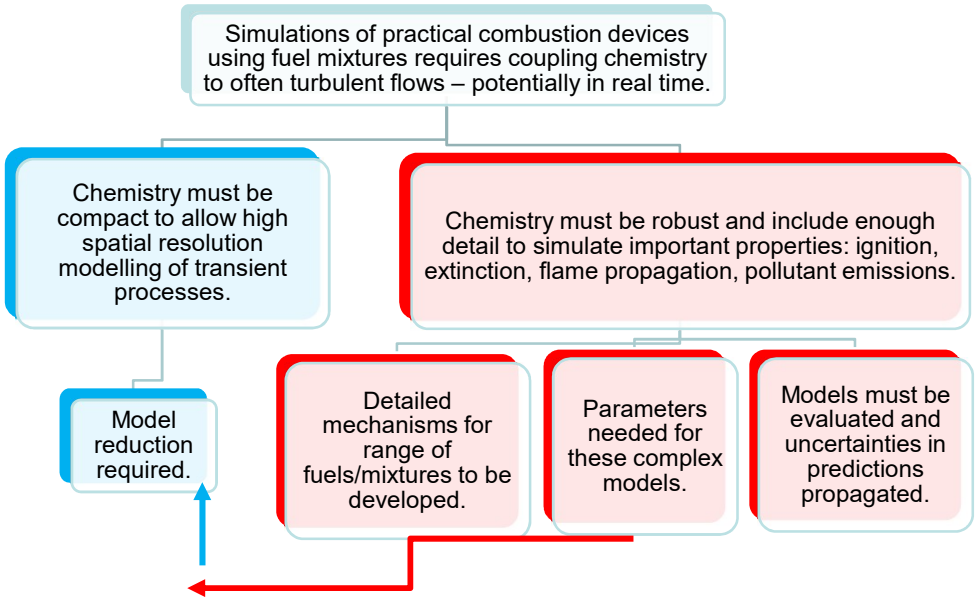

Summary of entire course…

1. A chemical kinetic model should never be treated as a black box.

- Always know basic details such as:
  - Origin of detailed chemistry (including how up to date).
  - Fidelity and level of accuracy/uncertainty in the data it contains.
  - Level of reduction that has been applied and assumptions made.

2. Even where machine learning/optimisation has been used to fit model data, the fidelity of the underlying data and how it has been used is critical.

Overview

DAY 1

- **Section 1** - Reaction kinetics basics: chemical mechanism structure; stoichiometry; rate equations for basic reactors; temperature and pressure dependence of rate coefficients; basic & statistical thermodynamics + ML.

Day 2

- **Section 2** - Determination of rate constants via (a) experimental and (b) theoretical methods (c) Multi-scale informatics.

DAY 3

- **Section 3a** - Generation of reaction mechanisms; machine learning.
- **Section 3b,c** - Ignition phenomena and low temperature chemistry, model validation via fundamental combustion experiments.

DAY 4

- **Section 4** - Future fuels and challenges.

DAY 5

- **Section 5** - Model uncertainties and sensitivity analysis.
- **Section 6** - Chemical model reduction methods.

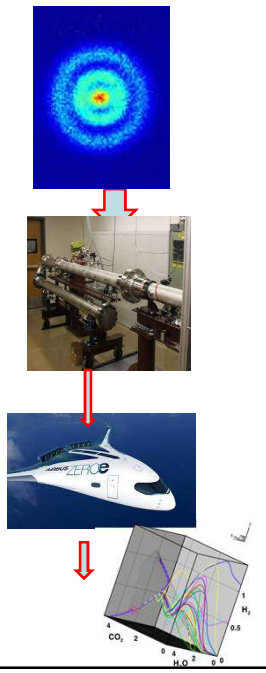

MODELLING FUNDAMENTALS

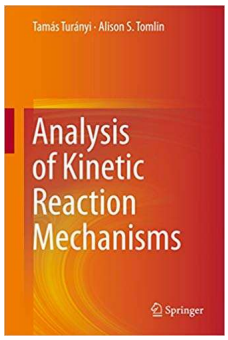

- ***Cleaner Combustion Developing Detailed Chemical Kinetic Models,*** *Editors:* ***Battin-Leclerc****, Frédérique,* ***Simmie****, John M.,* ***Blurock****, Edward (Eds.), Springer, 2013.*
- ***Analysis of Kinetic Reaction Mechanisms,*** *Tamás Turányi, Alison S. Tomlin, Springer, 2015.*
- *+ List of references provided with lecture notes and some refs included in slides.*

SECTION 1
REACTION KINETICS BASICS

- Chemical mechanism structure – importance of intermediate species.
- Stoichiometry; rate equations for basic reactors.
- Temperature and pressure dependence of rate coefficients.
- Basic transition state theory and concept of activation energy.
- Potential energy surfaces and brief summary of how they are computed.
- Basic & statistical thermodynamics + group additivity and machine learning. .

How do we define species in our model? Potential Energy Surface V(R)

- To a good approximation, the potential energy of a system containing atoms depends only on the positions R of all the atoms: V(R).
- Can compute V(R) using quantum mechanics.
- Usually V insensitive to certain changes in R (e.g. a uniform translation). So we work in subspace of R which significantly affects V, e.g. by change of variables to project out the uninteresting degrees of freedom. Called "internal coordinates" or "normal coordinates".
- Using classical mechanics, for thermalized systems, the probability of the system being at R scales as **the Boltzmann factor** $\exp(-V(R)/k_BT)$.
- Mostly the system is down in the "valleys" of small V(R), near the **minima of V(R).**
- If valleys with small V(R) separated by regions with high V(R), system gets stuck in valley for a long time: **natural definition of "Species".**
  - We call the R at minimum of V(R) in a valley the "**equilibrium structure**" or "**the geometry**" of that species. But really the atoms are always wiggling around, a species includes all atomic arrangements R down near the bottom of the valley.

Definition of "Species" Sets Definition of "Reaction"

- Definition of species as being a valley in V(R) implies "**dividing surface**" between species along the mountain ridge separating valleys A and B.
- Rate of reaction A → B is number of trajectories moving atoms from geometries in valley A to geometries in valley B, minus the reverse trajectories from valley B to valley A.
- All these trajectories cross the dividing surface, so count them there, no need to look at what is happening inside the valleys. Basis of transition state theory (TST).
  - **Analogy: To get change of number of cars in Manhattan, we can count cars crossing bridges and tunnels into and out of Manhattan. We don't need to watch what cars are doing inside the city.**

Chemical mechanism structure

- The ***overall reaction equation*** for a chemical process can be described by a single stoichiometric equation. The stoichiometric equation defines the molar ratio of the reacting species and the reaction products.

$$2\ H_2 + O_2 = 2\ H_2O$$

- In real systems reactants reacting with each other forming products immediately, is very rare.
- In most cases, ***intermediates are produced*** which react with each other and the reactants, with the final products formed at the end of many coupled reaction steps.
- Each individual step is called an ***elementary reaction***. Within elementary reactions, there is no macroscopically observable intermediate between the reactants and the products.

For: $2\ H_2 + O_2 = 2\ H_2O$

- **Reaction stoichiometry** 2:1:2 describes ratio of hydrogen, oxygen, water molecules.
- By re-arranging, all terms can be shifted to the right hand side:

$$0 = -2\ H_2 - 1\ O_2 + 2\ H_2O$$

- Any multiple of this equation is also true.
- If we denote the formulae of the chemical species by the vector **A** = (A_1, A_2, A_3), and the corresponding multiplication factors by vector $\boldsymbol{\nu}=(\nu_1, \nu_2, \nu_3)$. In this case A_1 = „H_2", A_2 = „O_2", A_3 = „H_2O", and $\nu_1 = -2$, $\nu_2 = -1$, $\nu_3 = +2$. The corresponding general stoichiometric equation is:

$$0 = \sum_{j=1}^{N_s} \nu_j A_j$$

where N_S is the number of species.
- The general stoichiometric equation of any chemical process can be defined in a similar way, where v_j is the stoichiometric coefficient of the *j*-th species, and A_j is the formula of the *j*-th species in the overall reaction equation.

Stoichiometric conditions and equivalence ratio

- Under **stoichiometric conditions** just enough oxidiser is available to completely burn the fuel to form CO_2 and H_2O.
- E.g. for methane and propane:

  $CH_4 + 2O_2 \rightarrow CO_2 + 2H_2O$ and $C_3H_8 + 5O_2 \rightarrow 3CO_2 + 4H_2O$

- For any general condition we can also define the Air/Fuel ratio – AFR, or the Fuel/Air ratio FAR.

$$\mathrm{AFR} = \frac{m_{air}}{m_{fuel}}, \qquad \mathrm{FAR} = \frac{1}{\mathrm{AFR}}$$

- The fuel-air equivalence ratio ϕ defines the **actual conditions relative to the stoichiometric** ones.

$$\phi = \frac{{m_{fuel}}/{m_{ox}}}{\left({m_{fuel}}/{m_{ox}}\right)_{stoich}}$$

- ϕ = 1 stoich; ϕ < 1 lean; ϕ > 1 rich.

Reaction order

- The exponent α_j is called the reaction order with respect to species A_j. The sum of these exponents:

$$\alpha = \sum_{j=1}^{N_S} \alpha_j$$

is the **overall order of reaction**.

- In the case of a global reaction equation such as $2\ H_2 + O_2 = 2\ H_2O$, the order is not usually equal to the stoichiometric coefficient v_j since there are intermediate steps in the system.
- For elementary reactions, the reaction order and the stoichiometric coefficient are commonly mathematically the same.

Importance of intermediates

- **Intermediates** are formed within most reaction systems.
- Hence to define the **time dependant dynamics** of a system accurately, a reaction model should include steps where intermediates are formed from reactants and go on to form products.
- E.G. for the oxidation of hydrogen we have: reactants (H_2, O_2), product (H_2O), and several intermediates (H, O, OH, HO_2, H_2O_2), in 30-40 total reaction steps.
- Critical steps are:

R1	$H_2 + O_2 = H + HO_2$	k_1
R2	$O_2 + H = OH + O$	k_2
R3	$H_2 + OH = H + H_2O$	k_3
R4	$H_2 + O = H + OH$	k_4
R5	$O_2 + H + M = HO_2 + M$	k_5
R6	$HO_2 + OH = H_2O + OH$	k_6

Stoichiometry

- Each elementary reaction step can be characterized by the following stoichiometric equation:

$$\sum_j v_{ij}^L \mathrm{A}_j = \sum_j v_{ij}^R \mathrm{A}_j$$

- The **stoichiometric coefficients** on the left hand side (v^L_{ij}) and the right hand side (v^R_{ij}) of an elementary reaction step should be distinguished.
- The stoichiometric coefficient belonging to species *i* in a reaction step can be obtained from the equation:

$$v_{ij} = v_{ij}^R - v_{ij}^L$$

- v^L_{ij} should be positive integers, while v^R_{ij} are integers for elementary reactions and can be positive or negative, integers or real numbers. Therefore, the overall stoichiometric coefficients can also be any numbers (positive or negative; integers or real numbers).

Time dependence

- The time dependant behaviour of an ***isothermal chemical system*** for the simplest practical case of one or more reactants reacting in a **well-mixed** vessel to form one or more products over time can be described as:

$$r = \frac{1}{\nu_j}\frac{\mathrm{d}Y_j}{\mathrm{d}t}.$$

  r is reaction rate and Y_j the mass or molar concentration of the j-th species.
- Within a narrow range of concentrations, the reaction rate r can always be approximated by the following equation:

$$r = k\prod_{j=1}^{N_S} Y_j^{\alpha_j}$$

  positive scalar k is reaction rate coefficient, α_j positive real numbers or zero, the operator Π means that the product of all terms behind it should be calculated.
- k is independent of concentrations, but may depend on T, P, and the quality and quantity of the nonreactive species present (for example an inert dilution gas or solvent). Hence the term ***rate coefficient*** is preferred to rate constant.

Rate equations for basic reactors

- The ***kinetic system of ordinary differential equations (ODEs)*** defines relationship between production rates of species and rates of reaction steps r_i:

$$\frac{\mathrm{d}Y_j}{\mathrm{d}t} = \sum_i^{N_R} \nu_{ij}\, r_i; \quad j = 1,\ 2,\ \ldots, N_S$$

  or in vector form $\dfrac{\mathrm{d}\mathbf{Y}}{\mathrm{d}t} = \boldsymbol{\nu}\mathbf{r}$

  i.e. number of equations equates to number of species.
- Generally eqns are coupled and must be solved simultaneously. **Leads to high computational cost for large mechanisms!**
- In adiabatic systems or systems with known heat loss rate, temperature is added as $(N_S+1)^{\text{th}}$ variable. DE for **rate of change of temperature** in a closed spatially homogeneous reaction vessel is given as:

$$C_p\frac{\mathrm{d}T}{\mathrm{d}t} = \sum_{i=1}^{N_R} \Delta_r H_i^{\ominus} r_i - \frac{\chi S}{V}\left(T - T_0\right)$$

T - temperature of system, T_0 - ambient T, C_p - constant pressure heat capacity of mixture, $\Delta_r H_i^{\ominus}$ standard molar enthalpy of reaction step i, S and V are surface and volume of the system, respectively, and χ - heat transfer coefficient between the system and surroundings.

Initial value problem

- The kinetic system of ODEs and its initial values together provide the following initial value problem:

$$\frac{\mathrm{d}\mathbf{Y}}{\mathrm{d}t} = \mathbf{f}(\mathbf{Y},\mathbf{k}) \qquad \mathbf{Y}(t_0) = \mathbf{Y}_0$$

- With the associated **Jacobian matrix** and normalised Jacobian:

$$\mathbf{J} = \frac{\partial \mathbf{f}(\mathbf{Y},\mathbf{k})}{\partial \mathbf{Y}} = \left\{\frac{\partial f_i}{\partial Y_j}\right\} \qquad \tilde{\mathbf{J}} = \left\{\frac{Y_j}{f_i}\frac{\partial f_i}{\partial Y_j}\right\}$$

- Reaction kinetic simulations frequently include the solution of partial differential equations, PDEs, that describe effects of chemical reactions, mass and thermal diffusion, convection and turbulence. In these PDEs *f* is the so called ***chemical source term***.
- Explicit numerical methods used to solve such initial value problems generally manipulate Jacobian matrix and hence **effort scales as N_s^2.**
- **Reducing species numbers** from a mechanism can therefore save a lot of computational time. **See later.**

Example

R1	$H_2 + O_2 \rightarrow H + HO_2$	$r_1 = k_1 [H_2] [O_2]$	
R2	$O_2 + H \rightarrow OH + O$	$r_2 = k_2 [O_2] [H]$	
R3	$H_2 + OH \rightarrow H + H_2O$	$r_3 = k_3 [H_2] [OH]$	
R4	$H_2 + O \rightarrow H + OH$	$r_4 = k_4 [H_2] [O]$	
R5	$O_2 + H + M \rightarrow HO_2 + M$	$r_5 = k_5 [O_2] [H] [M]$	*3rd order but not termolecular (under most conditions)*
R6	$HO_2 + OH \rightarrow H_2O + OH$	$r_6 = k_6 [HO_2] [OH]$	

$$\frac{\mathrm{d}[H]}{\mathrm{d}t} = +1r_1 - 1r_2 + r_3 + 1r_4 - 1r_5 + 0r_6$$

$$\frac{\mathrm{d}[\mathrm{H}]}{\mathrm{d}t} = k_1 [\mathrm{H_2}][\mathrm{O_2}] - k_2 [\mathrm{O_2}][\mathrm{H}] + k_3 [\mathrm{H_2}][\mathrm{OH}] + k_4 [\mathrm{H_2}][\mathrm{O}] - k_5 [\mathrm{O_2}][\mathrm{H}][\mathrm{M}]$$

$$\frac{\mathrm{d}[\mathrm{H_2O}]}{\mathrm{d}t} = k_3 [\mathrm{H_2}][\mathrm{OH}] + k_6 [\mathrm{HO_2}][\mathrm{OH}] \qquad \textit{Etc.}$$

Homework: Try forming the Jacobian for this simple system.

Closed vs. open systems

- In a **closed vessel**, system would tend towards a **final equilibrium point**.
- In an **open vessel** e.g. a continuously stirred tank reactor, CSTR, fresh reactants can flow into the vessel and products flow out. The system has a residence time t_{res} and can tend towards a **non-equilibrium steady-state concentration** or even a **limit cycle or chaotic attractor**.
- The system of ODEs is now modified to include inflow and outflow terms:

$$\frac{\mathrm{d}Y_j}{\mathrm{d}t} = \left(\frac{Y_i^0 - Y_i}{t_{res}}\right) + \sum_i^{N_R} \nu_{ij}\, r_i; \quad j = 1,\ 2,\ \ldots,\ N_S$$

$$C_p \frac{\mathrm{d}T}{\mathrm{d}t} = \sum_{i=1}^{N_R} \Delta_r H_i^{\ominus}\, r_i - \left[\frac{\chi\, S}{V} + \frac{C_p}{t_{res}}\right](T - T_0)$$

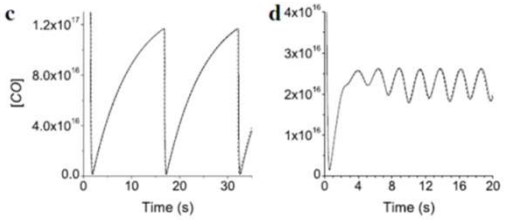

Oscillations in wet CO CSTR system
(Brad et al., 2007)

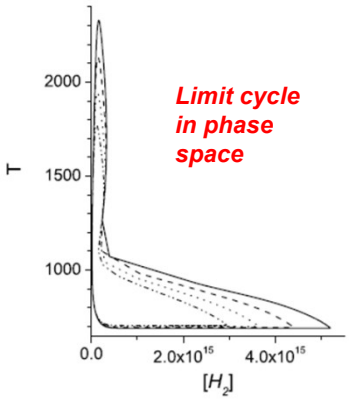

Limit cycle in phase space

Question - What are the components of a chemical mechanism?

Put another way, what do you need to provide to Chemkin or Cantera in order to be able to simulate the combustion of a fuel in different devices?

PARAMETERISATION OF RATE COEFFICIENTS FOR USE IN COMBUSTION MODELS

Temperature dependence of rate coefficients

- Arrhenius argued that for reactants to transform into products, they must acquire a minimum amount of energy: **activation energy E_a**.
- Consider reaction between molecules, A and B, and the associated **potential energy changes** during the reaction:
  - Reaction begins when molecules **collide** and interact, changing shape and exchanging atoms, momentum and energy.
- In this **transition state**, potential energy (PE) of reaction reaches a maximum, and small energy increase pushes reaction in direction of products, wherein PE falls.
- **Maximum PE can be described by activation energy E_a.**
- At absolute temperature T, fraction of molecules with kinetic energy greater than E_a can be calculated from statistical mechanics.
- ***Maxwell–Boltzmann (MB) distribution*** describes particle speeds in idealised gases where particles/gases move freely inside volume without interacting, except for brief collisions, when they exchange energy & momentum with each other or their thermal environment, assuming **thermodynamic equilibrium** reached.

Temperature dependence of rate coefficients

- Calculations for reaction rate coefficients involve **energy averaging over MB distribution** with E_a as lower bound.
- By assuming MB distribution, fraction of collisions with sufficient kinetic energy (KE) to pass over potential barrier is given by: $e^{-E_a/RT}$.

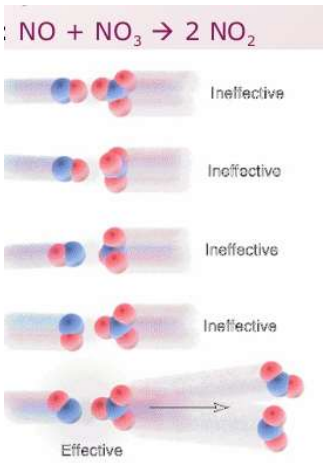

- ***Collision theory***, developed (Trautz and Lewis, 1916–18) suggests that molecules react if they collide with a relative KE along their **lines-of-centre** that exceeds E_a.
- **Hence both energy & orientation important.**
- Only a small percentage of total collisions have sufficient energy and appropriate orientations to form products.
- Formulation leads to an expression very similar to the Arrhenius equation which is given by:

$$k = AT^n \exp(-E/RT)$$

- Only molecules / collisions with energy above the reaction barrier can react.
  Small change in T can dramatically increase rate!

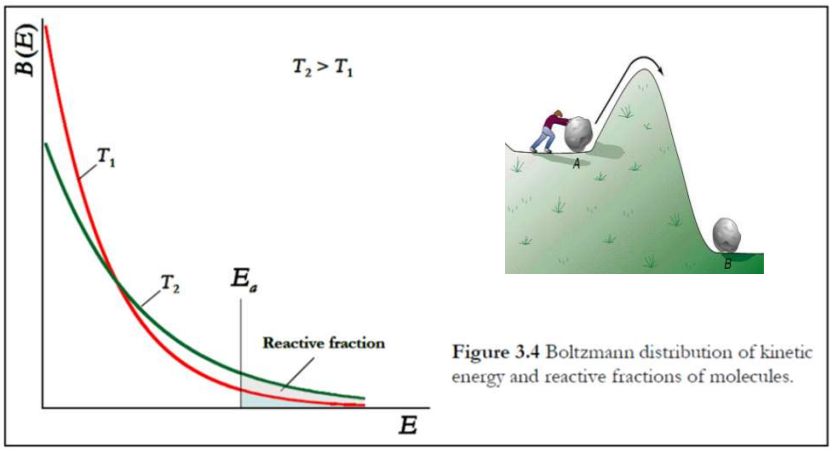

Figure 3.4 Boltzmann distribution of kinetic energy and reactive fractions of molecules.

Temperature dependence of rate coefficients

- If reaction between two molecules is elementary, and single step, *A* is related to frequency of collisions between reacting molecules.
- If E_a zero, *k* equals *A*, reaction occurs every time a collision occurs between reactant molecules.
- True for reactions in which no chemical bond is broken, such as the combination of atoms. Not all reactions have an activation energy….

- In transition-state theory, **activated complex** formed at transition state, considered to be in a **state of equilibrium** with reactants or to thermalize rapidly (*see later for challenges to this assumption*).
- Boltzmann-weighted number of states in each valley called Q, the partition function.
- K_{eq}'s are ratios of Q's.
- Rates are proportional to Q of transition state and Boltzmann factor of barrier energy.

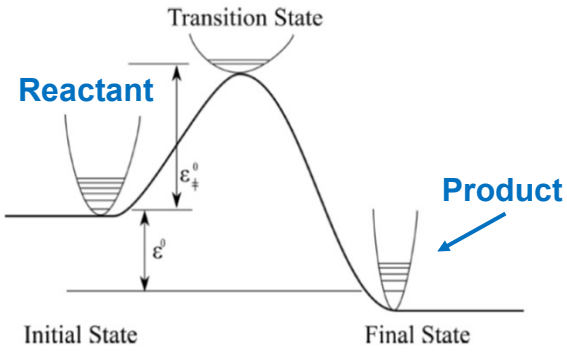

Transition State Theory

- The rate at which the final state is attained is determined by the **number of activated complexes formed** and the **frequency** with which they go over to the final state. These quantities may be calculated for simple systems by using statistical-mechanical principles.
- TST is now commonly used for calculating rate constants but requires knowledge of the **potential energy surface (PES)**.

We'll come back to this later but for excellent reviews on this topic see:

1. Zador et al., *Kinetics of elementary reactions in low-temperature autoignition chemistry, 2011.*
2. Klippenstein, *From theoretical reaction dynamics to chemical modeling of combustion, 2017.*

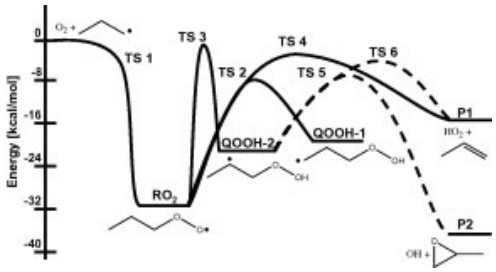

Example PES for n-propyl + O_2 (Goldsmith et al., 2017)

Temperature dependence of rate coefficients

- Due to more limited ranges of *T* in **liquid phase and in atmospheric kinetics** the temperature dependence of rate coefficient *k* is usually described by the classic Arrhenius equation:

$$k = A\exp(-E/RT)$$

where *A* is the pre-exponential factor, *E* is the activation energy, *R* is the gas constant and *T* is temperature. The dimension of quantity E/R is temperature and therefore E/R is called the activation temperature.

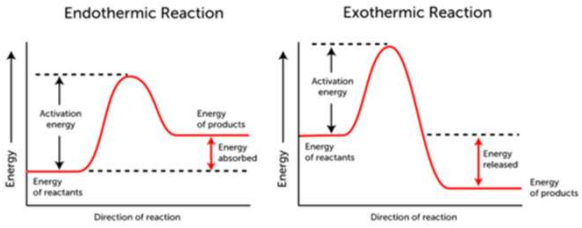

If the temperature dependence of the rate coefficient can be described by the original Arrhenius equation, then plotting *ln(k)* as a function of 1/*T* (Arrhenius plot) gives a straight line. The slope of this line is –*E/R*, and the intercept is *ln(A)*.

Narrow T range leads to approximate straight line.

Wider T range of relevance to combustion leads to approximate curve – non-classic Arrhenius behaviour.

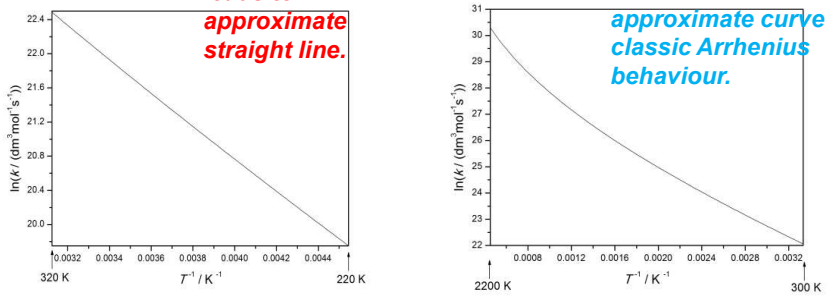

Arrhenius plot of the temperature dependence of the rate coefficient of reaction $CH_4+OH \rightarrow CH_3+H_2O$. (a) temperature range 220 K to 320 K; (b) temperature range 300 K to 2200 K.

- In high temperature gas phase kinetic systems, such as combustion and pyrolytic systems, the temperature dependence of the rate coefficient is usually described by the modified Arrhenius equation:

$$k = AT^n \exp(-E/RT) \quad \text{or} \quad k = BT^n \exp(-C/RT)$$

to distinguish that *B* is not the same as the classic *A*-factor.

- This form means that *A* or the **activation energy changes with temperature** and can be can be calculated from the slope of the curve, i.e. the derivative of the temperature function with respect to 1/*T*.

Worth remembering that the Arrhenius equation is basically a fit to data.

- Another type of unusual temperature dependence is when there are different routes from the reactants to the products leading to non-Arrhenius behaviour. In such cases the temperature dependence of the reaction step in a wide temperature range is sometimes described by the **sum of two Arrhenius expressions**.
- E.g. HO_2+OH=H_2O+O_2 (Burke et al., 2013) with expressions:

$$k_4(T) = 1.93 \times 10^{20} T^{-2.49} \exp(-294K/T) + 1.21 \times 10^{9} T^{1.24} \exp(658K/T) \ [\mathrm{cm^3\ mol^{-1}\ s^{-1}}]$$

Declared as duplicate reaction

Check point – do your mechanisms have such complex Arrhenius expressions?

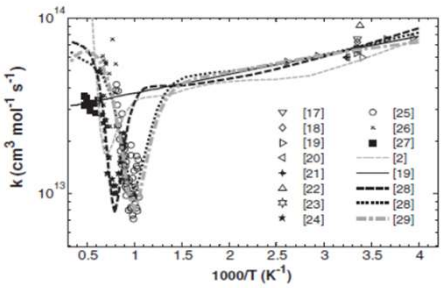

Fig. 1. Rate constants for $OH + HO_2 = H_2O + O_2$ (R4). Symbols represent experimental determinations [17–27], and lines represent proposed rate constant expressions [2,19,28,29] as indicated in the legend.

Pressure dependent rate coefficients

- The rate coefficients of **thermal decomposition** or **isomerization** reactions of some small organic molecules have been found to be **pressure dependent at a given temperature**.
- Model reaction: **isomerization of cyclopropane** yielding propene.
- Rate coefficient found to be first-order and pressure independent at high *P*, whilst second-order and linearly dependent on pressure at low *P*.
- Interpreted by Lindemann (1922) and Hinshelwood (1926) by assuming that the molecules of cyclopropane (C) are colliding with any of the other molecules present in the system ("third body", denoted by M) producing rovibrationally excited cyclopropane molecules (C*).
  - These molecules can then **isomerize** (transform into another molecule with the same atoms but with a different arrangement) yielding propene (P), or further collisions may convert the excited cyclopropane molecules back to non-excited ones: C + M ⇄ C* + M and C* → P.

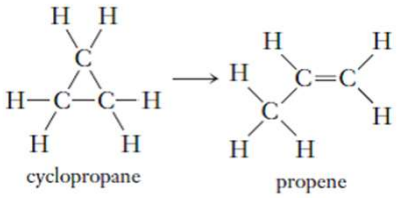

- Later shown that collisions create excited reactant species with wide range of rovibrational energies. Cyclopropane molecules **move up and down an energy ladder** and rate coefficient depends on energy of excited reactant.
- Example not of high practical significance but there are many other similar *unimolecular reactions* of importance in combustion.
- Decomposition of H_2O_2 is important in combustion of hydrogen, wet CO and hydrocarbons. See examples later….
- Due to collisions with any species present in mixture, rovibrational energy level of H_2O_2 moves up and down the energy ladder.
- Molecules with energy level higher than a threshold can decompose to OH with rate of decomposition energy dependent.

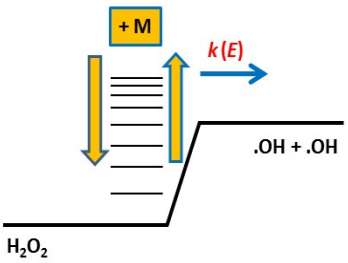

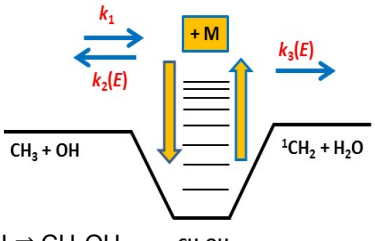

$CH_3 + OH \rightleftarrows CH_3OH$

$CH_3 + OH \rightleftarrows {}^1CH_2 + H_2O$

Example of dissociation reaction for CH_4

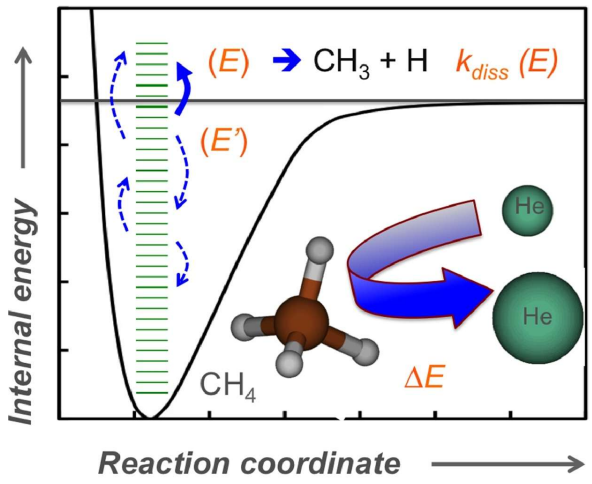

- Collisions with He atoms induce transitions up and down energy levels for CH_4 molecules.
- Occasionally, molecule excited to internal energy state exceeding dissociation threshold forming CH_3 and H - in competition with further collisions with bath gas, which may further excite or de-excite the molecule, perhaps back below dissociation threshold.
- **Competition** between **dissociation** and **collisional excitation/de-excitation** ultimately determines pressure dependence.

(Klippenstein, PROCI, 2017)

Example of dissociation reaction

- In low-pressure limit, every molecule excited above dissociation threshold dissociates.
  - Rate of dissociation determined by rate of exciting molecules above threshold.
  - Rate linearly dependent on number of collisions and thus pressure.
  - Rate roughly proportional to density of states at the dissociation threshold, $\rho(D_e)$, x a Boltzmann factor in the dissociation energy, $\exp(-D_e/k_BT)$.
- In high-pressure limit, molecules undergo numerous collisions even after they are excited above the dissociation threshold.
- Distribution of excited molecules maintains form of a Boltzmann distribution even above dissociation threshold and rate coefficient now independent of pressure.
  - Reduces to a Boltzmann average of the microcanonical dissociation rates.
- **At intermediate pressures**, rate is complicated function of **competition between dissociation** and **collisional energy transfer**.

How is this described? Fall-off

- At intermediate pressures reaction rate of unimolecular reactions neither second-order nor first-order.
- Apparent first-order rate coefficient in this "**fall-off region**" can be calculated using Lindemann approach (Pilling & Seakins, 1996).
- Arrhenius rate parameters required for both low- and high-pressure limiting cases, and Lindemann formulation blends them to produce a **pressure-dependent rate expression**.
- The low-pressure rate coefficient is given by the expression:

$$k_0 = A_0 T^{n_0} \exp\left(\frac{-E_0}{RT}\right)$$

and high-pressure rate coefficient by expression:

$$k_\infty = A_\infty T^{n_\infty} exp\left(\frac{-E_\infty}{RT}\right)$$

Apparent first-order rate coefficient at any pressure then calculated:

$$k = k_\infty \left(\frac{P_r}{1+P_r}\right) F$$

- In the equation above $F = 1$ in the Lindemann approach and the reduced pressure P_r is given by:

$$P_r = \frac{k_0[\mathrm{M}]}{k_\infty}$$

where [M] is the **third body concentration**.

- When calculating the effective concentration of the third body, the ***collision efficiencies*** $\boldsymbol{m_{y_i}}$ should also be taken into account:

$$[\mathrm{M}] = \sum_i m_{y_i} [Y_i]$$

- Metcalfe et al. (2013): [M] = 5.00 [H_2O] + 5.13 [H_2O_2] + 0.8 [O_2] + 2.47 [H_2] + 1.87 [CO] +1.07 [CO_2] + 0.67 [Ar] + 0.43 [He] + the sum of concentrations of all other species.
- Since N_2 is a commonly used "bath gas" within experiments, it often makes up the majority of the colliding species concentrations.
- N_2 therefore assumed to have unit collision efficiency and those of the other species are compared against it.
- NB: Recent work from Mike Burke's group has question the use of these simple linear mixture rules, suggesting sums should be on the basis of reduced pressure not pressure. **Watch his Webinar (https://youtu.be/AwOPvt09xY4?si=dMUu7h7IoZxp5SIE).**

- In H_2O_2 (+M) ⇄ 2 OH (+M), species with similar molecular energy levels to rovibrationally excited H_2O_2 (like H_2O_2 and H_2O) have large collision efficiencies, while noble gases have typically small collision efficiencies.
- General trend is that **larger molecules** with more excitable rovibrational frequencies have **larger collision efficiency factors**.
- Third body efficiency factors can also be considered as *T* dependent (Baulch et al., 2005), but approximate parameterisation is hindered by the ***lack of appropriate experimental data***.
  - contributes to **model uncertainties**.
- Jasper (2015) published ***a theoretical study*** of third body efficiencies for hydrocarbon collisions - linear, branched, and cyclic alkanes, alkenes, and alkyl radicals - with M = He, Ne, Ar, Kr, H_2, N_2, O_2. Trends extracted with respect to chemical structure and number of C atoms.
  - **Could be a way forward for determining more accurate values.**

Troe formulation

Lindeman equation can be improved by application of *P*, *T* dependent parameter *F*. In Troe formulation (Gilbert et al., 1983):

$$\log F = \log F_{\text{cent}} \left[1 + \left[\frac{\log P_r + c}{n - d(\log P_r + c)}\right]^2\right]^{-1}$$

with c=-0.4-0.67*log*F_{cent}, n=-0.75-1.271*log*F_{cent}, d=0.14 and

$$F_{\text{cent}} = (1-\alpha)\exp\left(-\frac{T}{T^{***}}\right) + \alpha\exp\left(-\frac{T}{T^{*}}\right) + \exp\left(-\frac{T^{**}}{T}\right)$$

so that four extra parameters *α, T***, T*, T*** must be defined to represent fall-off curve.

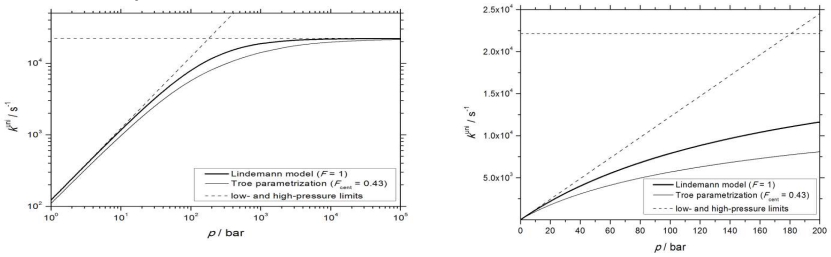

The change of the apparent first-order rate coefficient k_{uni} with pressure for reaction H_2O_2 ⇄ 2OH at temperature T=1000 K using bath gas N_2 (Troe, 2011).

Pressure dependence of bimolecular reactions

- ***Complex-forming bimolecular reactions*** may also be pressure dependent due to complex losing extra energy in collisions leading to thermal equilibration.
- E.G. reaction CH_3 + OH forming CH_3OH complex with main products the stabilization product CH_3OH and decomposition products CH_2+H_2O.

- The Troe formulation accurately represents the fall-off region for single-well PE surfaces (Venkatesh et al., 1997).
- For more complicated elementary reactions with **multiple wells**, differences between theoretically calculated rate coefficient and the best Troe fit can be as high as 40%.
- This has led to the so called "log p" formalism (see e.g. (Zádor et al., 2011)):

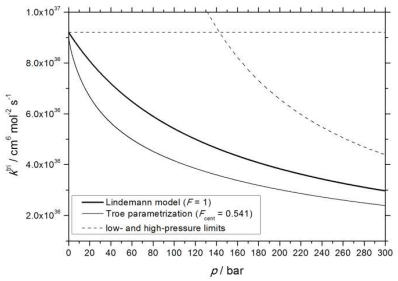

Ln P and Chebyshev polynomial formulations

- *k* is rate coefficient belonging to pressure *P*, while (p_i,k_i) pairs are a series of tabulated rate coefficients, defined by Arrhenius parameters, belonging to different pressures. Hence: an **interpolation method** which is linear in *ln p*.

$$\ln k = \ln k_i + (\ln k_{i+1} - \ln k_i)\frac{\ln p - \ln p_i}{\ln p_{i+1} - \ln p_i}$$

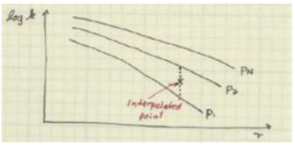

- Chebyshev polynomials can also be used for fitting *P* dependence of rate coefficients, but care needed when extrapolating outside of fitting ranges. For details see Venkatesh et al. (1997).

$$\log k(\tilde{T},\tilde{P}) \approx \sum_{i=1}^{N}\sum_{j=1}^{M} a_{ij}\varphi_i(\tilde{T})\varphi_j(\tilde{P}).$$

$$\varphi_i(x) = \cos[(i-1)\arccos(x)]; \quad i = 1,2,\ldots,$$

*Both formulations supported by **Chemkin and Cantera** if coefficients are provided within mechanisms.*

WARNING it is not always easy to track third body efficiencies using these methods but they still matter!

Check point – which type of *P* dependent expressions do your mechanisms use?

Non Boltzmann kinetics

- **Chemical activation** can occur due to exothermic/endothermic reactions occurring faster than heat/energy transfer, causing reacting molecules to have non-thermal energy distributions (**non-Boltzmann distribution**).
- Can result in "**chemically termolecular**" reactions of potential importance to combustion predictions. Involve reactive collisions occurring on same time-scales as thermalisation (equilibration).
  - **Typically gas phase termolecular reactions taught not to exist in standard Phys. Chem. texts.**
- Here, three reactants involved in bond breaking and forming products i.e. R + X +Y = products, not, R + X (+M) = RX (+M) (Burke & Klippenstein, 2017, Barbet et al. (2019).
- Examples: H + O_2 + R, and H + O_2 + M = HO_2 + M followed by HO_2 + R.
- H + N_2 + O = NH + NO, H + CO + H = H_2 + CO, and H + C_2H_2 + O_2/OH/H.

R is a radical

- Increasing the pressure increases the heat transfer rate between the reacting molecules and the rest of the system, reducing this effect.
  - **How important are such reactions for modelling practical systems? Yet to be fully determined.**
  - **May be important for interpreting low pressure measurements.**

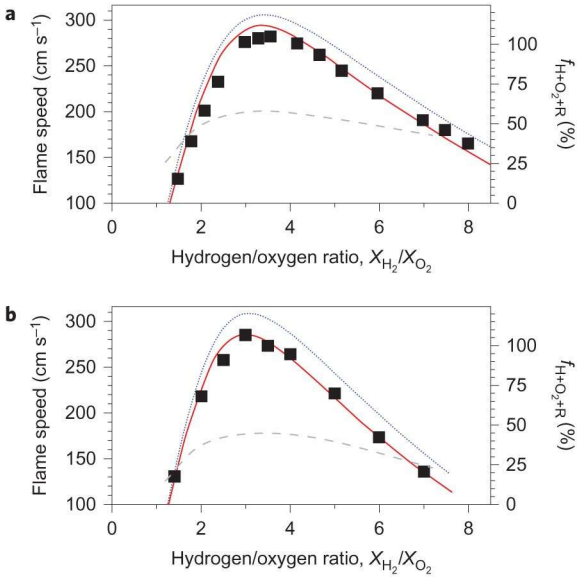

a) Hydrogen–air mixtures at atmospheric *T, P*

b) Hydrogen–oxygen flames diluted with helium at atmospheric *T* for a *P* of 5 atm and $X_{O2}/(X_{O2} + X_{He}) = 0.08$

- Symbols experimental;
- Blue dotted lines results from simulations where H + O_2 + R reactions were not included;
- Red solid lines indicate results from simulations where H + O_2 + R reactions were included.
- Thin grey dashed line: peak fraction of total HO_2 + R reaction flux through H + O_2 + R, $f_{H+O2+R} = \omega_{H+O2+R}/(\omega_{H+O2+R} + \omega_{HO2+R})$

Burke & Klippenstein, 2017

Thermodynamics/Thermochemistry

- In closed systems all kinetics is leading toward equilibrium. So good to start by figuring out where we are going (later we can worry about how fast we will get there… i.e. kinetics).
- **We need thermodynamic data to**:
  - Compute equilibrium compositions – useful e.g. for exhaust gas concentrations.
  - Determine the heat release in a combustion process.
  - Calculate the equilibrium constant for a reaction – this allows us to relate the rate coefficients for forward and reverse reactions.

- Other part, "**Thermochemistry**", is about reactions.

  - 1st Law gives energy density, final temperature.

  - 2nd Law related to detailed balance (and so reverse rate coefficients), final composition at equilibrium.

Basic thermodynamic quantities

Enthalpy

- Enthalpy *H* comprises a system's internal energy: energy required to create the system (internal energy, *U*), plus the amount of work required to make room for it by displacing its environment and establishing its volume and pressure: *H* = *U* + *PV.*
- The total enthalpy of a system cannot be measured directly, the ***enthalpy change*** of a system measured e.g. the enthalpy change during a reaction.

Enthalpy of reaction

- Enthalpy of formation for species expressed as a polynomial function of *T*.

$$\frac{H^{\Theta}}{RT} = a_1 + \frac{a_2}{2}T + \frac{a_3}{3}T^2 + \frac{a_4}{4}T^3 + \frac{a_5}{5}T^4 + \frac{a_6}{T}$$

a's NASA polynomials

- The enthalpy of reaction calculated by summing enthalpies of reactants and products at a given *T*:

$$\frac{\Delta H_j^{\Theta}}{RT} = \sum_{i=1}^{I} \nu_{ij} \frac{H_i^{\Theta}}{RT}$$

where ($\Delta_r H^{\ominus}_j$) < 0 for exothermic reaction (heat flows from system at constant *p* and overall enthalpy decreases), and ($\Delta_r H^{\ominus}_j$) > 0 for an endothermic one.

Tabulated thermodynamic quantities. Standard enthalpy of formation

Standard enthalpy change of formation, $\Delta_f H^\ominus$

The standard enthalpy change when 1 mole of a substance is formed from its elements in their reference states, at a stated temperature (usually 298 K). The reference state is the most stable state at that temperature, and at a pressure of 1 bar.

e.g. $C(s) + 2H_2(g) \rightarrow CH_4(g)$

$\Delta_f H^\ominus = -74.8$ kJ mol^{-1}

The standard enthalpies of formation of C(s) and $H_2(g)$ are both zero.

LHV of a fuel is computed easily from enthalpies

- Usually people define lower heating value (LHV) for a hydrocarbon fuel as standard heat of reaction of combustion, where the final products are CO_2 and steam (at room temperature).

$$LHV(CxHy) = x\, H_{f,298}(CO_2) + y\, H_{f,298}(H_2O, gas) - H_{f,298}(fuel)$$

- This gives a **"lower" heating value** than that obtained from a real bomb calorimetry experiment, where the final product is liquid water not steam (i.e. the latent heat of water condensation is not taken into account).

Definitions of HV

• LHV (or net calorific value, NCV) of a fuel is defined as amount of heat released by combusting a specified quantity (initially at 25°C) and returning the temperature of the combustion products to 150°C; **assumes the latent heat of vapourisation of water in the reaction products is not recovered**.
• Higher heating value (HHV, or gross calorific value, GCV) defined as amount of heat released by a specified quantity (initially at 25°C) once combusted and products have returned to a temperature of 25°C, which **takes into account the latent heat of vapourisation of water** in the combustion products. (cf condensing boiler).

1 Kg/scf Natural gas:
LHV: 47.13/983.0 MJ
HHV: 52.21/1089.0 MJ

1 Kg/scf H_2
LHV: 119.96/290.0 MJ
HHV: 141.88/343.0 MJ

Hydrogen will need to be compressed for storage….

Homework: *Compare HVs for other fuels based on weight and volume e.g. methanol, ammonia, sustainable aviation fuel vs. diesel and jet fuel.*

Basic thermodynamic quantities

Entropy:

- Related to the number Ω of microstates that are consistent with the macroscopic quantities characterising a system (e.g. *V*, *P*, *T*).
- Under the assumption that each microstate is equally probable, the entropy *S* is the natural logarithm of the number of microstates, multiplied by the Boltzmann constant k_B, $S = k_B \ln \Omega$.
- The **second law of thermodynamics** states that the entropy of an isolated system never decreases. Such systems spontaneously evolve towards **thermodynamic equilibrium,** the state with **maximum entropy**.
- In an open system where heat, work and mass can flow across the system boundaries:

$$\frac{dS}{dt} = \sum_{k=1}^{K} \dot{m}_k \hat{S}_k + \frac{\dot{Q}}{T} + \dot{S}_{gen}$$

rate of entropy production within system.

net rate of entropy flow due to flows of mass into and out of system ($\hat{S}$ = entropy per unit mass).

rate of entropy flow due to heat flow across boundary.

Why is entropy important for kinetics?

- Entropy measures:
  - How many microscopic arrangements are available
  - How "loose" or "tight" a configuration is
- This makes entropy essential for converting **potential energy surfaces** into **reaction rates**.
- Entropy determines:
  - The **density of states**
  - The number of accessible quantum states at a given energy
- In RRKM theory we will see that the rate depends on the ratio of:
  - States at the transition state
  - States in the reactant well
- More entropy → more states → higher probability of reaction.

Basic thermodynamic quantities

Gibbs free energy: $\Delta G^{\ominus} = \Delta H^{\ominus} - T\Delta S^{\ominus}$; J in SI units for standard conditions.

$$\Delta G^{\ominus} = \sum n\Delta G^{\ominus}_f(products) - \sum m\Delta G^{\ominus}_f(reactants)$$

- Described by Gibbs as "available energy:"
  - the **greatest amount of mechanical work** obtained from a given quantity of a substance in a given initial state, without increasing its total volume or allowing heat to pass to or from external bodies.
- A thermodynamic potential defining maximum amount of **non-expansion work** that can be extracted from a thermodynamically closed system (one that can exchange heat and work with its surroundings, but not matter).
- In a completely **reversible process**, when a system transforms reversibly from an initial state to a final state, the decrease in Gibbs free energy equals work done by system to its surroundings, minus work of the pressure forces.
  - **Sign** of standard free energy change $\Delta G^{\ominus}$ of a chemical reaction determines whether the reaction will tend to proceed in the **forward** or **reverse** direction.
- **It is the thermodynamic potential that is minimized when a system reaches chemical equilibrium at constant pressure and temperature.**

Equilibrium composition minimizes Free Energy

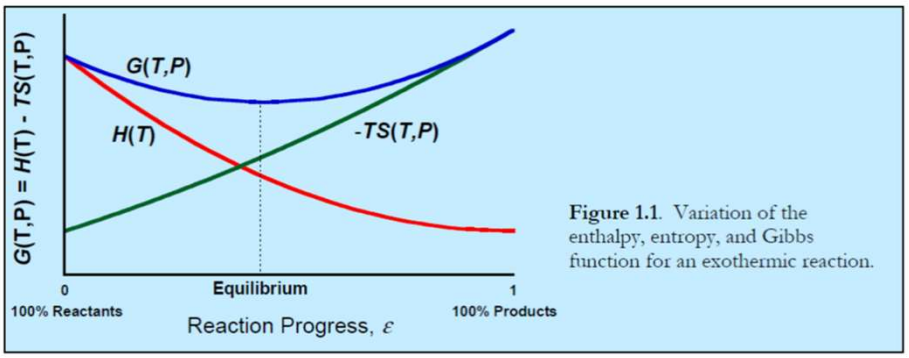

Figure 1.1. Variation of the enthalpy, entropy, and Gibbs function for an exothermic reaction.

Constrained minimization: conservation of C,H,O atoms; adiabatic

Free Energy Constrained Minimizer Software is Available.
See e.g. EQUIL in CHEMKIN package.

How do programs like EQUIL work to compute equilibrium concentrations?

- Input: **initial composition** and **temperature**.
- Input: thermochemical data (typically **NASA polynomials**).
- Assume ideal gas, ideal mixture, adiabatic so: $G = \sum_{i=1}^{Ns} \bar{g}_i N_i$

where $\bar{g}_i$ is the partial molal Gibb's function and N_i is the number of moles of each species i in the system. N_s is the total number of species.

- For ideal-gas mixtures, the partial molal Gibb's functions are given by:

$$\bar{g}_i = g_i(T,P) + RTln(X_i)$$

where $g_i(T,P)$ is the Gibb's function for the pure species i, evaluated at the system T and P; R is the universal gas constant; and X_i is the mole fraction of the ith species.

- **Equilibrium solution at given T and P is distribution of N_i that minimizes the system G**, subject to atomic population **constraints**:

  $\sum_{i=1}^{Ns} n_{ji} N_i = p_j$ where n_{ji} is number of jth atoms that appear in ith molecule, p_j is the total population in moles of the jth atom in the system, and M is the total number of elements present in system.

When might Chemical Equilibrium Calculations be Useful?

- For **final product prediction** in closed reactors.
- In cases where the chemical time-scales are much faster than other processes such as transport, crank angle rotation etc.
- For calculating properties such as **adiabatic flame temperatures**.

However:

- In general for complex flows and stirred continuous reactors the behaviour is far from equilibrium and we must solve for chemical kinetics.
- Although, most systems at least partially equilibrate and model reduction methods such as the ***rate-controlled constrained-equilibrium method*** (RCCE) make use of free energy minimisation.

67

Basic thermodynamic quantities

Specific heat capacities:

- Specific heat capacities vary with *T, P*. *C* = *C*(*P,T*).
- Expressed as values at:
  - Constant pressure C_p, where gas is allowed to expand performing work
  - Constant volume C_v, where gas is enclosed and pressure may change.
  - $C_V < C_P$
- At constant pressure heat capacity is equal to change in enthalpy divided by change in temperature $C_P = \frac{\Delta H}{\Delta T}$ (amount of energy applied to one unit of mass of substance for increase of one unit in temperature).

$$H_{Tf} = H_{Ti} + \int_{Ti}^{Tf} C_P dT$$

If we assume that C_p is independent of T this simplifies.

$$H_{Tf} = H_{Ti} + C_P(T_f - T_i)$$

Reversible reactions

- In theory, all thermal elementary reactions are reversible, which means that the reaction products may react with each other to re-form the reactants, denoted "⇄".
- The use of irreversible reactions denoted by a single arrow "→" means that either the reverse reaction has been neglected or that the reactions have been separated into forward and backwards rates.
- Forward rate expression given in Arrhenius or pressure dependent forms, and reverse rate calculated from thermodynamic properties through **equilibrium constant**:

$$k_{r_i} = \frac{k_{f_i}}{K_{c_i}}$$

Check point – do you know how many reactions are reversible vs. irreversible in your mechanisms?

Thermodynamic properties are evaluated at a given temperature *(T)*, e.g. standard molar heat capacity *($C_p^{\ominus}$)*, enthalpy *($H^{\ominus}$)* and entropy *($S^{\ominus}$)*. The standard molar reaction enthalpy *($\Delta_r H^{\ominus}_j$)* and entropy *($\Delta_r S^{\ominus}_j$)* can be calculated from the following equations:

$$\frac{\Delta S_j^{\Theta}}{R} = \sum_{i=1}^{I} \nu_{ij} \frac{S_i^{\Theta}}{R} \qquad \frac{\Delta H_j^{\Theta}}{RT} = \sum_{i=1}^{I} \nu_{ij} \frac{H_i^{\Theta}}{RT}$$

The equilibrium constant *K* in terms of normalised pressures is then obtained from:

$$\Delta_r G^{\Theta} = -RT \ln K \qquad K = \exp\left(\frac{\Delta S^{\Theta}}{R} - \frac{\Delta H^{\Theta}}{RT}\right)$$

The equilibrium constant in concentration units K_c is related to the equilibrium constant in normalised pressure units *K* by the following:

$$K_c = K\left(\frac{p^{\Theta}}{RT}\right)^{\Delta\nu}$$

where p^{Θ} is the standard pressure and $\Delta\nu = \sum_i \nu_i$ is the sum of stoichiometric coefficients.

Knowing thermodynamic properties of species allows reverse rate constant to be calculated. NB An error of 5 kcal/mol in Gibbs free energy results in an equilibrium constant that is off by a factor of 12 at 1000 K (Goldsmith 2012).

Representation in typical combustion models

Most models use 14 fitted polynomial coefficients - **the NASA polynomials** for each species (Burcat, 1984). Seven for T_{low} - T_{mid} and seven for T_{mid} to T_{high}. Typical values are T_{low} = 300 K, T_{mid} =1000 K and T_{high} = 5000 K.

$$\frac{C_p^{\Theta}}{R} = a_1 + a_2 T + a_3 T^2 + a_4 T^3 + a_5 T^4$$

$$\frac{H^{\Theta}}{RT} = a_1 + \frac{a_2}{2} T + \frac{a_3}{3} T^2 + \frac{a_4}{4} T^3 + \frac{a_5}{5} T^4 + \frac{a_6}{T}$$

$$\frac{S^{\Theta}}{R} = a_1 \ln T + a_2 T + \frac{a_3}{2} T^2 + \frac{a_4}{3} T^3 + \frac{a_5}{4} T^4 + a_7$$

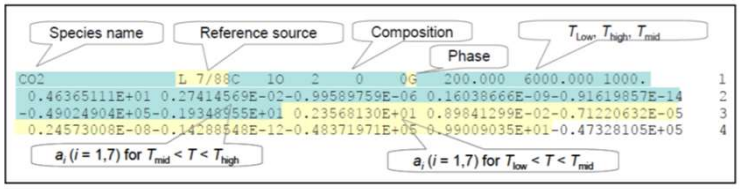

2nd Law and 3rd Law ways of computing entropy

3rd Law method:

integrate C_p/T from T=0 K, using fact that S=0 at 0 K.

$$S^0(T) = S^0(T^o) + \int_{T^o}^{T} (C_p(T')/T') dT'$$

2nd Law method: Set up an experiment where a reaction is equilibrated. Measure that reaction's equilibrium constant K by measuring the concentrations of all the species involved.

- Use $\Delta_r G^{\Theta} = -RT \ln K$
- If is $\Delta_r H$ known, use $\Delta_r G = \Delta_r H$ - T $\Delta_r S$ to determine $\Delta_r S$
- Else, measure K as a function of T: $\Delta_r S = d\, \Delta_r G/dT$.

Computing thermodynamic quantities: Statistical mechanics basics

- Based on quantity Q called the "**partition function**" for ensemble

$$Q = \sum_i g_i \exp(\frac{-E_i}{k_B T})$$

where E_i are the possible energies of the system (quantum mechanics only allows certain quantized energy levels), and g_i is the number of quantum states with energy E_i.

- Q contains enough information to compute all the normal thermochemical quantities. For example:

Internal energy $U(T,V) = \sum g_i E_i \exp(\frac{-E_i}{k_B T}) \frac{1}{Q} = {}^{-\partial(lnQ)}\Big/_{\partial(\frac{1}{k_B T})}$

All we need to know is the set of possible energies {E_i}

Helmholtz Free Energy: $F = U - TS = G - PV = -k_B T lnQ$

$$S = -k_B \ln Q + \frac{1}{T}\frac{\partial(\ln Q)}{\partial({}^{1}/_{k_B} T)}$$

Link to potential energy field

- The **potential energy field** (or *potential energy surface*, PES) describes how the energy of a molecule or system changes as the positions of its atoms change.
- Tells you **which molecular arrangements are stable, which are unstable, and how much energy it costs to move between them**.
- **Boltzmann distribution**, converts the potential energy field into probabilities of occupying different molecular states.
- **Partition function** used to calculate thermodynamic properties - essentially a weighted sum over all accessible states of the system:
- Each state's weight depends on its energy from the PES.
- Once you know the partition function, *all thermodynamic properties follow.*
- The PES is crucial because it determines:
  - The energies of molecular conformations
  - The spacing of vibrational levels
  - The depth and shape of energy wells

74

HOW DO WE COMPUTE THE ALLOWED ENERGIES $\{E_i\}$ FOR A SINGLE MOLECULE?

First we need the potential field V(R) for our molecule

- Can't measure V(R), need to compute it using
  - **Wave function based methods** - Schrödinger equation.
  - Solve for the electron density using **density-functional** (DFT) based methods.
- These are the fields of "quantum chemistry".
- Forces between atoms are electrostatic, but electrons are so light that quantum mechanics effects dominate, so we solve Schrödinger equation. This is an eigenvalue equation; the lowest eigenvalue is the value of V(R).
- Unfortunately, the Schrödinger equation is a Partial Differential Equation (PDE) in $\mathbf{3N_{electrons}}$ **dimensions**, with tricky constraints: too hard to solve exactly.
- We can **solve it approximately** by:
  - Expanding the solution wave-function in a finite basis set, and making many other approximations.

Overall summary of approaches

Vereecken et al, 2015

- Quantum chemical calculations can typically be divided into three categories:
  - **Ab initio calculations** based on a wavefunction description of the molecules,
  - **Density functional theory (DFT)** based on a description of the electron density in a molecule, and
  - Semi-empirical calculations that involve using parametrised integral approximations.
- Ab initio wavefunction calculations utilising sophisticated treatments of electronic correlation provide most accurate results **BUT** carry a high computational cost.
  - Mainly suitable for small molecules (4-6 atoms)
- DFT methods are less costly to execute, but rely on functionals, the exact form of which is unknown.
  - Accuracy is improving and commonly used for larger molecules.
  - There is no real convergence.

Brief Summary of Ab Initio Methods

- ***Ab initio quantum chemistry methods*** attempt to solve electronic Schrödinger equation given the positions of the nuclei and the number of electrons in order to yield useful information such as electron densities, energies and other properties of the system.
- Many electron function generally a linear combination of many simpler electron functions with the dominant function being the Hartree-Fock function.
- Each of these simple functions then approximated using only one-electron functions.
- The one-electron functions are then expanded as a linear combination of a finite set of **basis functions**.
- Approach has advantage that it can be made to **converge to exact solution**, when basis set tends toward limit of complete set and where all possible configurations are included (called "Full CI – full configuration interaction").

78

Born Openheimer and PESs

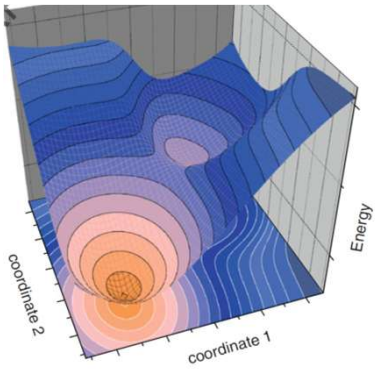

- **Separation** of nuclear and electronic motion due to **differences in mass**.
- Electrons have high KE: move very fast compared to nuclei.
  - expect nuclei to feel time-averaged force exerted by swarm of electrons.
- Electrons quantum mechanical (wave-like), described by Schrödinger Eq.
  - **Split into two parts.** Solve electron-motion problem first, assuming nuclei stationary at different geometries R, yielding potential field V(R) that nuclei move in.
  - Energy eigenvalues correspond to different electronic states.
  - Potential energy function corresponding to each electronic state of system (PES).

- Having determined V(R), quantify motion of nuclei - forces acting on the atoms, represented by the nuclei are derived from the PES.

Hartree-Fock (HF) theory

- Fundamental to much of electronic structure theory.
- Basis of molecular orbital (MO) theory, which posits that each electron's motion can be described by a single-particle function (orbital) which does not depend explicitly on instantaneous motions of other electrons.
- HF theory assumes that each electron moves in an average field created by all others, rather than tracking every tiny interaction directly
- Only for the H atom (or other one-electron systems, like He+) are orbitals exact eigenfunctions of the full electronic Hamiltonian.
- **Generally missing electron correlations.**
- As long as we are content to consider molecules near their equilibrium geometry, Hartree-Fock theory provides good starting point for more elaborate theoretical methods which are better approximations to the Schrödinger equation.
- Many types of calculations begin with a Hartree–Fock calculation and subsequently correct for electron-electron repulsion.
- Scales nominally as N^4 – N number of electrons.

80

Basis set expansion: the concept

The electronic Schrödinger equation, for fixed positions of the atomic nuclei $\underline{R}$, and ignoring complexities due to electron spin, is

$$H\Psi(\underline{r}) = V(\underline{R})\,\Psi(\underline{r})$$

where *H* is a linear operator that includes partial derivatives w.r.t to the electron positions $\underline{r}$.

- **Basis set expansion:** approximate $\Psi(\underline{r}) = \Sigma\, c_n \Phi_n(\underline{r})$, then multiply both sides with any desired test function $\chi_m(\underline{r})$ and integrate to convert the PDE into an algebraic equation in the unknowns $\{c_n\}$ and $V(\underline{R})$:

$$\int \chi_m H\Psi d\underline{r} = \sum c_n \int \chi_m H\Phi_n \, d\underline{r} = V(\underline{R}) \sum c_n \int \chi_m \Phi_n d\underline{r}$$

  i.e. Generalized eigenvalue problem A*c = V(R) B*c

- We want to know the lowest eigenvalue, that is the physically important one that corresponds to $V(\underline{R})$ – ground level potential energy.
- Bascially minimization of the energy of the wavefunction by optimizing the coefficients describing the wavefunction as a linear combination of basis set functions.

Basis set expansion: the concept

- The use of basis sets essentially turns a PDE into a set of coupled algebraic equations that can be efficiently solved computationally (**cf finite element methods in fluid flow – except here basis sets mimic molecular orbitals**).
- Single-particle states (molecular orbitals, MOs) expressed as linear combinations of basis functions giving approximate but not exact resolution.

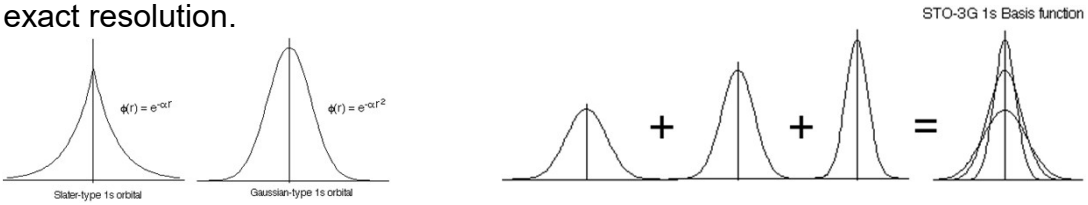

- The higher the number of basis functions in a basis set, the more flexibly the electron positions can be described (e.g. anharmonicity, polarisation) - **at of course increasing cost.**

Coupled Cluster Approach

- Accurately predicting molecular energies, reaction barriers, etc. depends on how well we describe **electron correlation** — electrons do not move independently, but respond to each other's presence.
- The **coupled cluster (CC) approach** treats electron correlation in a systematic way starting from a single, reference state (usually HF) and improves on it by allowing electrons to be excited in a coordinated manner representing correlated electron motion, e.g. two electrons adjusting positions simultaneously to minimise repulsion.
- Rather than adding corrections step by step, CC uses an exponential mathematical form that effectively sums many correlation effects at once e.g. two, three, or more electrons move in a linked way because of their mutual repulsion.
  - **EXPENSIVE**
- In practice, commonly used variants such as **CCSD** (including single and double excitations) and **CCSD(T)** (which adds a perturbative treatment of triple excitations) strike a balance between accuracy and computational cost.

83

Coupled Cluster Approach

- Instead of explicitly constructing linear combinations of basis functions in process of finding eigenvalues, instead do a **similarity transform of the Hamiltonian** operator *H*:

$$H \rightarrow \exp(-T(\underline{c}))\, H \exp(+T(\underline{c})) = H'(\underline{c})$$

- The Coupled Cluster equations are different, too:

$$\int \chi_m H'(\underline{c}) \Phi_0 d\underline{r} = V(\underline{R}) \int \chi_m \Phi_0 d\underline{r}$$

- Because the adjustable coefficients $\underline{c}$ are inside the exponentials, this is a large system of nonlinear algebraic equations.
- Empirically, Coupled Cluster approximation using F12 basis for the zero-order guess $\Phi_0(r)$ gives high-accuracy $V(\underline{R})$ values.
- **CCSD(T)-F12 is a high-accuracy method for computing $V(\underline{R})$ but expensive, CPU ~ N^7.**

Available Software

- Quantum chemists have developed efficient software for many of these approximate ways of computing V(R), and tested most of them so you can get an idea of their accuracy.
- Software is not perfect, but more packaged and easy to use than most CFD software.
- If you ask for same basis set and level of approximation with same geometry R in different software packages, you will usually get computed V(R) values which agree to many significant figures, i.e. the error is in approximation & basis set, not in implementation inside each software package.
- Some of the famous commercial software packages are **GAUSSIAN** and **MOLPRO** + many other commercial and free quantum chemistry packages.
- **All of them can compute V(R) to various degrees of accuracy with some differences in required CPU time and RAM.**

Check point: Key is to know what you are using – rather than treating as a black box!

Density Functional Theory (DFT)

- Different approach to ***ab initio*** methods – using **electron density functional** and not directly solving for wave function.
- DFT focuses on the **overall electron density** — how much negative charge is present at each point in space.
- Can capture many of the missing electron–electron effects that Hartree–Fock leaves out, often at a much lower computational cost.
- Need to find correct electron density, from which one can get the electronic energy at the selected molecular geometry.
- **Exact mathematical relationship** between electron density and energy is unknown.
- That relationship is called the **exchange–correlation functional**.
  - However, general mathematical form of energy functional not known.
  - Different functionals make different assumptions about how electrons interact and how localized or spread out they are. Choice of functional depends on applications.

Comparison between *ab-initio* and DFT

Property	Ab initio methods	Density functional theory methods
Object to find	Electron wave function	Electron density function
Way of improvement	Systematic	Empirical
Computational expense	Can be large	Small
Size of molecules routinely handled	Very accurate: 6 nonhydrogen average: 20–30 nonhydrogen atoms	Hundreds of atoms
Expertise needed	Very accurate: Significant, average: Medium	Little
Reliability	Very accurate: Large, average: Medium	Unpredictable
Systems not possible to handle	Large molecules, polyatomic transition metal complexes	Molecules where dispersion interactions are important

Assumptions - electron correlation

- Single MO methods (e.g. HF) ignore correlations between electrons (b not a in diagram below).
- In Complete Active Space (CAS) methods, the coefficients and the atomic orbitals in the MOs and the coefficients in the CI expansion are simultaneously optimized to overcome this.

- Coupled cluster methods essentially take the basic HF MO method and construct **multi-electron wave-functions** using the exponential cluster operator to account for **electron correlation**.
  - i.e. systematically add corrections.

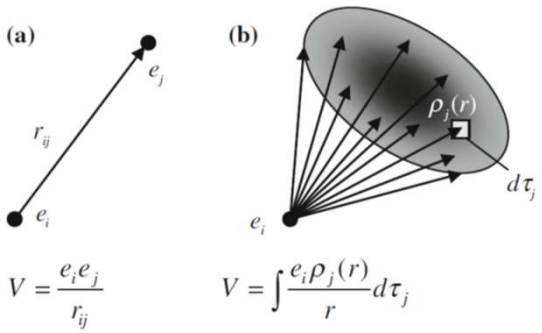

38

Level of theory

The combination of the method and the basis set used for MOs is referred to as "level of theory".

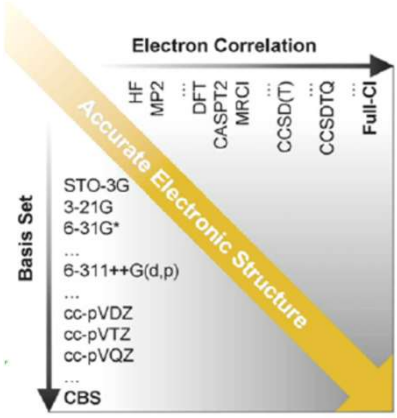

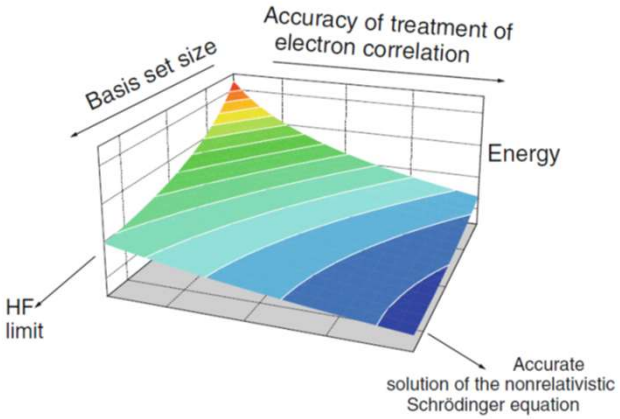

Composite Methods

- Combine methods with high level of theory and small basis sets with methods that employ lower levels of theory with larger basis sets.
- Examples are G2, G3, CBS-QB3, CBS-APNO.
- Somers and Simmie (2015) benchmarked composite methods against the Active Thermochemical Tables for the formation enthalpies of radicals with molecular formula $C_xH_yO_z$

If errors are random – average them. If bias - Methods like bond additivity correction

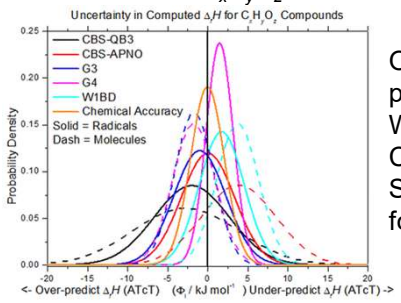

- Later we will look at the impact of uncertainties which result from choice of different methods for computing the PES in terms of the calculation of **phenomenological rate coefficients**.

Uses of PES

In practice, the PES is used in different ways depending on the level of detail required:

Harmonic approximation

- PES is approximated near minima as a set of springs
- Used to calculate:
  - Vibrational frequencies
  - Zero-point energies
  - Thermal corrections to enthalpy and entropy
- Used in quantum thermochemistry

Molecular dynamics (MD)

- Atoms move across the PES over time
- Thermodynamic properties obtained by time-averaging:
  - Energy
  - Pressure
  - Heat capacity

Monte Carlo sampling

- Random sampling of configurations on the PES; especially useful for equilibrium properties

Links to thermodynamic properties

Internal energy

- Average energy of the system.
- Obtained by averaging the potential energy (and kinetic energy) over all accessible states.

Entropy

- Measures how many energetically accessible arrangements exist
- Broad, shallow wells → higher entropy
- Narrow, steep wells → lower entropy
- The PES shape strongly influences entropy.

Free energy (Gibbs or Helmholtz)

- Combines energy and entropy.
- Free energy differences between states correspond to:
  - Reaction equilibria; Phase stability; Conformer populations

Heat capacity

- Depends on how energy changes with temperature.
- The curvature of the PES determines how vibrational modes are excited as temperature rises.

Importance of thermochemistry

- We will see later that many target outputs from combustion systems depend on accurate thermochemistry e.g:
  - Calculation of reverse rates.
  - Low temperature oxidation routes for hydrocarbon fuels involving RO_2 and QOOH species.
  - The prediction of heat release rates.
  - Prediction of adiabatic flame temperatures.
- Large molecules are challenging.
- Goldsmith et al. (2012) presented a method and data for 200 molecular species of interest in combustion chemistry.
- **A bond additivity correction (BAC)** was developed to account for shortcomings in the treatment of multiple bonds and to remove systematic errors that appeared for different bond types compared to Active Tables (see later): C—H, C—C, C═C, C≡C, O—H, C—O, C═O, and O—O.
  - **2σ uncertainties of 0.58 kcal/mol**
- A high level of theory can produce <0.2 kcal/mol uncertainty but at large CPU cost.

Active Tables (more later on this topic)

- New paradigm to develop accurate, reliable, and internally consistent thermochemical values for stable, reactive, and transient chemical species by utilizing to the fullest all available experimental measurements as well as state-of-the art theoretical data.
- **ATcT** is based on constructing, analysing, and solving the underlying **Thermochemical Network (TN).**
- Brings together both experimental and theoretical studies (**see earlier**) to reduce uncertainties in data (Burcat & Ruscic, 2005).
- Network of Computed Reaction Enthalpies to Atom-Based thermochemistry **(NEAT)** *Csaszar and Furtenbacher (2010)*
- **Results in highly correlated parameters – be careful of the effects of neglecting such correlations!**

Species Name	Formula	$\Delta_f H°(0\ K)$	$\Delta_f H°(298.15\ K)$	Uncertainty	Units	Relative Molecular Mass	ATcT ID
Dihydrogen	H2 (g)	0	0	exact		2.01588 ± 0.00014	1333-74-0*0
Helium	He (g)	0	0	exact		4.0026020 ± 0.0000020	7440-59-7*0
Heptane	C7H16 (l)	-201.46	-223.91	± 0.74	kJ/mol	100.2019 ± 0.0057	142-82-5*500
Octane	C8H18 (l)	-226.61	-249.73	± 0.79	kJ/mol	114.2285 ± 0.0065	111-65-9*500
2,2,4-Trimethylpentane	(CH3)2CHCH2C(CH3)3 (l)	-224.4	-258.9	± 1.5	kJ/mol	114.2285 ± 0.0065	540-84-1*500

Group Additivity

- Experimentally, for n-alkanes it is observed that *H*, *S*, and C_p all vary linearly with the number of carbons.
- One can assign a value to the increments caused by inserting one more CH_2 group into the alkane chain.
- This approach works for many different chemical functional groups: adding the group to the molecule adds a set amount to *H, S,* C_p called a GAV.
- For *S*, need to add a symmetry correction to the sum of the GAV.

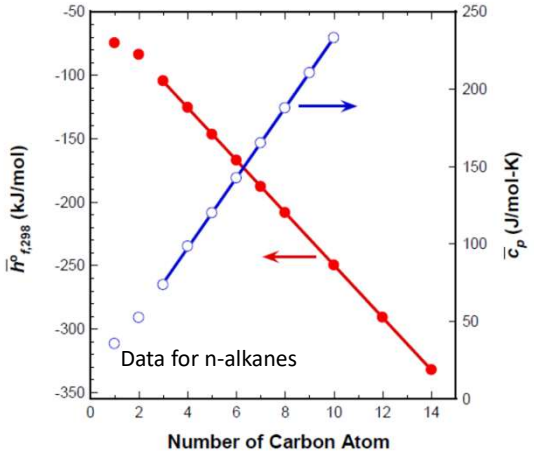

S.W. Benson constructed tables of these Group Additivity Values (GAV). Several researchers, especially Bozzelli and Green, have added to these tables using quantum chemistry to fill in gaps in experimental data.

Basic concepts

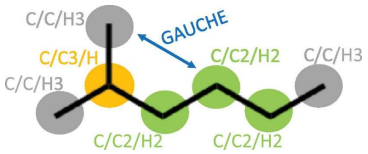

- $\phi_i(\Psi) = \sum_j^m a_{i,j}\Psi_j$
- where $a_{i,j}$ is the number of groups *j* in species *i* and ($\psi_j = \Delta h_{f,j}$(298 K), s^0_j(298 K), $c_{p,j}$ (*T*)).
- For the standard entropy, mixing effects due to symmetry and optical isomerism need to be taken into account additionally, so that it can be computed from the intrinsic standard entropy as:
- $s^0_j(298\ K) = s^0_{int,i}(298\ K) - R \ln(\sigma_i / n_{OI,i})$
- where σ_i is the symmetry number and $n_{OI,i}$ the number of optical isomers of the species.
- **Optical isomer contribution** is accounted for by means of adding one "OI" group with an entropy group value of *R*ln (2) for every chiral centre in the species.
- OI groups also added for OO and OOH groups in peroxy and hydroperoxide species, which are commonly regarded as pseudochiral centres.

(Vom Lehn, 2020)

Treatment of Radicals

- Typically the **hydrogen bond increment (HBI)** approach used, as implemented in THERM.
- Radical thermochemistry based on thermochemistry of **corresponding parent molecule** by adding a so-called **bond dissociation (BD) group**, that accounts for difference in thermochemistry between radical and its parent due to broken hydrogen bond.
- $\Delta h_{f,j,}^{radical}(298\ K)$
  $= \Delta h_{f,j,}^{parent}(298\ K) + \Delta h_{f,j,}^{BD}(298\ K) - \Delta h_{f,j,}^{H}(298\ K)$
- $\Delta h_{f,j,}^{H}(298\ K) = 217.998\ kJmol^{-1}$, enthalpy of formation of the abstracted hydrogen atom.
- Optical isomers may be different for a radical and its parent molecule.

97

Programs to estimate thermo with Group Additivity

- http://webbook.nist.gov/chemistry/grp-add/
- THERGAS (Nancy group, Blurock)
- THERM (Bozzelli)
- RMG (Green group, MIT)
- Several others...

➢ All of these programs are based on Benson's methods described in his textbook "Thermochemical Kinetics" and in several papers by Benson. See also several improvements to Benson's method by Bozzelli.

➢ Group additivity is related to the "functional group" concept of organic chemistry, and to "Linear Structure-Activity Relationships" (LSAR).

Problems with Group Additivity

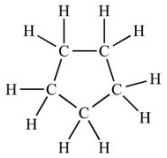

- While GA is intuitively simple, it has drawbacks stemming from the need to consider **higher-order correction terms** for a large number of molecules.
- Take cyclopentane, the addition of group contributions yields H^o = –103 kJ/mol, yet the experimental value is –76 kJ/mol. Difference is caused by ring strain, not accounted for in the group value of C–(C2,H2) obtained from unstrained, straight-chain alkane molecules.
- **Cyclics are biggest problem** for group additivity, but some other species also do not work well, e.g. halogenated compounds, and some highly branched compounds.
- Very small molecules are often unique (e.g. CO, OH), so group additivity does not help with those.
- Species with different resonance forms can also cause problems, e.g. propargyl CH2CCH can be written with a triple bond or two double bonds, not clear which should be used when determining groups.
- ***Many methods have been developed using straight chain alkanes but future fuels might not look like this….***

Use of ML for thermo

- Machine learning (ML) is increasingly replacing or supplementing traditional group additivity (GA) methods for predicting thermodynamic data.
- Can offer higher accuracy by accounting for complex, **delocalized molecular effects** that group contribution methods miss.
- Instead of summing fixed contributions from functional groups, ML models learn non-linear relationships directly from molecular structures.
  - relies on extensive high-quality data sets.
- **Hybrid approaches** combine two approaches by first training ML model on large set of group additive predictions, followed by refinement on limited high-quality dataset with transfer learning (fine tuning) (Ureel et al., 2023, Wang et al. 2026 (DeepTherm)).
- **Decision trees** can also overcome data requirement issues of direct use of deep neural networks (see later, Johnson et al. 2025).
- Can improve on representation of **e.g. steric effects, delocalized resonance effects**, reducing errors for hydrocarbon, predictions by factor of 2 and for radicals by factor of 4.

Check point – do we have enough high quality training data to use ML well?

Curated data set: functional group distribution

Functional group	Number of species	Functional group	Number of species
Vinyl carbon	341	Peroxide group	2117
Allenoic carbon	147	Epoxide group	320
Acetylenic carbon	123	Carbonyl group	1724
Aromatic ring	120	Ester group	426
Heterocyclic ring	1427	Anhydride group	38
Polycyclic aromatic rings	6	Ketone group	1655
Hydroxyl group	2558	Carboxyl group	89
Ether group	733	Peroxycarboxylic acids	26
Enol group	239	Aldehyde group	596
C-centered radicals	1765	O-centered radicals	936

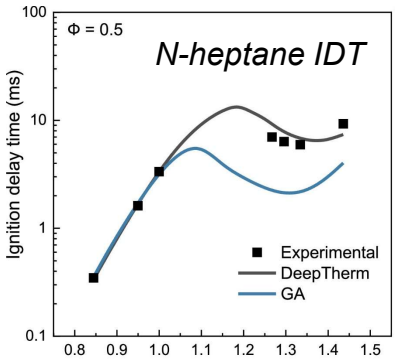

Summary

- Species concentrations in the Hot Exhaust Zone of a combustor are nearly in equilibrium due to the high temperature & high radical concentrations.
  - Whatever system you are studying, it is good to know what the equilibrium is, that is where the kinetics are heading!
- Can compute equilibrium composition using EQUIL and similar programs, but need **thermochemical parameters** for each species.
- Thermochemical parameters also allow us to **infer reverse rate coefficients** from forward rate coefficients.
- These parameters are obtained in a variety of ways, many of them not quite accurate enough for quantitative modeling.
  - Most convenient are **group contribution methods** - very fast.
- **High level quantum chemistry** methods and **Active Thermochemical Tables** can achieve excellent accuracy, **BUT** so far mostly for smaller molecules.
  - Still large **uncertainties** in important species for fuel combustion affecting ability to model heat release etc. (see later). **Scope for reducing through ML.**

Section 2a

Measurement of rate coefficients for elementary reactions

With thanks to Prof Mike Pilling for many of these slides

- Design of measurement systems
- Common systems: laser photolysis; cavity ringdown; shock tubes; flow tubes.
- Example for the H_2+O_2 system.
- Multi-scale informatics.

What does a measurement system look like?

- Ideally, we want to isolate the individual reaction and study it at the appropriate combustion conditions.
  - ➢ i.e. no sensitivity to other possible secondary reactions occurring in the system.
  - ➢ Experiment can be conducted at *T*, *P* required for application of rate constant.
- Not always possible:
  - ➢ May have to model the system to extract rate coefficients of interest.
    - **Rate then subject to uncertainties in the model.**
  - ➢ May need to extrapolate to appropriate *T, P*. Ideally achieve this with the help of theory (**see next section**).

Techniques covered

- Pulsed laser photolysis (laser flash photolysis).
- Shock tubes.
- Flow tubes for elementary reactions and whole systems.
- Static studies of whole systems.
- Multi-scale informatics.

Pulsed laser photolysis

Principles (Pilling and Seakins, 1996)

- Reactant and precursor species are premixed and flow into **photolysis cell**.
- **Pulse of light** used to produce a transient species e.g. a radical or excited state atom using photolysis.
  - E.g. H_2O_2 or t-butyl hydroperoxide photolysed to produce OH radicals.
- Concentration of species then monitored as a function of time.
- If photolysis beam of uniform intensity and reactant well mixed – uniform reactant concentration obtained.
- Pulsed laser photolysis allows to study short reaction times.
- Key is to **minimise secondary reactions** e.g. transient with precursor.
  - Measurement distant from reactor walls.
  - Low precursor concentrations – use of high pulse energy lasers e.g. excimer laser.

Detection methods

1. Absorption spectroscopy

- Light of a frequency corresponding to a **vibrational or electronic absorption** of radical is passed through cell and detected by suitable detector.
- Decay of absorption signal represents change in concentration of transient via **Beer-Lambert Law**.
- $I = I_0 \exp(-\varepsilon c l)$, ε absorption coefficient, c concentration, l path length.
- Example: voltage change ΔV from photomultiplier $\propto$ to change in light intensity and hence related to c.
  - if path length, ε known.

- Differences in light intensities difficult to detect with accuracy.

$C_3H_5 + C_3H_5$:Absorption spectroscopy

- Reaction is second order in C_3H_5
- Need to know absolute concentration of radical – absorption spectroscopy provides a good route to this (see Macpherson, 1985 for discussion for CH_3).
- $I/I_0 = \exp(-s[C_3H_5]L)$ where I_0 is the incident and I the transmitted light intensity, s is the absorption cross section and L is the path length.
- Similar method applied to $CH_3 + CH_3$.

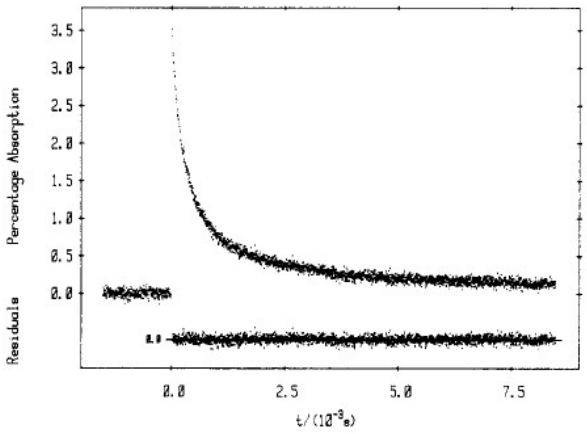

Detection methods

2. Laser Induced Fluorescence (LIF)

- Signal detected relative to zero background.
- Increases linearly with excitation intensity.
- Can detect much lower concentrations ~10^8 molecules.
- Dye laser used to excite radical to upper electronic state (matched to rovibronic transition).

- Relaxation leads to fluorescence.
- Provides **relative measure of concentration**.
- Experiment designed to minimise scattered light.

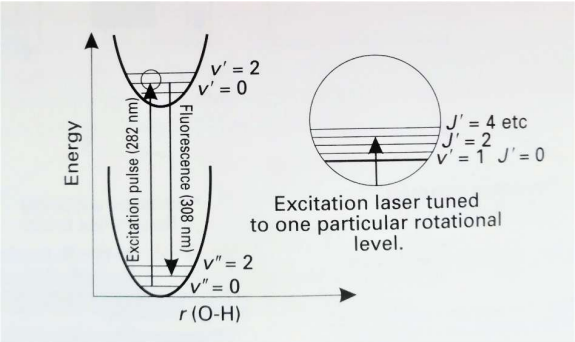

Laser flash photolysis (LFP) / laser induced fluorescence (LIF) for the study of OH + reactant

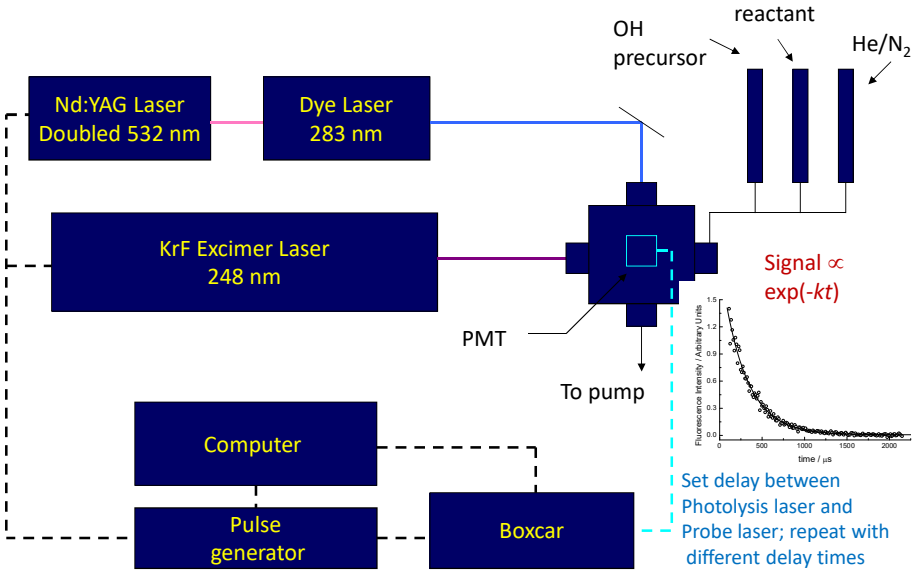

Procedure for determining rate coefficients for pseudo first order reactions using LFP for OH + SO_2

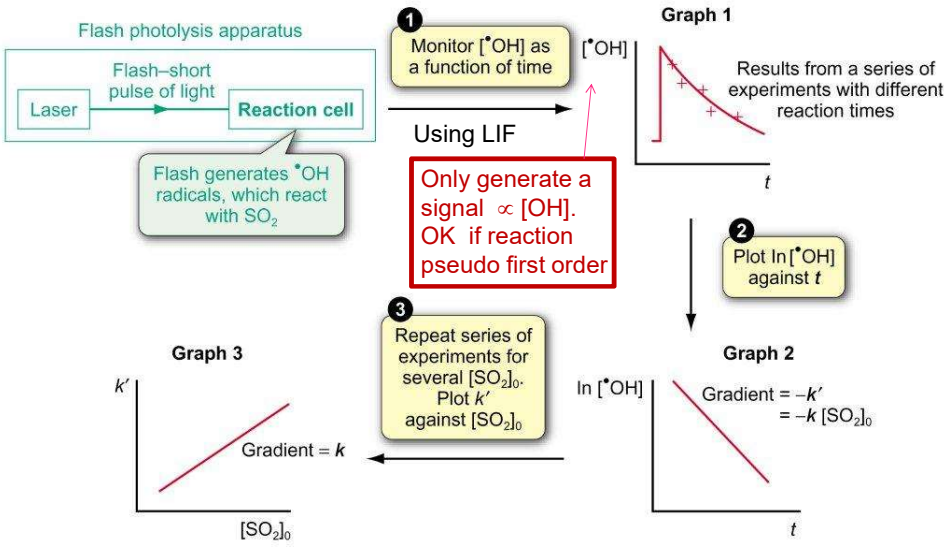

$$OH + C_2H_2 + M \rightarrow C_2H_2OH + M$$

- Pressure dependent (association) reaction.
- Study as a function of temperature and pressure.
- Results fitted to Troe expression

(McKee, 2007)

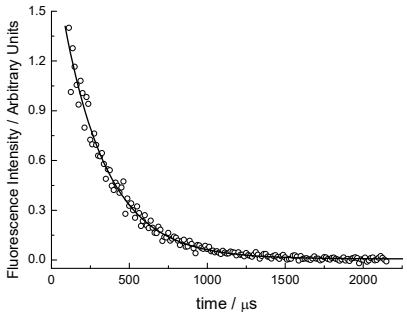

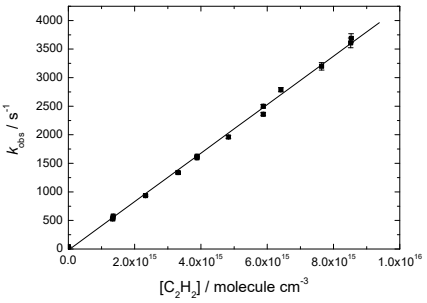

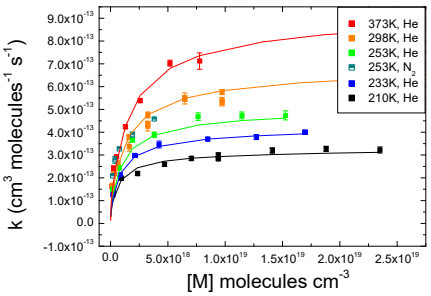

OH + acetone, (Wollenhaupt, 2000)

Laser flash photolysis, resonance fluorescence/laser induced fluorescence to measure [OH] (relative). Optical measurement of [acetone] before and after reactor.

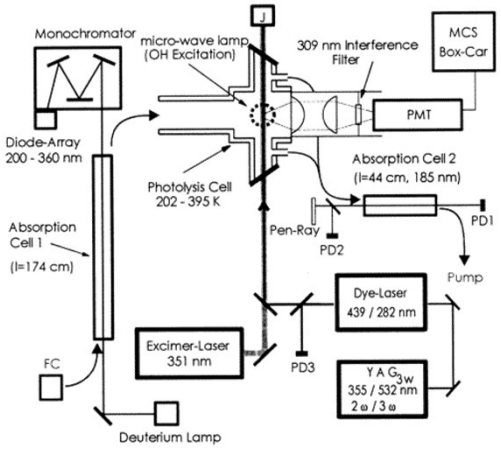

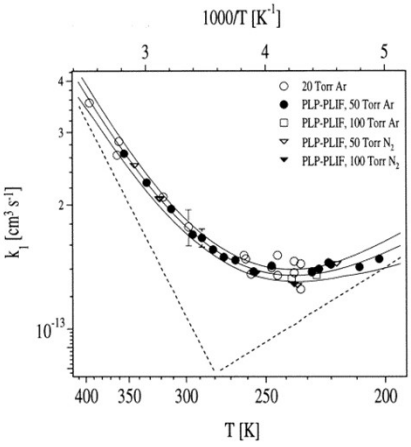

k_1 (202−395 K) = 8.8 × 10^{-12} exp(−1320/T) + 1.7 × 10^{-14} exp(423/T) cm^3 s^{-1}, indicating that simple H atom abstraction may not be only mechanism

Minimising secondary reactions

- In order to be able to use a simple pseudo first-order approach to the analysis of the data, **secondary reactions must play a negligible role**.
- This involves keeping the **initial radical concentration low**.
- See Vaghjiani and Ravishankara (1991) for a classic experimental analysis of problem for OH + CH_4 → CH_3 + H_2O.
- Typical radical decay timescales in pulsed photolysis reactions are ~ 0.1 – 1 ms.
- k(OH + CH_3) is ~ 10^{-10} cm^3 $molecule^{-1}$ s^{-1}. The timescale for removal of OH by this reaction is ~ 0.1 s for [CH_3] = 10^{11} cm^{-3} and 1 ms for [CH_3] = 10^{13} cm^{-3} .
- So essential to keep amount of OH generated in photolysis pulse low if this secondary reaction is to make a negligible contribution to the observed decay of OH.
- Need a **sensitive detection technique** – LIF is ideal.

Detection methods

3. Mass spectrometry

- MS works by turning molecules into charged particles and measuring how they move in an electric or magnetic field.
- Ionisation achieved e.g. by bombardment with electrons or photo-ionisation e.g. using pulsed laser.
- **Time-of-flight (TOF) analysers** use electric field to accelerate ions through the same potential measuring time taken to reach detector.
- If particles have same charge, velocities will depend only on their masses. Initial velocities vary and time-lag techniques used.
- Separated ions hit a detector, which measures: how many ions arrive; at which mass-to-charge ratio (*m/z*).
- Typically presented as plot of ion intensity as a function of the mass-to-charge ratio - the **mass spectrum**.

- Not *in-situ* method – requires sampling.
- Can measure several species simultaneously. Extremely sensitive. Quantitative.

TOF schematic (tofwerk, 2026)

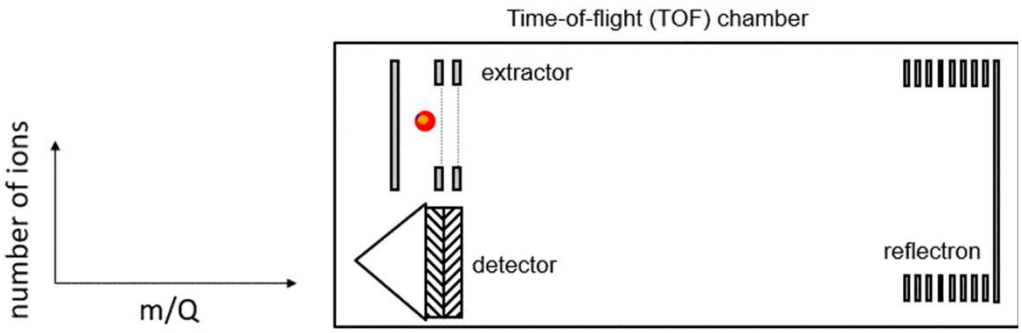

- Ions with smaller *m/z* fly more quickly through the TOF chamber and reach the detector earlier.
- The instrument measures the time of flight of each ion from extractor to detector, which is then converted into a mass spectrum.

117

Detection using time of flight mass spectrometry

Blitz et al. 2007

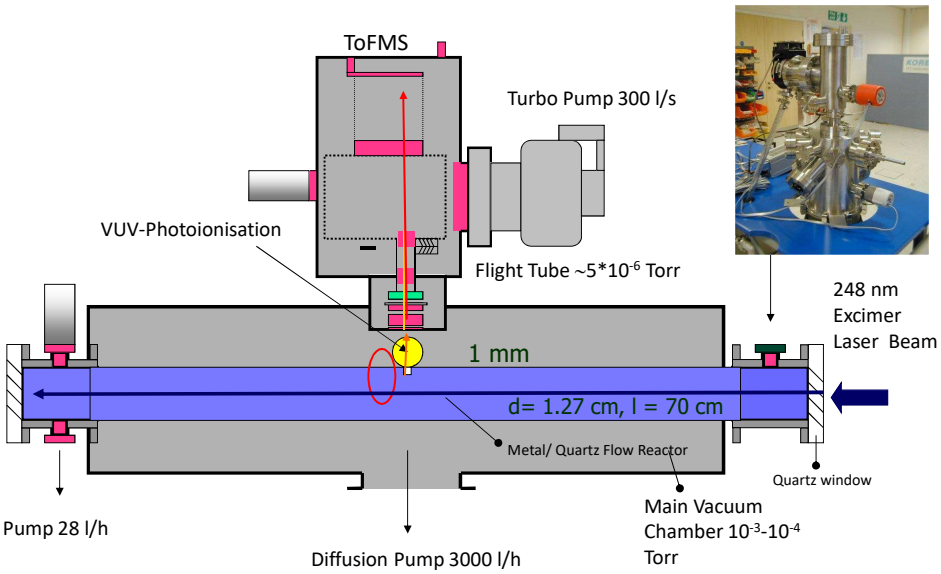

Detection of NO, NO_2, SO allows determination of rate constant for SO+NO_2

Individual mass kinetic traces fitted to exponential growths/decays. NO_2 in excess, pseudo 1st order.

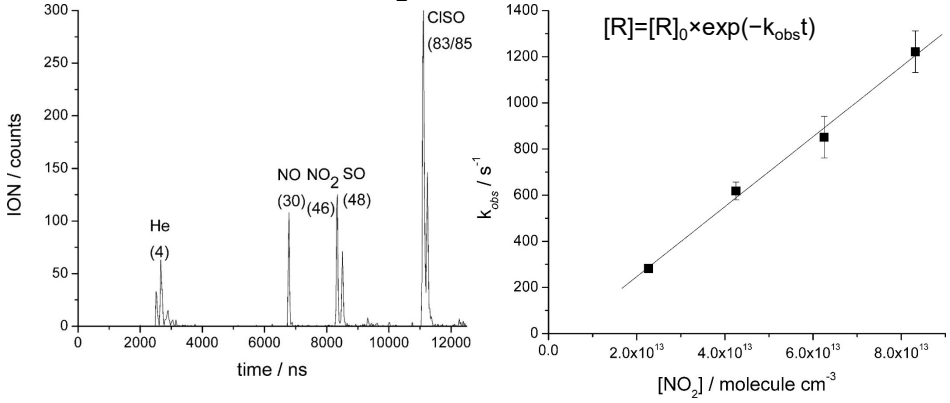

TOF-MS from 248nm photolysis of Cl_2SO/NO_2, 500 shot averaging. The two masses at ~8300ns are fully resolved and correspond to NO_2 (46amu) and SO (48amu).

Application of synchrotron radiation to distinguish enols from aldehydes in flames (ALS, Lawrence Berkley)

Taatjes et al. *Science* 2005, **308**, 1887

- Synchrotron tuneable vacuum ultraviolet (SVUV) light - pulsed-extraction TOFMS.
- **ALS is tuneable** (different photon energies used) making it feasible to **distinguish isomers, with same mass**, through their differing photoionization efficiency curves.
- Mole fractions for acetaldehyde and ethenol are derived by scaling the observed ion signals from species in the flame by their relative photoionization cross sections.

  acetaldehyde: CH_3CHO

  ethenol: CH_2=CHOH

Photoionization efficiency curves taken for m/z 0 44 ions

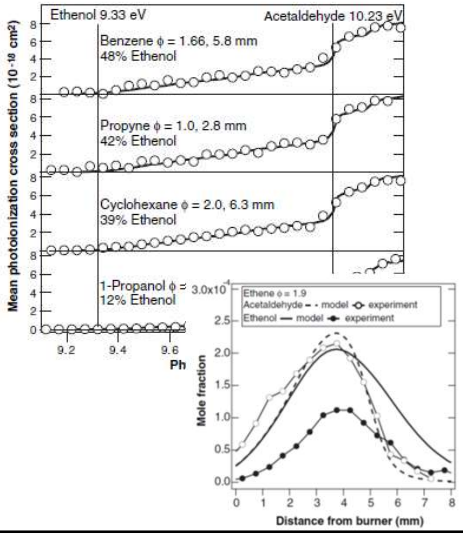

Importance of accurate cross sections

Photoionization cross section is the probability that a molecule will be ionised when it absorbs a photon of a given energy.
• Large cross section → ionises easily → strong signal
• Small cross section → ionises weakly → weak signal
Depends on:
• the **species**
• the **photon energy** (or wavelength)

A big signal does not necessarily mean a high concentration.
Two species at the same concentration can give signals differing by orders of magnitude because their cross sections differ.

Accurate cross sections needed to distinguish between species.

Yang et al. (2007)

NSRL China
Various butanol flames,

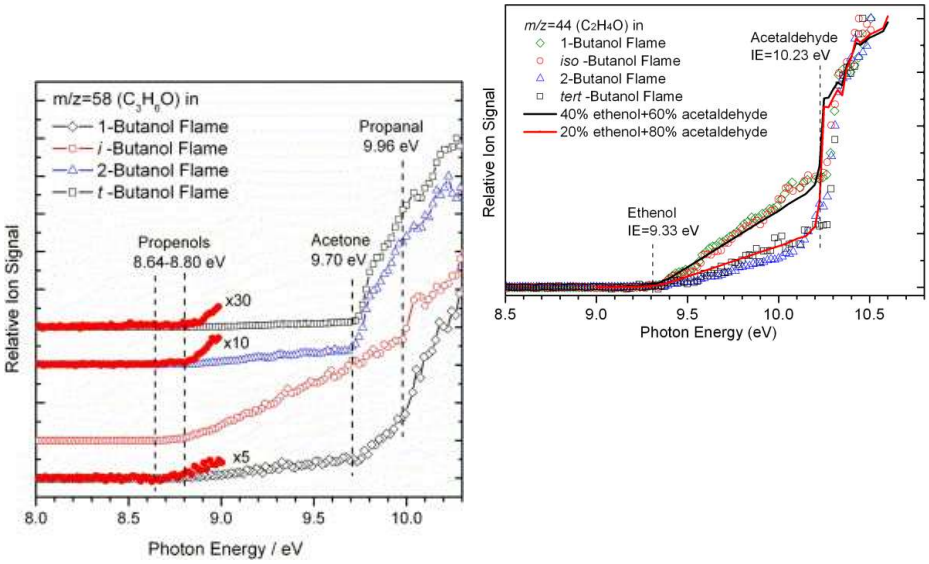

Cavity Ring Down Spectroscopy

- Used to study gas samples which absorb light at specific wavelengths, and to determine mole fractions down to the parts per trillion level (extremely sensitive due to long path length).
- Consists of a laser which illuminates a high-finesse optical cavity, - two highly reflective mirrors.
- Resonance with a cavity mode, builds up intensity in the cavity due to constructive interference.
- When laser turned off - **measurement of exponentially decaying light intensity leaking from cavity**.
- Reflection back and forth between mirrors gives effective path length for extinction on the order of a few kilometres.
- Insensitive to the intensity fluctuation of the light source.

- If light-absorbing material placed in cavity, mean lifetime decreases.
- A CRDS setup measures time for light to decay to 1/e of its initial intensity.
- This "ringdown time" can be used to calculate the concentration of the absorbing substance in gas mixture in the cavity.

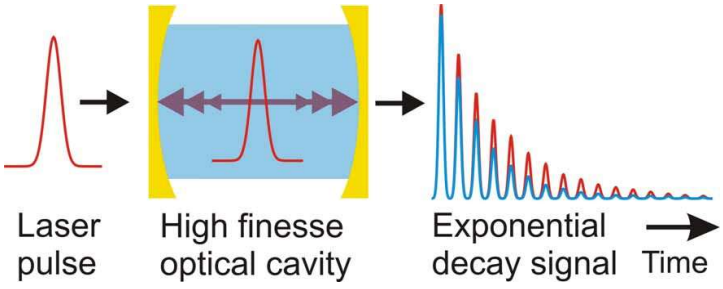

https://www.chem.ualberta.ca/

Atomic Resonance Absorption Spectroscopy (ARAS)

- Used to detect and measure specific atoms by exploiting the fact that free atoms absorb light at very precise, element-specific wavelengths.
- Often used for detecting atomic radicals (O, H, N etc.).
- A light source (e.g. tunable laser) emits radiation at a wavelength that matches an allowed electronic transition of the atom.
- As light passes through sample atoms absorb photons following the Beer–Lambert law.
- Absorption occurs only when the photon energy matches exactly an atomic energy level difference making the technique highly selective and sensitive.
- In common with other techniques, accurate absorption cross sections are key.

124

Shock tube - basics

Basic concept:

- High-pressure driver gas expands (usually helium) upon diaphragm opening, creating shock wave.
- Test gas is instantaneously compressed and heated to combustion temperatures by incident and reflected shocks.
- High-temperature experiments monitored near end wall.

- Test time defined by difference between shock wave reflection and arrival of expansion wave at end wall.
- Several possible methods to delay expansion wave arrival
  - ➢ extend driver section
  - ➢ slow down the expansion wave by decreasing sound speed of driver gas by adding heavier gasses.

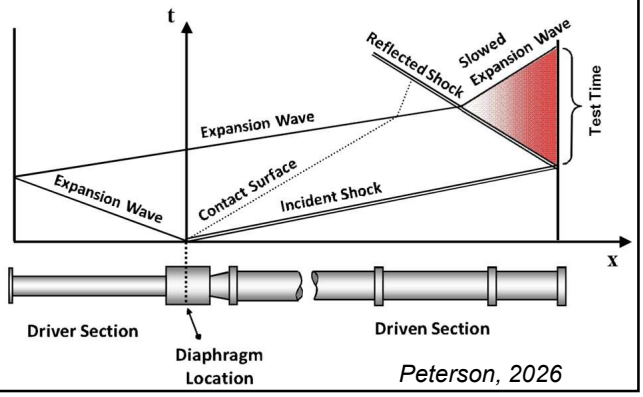

Peterson, 2026

Shock tube:
Hanson lab at Stanford

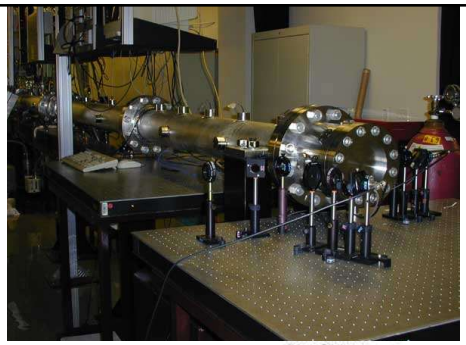

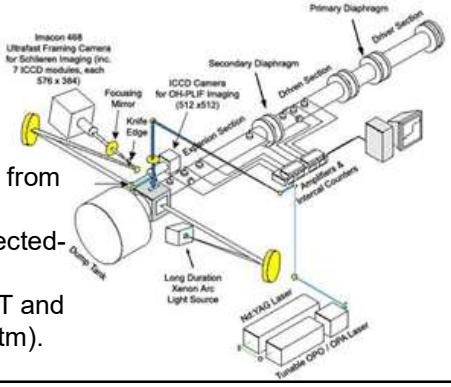

- ➢ Instantaneous heating/compression from shock waves.
- ➢ Accurately known incident- and reflected-shock conditions.
- ➢ Wide range of post-reflected shock T and P possible (600-4000 K, 0.1-1000 atm).

Shock tubes

- Radicals generally formed from **thermal dissociation of precursor**.
- Test times 1-10 ms.
- **Single shot**, so no signal averaging, but impressive optimisation of signal.
- Generally need to assess secondary reactions and use numerical chemical model with sensitivity analysis to show viability of measurements.
- Example: Measurement of CH_3 + OH by Hanson group.

Vasudevan et al, (2008)

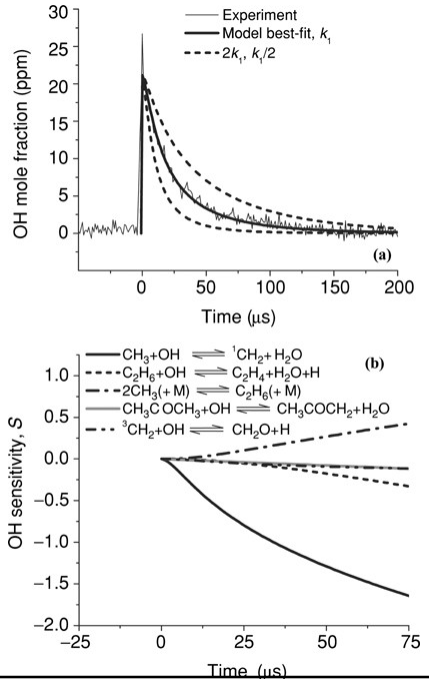

OH + HCHO, 934 K to 1670 K, 1.6 atm

- OH radicals - shock-heating tert-butyl hydroperoxide.
- 1,3,5-trioxane [$(CH_2O)_3$] was used in the pre-shock mixtures to generate reproducible levels of CH_2O
- OH concentration time-histories were inferred from laser absorption using the R1(5) line of the OH A-X (0, 0) band near 306.7 nm.
- Other reactions contribute to the OH time profile, especially CH_3 + OH.
- **Rate coefficient determined by fitting to detailed model** (GRI-Mech), with addition of acetone chemistry, deriving from dissociation of OH precursor (t-butylhydroperoxide).
- Detailed uncertainty analysis.

Vasudevan et al, (2005)

Determination of *k* and uncertainty analysis

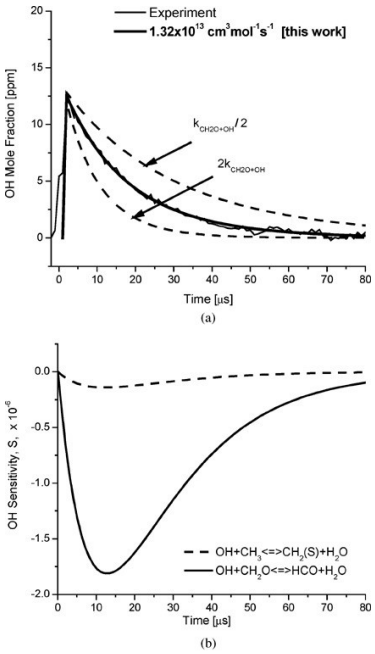

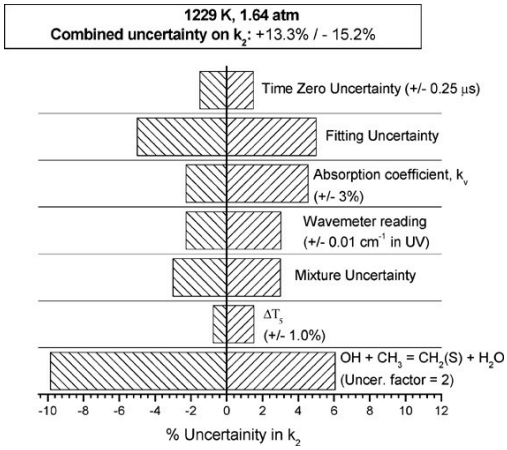

Check-point: if you are measuring rate constants are there secondary reactions in your system? Have they been accounted for?

Arrhenius plot for OH + HCHO

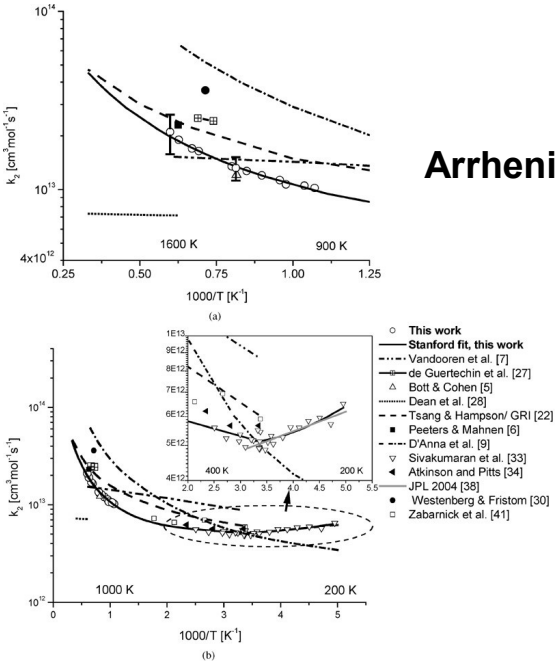

$k_2 = 7.82 \times 10^7 T^{1.63} \exp(531/T) / \text{cm}^3\ \text{mol}^{-1}\ \text{s}^{-1}$

OH + Aldehydes
(Wang et al., 2017)

- Absorption technique; 976 – 1346 K, 0.6 atm.
- Some dissociation of aldehyde at higher T.
- Monitor by CO absorption.

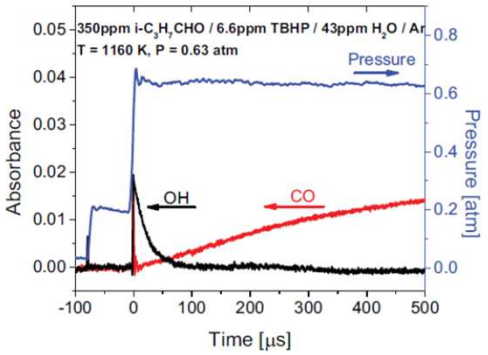

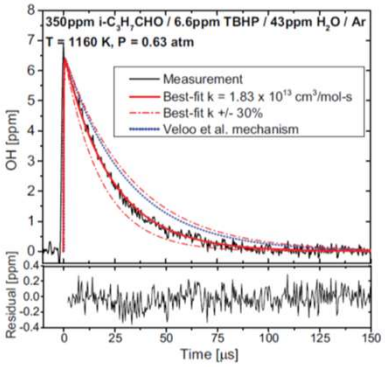

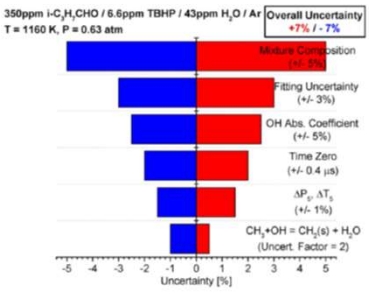

OH + aldehydes contd.

$k_{iC_3H_7CHO+OH} = 7.70 \times 10^{13} \exp(-1700\ K/T) \pm 7\%$;

$k_{nC_4H_9CHO+OH} = 1.03 \times 10^{14} \exp(-1730\ K/T) \pm 7\%$;

$k_{iC_4H_9CHO+OH} = 1.02 \times 10^{14} \exp(-1750\ K/T) \pm 10\%$;

$k_{(CH_3)_3CCHO+OH} = 7.20 \times 10^{13} \exp(-1670\ K/T) \pm 8\%$;

$k_{C_2H_5CHCHCHO+OH} = 6.93 \times 10^{13} \exp(-1340\ K/T) \pm 8\%$;

$k_{C_6H_5CHO+OH} = 3.10 \times 10^{13} \exp(-1380\ K/T) \pm 8\%$.

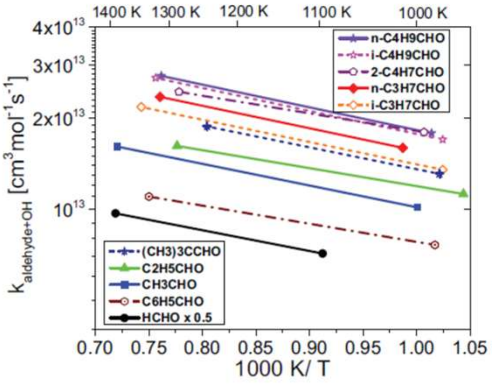

Flow tubes for elementary reactions and whole systems

Pyrolysis of n-butanol using molecular beam sampling from a plug flow reactor

Cai et al. (2012)

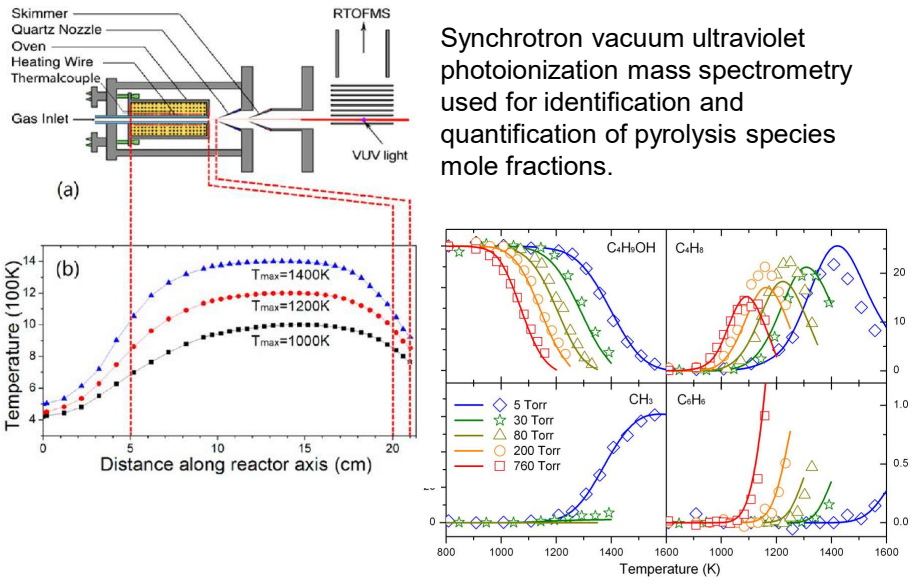

Synchrotron vacuum ultraviolet photoionization mass spectrometry used for identification and quantification of pyrolysis species mole fractions.

Use of species concentrations in flow reactor to determine rate coefficients: butanol dissociation

Cai et al. (2012)

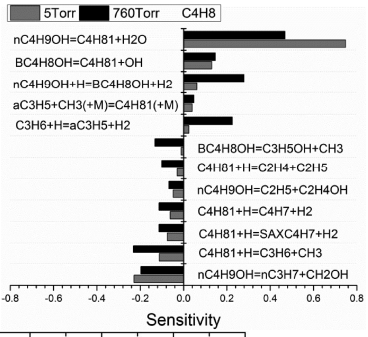

C_4H_8 sensitivity
T_{max} = 1450 K under 5 Torr (gray) and
T_{max} = 1100 K under 760 Torr (black)

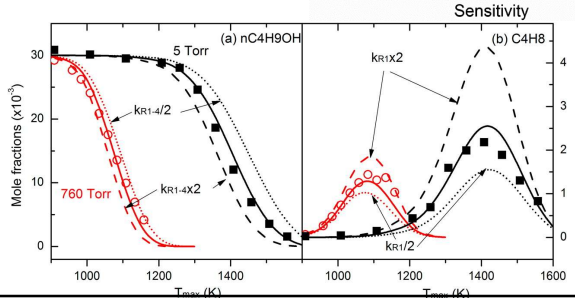

Experimental mole fraction profiles (symbols) and modelling results (lines) of nC_4H_9OH pyrolysis at 5 and 760 Torr.

Examples from the $H_2 + O_2$ system

Reminder: Interaction of elementary reactions in $H_2 + O_2$

- **Three ignition (explosion) limits.**
- **Competition** between **termination** (removing radicals, decelerating rate) and **branching** (accelerating rate).
- **First limit** – competition between wall termination e.g. H → wall (rate ↑as pressure ↓) and H + O_2 → OH + O.
- **Second limit** – competition between H + O_2 + M → HO_2 + M (rate ↑as pressure ↑) and H + O_2 → OH + O.
- HO_2 is low reactivity radical and reacts mainly by HO_2 + HO_2 + M → H_2O_2 + M.
- **Third limit –** H_2O_2 dissociates generating OH radicals (H_2O_2 + M → 2OH) and propagation and branching recommence.

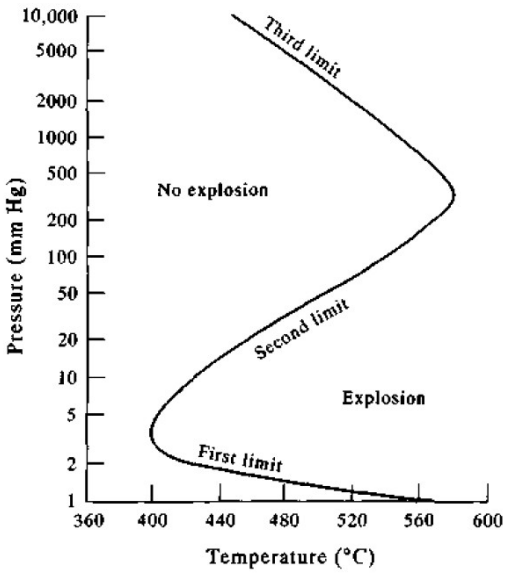

Hydrogen oxygen system

- Burke (2012) presented full evaluation of system showing sensitivities of target outputs to each reaction.
- Note the significance of
  - ➢ H + O_2 branching step,
  - ➢ termination step H + O_2 + M
  - ➢ and H + HO_2 steps for both ignition and burning velocities.

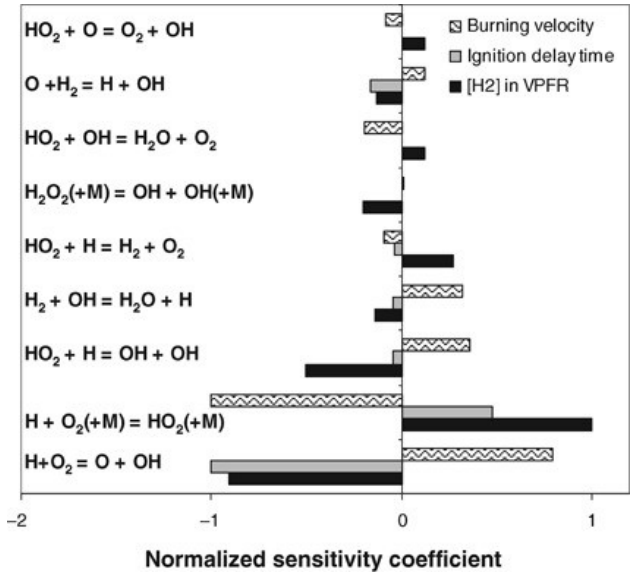

$H + O_2 \rightarrow OH + O$

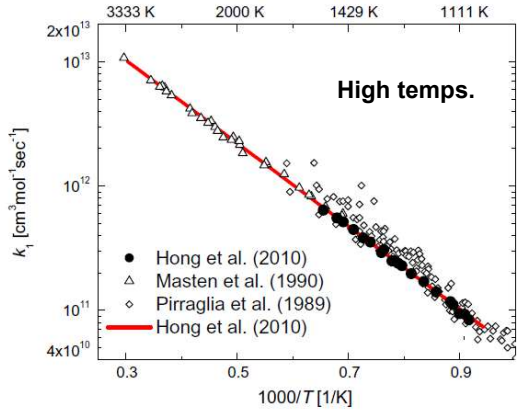

- From Hong et al. (2011) shock tube measurements.
- $k = 1.7\times 10^{-10} \exp(-7670/T)$ (1100 – 3370 K). Uncertainty ± 10%.
- See Burke et al. (2012), who support the rate coefficient.

Second branching step $O + H_2 \rightarrow OH + H$

- Sutherland et al. (1986) used
  - flash photolysis, monitoring O by resonance fluorescence, and
  - shock tube, generating O by flash photolysis of NO and monitoring by Atomic Resonance Absorption Spectroscopy (ARAS).
- Davidson and Hanson (1990) used a shock tube, generating O by laser flash photolysis of NO and by pyrolysis of N_2O. O monitored by ARAS: 2120 – 2750 K.
- Javoy et al. (2000). ARAS: 2021 – 3356 K.

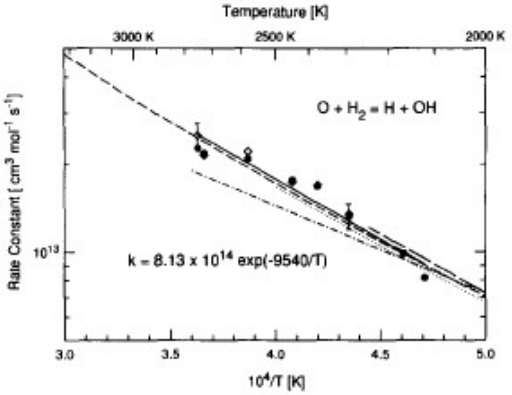

Fig. 2. Arrhenius diagram: $O + H_2 \rightarrow OH + H$. Filled circles—data derived from photolysis method. Open diamonds—data derived from pyrolysis method. Error bars represent ±10%. Solid line—best fit to present data. Dotted line—Sutherland et al. [8]. Dashed line—Nataranjan and Roth [9]. Dot-dashed line—Pamidimukkala and Skinner [10]. Long-dashed line—Shin et al. [11].

Sutherland et al. (21st Symp(Int) Comb, 1986, 929).

$H + O_2 + M \rightarrow HO_2 + M$

- Termination step at lower *T,* converting reactive H into less reactive HO_2.
- At higher *T* acts as a route to branching through formation of H_2O_2 through HO_2 + HO_2 (and HO_2 + RH in hydrocarbon combustion).
- Reaction is at the third-order limit except at higher pressures.
- Michael et al. (2002) used flash photolysis at room *T* for a wide **range of third bodies**, and a shock tube at higher *T* for Ar,. O_2 and N_2. Showed that H_2O is an unusually effective third body.
- Detailed analysis of collision frequencies and energy transfer parameters.
  A + B $\rightleftharpoons$ AB* $\rightarrow$ AB

$$k = \frac{k_0[\mathrm{M}]k^{\infty}}{k^{\infty} + k_0[\mathrm{M}]}$$

$H + O_2 + M \rightarrow HO_2 + M$

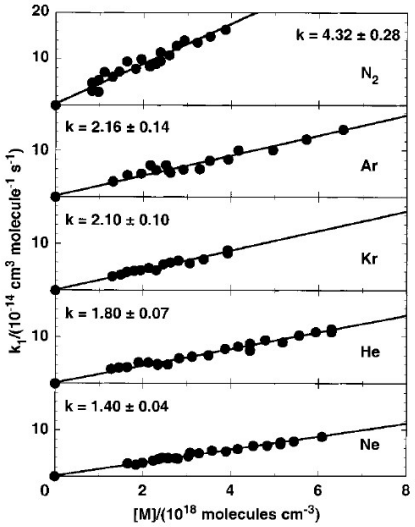

Units of k: 10^{-32} cm^6 $molecule^{-2}$ s^{-1}

T dependence of Z_{coll}

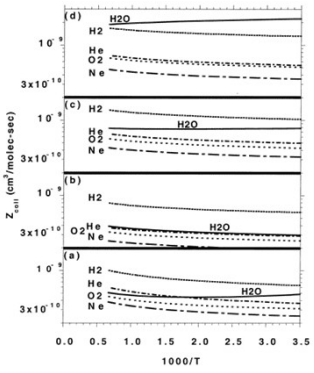

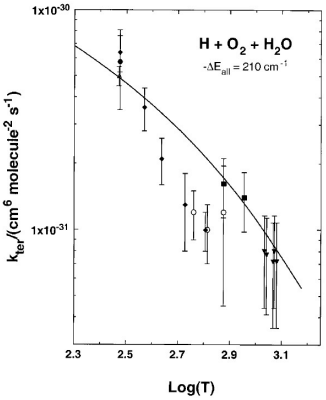

Check-point: all mechanisms contain this reaction. Do you know in yours how *P* dependency is parameterised and how 3rd body efficiencies are represented?

High pressure pulsed photolysis / flow reactor

(Fernandes et al., 2008)

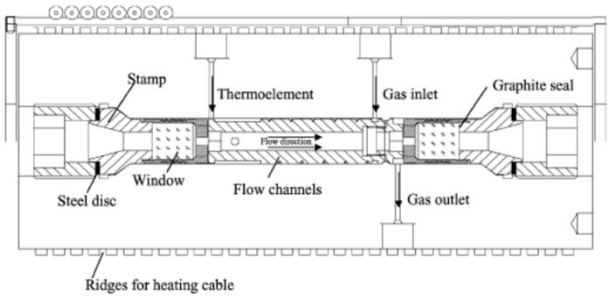

- $H + O_2 + M \rightarrow HO_2 + M$, 300 – 900 K, 1.5 – 950 bar
- H from photolysis NH_3 at 193 nm.
- HO_2 detected by absorption spectroscopy at 230 nm.
- At these higher pressures, the reaction moves into the fall-off region.

$H + O_2 + M \rightarrow HO_2 + M$

- Data for different third bodies and temperatures can be rationalised and placed on the same plot using reduced falloff curves.
- Requires calculation of high pressure limiting rate coefficient (that isn't accessible to experiment for this reaction).

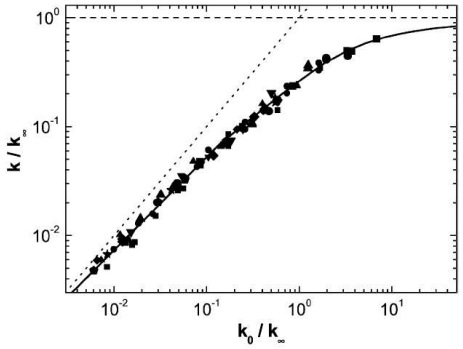

Fig. 7 Doubly reduced falloff curves for the recombination H + O_2 (+M) → HO_2 (+M) in the bath gases M = He, Ar, and N_2 (experimental points from this work from Tables 1–3; T/K = 300 (■), 400 (●), 500 (▲), 600 (▼), 700 (♦), 800 (★), and 900 (⬟), see text).

Evaluation: Burke et al., 2012

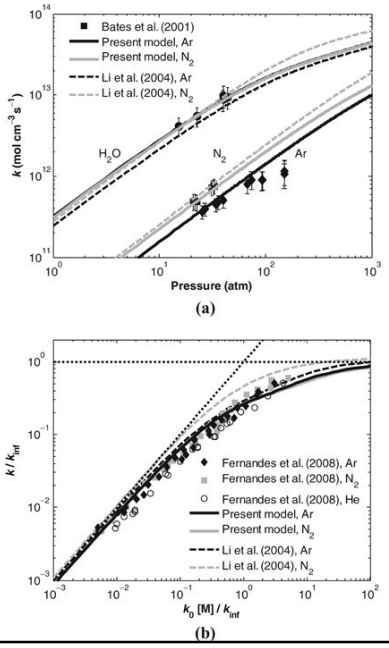

- Full model evaluation for high pressure combustion.
- Fall-off updated using **high pressure limit values** from ab initio studies of Harding and Troe.
- Mostly consistent for different bath gases bar fall off region for Ar.
- Bath gas mixture rules add additional uncertainty.

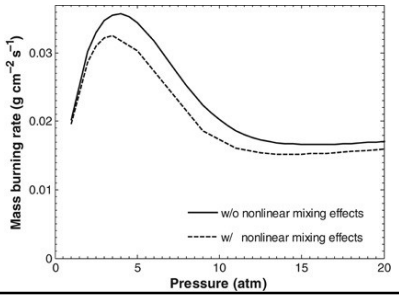

Latest comparison of purely *a priori* theory and experiment, M=Ar (Klippenstein, 2017)

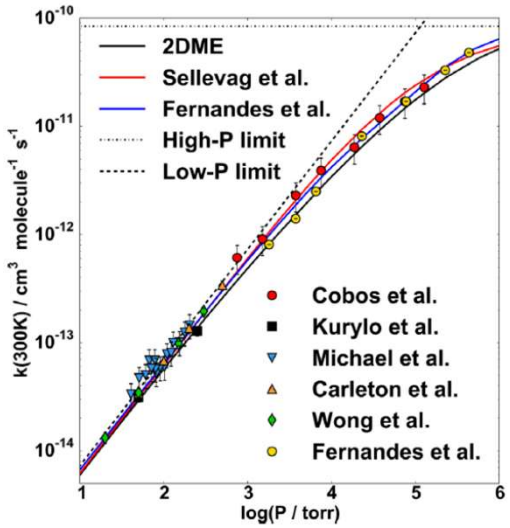

1. **solid black line**: *a priori* energy transfer based 2D-ME predictions, coupled with dynamically corrected variable reaction coordinate TST based on a high accuracy well-validated MRCI PES

2: **solid red line**: fitted master equation results of Sellevag et al. J Phys Chem A 2008, 112, 5085.

3. **solid blue line**: analytic fit of Fernandes et al. Phys Chem Chem Phys 2008, 10, 4313

A priori theory values within error bars of experiments.

$H_2O_2 + M \rightarrow 2OH + M$

(Troe, Combustion and Flame 2011, 158, 594–601)

- The thermal dissociation/recombination reaction of hydrogen peroxide $H_2O_2 \rightleftharpoons 2OH$. Analysis and representation of the temperature and pressure dependence over wide ranges.
- Reaction is far from the high pressure limit. To obtain a representation of *k(T,P)*, Troe used the statistical adiabatic channel model to calculate k_∞, using an ab initio surface (Phys. Chem. Chem. Phys. 10 (2008) 3915; J. Chem. Phys. 111 (1999) 2565).
- An important aspect of this work was the use of thermodynamics to relate forward and reverse reactions, using the revised enthalpy of formation of OH.

H_2O_2 dissociation

(Hong et al. Comb Flame 2011, 158, 633)

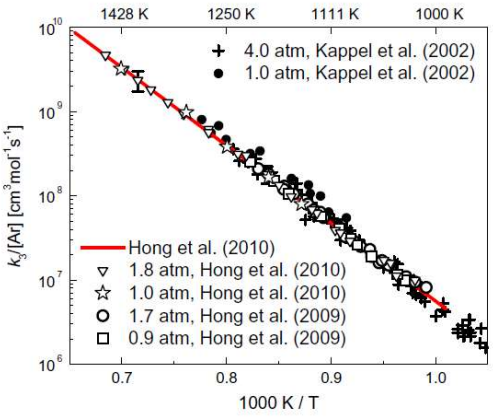

- Data refer to low pressure limit. Used shock tube with laser absorption detection of H_2O and OH.

MULTI-SCALE INFORMATICS (MSI)

$OH + HO_2 = H_2O + O_2$
An example of multi-scale modelling

- Focusses on H_2O_2 decomposition system where large uncertainties persist in *T/P/*M dependence.
- *T* dependence of rate for $HO_2 + OH = H_2O + O_2$ subject of debate.
  - Radical-radical reactions are difficult to study experimentally.

- Experimental data mostly low *T*.
- **Non-Arrhenius behaviour** between 900 - 1300 K.
- Deep, narrow "well" with a minimum ~ order of magnitude lower than atmospheric and high-temperature values.
- Later data from Srinivasan et al. and Hong et al. suggest weaker *T* dependence.
- **HOW TO RESOLVE?**

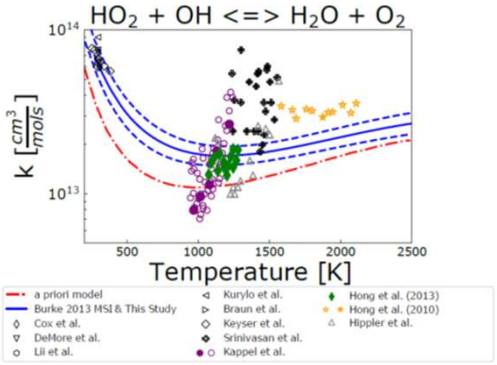

Burke et al., 2013, 2021

$OH + HO_2 = H_2O + O_2$
An example of multi-scale modelling

- Multi-scale modelling approach uses combination of **exp. data** (at limited conditions), **coupled with theory** within an **optimisation approach** to find a functional form consistent with all sources.

- *ab initio* transition-state theory within their associated uncertainties.
- Uncertainties in barrier heights, frequencies, exp. *T*, *P*, third body efficiencies included in optimisation.
- Finds rate minimum near 1200 K, although *T* dependence is substantially less pronounced than previously suggested.

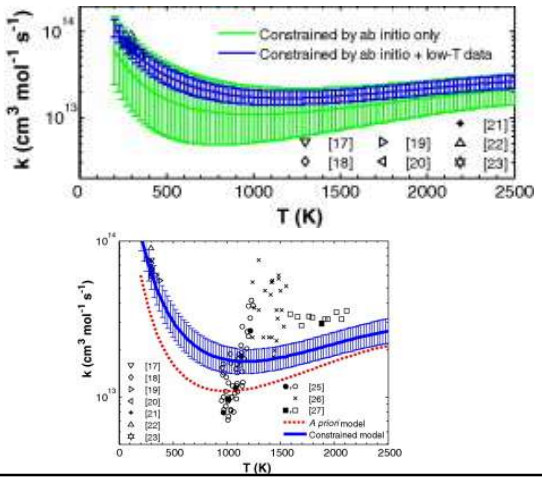

$HO_2 + HO_2 \rightarrow H_2O_2 + O_2$

- < 800 K: flash photolysis, absorption spectroscopy.
- Open circles: shock tube, absorption spectroscopy *(Kappel et al, Phys Chem Chem Phys, 2002, 4, 4392)*.
- Reference 5: Hippler et al. J Chem Phys 1990, 93, 1755
- Significant disagreement > 1000 K
- Burke et al. (2012) 'Difficult to discern which, if any, (of the high T) determinations is reliable.' More measurements needed under combustion conditions.

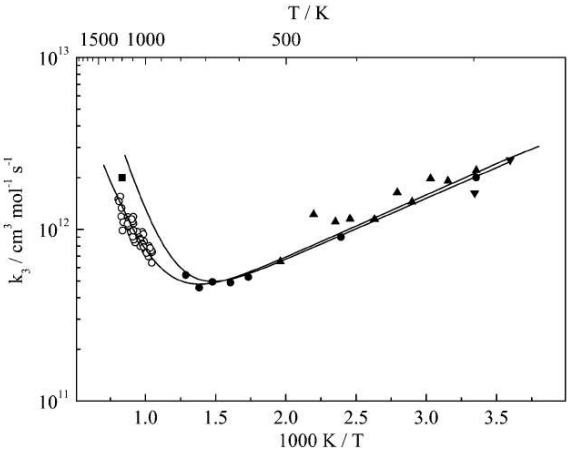

Fig. 10 Rate constants k_3 (■: ref. 2, ▲: ref. 35, ▼: ref. 36, ●: ref. 37, ○ and lower line: this work, upper line: ref. 5).

New channel (Klippenstein et al., 2022)

- High level theory applied (CCSD(T) with extrapolation to CBS limit and various corrections for e.g. higher order excitations, anharmonicity).
- Uncertainties in stationary point estimated at 0.2 - 0.4 kcal mol^{-1}.
  - VRC-TST calculations implemented for singlet channels within ME analysis.

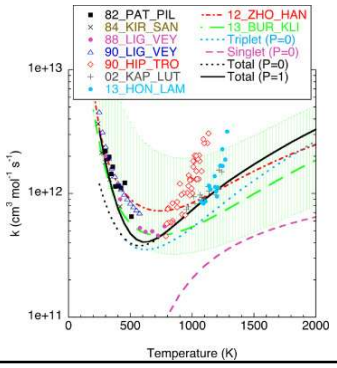

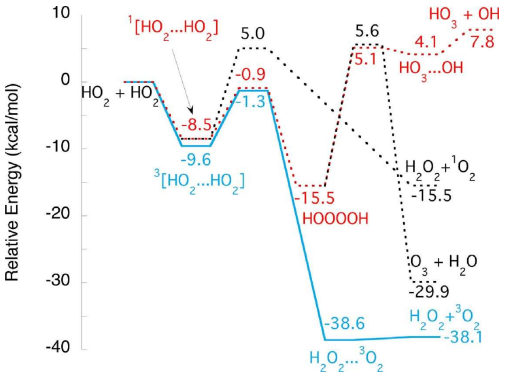

HO_2 + HO_2 new channel proposed, MSI approach

- Scatter, leading to discrepancies between experimental data. Most recent data – shock tube study of Hong et al.
- Two channels now proposed:
  $HO_2+HO_2=H_2O_2+O_2$; $HO_2+HO_2=OH+OH+O_2$
- MSI resolves data and supports new channel.
- Both reactions of importance for high T flame speeds in various flames + perhaps surprisingly predictions of NTC for alkanes.

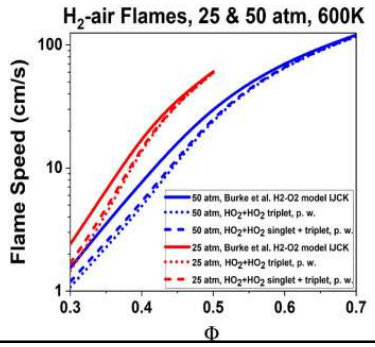

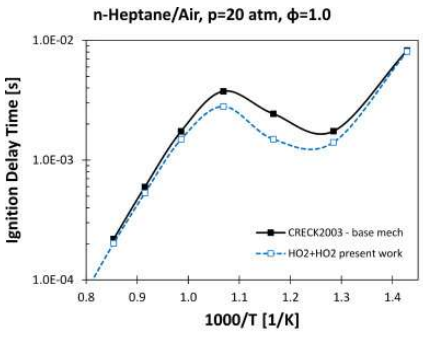

Section 2b
Theoretical basis of Chemical Kinetics

- Why theory?
- Collision theory
- Transition state theory
- RRKM theory
- Barrierless reactions
- Master equation methods
- Combining theory with experiment

WHY USE THEORY?

- Models help us to **extrapolate** thermo-kinetic data to *P*/*T* where experiments don't exist or are not possible.
- A single highly accurate source of data would help us to establish **consistency between mechanisms**.
- At least for small molecules, theory can now achieve **comparable levels of accuracy** to experiments.
- Can perhaps be more easily **automated** for large number of reactions than developing laboratory robots?
- To design and improve rate rules in a hierarchical framework.
- To support **fundamental understanding** of kinetic systems.
- "Future progress in the fidelity of the chemical modelling of combustion will benefit from more widespread applications of theoretical chemical kinetics and from **increasingly intimate couplings of theory, experiment, and modelling**." Klippenstein (2021) paper reviews these links.
  - Combustion chemistry in the twenty-first century: Developing theory-informed chemical kinetics models, Miller et al. 2021.

Basis of Theory

- Theory of chemical kinetics should ideally predict rates at which reactants with a given **energy distributed about specific excitation modes** pass over to products of equally well defined energy within a **multi-dimensional PE hypersurface**.
- Requires:
  - Complete description of PES.
  - Energy distributions of reactants and products.
- Even with developments of CPU resource difficult for all but smaller molecules.
  - Simplifications made e.g. Collision theory, Transition State Theory.

Simple Collision Theory (Wayne, 1969)

Check-point: CT provides an upper limit for rate constants which should not be violated.

- Assumes hard spheres.
- Rate of reaction relates to **collision frequency** for collisions with relative kinetic energy greater than critical value E_c along lines of centre.
- Derived by applying Boltzmann distribution to the relative velocity of two colliding species (A, B say).
- Gas collision rate:

mean relative speed

Collision cross section *Reduced mass*

$$Z\ (\varepsilon > \varepsilon_c) = n_A n_B \sigma^2 \left(\frac{8\pi kT}{\mu}\right)^{1/2} e^{-\varepsilon_c/kT}$$

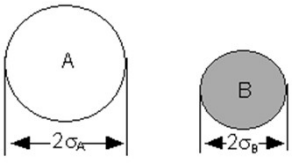

where ε_c is the critical energy per molecule, $\sigma = \frac{1}{2}(\sigma_A + \sigma_B)$, $\mu = m_A m_B/(m_A+m_B)$

- When using per mole *k* is replaced with *R* in equation.
- Limited by lack of consideration of:
  - Steric factors/Longer range interactions (simple factor could be added).
  - Activation through internal degrees of freedom such as vibration (important for uni-molecular reactions).
- Use of Lennard-Jones potentials allow improvement on hard sphere assumption.

Transition State Theory (TST)

- Simple collision theory takes no account of nature of colliding species except to consider if they carry enough energy to get over an energy barrier to reaction.
- TST focuses on configuration of reactants at highest point on PES – the ***transition state*** or ***activated complex***.
  - Activated complexes studied near the saddle point of a PES.
- **Assumes quasi equilibrium between reactants and activated complexes.**
- They are converted into products and kinetic theory used to calculate rate of conversion.
- TST assumes that all trajectories originating from reactant region cross a reactant/product dividing surface in phase space only once
  - all forward-crossing trajectories lead directly to products
  - dividing surface assumed to be dynamical bottleneck.
- Conventional TST - dividing surface passes through saddle point on PES.

Main idea of TST

Identify a 3*N*-1 dimensional dividing surface, a Transition State (TS), that represents a **bottle neck** for going *from an initial to a* final state:

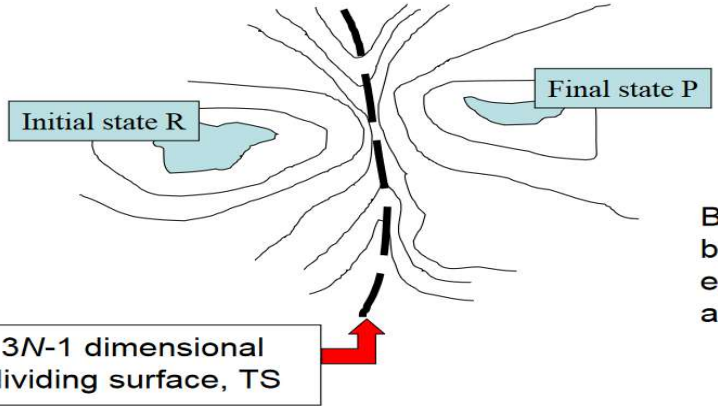

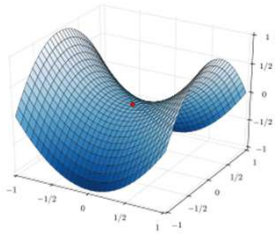

Bottle neck can be due to an energy barrier and/or entropy

$$k^{TST} = \text{(probability of being in TS)} \cdot \text{(flux out of TS)}$$

TST formulations

- Both **classical** and **statistical** versions of TST can be formulated.
- Statistical thermodynamic formulation allows calculation of equilibrium constant between reactants and complex from partition functions.
  - **Of course accurate knowledge of partition functions requires accurate methods for calculating PES.**
- Collision theory requires that only the height of the energy barrier is known.
- TST requires information about **shape of PES around the saddle point**.

Transition State Theory

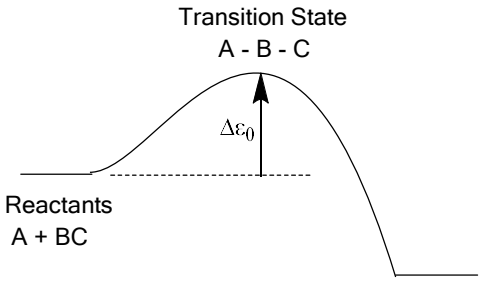

Flux s^{-1} *P of TST*

$$k(T) = \alpha \frac{k_B T}{h} \frac{Q_{TS}^{\ddagger}}{Q_A Q_{BC}} \exp\left(\frac{-\Delta\varepsilon_0}{k_B T}\right)$$

Contributions from translation, rotation and all internal degrees of freedom

- Transition State Theory provides a method for calculating the rate constant, $k(T)$, using statistical mechanics.
- Q is the molecular partition function, q, divided by the volume, V.
- The ‡ sign indicates that one vibrational mode (along reaction coordinate) has been removed from the partition function for TS – constraint along reaction coordinate.
- Need barrier height and good description of partition functions.

α is a correction factor: most common source from incorporation of tunnelling through the barrier in H atom transfer reactions and symmetry factors.

Molecular degrees of freedom

- A molecule composed of N atoms has a total of 3N nuclear degrees of freedom:
  - **3 translation** (motion in x, y, z directions).
  - **2 rotation** (linear molecule, rotation about bond axis does not change orientation), **3 rotation** (non-linear, can rotate about three independent axes).
- Remaining degrees of freedom correspond to internal vibrations (bond stretching and bending).
  - **3N-5 vibration** (linear), **3N-6 vibration** (non-linear).
- The interaction between the electrons and the nuclei provides a potential energy surface that defines the equilibrium geometry of the molecule and the response to the relative motion of the atoms – the **vibrations and internal rotations**.
- The molecule is described by an overall wavefunction, ψ; remember the Born-Oppenheimer principle states that this can be separated into nuclear and electronic components, because of the difference in masses.

$$\psi = \psi_{electronic}\, \psi_{nuclear}$$

Vibration

- A periodic motion of the atoms of a molecule relative to each other, such that the centre of mass of the molecule remains unchanged.
- A **diatomic molecule** has **one normal mode** of vibration - it can only stretch or compress the single bond.
- Vibrations of polyatomic molecules are described in terms of independent normal modes.
- Molecular vibration is excited when molecule absorbs energy, ΔE, corresponding to the vibration's frequency, v: $\Delta E = hv$.
- Motion in normal vibration approximated using **harmonic oscillator**. Vibrational energy is a quadratic function (parabola) with respect to the atomic displacements.
- In reality motion is anharmonic and first overtone has frequency that is slightly lower than twice that of the fundamental.
- Excitation of higher overtones involves progressively less and less additional energy and **eventually leads to dissociation**.

Partition Functions and Reaction Coordinate

- To evaluate rate constants using statistical thermodynamic formation of TST we need the partition functions for reactants and activated complex.
- Needed for various degrees of freedom.
  - $Q = Q_{trans}Q_{vib}Q_{rot}Q_{elec}$
- Calculation of these requires accurate knowledge of the form of the PES at the transition state.
- Special cases exist.
- Use of **reaction coordinate** assumes reaction system treated as motion along just one path.
  - Allows determination of vibrational term to be omitted from partition function for activated complex.
  - Obtained via normal mode analysis of vibrations.

Reminder - approaches to accurate electronic structure calculations

- A basis set is composed of atomic orbitals, yielding linear combination of atomic orbitals approach (LCAO).
- The CBS limit is extrapolated estimate of result obtained using an infinitely large (**complete) basis set**.
- Electron correlation is interaction between individual electrons.
- Hartree Fock method has minimal electron correlation.
- **Full configuration interaction** (or **full CI**) is a linear variational approach which provides numerically exact solutions (within infinitely flexible complete basis set) to electronic Schrodinger equation.

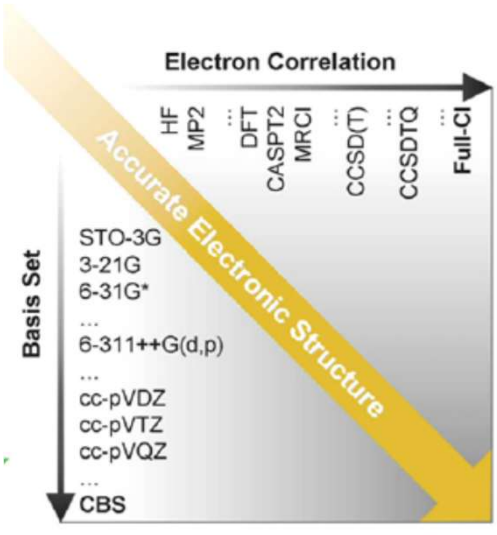

Zador et al Prog Energy Comb Sci 2011, 37, 371

Approach to calculating rate coefficients using TST

- The approach is most simple for a constrained transition state – one where there is a significant maximum on the reaction coordinate.
- The PES is calculated using electronic structure methods and the TS located.
- The energy of the TS relative to the reactants is determined along with the structure of the TS (which allows the moments of inertia to be calculated) and the vibrational frequencies.
- *k* (T) can then be calculated using Transition State Theory, and assuming rigid rotor – harmonic oscillator (RRHO) behaviour.
- Problems arise with hindered internal rotors and more complex calculations are needed.
- Classical mechanics assumes that probability of particle overcoming an energy barrier is 0 if it has less energy that barrier height.
- **However**, quantum mechanical **tunnelling** through the energy barrier can also be important for particles of small mass and H transfer reactions.

Accuracy of TST calculations

- **Kinetic accuracy**
  - Uncertainty of barrier height is typically ~ 4 kJ mol^{-1} (1 kcal mol^{-1}). Graph shows a plot of exp(E/RT) vs T with E = 4 kJ mol-1, which represents the uncertainty factor in *k* deriving from the uncertainty in the activation energy.

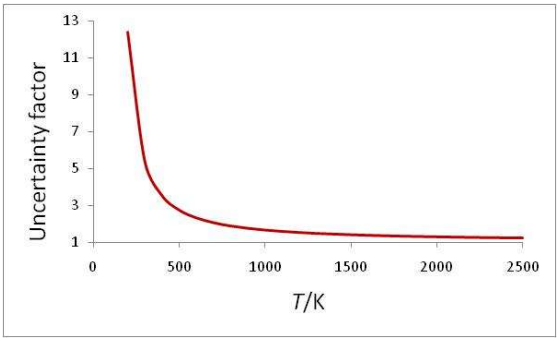

- **Deficiencies** in the TS model
  - Rigid rotor harmonic oscillator model
  - Tunnelling model – generally use Eckart.
- **Improvements via** – higher level ab initio calculations, variational effects, anharmonicities, multidimensional tunnelling …
- Often tune the barrier height obtained from lower level calculations to experimental data, allowing improved extrapolation of the latter.
  - **See later examples from Shannon, Burke etc.**

Microcanonical rate theory

- Microcanonical rate theory examines the rate at a specific energy; it gives:

$$k(E) = \frac{hW^{\ddagger}(E)}{N(E)}$$

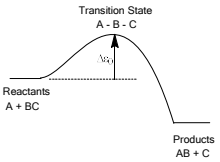

- where $W^{\ddagger}(E)$ is the sum of states at the transition state, from energy zero at the TS to E and $N(E)$ is the density of states at energy E for the reactant(s).
- This approach is used when dealing with **master equation** calculations.
- Integrating this expression over a Boltzmann distribution of reactants gives the TST result for $k(T)$.

Variational TST (VTST)

- Some reactions have only a **small or no energy barrier**.
  - exact location of the TS is problematic
  - e.g. radical-radical reactions.
- In **variational transition state theory (VTST)** location of dividing surface is variationally optimized either to:
  - maximize Gibbs free energy of activation in a canonical ensemble.
  - minimize number of states of generalized transition state in a microcanonical ensemble.
- Microcanonical VTST achieved by **optimizing the TS for each internal energy E**, and even for each J quantum number for molecular rotation.
- Once energy-specific optimal TS is known, temperature-dependent rate coefficient recovered for each T by averaging over appropriate Boltzmann distribution.
- Every additional dimension that is optimized increases the computational cost, but also improves the quality of description.

Further limitations of Transition State Theory (TST)

- Valid in gas phase bimolecular reactions - inelastic collisions of reactants efficient enough to repopulate rovibrationally excited states maintaining local equilibrium.
- Problems in gas-phase **unimolecular reactions** unless pressure is extremely high, since **rovibrationally excited states not in local equilibrium**, and rate constants **fall off** as pressure is lowered and reactive states are depleted faster than they can be repopulated.
- Need a different set of methods for **pressure dependent reactions.**

RRK (Rice–Ramsperger–Kassel theory) Theory

- Recognises that a minimum amount of energy must be localised in **specific modes of molecular motion** in order for unimolecular step to take place.
  - i.e. a molecule can only react or fall apart if enough energy happens to collect in the *right bond*.
  - activation is by collision, molecules have many internal degrees of freedom, and reaction occurs when some special degree of freedom acquires at least a critical amount of energy.

RRK theory assumes:

- The total energy is spread out among all the vibrational modes
- Energy is constantly being shuffled between these modes
- Treated statistically RRK theory asks
  - What is the chance that one bond temporarily gets enough energy?
- The more total energy the molecule has, the more often this happens.

RRKM

- Standard TST theory assumes perfect thermal Boltzmann population with clear temperature *T*: *k*(*T*).
- Many combustion reactions are so fast that a Boltzmann distribution cannot be established. For those cases better to use *k*(E), and average as necessary over the true energy distribution.
- RRKM theory calculates reaction rates by counting how many quantum states allow a molecule with a given energy to reach the reaction pathway:
  - a microcanonical formulation of TST which can then be averaged to get *T/P*-dependent rates.
- Improves on RRK:
  - Uses the **actual vibrational modes** of the molecule
  - Explicitly includes the **transition state**
  - Accounts for how energy is distributed at the reaction bottleneck
  - Still assumes energy is randomized, but in a structured way
- RRKM theory depends on assumption that the total phase space of a molecule at a particular energy is uniformly populated as the molecule passes from reactant to product through the TS, and the time scale for energy randomization is << that of reaction
  - **thermal Boltzmann distribution is maintained** at all energies, which is true at sufficiently high pressures.

Barrierless reactions

- RRKM theory is applicable for TS dividing surfaces located at a constrained geometry with a well-defined energetic barrier.
- RRKM recognises that:
  - Not all vibrations are equal
  - Some motions help reach the transition state, others don't
  - The "bottleneck" controls the reaction rate
- When reaction in question is **barrierless**, a first principles determination of *k(E)* requires a **variational approach** – i.e. is calculated by minimizing rovibrational sum of states, *W*(*E*), on the PES in question.
- Alternative approach is using inverse Laplace transformation (ILT).
- Unimolecular microcanonical *k*(E) is determined from either experimental measurements or theoretical determinations of the canonical high pressure limiting rate coefficient, $k_\infty(T)$.
- Well suited for radical-radical reactions.

Limits of Commonly Used Methods

- The most commonly used theoretical models for describing chemical kinetics are accurate in two limits.
- When relaxation is fast with respect to reaction timescales, **thermal transition state theory (TST)** is the right tool.
- In the limit of slow relaxation, an energy resolved description like **RRKM theory** is more appropriate.
- More recently, Master equation approaches have been successfully used to analyse and predict non-equilibrium chemical kinetics for a range of intermediate relaxation regimes.
- Suitable for cases where the reactions are so fast that a Boltzmann distribution cannot be established. For those cases it is better to use k(E), and average as necessary over the true energy distribution.
- MEs facilitate kinetic simulations over multi-well molecular energy topologies where energy transfer with an external bath impacts phenomenological kinetics.
  - i.e. the timescales for thermalization are competitive with kinetic timescales.

Master equation model for pressure dependent reactions

Answers question: given collisions, energy transfer, and reactions, what rate do we observe at a given temperature and pressure?

Master Equation Modelling - Intro

The **master equation** tracks how a population of molecules:

- Gains or loses energy in collisions
- Reacts while at different energy levels

It treats the system as moving between **energy "bins"** over time.

Modern master-equation modelling combines:

- **RRKM theory** → energy-dependent reaction rates
- **Collision models** → energy transfer with the bath gas
- **Thermodynamics** → equilibrium distributions
- **Pressure and temperature effects**

Allowing prediction of:

- Pressure-dependent rate constants; fall-off behaviour; product branching ratios
- Chemically activated reactions

Energy Grained Master Equation (EGME)

- EGME typically involves the calculation of energy resolved rate coefficients using microcanonical transition state theory (μTST) and collisional energy transfer models.
- Combined to construct a model describing phenomenological rate coefficients that arise from competition between reaction and thermalisation of non-equilibrium ensembles.
- Typical application is via a one-dimensional ME, wherein the total **rovibrational energy of the system, *E*,** is the independent variable, where angular momentum, *J* is averaged. E.g. in MESMER.
- **Assumption** - errors in molecular properties (e.g., energies and frequencies) and experimental measurements (e.g., of rate coefficients or product yields) tend to have more impact on ME results than errors introduced by neglecting *J*.

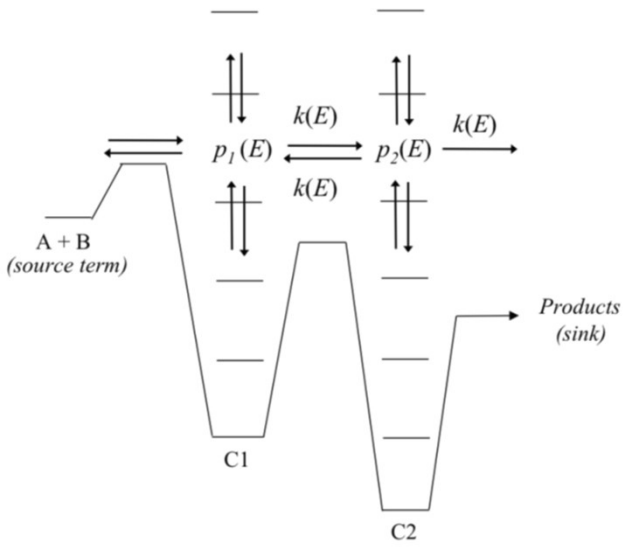

- Energy barrier to inter-conversion of species, and TS corresponds to first-order saddle point on the molecular PES.
- Thus, the reactant must be **activated and energy supplied to overcome barrier**.
- Typically, supplied through collisions with bath gas molecules.
- Some collisions are activating and some deactivating.
- Since collision events and amount of energy transferred are random quantities, energy transfer process can be regarded as random walk, and treated using techniques from stochastic process theory.

EGME Method

- Provides macroscopic kinetic description of reaction system in terms of the behaviour of isomers at **energy resolved** (or microcanonical) level.
  - Need microcanonical rate constants.
- Overcomes number of states by bundling together rovibrational states of similar energies into ‘grains’, and then describing the time evolution between these energy grains, which generally span no more than a few kJ mol^{-1}.

EGME method

Mesmer manual, Glowacki et al.

- ω is Lennard-Jones collision frequency, and $P(E|E')$ is the probability that collision with bath gas will result in a transition from a grain with energy E' to a grain with energy E.
- Q_m is the rovibrational partition function for the molecular species corresponding to isomer m, n_A is the number density of reactant A, and p_B is the population in reactant B.

Population density within grain

collisional energy transfer from other energy grains in that isomer

population loss from grain $p_m(E)$ via collisional energy transfer

$$\frac{dp_m(E)}{dt} = \omega \int_{E_{0m}}^{\infty} P(E \mid E')p_m(E')dE' - \omega p_m(E)$$

reversible population gain/loss into grain $p_m(E)$ by reactions that transfer population from isomer n/m to isomer m/n at a particular energy E

$$+\sum_{n \neq m}^{M} k_{mn}(E)p_n(E) - \sum_{n \neq m}^{M} k_{nm}(E)p_m(E)$$

reversible population loss from $p_m(E)$ via reactions that transfer population from isomer m to products S

$$-k_{Sm}(E)p_m(E)$$

$$+K_{Rm}^{eq}k_{Rm}(E)\frac{\rho_m(E)e^{-\beta E}}{Q_m(\beta)}n_A p_B - k_{Rm}(E)p_m(E)$$

Population gain/loss via association/redissociation

ME methods

- Also needed for closure:

$$\frac{dp_B}{dt} = \sum_{m=1}^{M} \int_{E_{0i}}^{\infty} k_{Rm}(E)p_m(E)dE$$

$$- n_A p_B \sum_{m=1}^{M} K_{Rm}^{eq} \int_{E_{0i}}^{\infty} k_{Rm}(E)\frac{\rho_m(E)e^{-\beta E}}{Q_m(\beta)}dE$$

- Whole system then solved by matrix diagonalization techniques using discrete form:

$$\frac{d}{dt}\mathbf{p} = \mathbf{M}\mathbf{p}$$

- **M,** the transition matrix**,** determines population evolution due to the collisional energy transfer and reaction processes.
- The total number of eigenvalues is equal to the number of grains.
- Grain size is a balance between cost and microscopic non-equilibrium detail.
- **Eigenvalue of smallest magnitude gives rate coefficient.**

Example of isomerization and dissociation system

The Kinetic Model

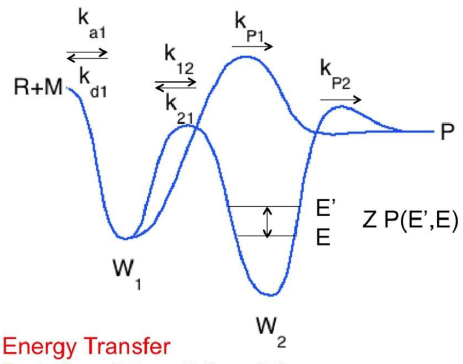

Energy Transfer
Bath Gas; [B] >> [M] >> [R]
Z; Lennard Jones Collision Rate
P(E',E); Exponential Down

Microcanonical
RRKM Theory
$k_{a1}(E)$
$k_{d1}(E)$
$k_{12}(E)$
$k_{21}(E)$
$k_{P1}(E)$
$k_{P2}(E)$

Phenomenological
Master Equation
$k_{R+M \rightleftharpoons P}(T,P)$
$k_{R+M \rightleftharpoons W1}(T,P)$
$k_{R+M \rightleftharpoons W2}(T,P)$
$k_{W1 \rightleftharpoons W2}(T,P)$
$k_{W1 \rightleftharpoons P}(T,P)$
$k_{W2 \rightleftharpoons P}(T,P)$

(Klippenstein, 2017)

Chemically Significant Eigenvalues (CSE)

- The eigenvalues of **M** exhibit a separation in magnitude:
  - all are negative
  - majority are large in magnitude and govern the time evolution of the energy transfer process (IERE).
  - a smaller group of eigenvalues (CSE) govern the chemical evolution of the system.
- At low temperatures the number of CSE corresponds to the number of distinct chemical species being modelled and is usually the sum of the number of wells and source terms in the model.
- Separation in time scales allows a matrix rate equation to be set up relating purely to the CSEs that is identical to the rate equation for the chemical system.
- Rate constants determined from an eigen-pair analysis of the ME.
- This is only possible provided the IEREs and CSEs are well separated in time
- References: J. Chem. Phys., 1974, 60, 3474; J. Phys. Chem. A, 2002, 106, 9267; J. Phys. Chem. A, 2006, 110, 10528; Phys. Chem. Chem. Phys., 2007, 9, 4085–4097.

Master Equation Solver for Multi-Energy well Reactions (MESMER)

- Open source, object oriented code (C++).
- http://sourceforge.net/projects/mesmer/
- Facilitates kinetic simulations of multi-well systems where energy transfer with a bath gas impacts phenomenological kinetics.
- Provides interface with results of electronic structure calculations to allow set up of multi-well system.
- Output choices include chemically significant (and other) eigenvalues, species concentrations vs time, phenomenological rate constants.
- Allows **fitting to experimental data** using χ^2 minimisation.
- Includes MPI parallelization.
- Allows fitting to experimental decay traces.

Other master equation approaches/available software

1. Multiwell. Uses a stochastic approach rather than the matrix methodology used in MESMER. Developed by John Barker. See:
   http://clasp-research.engin.umich.edu/multiwell/. and Int J Chem Kinet. 33, 232-45 (2001), 41, 748-763 (2009)

2. MESS. A matrix method, developed at Argonne National Labs by Georgevskii et al. See: http://tcg.cse.anl.gov/papr/codes/mess.html
   J. Phys. Chem. A 2013, 117, 12146−12154
3. AutoMech developed by Elliot et al. at ANL. Attempts to combine automated reaction discovery with a wide range of theoretical methods for estimating thermochemical and reaction rate parameters (Elliot et al. 2021).

Master equation
Some examples and Discussion of Uncertainties

Level of detail in rate constant calculations

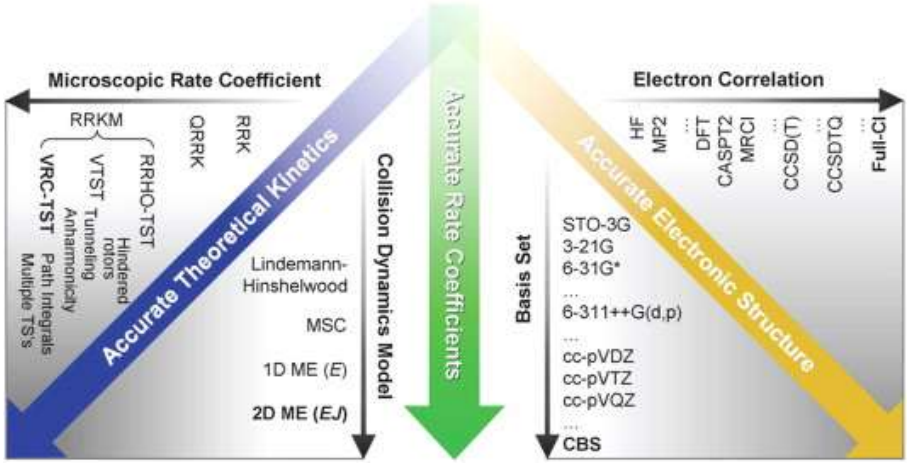

Uncertainties in derivation of phenomenological rate coefficients from theory: n-propyl radical oxidation

- Like other models Master Equations require a variety of **input parameters** which are **not known exactly**.
  - barrier heights, well depths, vibrational frequencies, collision frequency, and energy transfer parameters.
- Often determined from ab-initio calculations which have differing uncertainties depending on **level of theory**.
- Few studies emerging that propagate such uncertainties.
  - MESMER also has option to do this.
- Will take Goldsmith et al. (2013) **n-propyl oxidation** as example.
  - Theory used for PES described in Goldsmith (2012).

Inputs to ME

- Variations of ±0.5 and ±1.0 kcal/mol considered for electronic energy relative to O_2 + *n*-propyl for stable species and the transition states respectively.
- For each stationary point 3-5 lowest-frequency vibrations considered uncertain, except for O_2.
- $\langle \Delta E_{down} \rangle = (200 \pm 50\%)(T/298)^{(0.85\pm0.15)}$ cm^{-1}.
- Lennard Jones parameters varied by 20%.

67 parameters varied in total

- *Frequencies varied by:*
  - *±20% for hindered-rotors, and transition-state imaginary frequencies (for Eckart tunneling estimates)*
  - *±10% for harmonic vibrations*

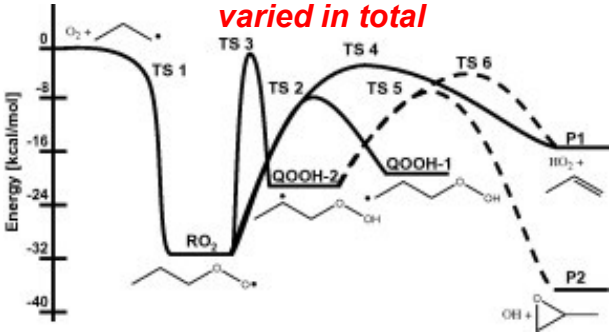

Resulting reaction rate distributions

$O_2 + n - C_3H_7 \rightleftharpoons RO_2$ (R1)

$\rightleftharpoons QOOH - 1$ (R2)

$\rightleftharpoons HO_2 + \text{propene}$ (R3)

$\rightleftharpoons OH + \text{propene-oxide}$ (R4)

$RO_2 \rightleftharpoons QOOH - 1$ (R5)

$\rightleftharpoons HO_2 + \text{propene}$ (R6)

$\rightleftharpoons OH + \text{propene-oxide}$ (R7)

$QOOH - 1 \rightleftharpoons HO_2 + \text{propene}$ (R8)

$\rightleftharpoons OH + \text{propene} - \text{oxide}$ (R9)

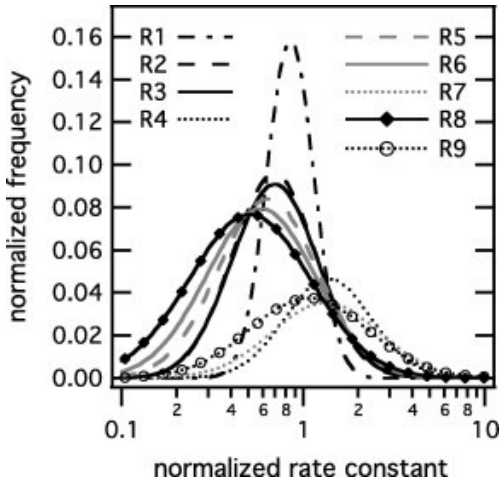

Rates at 3σ variances typically differ from most frequent values by factors of 4–6, decreasing with increasing temperature.

Sensitivity Analysis – which are most influential parameters?

1 atm			100 atm	
Reaction R5 RO_2 ↔ QOOH-1				
Parameter	S_i, 600 K	S_i, 800 K	S_i, 600 K	S_i, 800 K
TS2 energy	0.667 (−)	0.621 (−)	0.697 (−)	0.701 (−)
RO_2 energy	0.198 (−)	0.169 (−)	0.184 (−)	0.182 (−)
Reaction R6 RO_2 ↔ HO_2 + propene				
TS4 energy	0.665 (−)	0.584 (−)	0.643 (−)	0.627 (−)
RO_2 energy	0.143 (−)	0.074 (−)	0.166 (−)	0.156 (−)
RO_2 $\langle \Delta E_{down} \rangle$ prefactor		0.080 (+)		

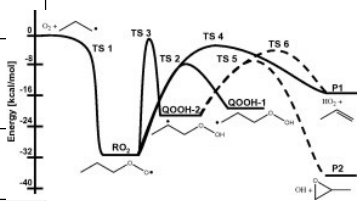

$CH_3CH(OH)CH_3$ + OH study (Prager, 2013)

- Importance to low temperature alcohol combustion.
- Branching fractions require extensive isotopic substitution that is difficult for larger alcohols.
  - **See example later for why these are important.**
- Theory therefore necessary and comparisons can be made against total fuel+OH rates from measurement.
- A range of theory calculations were compared for the calculation of optimized geometries and harmonic frequencies of the reactants and the transition state (TS) for the reaction channel:

  $CH_3CH(OH)CH_3 + OH \rightarrow CH_3C\cdot(OH)CH_3 + H_2O$
- Methods included DFT, Møller–Plesset perturbation, CASPT2, CBS-QB3, G3B3 and G3MP2 using Gaussian and Molpro.

Results of use of theory only

- Considerable scatter in calculated barrier height E, ranging from −1.94 kcal mol^{-1} (MP2) to −0.41 kcal mol^{-1} (G3B3).
- Less scatter in calculated frequencies although second lowest frequency ν_2, and the imaginary frequency ν^* show differences of up to a factor of 1.8.
- These parameters feed into uncertainties in predicted rate constants for the reaction.
- Energy transfer not included in UQ analysis.

Total uncertainty assuming uncorrelated parameters is factor of ~10 at 300 K, decreasing to ~2.5 at 800 K.

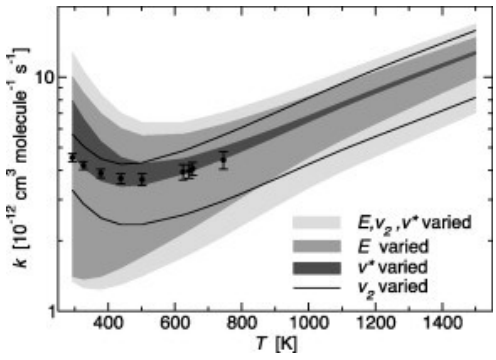

Combining theory with experiment

- Bayesian inference used to constrain input parameter distributions using available experimental data.
- Posterior distributions much more tightly constrained than those based on theory only.
- Significant correlations are seen.

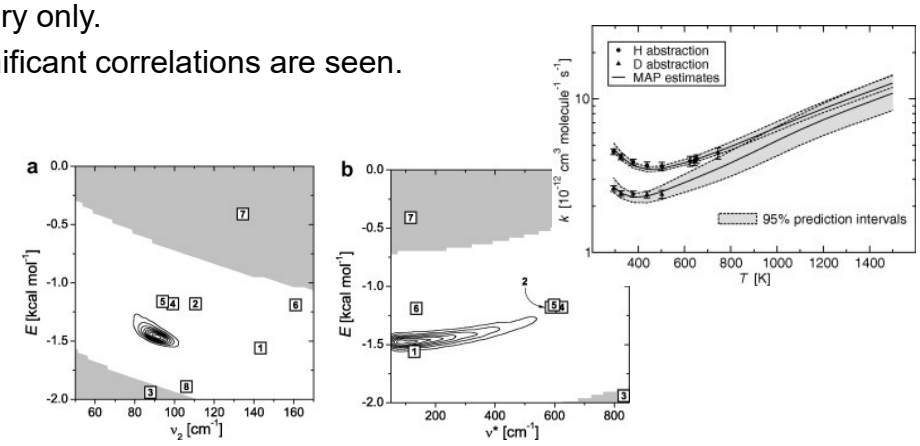

Which theory is best?

- Can we even answer this question?
- CASPT2 (multi-reference second-order perturbation theory), M062x, B3LYP (the two DFT methods), and CBS-QB3 (composite method) give energies close to the posterior estimates of *E.*
- However, B3LYP and CBS-QB3 yield values of ν_2 larger by ~50% compared to the posterior estimates.
- CASPT2 and M062x predict imaginary frequencies ν^* much higher than the posterior estimate.
- The TST calculations are however found to be consistent with the experimental data within their suggested uncertainties.

Use of MESMER to fit experimental data

- MESMER has a fitting facility that uses the Marquardt algorithm to fit to extensive sets of experimental data by **minimising χ^2.**
- The method is often **linked to electronic structure calculations of the PES**, with sensitive parameters (e.g. a transition state energy) allowed to float in the fitting process.
- Other parameters that are often fitted include those for energy transfer.
- MESMER can cope with different experiments using different bath gases.
- It is difficult to calculate association rate constants accurately (see earlier), but MESMER allows them to be fitted to experimental data using inverse Laplace transformation (ILT).

Can theory be used to optimise experimental design?

- PES parameters may be constrained further using experimental data.
- By using sensitivity analysis of the ME can we determine **which experimental conditions will best constrain inputs** such as barrier heights, frequencies etc. ??
- Shannon et al. (2015) applied this approach to the DME oxidation system. CBS-QB3 theory used within Master Equation.
- Energy transfer:

$$\langle \Delta E \rangle_{\text{down}} = \langle \Delta E \rangle_{\text{down,ref}} \left(\frac{T}{T_{\text{ref}}} \right)^{d}$$

- For barrierless association of CH_3OCH_2 with O_2, microcanonical rate coefficients calculated using inverse Laplace transform (ILT) method.

$$k_a(T) = A \left(\frac{T}{T_0} \right)^{n} \exp(-E_a/(k_B T))$$

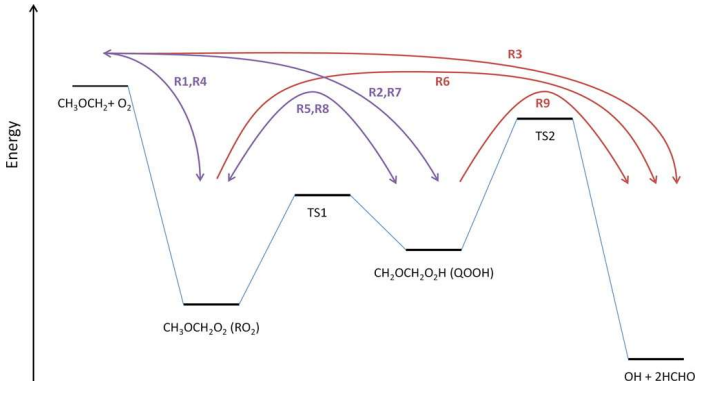

Sensitivity Analysis

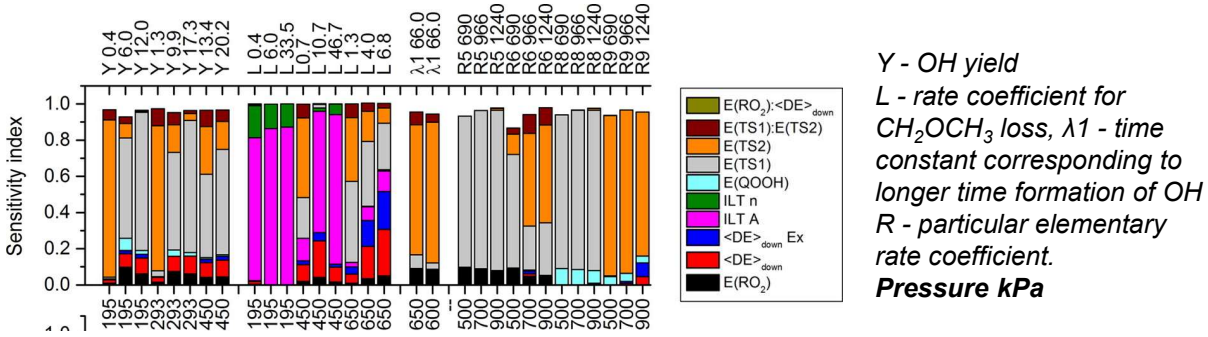

Y - OH yield
L - rate coefficient for CH_2OCH_3 loss, λ1 - time constant corresponding to longer time formation of OH
R - particular elementary rate coefficient.
Pressure kPa

- A **global sensitivity analysis** was carried out to simulate possible experimental targets.
- Helps determine **which experiments constrain which parameters**.
- Rate coefficients at combustion conditions most sensitive to barrier heights TS1,TS2.
- OH yields best constrain TS1,TS2 and even do this at low pressures where experiments are performed.

Extrapolation

- We said at the beginning that models are only useful if we can use them to **extrapolate** to conditions where we have no experimental data.
- Constraining a model across wide ranges of P,T,X_i can often not be afforded in terms of time or cost.
- **BUT** ME model inputs (e.g. barrier heights, frequencies, energy transfer parameters) are not dependent on thermodynamic conditions.
- Hence we can constrain these using combined theory/experiment and use the ME model to extrapolate to new conditions.
  - **Multi-Scale Informatics.**
  - **See earlier examples from Burke et al. and Shannon et al.**
- Watch Mike Burke's Combustion Webinar on this topic.

Final Remarks

- High level theory can increasingly play an important predictive role in determining phenomenological rate coefficients.
- Uncertainties are reducing as the level of theory possible increases with increasing CPU power. But they still remain.
- Theory allows us to understand and interpret experimental studies.
  - This interaction is key to understanding the validity of the more accessible theoretical methods.
- Theory provides a more flexible approach than experiment to determining rate data over a wide range of conditions – it is essential we understand both its strengths and its weaknesses and uncertainties involved.
- **Combined theory/experiment may help us to extrapolate**.

SECTION 3
CONSTRUCTION AND EVALUATION OF REACTION MECHANISMS

- Reaction classes and functional groups
- Automatic mechanism generation methods
- Importance of training data, particularly for new fuels.
- Use of ML.

- Low temperature chemistry and autoigntion.
- Use of ignition delay times for low temperature mechanism evaluation.

Pre-amble in the context of low carbon economies

- The kinetics of different fuels drives how they behave in different practical devices.
- Historically, the energy sector has focussed on fossil fuels which have been **designed (and legislated) to be fairly similar** in their properties.
  - When you buy diesel, gasoline, jet fuel, natural gas they do not differ widely.
- The **low carbon economy** will drive the use of alternative fuels and their blends which could be derived from a huge range of feedstocks.
  - **Different** biomass **feedstocks** – oils, tars, lignocellulosic wastes.
  - Power to liquid fuels from Fischer Tropsch processes + H_2 and captured CO_2.
- The same feed stock components can be used to produce very different fuel types.
  - Alcohols, alkanes, ethers, ammonia, sustainable jet fuels, biodiesel etc.
- If we want to understand their kinetics and that of their blends we need to quickly develop models.
- What have we learned from the fossil fuel era that can help us do this?
- How can we build relevant models quickly?

Question – how would you go about constructing a chemical mechanism for a new species that say contains C/H/O atoms? What are the main steps?

Constructing Chemical Mechanisms - Manual

- Historically mechanisms result from careful development work by experts.
- Begins with the selection of important species:
  - **reactants and products**
  - important **intermediates** necessary to predict production rates of key products or key quantities such as ignition delays, flame speeds or dynamic features such as extinction and oscillations.
- **Types of reactions** that can occur between these coupled groups of species then need to be specified along with appropriate descriptions of rate coefficients, and thermodynamic data.
- Growing expertise led to **protocols** for different types of application.
  - Indicate ***reaction classes*** for each category of important species.
- Typically, certain reaction classes ignored if
  - rates **very slow** compared to overall time-scales of interest,
  - they are **too endothermic or too complex** (e.g. too many bonds are broken or products produced (Yoneda, 1979; Németh et al., 2002)),
  - pathways to **minor products** also often ignored (Saunders et al., 2003a).

The concept of reaction classes

(Blurock, Battin-LeClerc, 2013)

- Developing detailed combustion mechanisms for oxidation of fuels/atmospheric species with a large number of C atoms presents challenges in mechanism production philosophy.
  - Not possible to source parameters exclusively from experiments/detailed theory.
  - Estimates of reaction rate constants/thermo must come from physical/chemical principles based on fundamental kinetic studies for a smaller number of fuels.
- One way of encompassing general principles into specific reactive properties is to define ***reaction classes***.
- ***Reaction classes*** - kinetic generalisations that systematically embody analogies and physical principles a modeller uses to estimate rate constants where no specific evidence exists.
- Based on a local set of **functional features around the reactive centre of molecules** that are significant when determining numeric value of rate constant.
- Used in both ***automatic*** and ***manual generation*** of reaction mechanisms e.g. n-hexadecane mechanism of Westbrook et al. (2009).

How to define reaction classes

- A reaction class has three sets of information:
  1. A **pattern or rule** to recognise within the chemical reactants (can be more than one) when the reaction class should be applied.
  2. A **transformation** of how the specific reactants are converted to products.
  3. The **rate coefficients** associated with the transformation.
- Generally built from years of chemical experience and intuition.
- May also be suggested by automatic computer codes designed to explore chemical pathways automatically for reactions that are relevant in gas phase chemical problems e.g. KinBot (Zador & Van De Vijver https://www.osti.gov/biblio/1464498-kinbot).
  - KinBot uses a chemical network approach coupled with knowledge of the **potential energy surface** determined for the particular system.

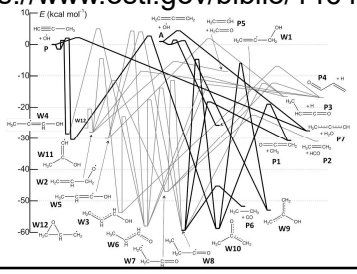

Examples of high temperature reaction classes

(Sarathy et al., 2011, Curran et al., 1998)

1. Unimolecular fuel decomposition
2. H-atom abstraction from the fuel
3. Alkyl radical decomposition
4. Alkyl radical isomerization
5. H-atom abstraction reactions from alkenes
6. Addition of radical species O and OH to alkenes
7. Reactions of alkenyl radicals with HO_2, CH_3O_2, and $C_2H_5O_2$
8. Alkenyl radical decomposition
9. Alkene decomposition
10. Retroene decomposition reactions

Fuel molecule breaks apart

Something pulls off a H atom leaving alkyl radical

Alkyl radical either breaks apart or internally reorganises to new structure etc. etc.

Examples of Low Temperature Reaction Classes

(e.g. RH any general alkane, Sarathy et al. 2011)

11. **Addition of O_2 to alkyl radicals (R + O_2 = ROO)**
12. R + ROO = RO + RO
13. R + HO_2 = RO + OH
14. R + CH_3OO = RO + CH_3O
15. **Alkyl peroxy radical isomerization (ROO = QOOH)**
16. Concerted eliminations (ROO = alkene + HO_2)
17. ROO + HO_2 = ROOH + O_2
18. ROO + H_2O_2 = ROOH + HO_2
19. ROO + CH_3O_2 = RO + CH_3O + O_2
20. ROO + ROO = RO + RO + O_2
21. ROOH = RO + OH
22. RO decomposition.
23. QOOH = cyclic ether + OH (cyclic ether formation)
24. QOOH = alkene + HO_2 (radical site beta to OOH group)
25. QOOH = alkene + carbonyl + OH (radical site gamma to OOH group)
26. **Addition of O_2 to QOOH (QOOH + O_2 = OOQOOH)**
27. **Isomerization of OOQOOH and formation of ketohydroperoxide and OH**
28. **Decomposition of ketohydroperoxide to form oxygenated radical species and OH**
29. Cyclic ether reactions with OH and HO_2
30. Decomposition of large carbonyl species and carbonyl radicals

Typical low temperature chain branching route for alkanes

Rate constants and functional groups

- Every chemical environment, meaning an atom and its bonding, has an effect on the neighbouring atoms and bonds.
- For example, a radical on a carbon atom is more energetically stable on a **tertiary** carbon atom than on a **primary** carbon atom which has the consequence that a **tertiary** hydrogen atom is more easily extracted from the carbon atom.

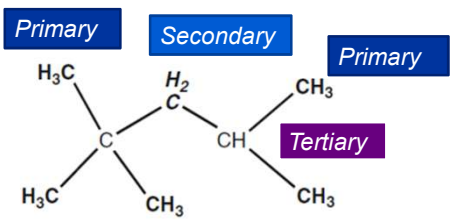

- Mechanisms for larger fuels can be built using this **concept of reaction classes** and populated by data based partly on experimental measurements or detailed theory calculations and partly on **extrapolations** of this data to larger and larger molecules using the concept of **functional groups**.

Use of functional groups: example of hydrogen atom abstraction from the fuel

Table 2.1 Rate constants for alkylic hydrogen atom abstractions, expressed in the form $k = A\ T^b \exp(-E/RT)$, with the units cm^3, mol, s, kcal, by hydrogen atoms which can be abstracted (Buda et al. 2005)

H-abstraction	Primary H			Secondary H			Tertiary H		
by	lg A	b	E	lg A	b	E	lg A	b	E
O_2	12.84	0	ΔHr	12.84	0	ΔHr	12.84	0	ΔHr
·H	6.98	2	7700	6.65	2	5000	6.62	2	2400
·OH	5.95	2	450	6.11	2	−770	6.06	2	−1870
$\cdot CH_3$	−1	4	8200	11.0	0	9600	11.00	0	7900
$HO_2\cdot$	11.30	0	17000	11.30	0	15500	12.00	0	14000

The structure of reaction mechanisms

- Reaction classes can vary with temperature and hence size of required mechanism can be reduced by, e.g., restricting to low *T* classes (e.g. ignition problems), or high *T* mechanisms (e.g. flame propagation).
- Additional classification of sub-mechanisms can be based on:
- ***Hierarchical sub-mechanisms*** based on size of reactants: within a given sub-mechanism, only species of a given size are consumed. Smaller products (produced but not consumed within this sub-mechanism) are consumed by sub-mechanisms 'lower' in the hierarchy.
- **Primary**, ***secondary***, and ***base*** mechanisms: special case of hierarchical structure.
  - The **primary mechanism** - reactions of initial reactants and directly derived radicals.
  - The **secondary mechanism** – consumes products of primary mechanism. It would be possible to define iteratively tertiary and even n-ary mechanisms, but in practice in most combustion models, secondary mechanisms are designed to lead to intermediate species, which are finally consumed in a **base mechanism**.
- **Pathways**: A chain of reactions or reaction classes. The remaining species at the end of this chain should be consumed by other sub-mechanisms.

Hierarchical development of mechanisms

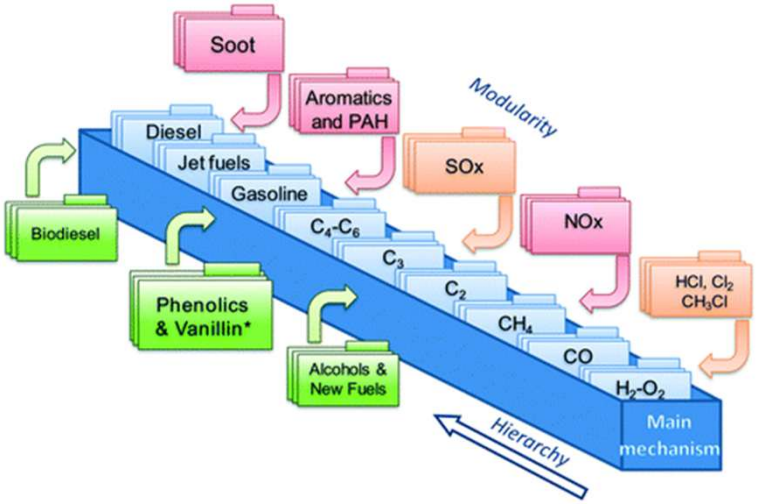

Pelucchi , 2019

The base mechanism

- Usually, a well-validated detailed mechanism of smaller species (e.g. up to C2-C4), which includes reactions taken from databases.
- Has usually been validated under the conditions being considered.
- **Estimated rate constants are not usually used** within base mechanisms, rather data is obtained from ***measurements***, ***theory calcs***, ***evaluations*** or even from ***optimised mechanisms***.
- Likely to be known with **lower uncertainty** than the reaction pathways for the larger hydrocarbons.
- Needs to be updated frequently but often in larger mechanisms "legacy" mechanisms may still be present.
- Care needs to be taken when updating base mechanisms within larger schemes since other reaction steps may have been "tuned" based on the existing base scheme.
- Example:
  - Aramco mechanism (2.0 http://www.nuigalway.ie/c3/aramco2/frontmatter.html)

AramcoMech2.0

- A C1-C4 mechanism that has been developed in a hierarchical way 'from the bottom up'
  - starting with a H_2/O_2 sub-mechanism,
  - followed by a C1 sub-mechanism
  - grown to include larger carbon species such as ethane, ethylene, acetylene, allene, propyne, propene, n-butane, isobutane, isobutene, 1-butene and 2-butene, and oxygenated species including formaldehyde, acetaldehyde, methanol, ethanol, and dimethyl ether.
- Has been **validated against a large array of experimental** measurements including data from shock tubes, rapid compression machines, flames, jet-stirred and plug-flow reactors.

Theoretically Informed Kinetics (ThInK, Klippenstein et al., 2025))

- Small molecule combustion chemistry (H_2 and C_1 – C_3 species) based on the extensive use of theoretical predictions for reaction rate coefficients, thermochemistry, and transport parameters.
- Claim is that for small molecules, theory can now achieve same accuracy as experiments
- Hence it is possible to build a mechanism from theory that is almost entirely **predictive**.
- Means that no parameters are tuned for selected sets of experiments and the model should be **extrapolatable** to any conditions and to coupling with schemes for larger molecules.

✓ Includes detailed table of level of theory used for each reaction.
✓ Comparison of data with other models in the literature.
✓ Extensive validation data set.
✓ Mechanism, thermo and transport parameters

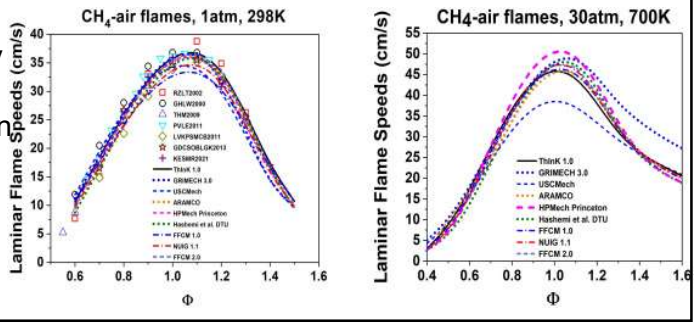

Primary and secondary mechanisms

- **Primary mechanism** represents reactions of the primary fuels and their derived radicals.
  - Usually kept in detail.
- **Secondary mechanism** consumes the products of the primary mechanism forming smaller species.
- In secondary mechanisms often simplifications are made even at the generation stage to keep the number of reactions as low as possible:
  - **Vertical reaction lumping** is applied so that reactants go directly to smaller products via one reaction step without passing through intermediates (*see later for methodology*).
  - **Species lumping** where parallel pathways of similar isomers are grouped (*see later*).
  - Reaction classes of **low importance** can be removed.

Automatic Reaction Generation Methods

- Several reasons why this is important for mechanisms describing the oxidation of larger and more complex fuels:
  - simply too large a task for a single human
  - humans make mistakes
  - the production of larger mechanisms has to be careful and systematic to generate what could be mechanisms with thousands of species and reactions
  - data for individual reactions is unlikely to be obtained from experiment/evaluation. Estimations based on Reaction Class rules will be required.

- **Why not use the help of a computer informed by decades of human knowledge?**

Principles of Automatic Generators

- Expert systems using a database of chemical principles to systematically and efficiently produce large detailed mechanisms (Blurock et al., 2013, Cleaner Combustion, p59-92).
- The developer or modeller determines which sub-mechanisms and reaction classes should be generated.
- Therefore **expert system** based on **similar rules and reaction classes** discussed earlier but these are now encoded rather than applied by hand.
- Reduces errors and apply rules in a systematic way.
- If rate constants are changed for a whole class then should be easier to regenerate the mechanism.
  - EXGAS – Developed at CNRS Nancy (Côme et al., 1996).
  - RMG – Developed at MIT (Green et al., 2001; Van Geem et al., 2006).
  - REACTION – Developed by Ned Blurock (Blurock,1995; Moreac et al., 2006).
  - MAMOX++ – Developed by Milan (Ranzi et al., 1995).

Mechanism Truncation Error: Which reactions must be included in the model?

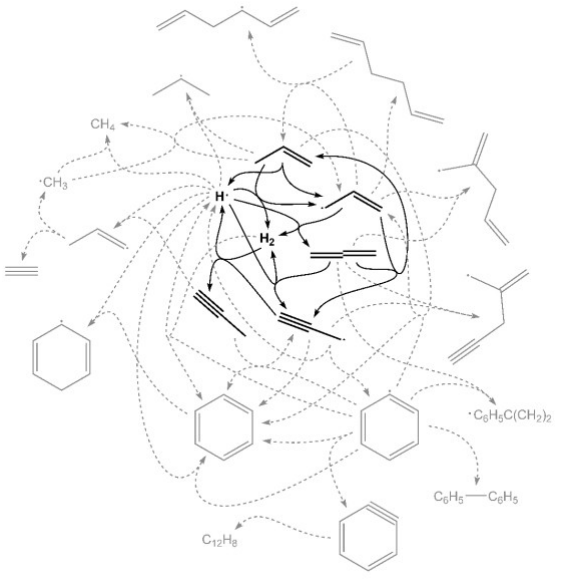

- Often too many species & reactions to include them all in final model, or even to compute all their rate & thermo parameters using high-accuracy methods.
- So need to use **lower-accuracy estimation methods** to make initial decisions about which species/reactions need high accuracy numbers.
- Need to include **the important ones**, can neglect the rest.
- "Important" depends on reaction conditions, the observables you care about, and your error tolerance.

Different AMG codes and specificities

- **MAMOX ++**
  - Produces hierarchy of (highly) **lumped mechan**isms derived numerically from automatically generated detailed mechanisms.
- **EXGAS**
  - Has comprehensive reaction class database and large choice given to user for **mechanism tailoring**: e.g. low *T* vs high *T*, degree of lumping used etc.
- **RMG**
  - Uses a "**generate and test**" algorithm which generates a fundamental mechanistic step, estimates rate constants and then uses an "on-the-fly" reduction processes to determine whether the reaction should be included in the final mechanism.
  - Publicly distributed automatic generator of pressure-dependent reaction networks.
- **REACTION**
  - Uses concept of Reaction Pathways rather than exhaustive list of Reaction Classes.
  - Fundamental chemical information solely based on external databases so that it can be updated without modifying or recompiling the software.

Particular Challenges Posed by Biofuels

- **AMG codes initially developed for alkanes.**
- Wide range of biofuels now being used for applications in vehicles e.g. as additives or in blends with gasoline and diesel.
- Most common examples include:
  - Alcohols e.g. ethanol, butanol isomers, methanol
  - Methyl Esters e.g. in biodiesel, furans, etc.
- **Molecules contain oxygen** and have **different functional groups and bond energies** compared to e.g. alkanes.
- Modifications need to be made in terms of
  - Reaction classes
  - Relevant rate data for existing classes compared to alkanes, alkenes
  - Species present, groups included for group additivity calculations.
- The existence of measured data for the reactions of such compounds is pretty SCARCE!

Bond energies for alcohols (Pelucchi, 2020)

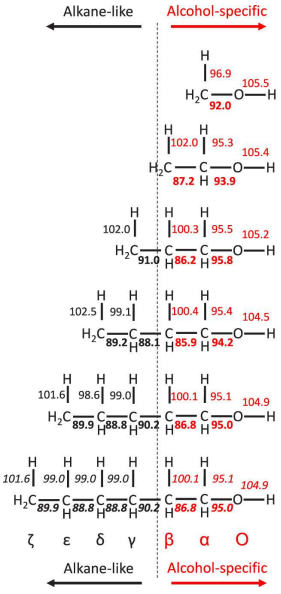

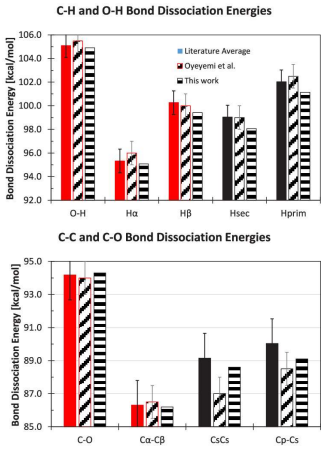

- Derived from theory and ATChTs.
- Will affect H abstraction rates at different *T*s, and therefore low *T* pathways.

Example of H abstraction Reactions

- We saw for alkanes that H abstraction rates were determined based on whether the H was attached to a primary, secondary or tertiary carbon atom.
- For oxygenated species there are more types of H atom.

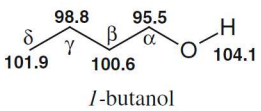

1-butanol

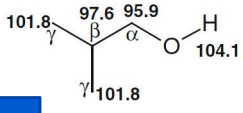

iso-butanol

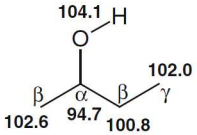

2-butanol

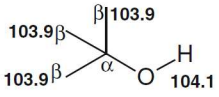

tert-butanol

C-H bond energies for butanol isomers

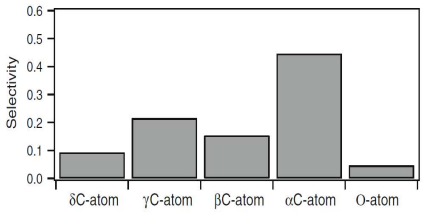

Selectivities for abstraction by OH (Frassoldati et al., 2012)

RMG Case Study: Advanced Oxygenated Biofuels

Christian Michelbach (2024a,b)

- We want to predict the combustion behaviour of advanced biofuel blends composed of ethyl levulinate, ethanol, and diethyl ether.
  - There is an interest in such fuels for use in SI and CI engines as they can be made from lignocellulosic biomass (2nd gen).
  - This requires predictions that cover a wide range of temperature, pressure, stoichiometry, and fuel blending conditions.

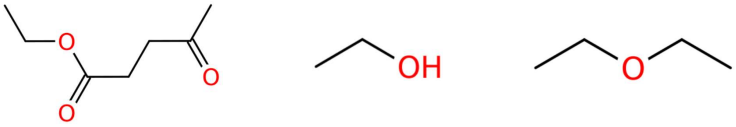

- Using RMG, can we produce a detailed kinetic mechanism that suits our needs?
- Can we then extend the methodology to a butanolic version where less data is available?

RMG Case Study: Seeding

- Building RMG models is an iterative process. Requires user to analyse produced model, making incremental improvements with each step.
- An initial model generated, using only RMG database reaction families and training reactions.
  - Model clearly insufficient, as shown by the IDTs of diethyl ether.
  - Holes in the current kinetic database for oxygenated species.
- Introducing seed mechanism provides key reaction steps (e.g. initiation and chain branching).
  - RMG typically good at filling in remaining propagation and termination steps.
  - Including a diethyl ether sub-mechanism (Tran et al., 2019) greatly improves IDT predictions.
  - Still room for improvement.

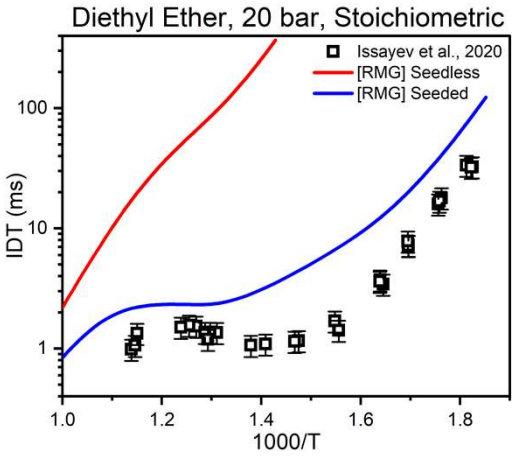

RMG Case Study: Kinetic Database

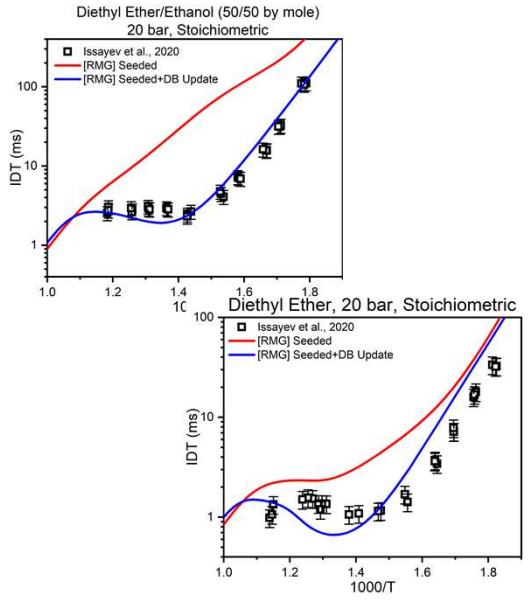

- Prediction of component IDTs has improved, but what about blends?
- Even with kinetic and thermodynamic seeding for diethyl ether and ethanol, the prediction of blended IDTs is poor.
- RMG database is largely lacking training reactions and groups specific to oxygenated species.
  - Alcohols are reasonably covered.
  - Ethers, esters, and ketones need database updates for many reaction families (i.e. H abstraction, intra H migration, cyclic ether formation, radical recombination).
  - Rate constants can be sourced from literature – be sure to consider uncertainty when adding data.
- After making database updates for oxygenated species, predictions are improved significantly.

RMG Case Study: Database Updates

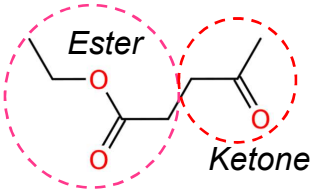

- For database training, ethyl levulinate can be split into a ketone and ester functional group.
- We can use literature to find appropriate training data for these groups.
- As an example reaction, consider hydrogen abstraction by a H radical, to form H_2 and EL3J.

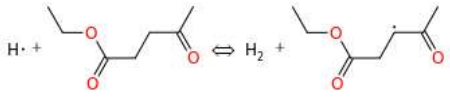

- Methylethyl ketone (MEK) can represent ketone group.
  - Thion (2017) calculated H abstraction rates for MEK at G3//MP2/aug-cc-pVDZ level of theory.
  - In RMG, create a library of new training reactions. Then use the 'kinetics_library_to_training.ipynb' tool.
- May need to add new group structures to RMG.
  - Done 'by-hand', using adjacency list format.
  - Prevents ambiguous group definition and incorrect training reaction selection during reaction generation.
  - High potential for human error. Needs care.

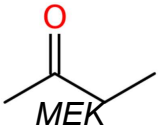

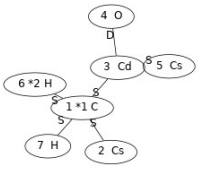

Group Drawing (RMG)

```
entry(
    index = 537,
    label = "C/H2/Cs/Cd\Od\Cs",
    group =
"""
1 *1 C   u0 {2,S} {3,S} {6,S} {7,S}
2    Cs  u0 {1,S}
3    Cd  u0 {1,S} {4,D} {5,S}
4    O   u0 {3,D}
5    Cs  u0 {3,S}
6 *2 H   u0 {1,S}
7    H   u0 {1,S}
""",
```

Group Definition

RMG Case Study: Final Model

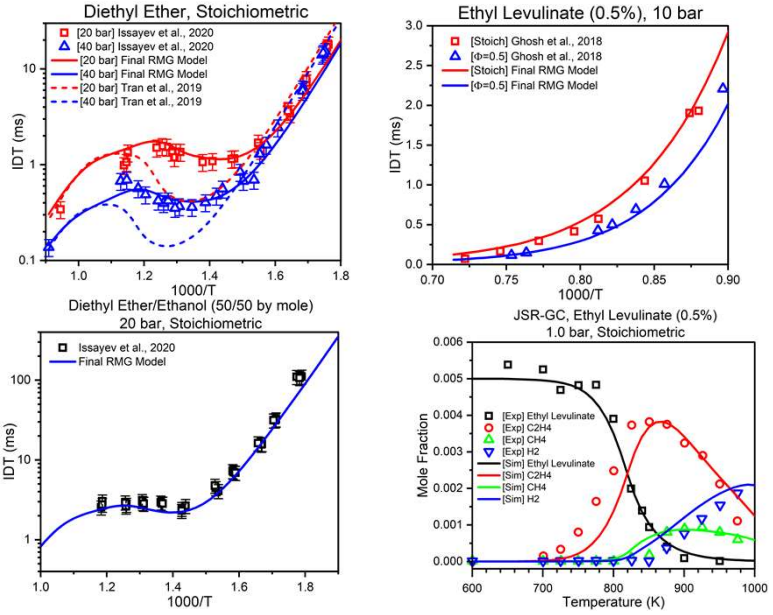

- Using the outlined process, we can produce a final model that performs extremely well for complex fuels.
- Model can be extrapolated beyond regime of original seed mechanisms, outperforming them.

What we learned…

- Robust and accurate mechanism generation can contain some automisation but also requires careful human interaction.
- A reasonable **seed mechanism** was required.
  - Composed using human expertise – particularly when new reaction classes are needed.
- **New groups/training** data were required – we need an automatic way to pull this in. LLMs?
- Physical reality checks were needed outside the developed region of the seed mechanisms.
  - Many violations of **collision limits** found.
- **Sensitivity analysis** and rate constant updates (based on **high level theory**) were needed to get final good accuracy.
- **Validation data** is sparser than we would like – particularly for mixtures.

Other approaches: HyChem

- HyChem separates fuel combustion into two parts:
  - Fuel-specific chemistry that breaks the fuel into small fragments
  - Universal small-molecule chemistry that is already well known
- A physically motivated hybrid approach with detailed data rather than a reduced mechanism or a ML/AMG type approach.
- Mainly for application to high temperature systems where fuel decomposition dominates but recent developments for LT chemistry (Choudhary et al., 2025).
- Avoids explicitly modelling thousands of uncertain reactions for large fuels.

1. Fuel decomposition (fuel-specific part) - small number of reactions
   a. Describes how the fuel initially breaks into: C_2–C_4 hydrocarbons radicals like CH_3, C_2H_3, C_2H_5
   b. Rates are derived from: quantum chemistry, RRKM theory, experiments.
2. Uses well validated core C1-C4 hydrocarbon chemistry + NOx reactions.

- Recently coupled with constraints from FTIR measurements for SAF combustion predictions (Biswas et al., 2025).

Use of Machine Learning in automated mechanism generation

- For almost all complex fuels (beyond C4 say) the rate constants (and in some cases equilibrium constants) used for elementary reactions describing their oxidation are **based on estimates**.
- Detailed data for smaller molecules can be used to estimate rates for larger molecules with similar chemical structures e.g. in RMG.
- However, data is often sparse and potentially a **mixture of experimental and ab initio/theory computations.**
- Machine-learned models trained on large datasets can improve accuracy of estimates, allowing better integration of quantum chemistry and experimental data (Green, 2024).
- Challenges – newer fuels (potentially oxygenated) that have more complex structures and for which **available training data is sparse**.
- Care needed in application of ML – we can't just throw all available data to a neural network (NN) and expect the best fits. **Improved estimates gained from utilizing information on chemical structure and reaction classes that are used in traditional estimation methods.**

Use of Deep Learning Methods for rate coefficient prediction across reaction classes

- Li et al. (2024) use a ML method to predict rate constants for various reactions in combustion kinetic models.
- Use a **generalised deep learning method** which operates **across reaction classes** – using natural language processing (NLP) methods to infer reaction classes using only the text-based information of reactions (simplified molecular-input line-entry system, SMILES).
- Training data mostly based on high-level quantum chemistry calculations for 9 reaction classes across 8 fuels – 242 reactions.
- Reaction fingerprints serve as inputs of deep neural network (DNN) models to predict modified Arrhenius parameters ln A, n, and E_a.

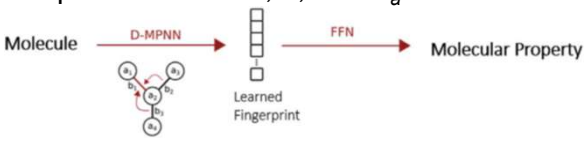

- Of course the inputs from theory contain uncertainties – but in this work they are assumed to be zero, although the impact of this assumption is tested.

233

Reaction Classes

- Reaction classes are typical of those found in complex fuel oxidation mechanisms.
- See earlier Low T reaction classes.

Table 1
Reaction classes considered in the dataset.

No.	Reaction class	Number of reactions
1	Unimolecular decomposition, RH=R'+R"	13
2	H-atom abstraction, RH+X = R+HX	103
3	Fuel radical decomposition	18
4	1st O_2 addition, R + O_2=RO_2	10
5	RO_2 isomerization, RO_2=QOOH	34
6	QOOH=Cyclic ether + OH	22
7	QOOH decomposition (β-scission)	19
8	2nd O_2 addition, QOOH+O_2=O_2QOOH	9
9	O_2QOOH = ketohydroperoxide + OH	14

234

Approach

- Using this general approach and reaction fingerprints carries the risk of **overfitting** because the dimensionality of the input features is comparable to the size of the dataset.
- Hence mitigating overfitting during the model training phase is an important part of the methodology using a drop-out method.
- An automatic method (OPtuna) is used to optimize the hyper-parameters of the NN:
  - the number of hidden layers,
  - the number of neurons per layer,
  - learning rate, batch size,
  - drop out ratio,
  - weight decay in the optimizer.
- Reaction classes were almost always successfully identified from fingerprint data.

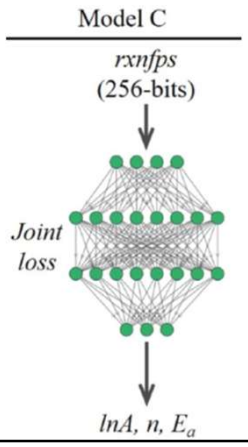

235

Uncertainties in predictions

- The uncertainty factor for most reactions (about 70%) is less than 4, roughly comparable with uncertainties of high-level calculations.
- Uncertainty factors for some reactions (about 18 %) are 4 – 10. Small number of predicted rate constants with uncertainty factors above one order of magnitude, mostly from the complex low-temperature reaction classes – likely due to sparsity of training data.

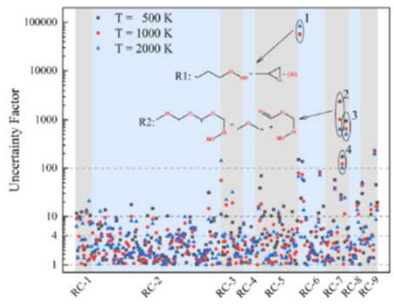

Fig. 10. Uncertainty factor of rate constants predicted by model C. Horizontal coordinates are reactions sorted by reaction class.

Table 6
RMSE of predicted rate constants by Model C and rate rules/group additivity estimations in RMG [78].

DMM:	ln A	n	Ea	ln k
RMG_RateRules	11.63	1.38	6694	4.86
RMG_GroupAdditivity	16.28	2.02	11,971	6.20
This work	6.51	0.89	2597	1.75
Propane:				
RMG_RateRules	15.25	2.16	4462	2.92
RMG_GroupAdditivity	15.96	2.32	9772	5.18
This work	11.68	1.58	4356	2.69

Better than traditional rate rules approach

236

What is this approach lacking?

- It is dependent on the reaction classes being successfully identified – but the list of included classes is predetermined.
- It is not actually building a mechanism from scratch and so is not an automated reaction generator.
- The uncertainties remain high for systems with sparse training data sets.
- **How can machine learning (ML) be used to generate reaction mechanisms and populate their required data even for systems where data is sparse?**

What do we need to build a mechanism for a particular process? (Johnson and Green, 2024)

- A systematic method both to propose candidate reactions and species, and to decide which are actually important.
  - Build new reaction classes by systematically generating all possible reactions from important species, then numerically test and prune reactions calculated to be too slow to be important based on **selected error tolerance**.
  - Requires calculations (or estimations) for large numbers of reaction rates. Number of reactions can build quickly. Also, some slow reactions may lead to important intermediates and be missed with the wrong tolerances.
  - Sometimes there are so many possible isomers that it is difficult for a human to correctly enumerate them all. **KinBot** attempts to overcome this, but still challenging to solve numerical eqs resulting from complex systems with thousands of species.
  - Currently not possible to compute accurate rates for all possible reactions in a system using higher level quantum methods. So even in order to build a mechanism we rely on accurate estimates.

Problems with sparse data

- Traditional approaches are based on identifying functional groups within molecule, or bond changes, and then using simple (e.g. least squares regression) fits to data from smaller molecules.

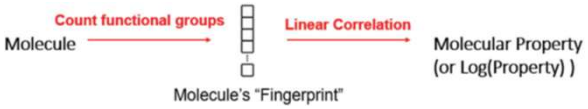

- For example, one entry in the fingerprint could be the number of a certain functional group in the molecule.
- Methods such as Li et al. and Chemprop use machine learning to improve estimates over simple regression approaches.
- However, problems where data sets are sparse and the newer the system of interest, the sparser the data sets will be.
- Often in kinetics, the data available is very "clumpy", with many data for certain types of molecule or reactions, and zero data on some other types of molecules or reactions (e.g. new systems or fuels).

239

Using tree structures

- Typical successful applications of NNs for predicting rate constants can be based on datasets containing more than 10,000 reactions.
- Typical reaction families in AMG codes such as RMG have to be estimated based on data from fewer than 20 reactions.
- According to Johnson and Green (2024) the best way to use such sparse training data is to incorporate ML within a similar tree structure to that used for developing RRs e.g. as used in RMG.
- Have developed an approach based on the use of decision trees.

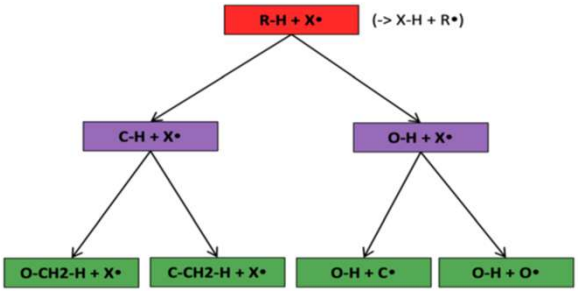

Example of a subgraph isomorphic reaction template decision tree.

What are decision trees?

- Decision trees are classifiers that start with an item at a single root node with no parents.
- At each node the item is checked against each descendant "child" node and moves to the first child node that it matches and so on until it reaches a node where it doesn't match any children.
- That final node becomes its classification.
- In this context the items are **reactions, i.e. molecular graphs of reactant(s) and product(s) with atom mapping** with matching done by subgraph isomorphism checks.
- **Automation:**
  - iterate starting from a single root node adding the new node that best optimizes the tree each iteration
  - end tree generation process when some termination criterion related to the number of tree nodes or tree depth is satisfied
  - new nodes are added that best divide those reactions into groups with similar rate estimates.

241

The mechanism building process

- Extension chosen that minimizes $\Pi = N_1\sigma_1 + N_2\sigma_2$ where N_i is the number of reactions in partition i and σ_i is the standard deviation in log(k(1000 K)) within partition i.
- I.e. choose the extension that clusters reactions with similar rates into the same partitions at chosen T of 1000 K where the training data is expected to be the most accurate.

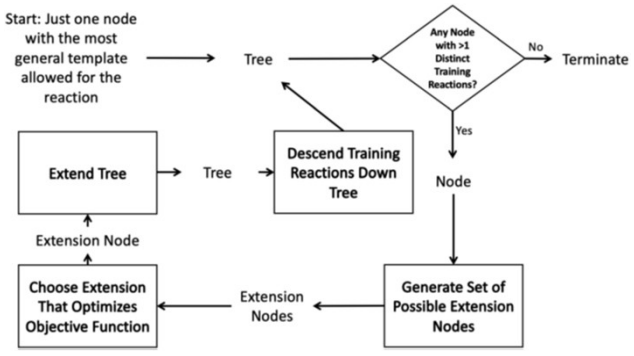

242

- A rule is defined at each node. All training reactions matching a given node (top node has all reactions) are fitted to a to estimate Arrhenius parameters essentially using a least squares method.
- Uncertainties for input reactions (e.g. from kinetics experiments, theory, optimization studies incorporating bulk experimental data), the interpolant, and for *k(T)* estimates for a new reactions where no data is available. Challenging!

- Normal distribution for $\Delta\log(k_i) \sim N(\log(k_{\text{best fit},i}) - \log(k_{\text{true},i}), \sigma^2_{\text{rxn,i}} + \sigma^2_{\text{model,i}})$

- i.e. uncertainties are due to limitations in the model's ability to represent the chemical space and the errors in the training data.
- **Estimation of uncertainties allows the appropriate node to be selected for rate constant estimation.**
- **At nodes near top** of tree - many reactions providing accurate calculations, but chemical space spanned can be quite large making it difficult for a single model fit to represent all involved reactions.
- **At nodes near bottom** of tree - chemical space spanned is much smaller and the model can better represent the space, but there are fewer reactions, making the fit more sensitive to errors in the training data.

Testing against RRs

- Method has been tested for several commonly used reaction families where Rate Rules have previously been applied and outperforms RR methods.

Table 1 Comparison of accuracy of RMG rate rules (RR) and the subgraph isomorphic decision tree (SIDT) estimator for three different RMG families oxygen substitution (O-Sub), intra-molecular hydrogen transfer (intra-H), internal endocyclic radical addition (Int-Endo) and radical addition (R-Add)

Estimator	O-Sub RR	O-Sub SIDT	Intra-H RR	Intra-H SIDT	Int-Endo RR	Int-Endo SIDT	R-Add RR	R-Add SIDT	H-Abs RR	H-Abs SIDT
Median absolute error factor	10.3	5.28	8.94	3.56	9.67	1.73	2.25	1.88	5.11	4.05
MAE factor	18.5	10.1	38.1	10.9	24.7	2.95	3.07	2.34	16.4	8.02
RMSE factor	61.7	27.6	575	79.3	98.3	7.07	5.59	3.51	89.7	23.7
2-Sigma error factor	3876	770	333 000	6320	9710	50.1	31.3	12.3	8040	564

244

Final remarks

- There is definitely significant scope for ML methods to assist in building mechanisms for new fuels and processes.
- **BUT!**
- The success of such methods depends on
  - The **available training data**, its quality and how well it covers the space of interest.
  - Training data from both quantum and experimental methods is needed.
  - Effective **data sharing and curation** will be important. Not an easy and an often thankless task.
  - The use of ML methods which maximise the value in this training data, including in cases where it can be sparse.
- This means using approaches that effectively partition the data to give optimal error minimisation.
- Finally (**at the risk of sounding like a broken record**) we need to track uncertainties, and consistently!

245

Model validation using fundamental experiments: Low temperature chemistry and ignition

Fundamental experiments and simulations

- Ultimately, we are working towards applying chemical kinetics models in the design of efficient, low pollution, practical combustors:
  - **Engines**
  - **Gas turbines**
  - **Boilers, fires, furnaces.**
- Validating models in such reactors is however, tricky, as chemistry is coupled to complex, often 3D flows.
  - ***Too many sources of uncertainty, how to identify the main ones?***
- Hence, we use more simple reactors to **limit flow complexity** to:
  1. Learn about fundamental combustion properties e.g. ignition delay times, laminar burning velocities, flame temperatures, species profiles.
  2. Provide data for validation/evaluation of certain aspects of the models e.g. chemical source terms, by isolating these processes.

Combustion Chemistry Varies Dramatically at Different Reaction Conditions!

- Consider a fuel+air mixture – at room temperature the mixture is stable, negligible reactions.
- But if you add a spark, many reactions happen quickly: explosion!
- If temperature is maintained low enough: aldehydes and peroxides are formed.
- At higher T & moderately rich: reactions form syngas (H_2+CO) – A little bit richer: reactions form acetylene, benzene, and soot.
- NOx chemistry also depends on temperature.

So: if a mechanism is to be general enough for device design over varying conditions we need to validate across all these regimes.

Starting with low temperature - what is auto-ignition and what causes it?

- Combustion chemistry driven by chain reactions of reactive radicals.
- Progress of combustion depends on the balance of chain-branching and chain-terminating reactions.
- Auto-ignition, **the spontaneous ignition of a fuel-air mixture**, occurs when initially slow thermal reactions have a large enough chain-branching component to sustain and accelerate oxidation.
- Increasing radical concentrations and reaction rate build on themselves and eventually lead to a rapid **explosive rise in radical concentration**, oxidation rate, **and temperature** – ignition!
- Reactions typically release heat, increasing temperature of system, and at same time their rate is strongly dependent on temperature and pressure.

Example - auto-ignition of H_2/O_2 mixtures

Initiation reactions (generation of first radicals)

	$\Delta H_{J\ (kcal)}$	
$H_2 + M \rightarrow H + H + M$	106	*Require lots of heat*
$H_2 + O_2 \rightarrow HO_2 + H$	109	
Chain branching (1 radical makes 2 radicals)		
$H + O_2 \rightarrow OH + O$	16	*Require small heat input*
$O + H_2 \rightarrow OH + H$	2	
Chain propagation (conversion between radicals)		
$OH + H_2 \rightarrow H_2O + H$	-15	*Produce heat*
$H + O_2 (+ M) \rightarrow HO_2 (+ M)$	-24	
Termination (radicals are lost to form stable species)		
$O + O + M \rightarrow O_2 + M$	-59	*Produce heat*
$OH + H + M \rightarrow H_2O + M$	-58	
$H, HO_2, O, OH \rightarrow$ *wall*		

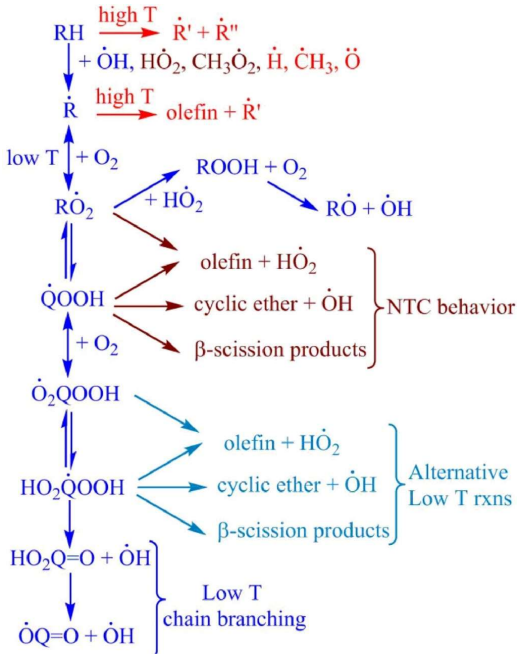

General scheme for fuel oxidation (Curran, 2019)

Competition between pathways depends on stoichiometry, T, P

The Auto-ignition Temperature (AIT)

- The auto-ignition temperature is defined as:
  - the lowest temperature that a substance needs to be at to sustain combustion without the application of an ignition source.

Fuel	AIT °C	Flash point °C
Diesel	200	70
Hexane	233	-22
Kerosene JA1	250	37
Petrol/gasoline	450	-20
Acetone	535	-18

- Note that there is no link between the auto-ignition temperature and the flash point.
- The **flash point** of a volatile material is the lowest temperature at which it can vaporise to form an ignitable mixture in air.

AIT of Paraffin hydrocarbons at atmospheric pressure

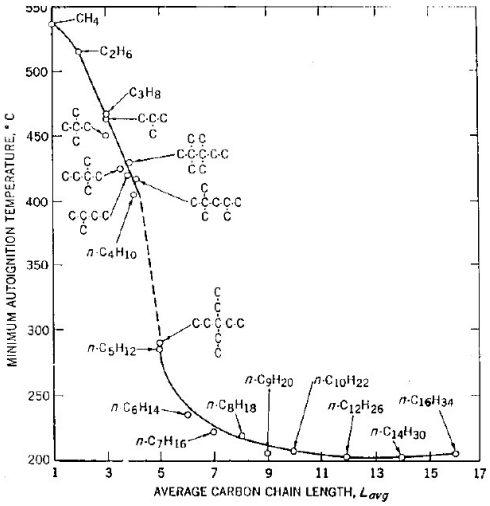

Both pressure and stoichiometry would also affect AITs.

For many of the heavier liquid hydrocarbons the auto-ignition temperature is close to 200°C

Ignition delay times

- As well as explosion characteristics we may also study the ignition delay of fuel/air/O_2 mixtures at different *T,P*.
- Tells us about reactivity and the ability of a fuel to auto-ignite e.g. under compression within a piston.

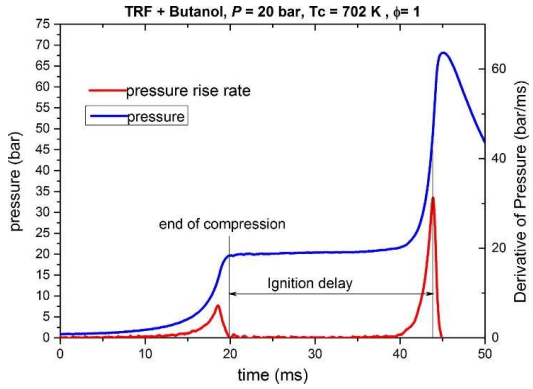

Example from single piston rapid compression machine
(*Agbro et al., 2017*)

Ignition regimes for hydrocarbons

Model predicted ignition delay times for n-pentane oxidation in 'air' at 20 atm

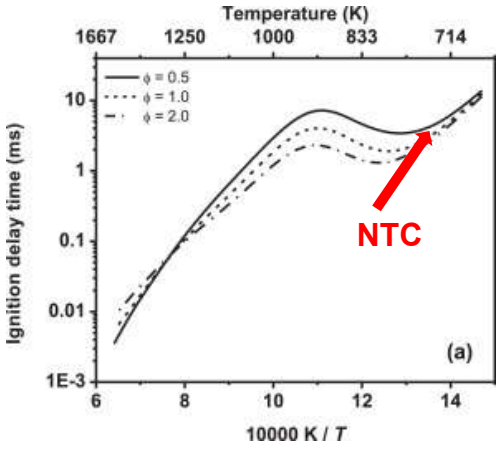

Bugler et al., 2016

Data shows three distinct temperature ranges of reactivity:

- low (600–750 K)
- intermediate (900–1250 K)
- high temperatures (>1300 K).

Both low and intemediate temperatures are included in the **negative temperature coefficient (NTC)** regime where ignition delays increase with increasing *T*.

Non- Arrhenius behaviour.

Do all fuels show an NTC?

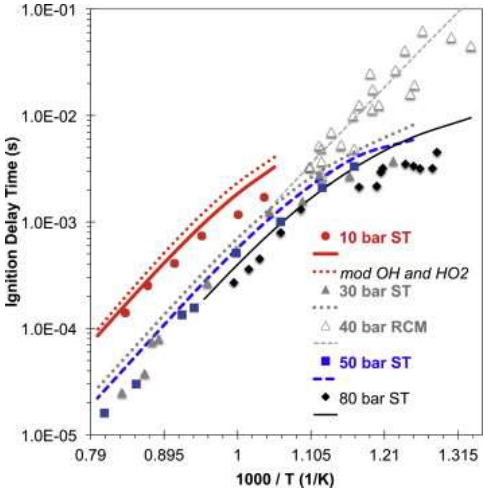

No, for example several of the smaller (lower C numbers) alcohol type fuels exhibit more Arrhenius type behaviour where log(ignition delays are closer to linear with respect to 1/T.

As the chain length gets longer the alcohols behave more like alkanes (Sarathy et al., 2014).

Ignition delay times of ***ethanol/air mixtures*** at stoichiometric conditions (Sarathy et al., 2014)

Competition between branching and termination for generic alkane RH

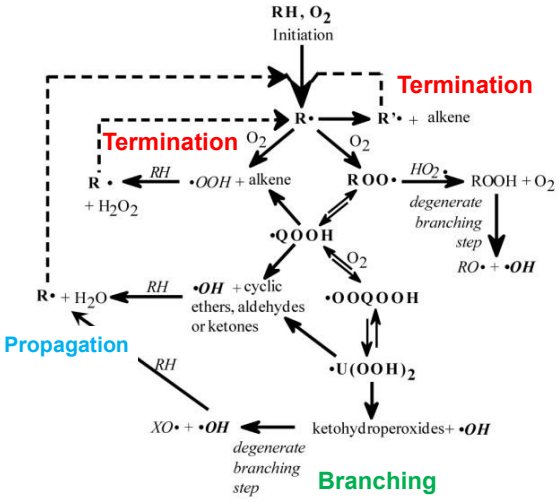

Depending on the *T*/*P*/stoichiometric conditions, either chain branching or termination can dominate, leading to ignition or not.

(Battin LeClerc et al., 2011)

What causes the NTC?

- Key to reactivity is **fate** of **alkylperoxy (RO_2) radicals** which undergo a number of reactions depending on *T* and *P*.
- Most relevant for chain branching is isomerisation of RO_2 via internal hydrogen abstraction onto the oxygen radical site through a transition state ring resulting in formation of **hydroperoxyalkyl radical** ($QOOH$, where $Q = R_{H-1}$).
- QOOH can undergo second O_2 addition with subsequent formation of OH + ketohydroperoxide, which again can form an additional OH. **Branching**
- At lower temperatures RO_2 can reform original alkyl R + O_2 or can dissociate to produce an alkene + HO_2.
- Formation of HO_2 and its fate is key to NTC. It is lower in reactivity than OH and at intermediate temperatures can go on to form H_2O_2.
- H_2O_2 is stable up to higher temperatures and hence its formation reduces overall radical pool, lowering reactivity increasing IDTs.
- At higher temperatures H_2O_2 can decompose to form two OH radicals, thus increasing reactivity again (remember hydrogen chemistry from earlier).

Differences between alkanes and short chain alcohols (Sarathy at al., 2014)

- Addition of **iso-butanol supressed low *T* heat release**.
- This is generally true for short chain alcohols, especially ethanol.
- **H abstraction from α-site tends to dominate** due to lower energy barrier, leading to carbonyl + HO_2 pathways being favoured over those leading to QOOH + O_2 which occur for iso-butanol.
- Relative rates for these two abstractions is crucial for predicting ignition for alcohol fuels.
- Same is true for n-butanol – see diagram below.

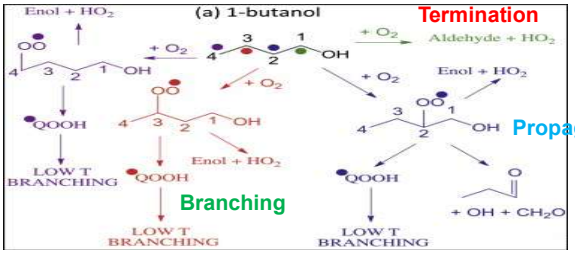

Pathways for linear alcohols (Sarathy, 2014)

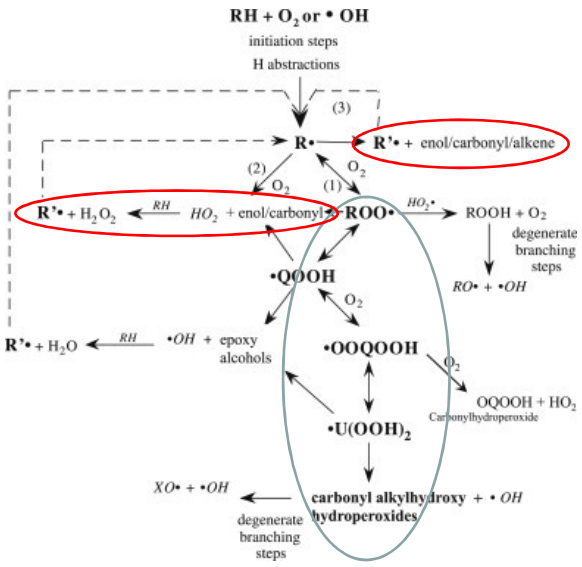

- Site of initial abstraction determines whether branching or termination routes dominate.

Differences between alcohols and gasoline/surrogate – n-butanol

- N-butanol shows Arrhenius response.
- Gasoline and surrogates show NTC which is gradually reduced by addition of n-butanol.

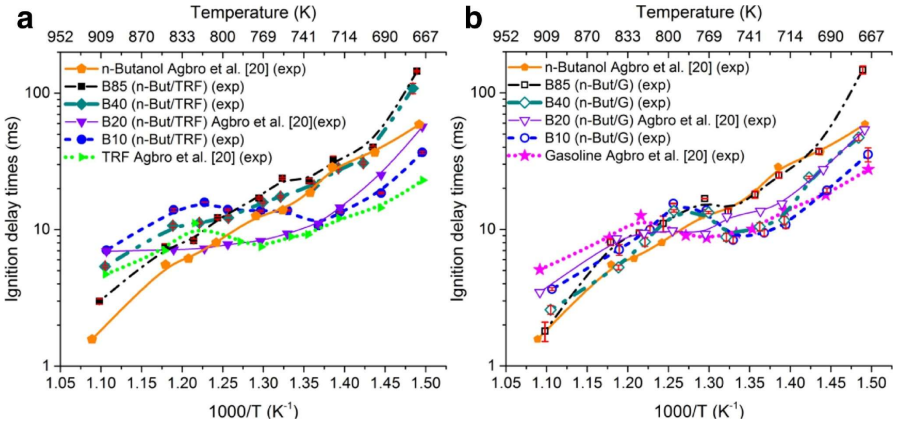

Sensitivity analysis for IDTs – stoichiometric n-butanol in air, 725 K

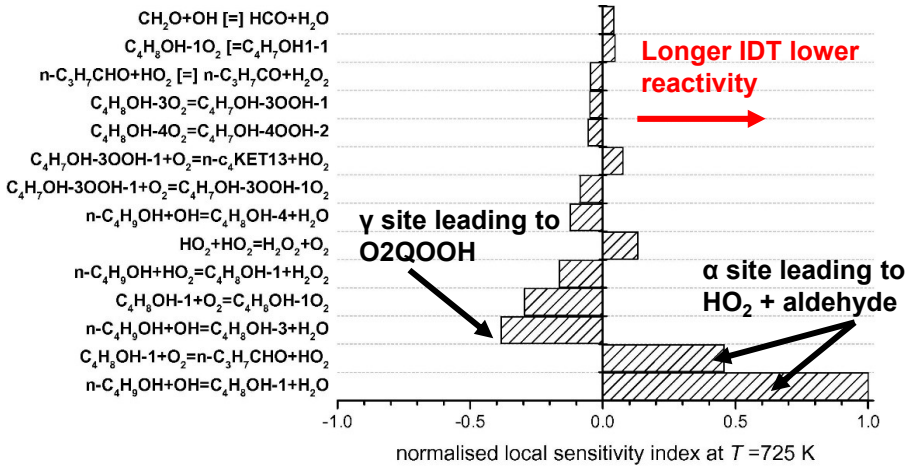

Global sensitivity analysis – contributions of reaction uncertainties to variance in predicted IDTs (see later)

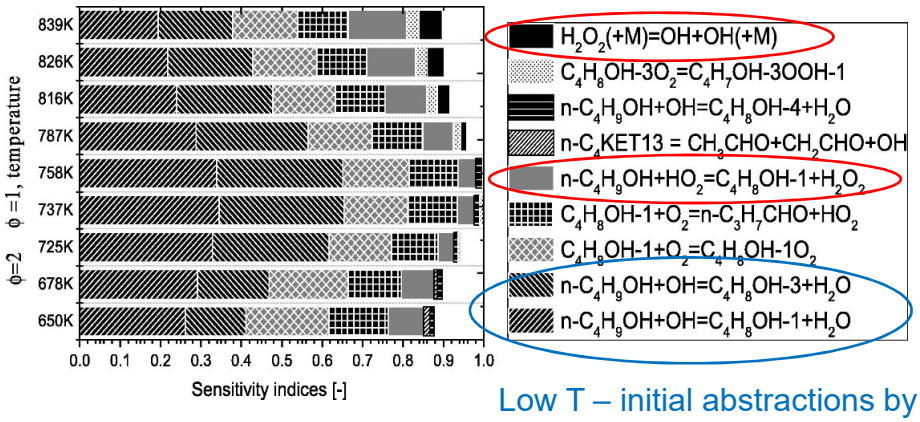

Low T – initial abstractions by OH dominate.

High T – HO_2, H_2O_2 chemistry increases in importance.

Global sensitivity analysis

Component functions of simulated log IDT on-top of the scatter
a) n-C_4H_9OH + OH = C_4H_8OH-1 + H_2O **α site**
b) for n-C_4H_9OH + OH = C_4H_8OH-3 + H_2O **γ site**
15 bar, ϕ = 1, 725 K.

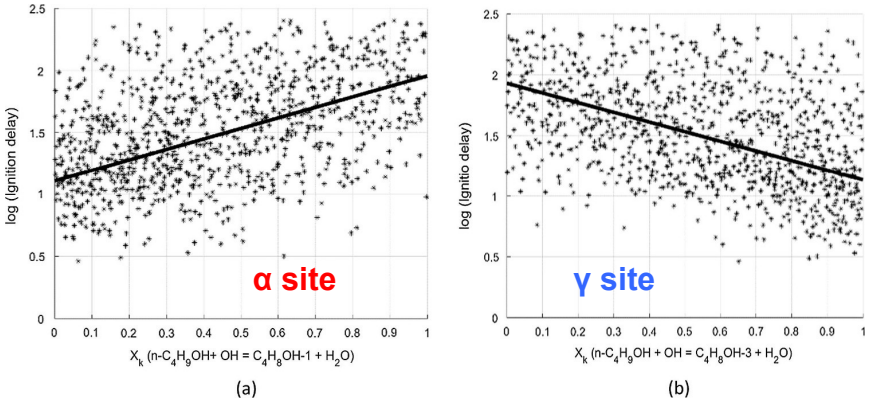

Sensitivity to scaled branching ratio for α and γ H abstraction reactions

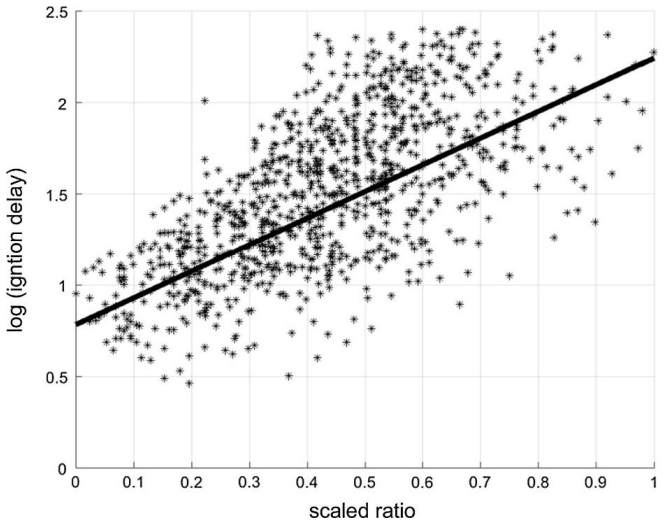

S index for ratio = 0.7.

S index for total rate of n-butanol + OH < 0.1.

It is the relative and not total rates that matter!

Validation data: Ignition delay time (IDT) measurements from RCM

IDT can be measured in a variety of experimental set-ups but of relevance to engines is the **rapid compression machine** (RCM) where IDT studied as function of equivalence ratio/thermodynamic conditions for different fuels and blends.

Single or dual piston machines operating at 600-1000 *K,* 1- 70 bar, with compressed temperatures depending on diluent used.

- **Compression stroke** followed by **auto-ignition** for reactive mixtures.
- Pressure rise captured by pressure transducers. Laser based piston location measurements used to determine volume changes.
- Some newer designs are able to perform rapid sampling of intermediates.

The Leeds RCM

Optimal RCM design features

- Fast as possible compression time (10-70 ms) - adiabatic process.
- Constant as possible piston location at end of compression - breaking and damping.

Issues:

- Cold boundary layer can be rolled up by piston, creating inhomogeneities (Lee & Hochgreb, 1998).
- Use of creviced pistons attempt to reduce this effect as does the use of twin-pistons creating symmetry (Sung & Curran, 2014).
- Optical diagnostics can be used to investigate inhomogeneities in RCM leading to hot-spots and pre-ignition.
- Inhomogeneities bigger issue for lower reactivity fuels and low *T*s.
  - Methods to exclude pre-ignition profiles can be used.

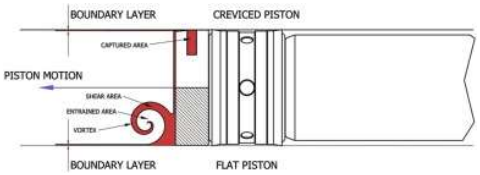

Ignition delay measurements

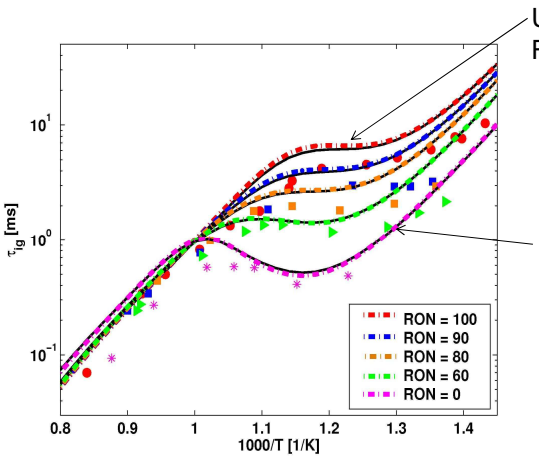

Unreactive fuel – iso-octane
RON = 100

Highly reactive fuel e.g. *n*-heptane – RON = 0

RON = Research Octane Number

Source: Stanford

RON and MON

- In an SI engine, efficient fuels are required but we do not want fuels that will create the potential for knocking.
- Historically the anti-knock quality is expressed by **octane numbers** by comparison to mixtures of *n*-heptane + iso-octane.
- The higher the octane number, the more compression the fuel can withstand before igniting. **Adding octane boosters e.g. alcohols potentially useful.**
- RON – Research Octane Number
  - *Determined by running fuel in test engine with variable compression ratio under controlled conditions, and comparing the results with those for mixtures of iso-octane and n-heptane. Low speed, milder driving.*
- MON – Motor Octane Number
  - *Determined at 900 rpm engine speed and not 600 rpm for RON using variable ignition timing.*

RON and MON have been useful measures of fuel tendencies to auto-ignite but cover specific conditions and not easily extrapolated to those of modern down-sized, boosted engines.

Cetane number, CN

- Inverse function of a fuel's ignition delay used to define fuels for use in **compression ignition engines**.
- **Higher cetane** fuels have **shorter IDTs** than lower ones.
- Comes from cetane *n*-$C_{16}H_{34}$, which has a defined CN of 100 i.e. very readily ignites under compression.
- Typical range for diesel engine operating well is 48-50.
- Lower CNs mean longer IDTs needing longer for the fuel to combust.
  - Higher speed engines require higher CN fuels.
- Minimum CN in Europe = 51, US = 40.
- **Alternative fuels and their blends must meet standards**
  - See later.

Modelling chemistry within the RCM

- If we can develop models that well represent fuels/mixtures across different temperatures and pressures, better detail for use in engine design.
  - **RCM provides validation opportunities for such models**.
- Most validation studies assume **adiabatic core hypothesis**.
  - Assumes a boundary layer exists along the walls of the combustion chamber and is the only location where heat loss to the walls occurs.
  - Used to determine temperature within chamber at end of compression.

$$\frac{T_c}{T_i} = \left(\frac{P_c}{P_i}\right)^{\frac{\gamma-1}{\gamma}}$$

  - γ is temperature dependent ratio of specific heats for the mixture
- Simplest modelling approach closed, constant volume, well mixed reactor - in reality heat losses occur during compression.
- Thus "***non-reactive***" data also obtained using mixture with thermodynamic properties as reactive condition but inert.
  - Achieved by replacing oxygen with nitrogen.
  - **Volume profile then used in subsequent modelling of reactive case.**

New experimental targets from ICM?

Speciation

- IDTs can reach high pressures but only provide sensitivities to certain reactions that influence **branching vs termination** reactions.
- Jet Stirred Reactors etc. tend to be at low pressures.
- Need high pressure, low temperature species measurements to extend model validation regime.

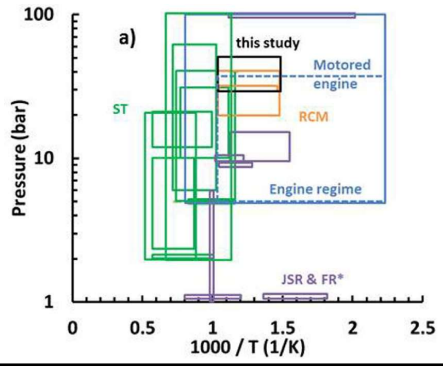

- Sampling method required that **provides representative sample** i.e. no change in composition due to sampling.
  - quenching entire reactive mixture into a large volume by puncturing diaphragm.
  - fast-acting sampling valve mounted on reactor end-wall which samples from reaction core and quenches into sampling volume
- Subsequent GCMS and FID.
- See review by Goldsborough et al. 2017.

Example for propane oxidation (Ramalingham, 2020)

- New targets for species concentrations as function of time.

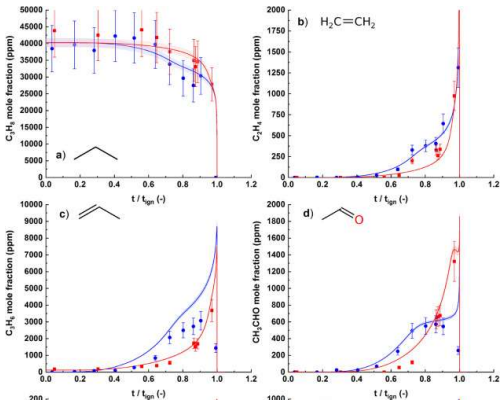

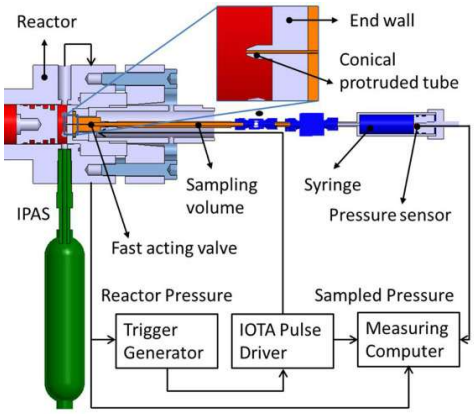

Example for Methyl *trans*-3-Hexenoate Autoignition (Wagnon et al., 2014)

- While ignition delay time predictions were in agreement with experimental data, speciation highlighted uncertainties in the reaction chemistry of unsaturated esters and small hydrocarbon intermediates.

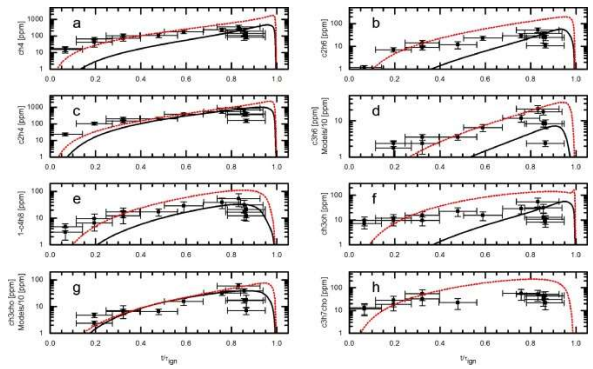

The black solid, and red dotted lines indicate the original and updated model results, respectively. Average conditions for the experiments were T_c = 934 K, p_c = 10.4 bar, φ = 0.30, diluent:O_2 = 3.76.

Iso-butanol example (Ji et al, 2015)

- Species sampling showed that best available mechanism well predicted IDT but:
  - overpredicted ethene by a factor of 6–10
  - underpredicted iso-butene by a factor of 2
  - overpredicted iso-butyraldehyde by a factor of 2.

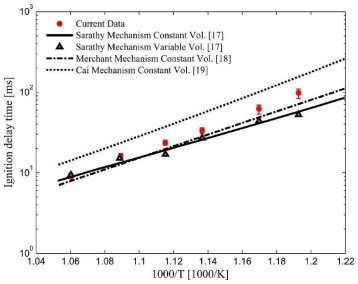

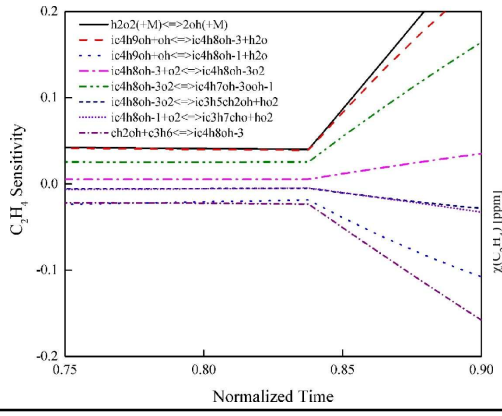

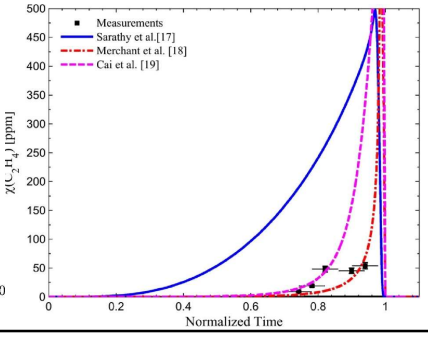

Heat Release Analysis

- Goldsborough (2019) developed a method to perform **heat release analysis (HRA)** from pressure traces for RCM experiments.

$$\frac{dU_s}{dt} = \dot{Q}_{chem} - \dot{Q}_{wall} - \dot{W}_{piston} - \dot{H}_{out} + \dot{H}_{in}$$

- U_s - total sensible internal energy, $\dot{Q}_{chem}$ - rate of heat released, $\dot{Q}_{wall}$ - rate of heat exchange with the chamber walls, $\dot{W}_{piston}$ - rate of work done by piston on gas and $\dot{H}_{out}$ and $\dot{H}_{in}$ are the rates of enthalpy flow out and in of the reaction chamber.
- Adiabatic core assumed. Non-reactive experiments used to account for heat losses from chamber.

$$HRR = \frac{\gamma}{\gamma - 1}\frac{dV}{dt}(P - P_{nr}) + \frac{1}{\gamma - 1}V\left(\frac{dP}{dt} - \left.\frac{dP}{dt}\right|_{nr}\right) - \frac{PV}{(\gamma - 1)^2}\left(\frac{d\gamma}{dt} - \left.\frac{d\gamma}{dt}\right|_{nr}\right)$$

  - γ - ratio of specific heats, V - reaction chamber volume (as calculated from the non-reactive pressure history.

Example for iso-butanol gasoline surrogate blend

(Michelbach, 2021)

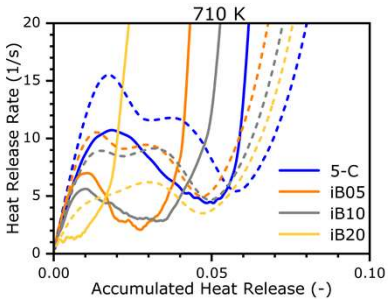

- Dashed lines from simulations using LLNL/Sarathy mechanism show very different behaviour than experimentally derived traces.
- Model predicts two stages of LTHR not seen in experiments.

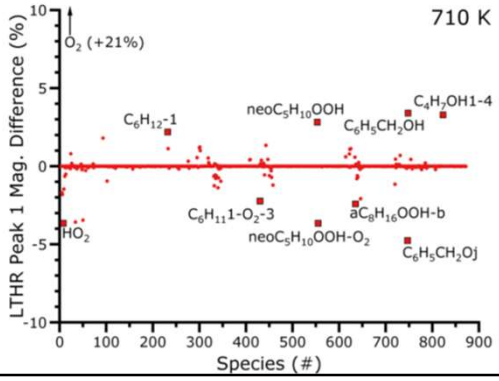

- % change in predicted LTHR peak for 5-C constant volume simulations, due to a +5 kJ mol^{-1} change in species enthalpy of formation. P_c=20 bar, Φ=1.0.
- **Thermo data strongly affects HRRs.**

Example for gasoline surrogates (FACE-F) and blends with ethanol (Cheng et al., 2021)

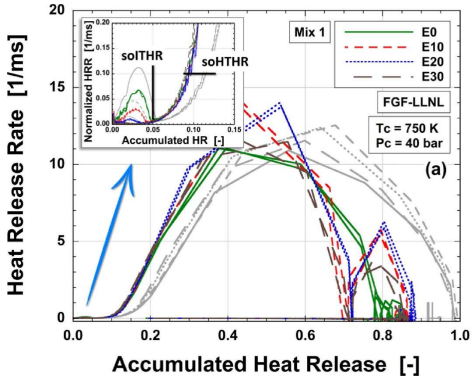

FGF/E0–E30 blends at 40 bar, ϕ = 1, Tc = 750 K. Colour lines are experimental results; gray lines are model results.

- Model over-predicts LTHR as well as failing to fully distinguish between two surrogate designs tested in the work.

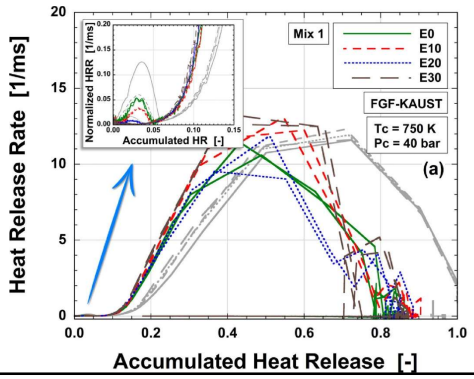

Categorising fuels

- Some controversy in using simple values of RON and MON within modern engines.
  - Can they be extrapolated to new *T, P* regimes?
- **Octane sensitivity *S*** (RON-MON) was developed to partially overcome this.
- Kalghatgi (2001) pioneered a practical method to correlate RON and MON to knock-limited spark advance (KLSA) using parameter *K*.
- **Octane index** OI = RON – *KS.*
- Where *K* is positive, higher OI → better anti-knock quality of fuel.
- In some cases *K* is negative; i.e. for a given RON, a fuel of *lower* MON has better anti-knock quality and will lead to better performance. Depends on engine conditions.

SECTION 3 CONT… MODEL VALIDATION USING FUNDAMENTAL EXPERIMENTS: Shock tubes, flow reactors and flames

Validation data: IDT and species profiling from shock tubes, Ch 6 in Cleaner Combustion

- IDT - time interval between arrival of reflected shock wave and onset of ignition at test location determined by *P* measurements or CH* and OH* emission. (Gauthier et al., 2004)
- Low T measurements limited by available test time
  - interval between arrival of reflected shock at observation port and the arrival at same location of a significant pressure disturbance from the predicted or measured reflected shock pressure.
- Not suitable for long IDTs.

- **Time-of-flight mass spectrometry** or multi-species optical diagnostics can be used for continuous sampling and species analysis.
- **Gas chromatography** used for product analysis at end of process.
- Species data allows for wider mechanism validation vs IDT.

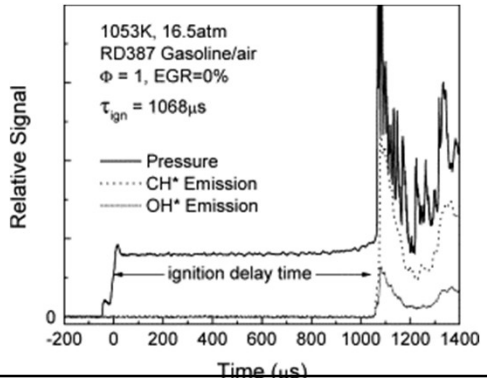

Aerosol Shock Tube

(Davidson, 2008)

- Developed to enable studies of shock wave interactions with **liquid aerosols**, including **droplet evaporation kinetics** and subsequent chemical reaction of the vapour.
- Useful for studies of low vapour pressure fuels e.g. long chain hydrocarbons.
- Uniform spatial distribution of aerosol important for well behaved shocks.
- Also need narrow micrometer-sized aerosol size distribution that rapidly evaporates.
- Used for IDT measurements of high carbon number fuels e.g. n-dodecane/O_2/argon and JP-7/O_2/argon mixtures.

Example from aerosol shock tube study - fatty acid methyl esters

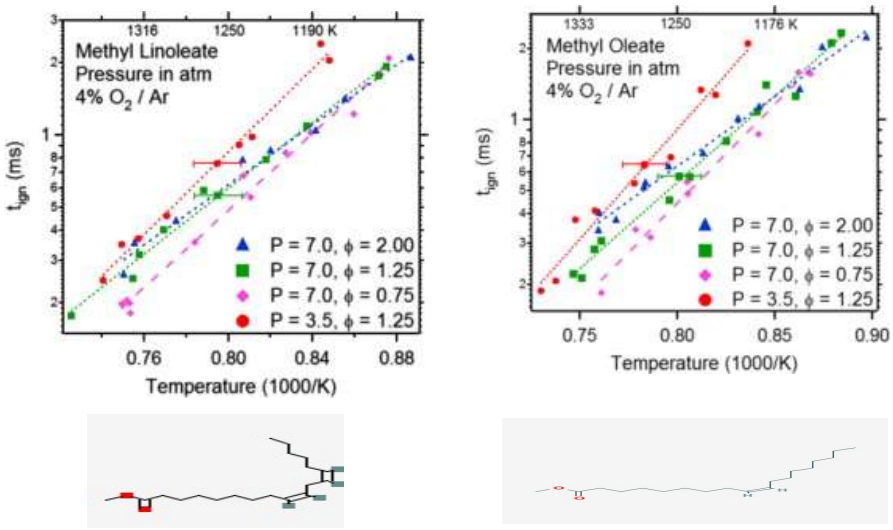

Validation data: Species profiles from Jet Stirred Reactors (JSRs)

- Can more easily give information about reactants products and intermediates over a range of *T* when operated at steady state or under oscillatory conditions.
- Turbulent jets used for enhanced mixing in order to create **homogeneous reactor**.
- Preheating of mixture improves *T* homogeneity.
- Higher pressures can be achieved - quartz reactor encased in pressure resistant jacket.
- Modelled using well mixed **open reactor equations** with heat transfer - *shown earlier*.
- Usually operated **isothermally**.
- Heat losses, losses of radicals to walls and residence times are important physical parameters in models.
  - Radical wall losses reduced by use of fused silica vessels.

Species observations

- Coupled with species measurement systems including gas chromatography, IR spectrometry e.g. butane oxidation shown here. (Hébrard et al., 2015).
- Recent use of **synchrotron** vacuum UV photo ionisation mass spectrometry for detecting **intermediates** for the first time e.g. ketohydroperoxides/enols.

- Identification of intermediates helps to confirm reaction pathways.
- **Stringent test** of reaction mechanisms' ability to predict species in reaction chain

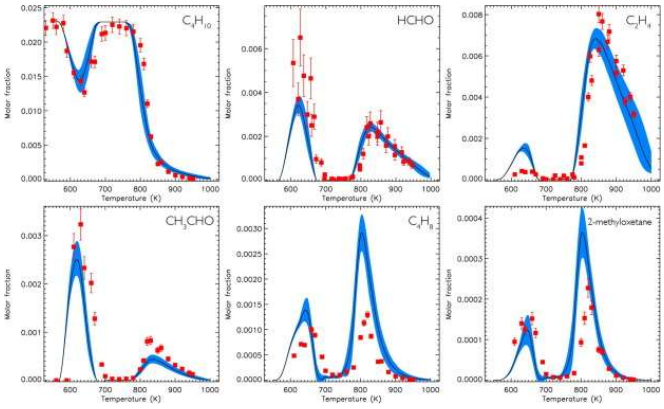

Differences in sensitivities for different targets: IDT vs C_4H_{10} mole fraction in JSR

- **BLUE:** Fuel specific reactions. **RED:** Base C2 chemistry.

At low *T*, JSR sensitivities dominated by radicals generated from ketohydroperoxides decomposition e.g. $C_2H_5O \rightarrow HCHO + CH_3$

At high *T*, only reactions of HO_2, CH_3, HCHO, less so CH_3CHO

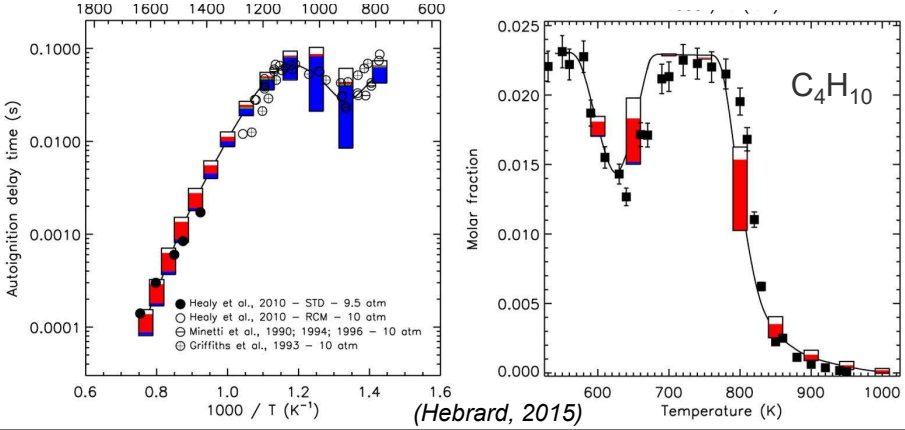

(Hebrard, 2015)

N-butanol study (Sarathy, 2009)

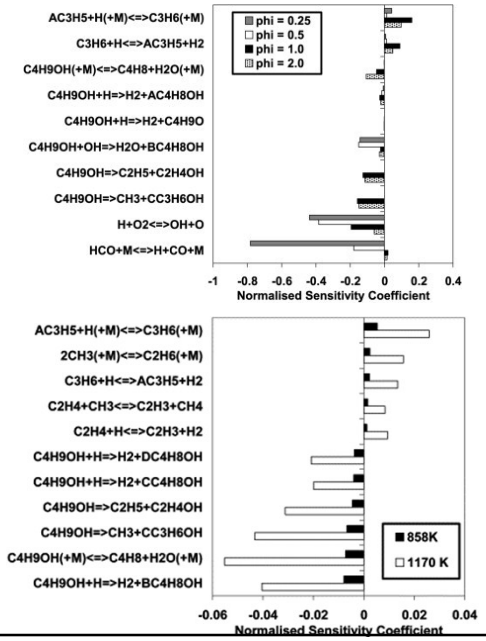

Sensitivity of *n*-butanol to select reactions in

TOP

JSR at ϕ = 1, P = 1 atm, τ = 0.07 s, T = 1160 K

BOTTOM

Opposed flow diffusion flame.

Fuel decomposition highlighted along with small molecule chemistry.

Variable and atmospheric pressure flow reactors (Dryer etc.)

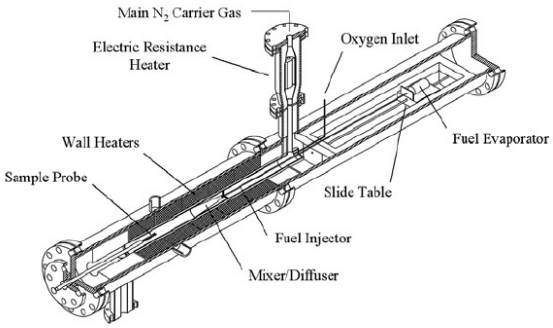

Reaction time varied by moving point of fuel injection

- APFR high temperature facility at atmospheric pressure.
- VPFR can access a wide range of conditions: T (550–1200 K), P (0.3–20 atm), and φ (pure pyrolysis to oxy-gen-rich conditions).
- Carrier gas is a turbulent flow of preheated nitrogen into which oxygen and water vapour are injected and premised to dilute amounts.

- Rapid mixing within quartz diffuser section, gives **quasi-steady reaction** along the length of a constant-diameter quartz test section.
- Dilute system used to limit heat release and establish quasi-isothermal conditions.

DME oxidation

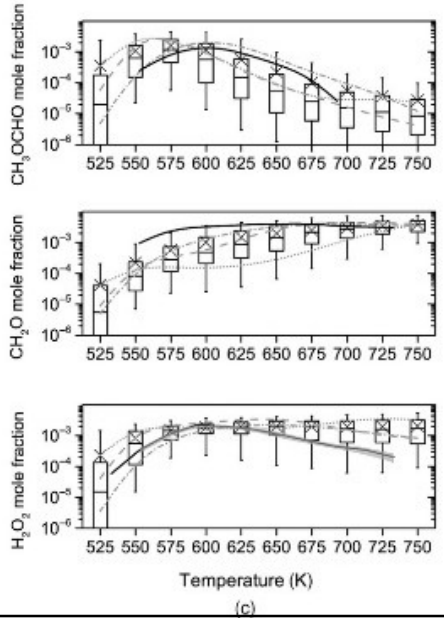

- Data from Princeton flow reactor (solid line, Guo 2013) is compared against uncertainty profiles from simulations using Aramco Mech1.3 (2013).
- Dashed line original model.
- Boxes and whiskers represent uncertainty percentiles (*25th and 75th*).
- Overlap exists but **uncertainty ranges are large**
  - ➢ Further model constraints are needed.

Tomlin et al., 2014

Comparison of sensitivities, DME flow reactor, note mechanism dependencies

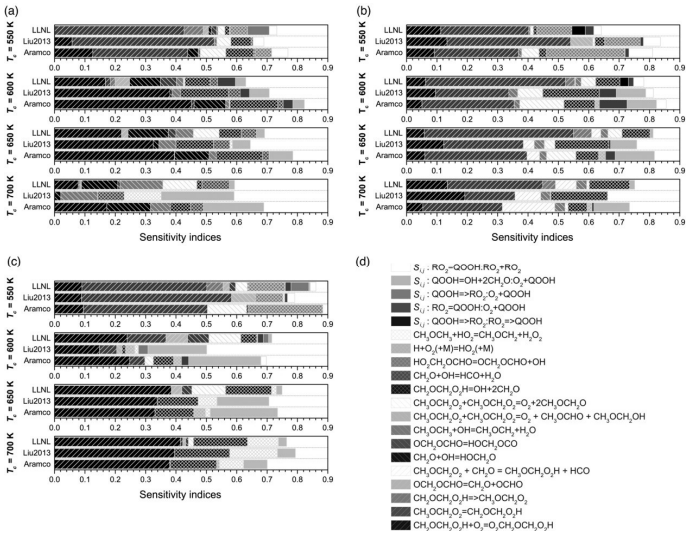

(a) CH_2O mole fraction, (b) CH_3OCHO mole fraction, (c) H_2O_2 mole fraction

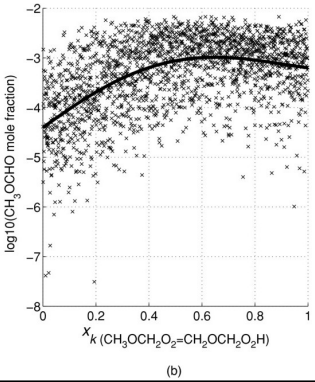

Example – quantification of ketohydroperoxides during DME combustion

- Molecular beam mass spectrometry with single-photon ionization via tunable synchrotron-generated vacuum-ultraviolet radiation.
- Quantified profiles for 17 components including hydroperoxymethyl formate ($HOOCH_2OCH_2O$), a key intermediate in low-temperature oxidation of DME.
- Allows stringent model validation.

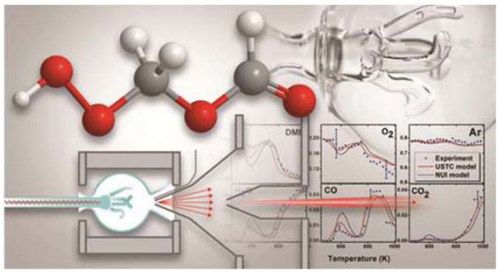

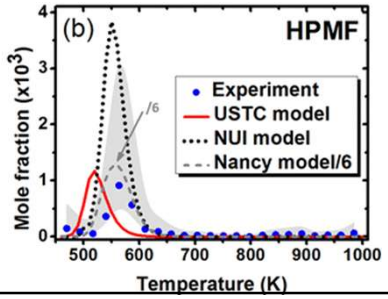

Moshammer et al. 2016

Laminar Burning Velocity, LBV

- Laminar burning velocity is a physiochemical constant for a given combustible mixture, *T, P*, ϕ.
  - Velocity, relative to unburnt gas, with which a planar one dimensional flame travels along the normal to its surface into the mixture.
- Unfortunately, although its theoretical definition is simple, the same cannot said of its practical measurement .
- **Burning velocity** is a measure of how fast reactants are moving into the flame zone in a moving frame of reference.
  - E.g. in a spherically expanding flame.
  - The spherical flame has no heat losses and burns at the adiabatic flame temperature.
- **Flame speeds** are measured relative to a fixed point and are influenced by the expansion of burnt gases.

Why does LBV matter?

- Sensitivities for LBV both pre-mixed and non-premixed flames similar to those for extinction so good test of model's ability to **predict extinction for practical devices**, Egolfopoulos, 2014.
- Useful measure for estimating turbulent burning velocities.

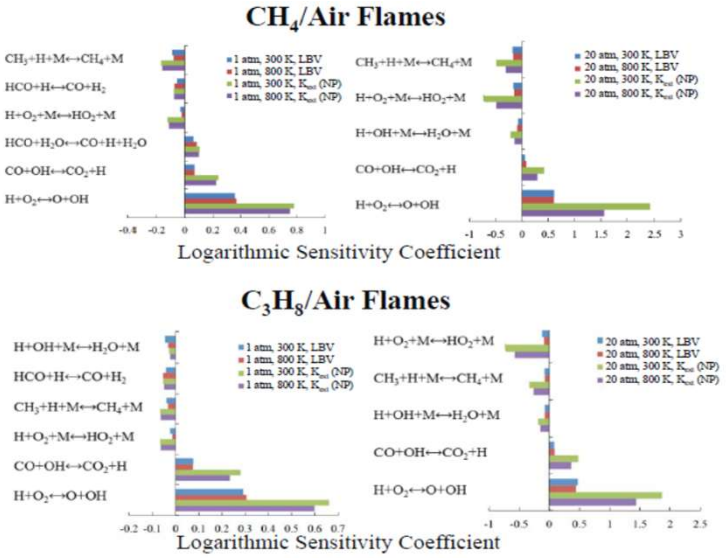

Measuring burning velocity - spherical bomb

- S_L can be measured in a constant volume spherical vessel.
- Pressure measurements or Schlieren photography can be used to evaluate burning velocities but requires interpolation.
- Instabilities, curvature and stretch cause measurement difficulties, particularly for pressure method. Need to extrapolate to zero stretch.
- Can also be used for turbulent velocities by use of fans and at varying pressures.

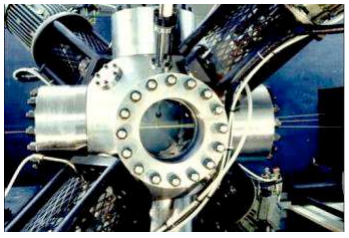

The bomb!

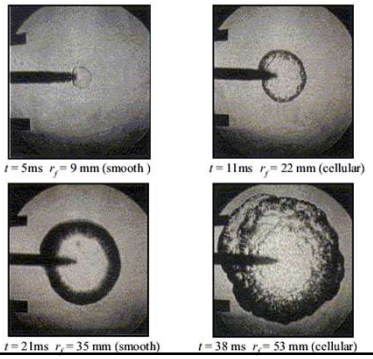

Measuring burning velocity, flat flame burner

- Heat flux method is used by creating adiabatic conditions on a flat stable flame.

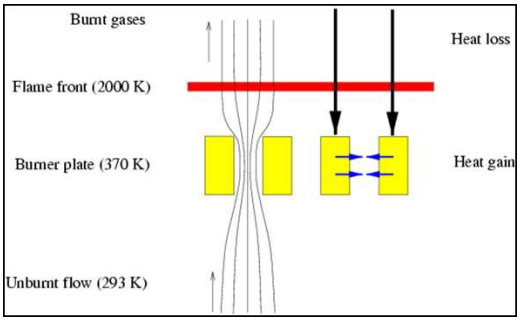

http://cms.heatfluxburner.org/home/

Measuring burning velocity – flat flame burner

- When gas inlet velocity < laminar burning velocity, flame is stabilised on the burner.
  - As a result the heat loss of the flame to the burner plate is larger than the heat gain of the gas mixture from the burner plate.
- When unburnt gas velocity > laminar burning velocity heat gain of gas from burner plate is larger than heat loss of flame.
- Both of these are non adiabatic situations.
- An **adiabatic** situation is found when there is no net heat loss to the burner, meaning heat loss and gain level each other off.
- In this case **laminar adiabatic burning velocity equals inlet velocity of the gas mixture.** *T* profile is flat across the flame.
- Various inlet gas velocities are tested *T* profile measured and interpolation used to obtain zero heat flux conditions.

Interpolation method

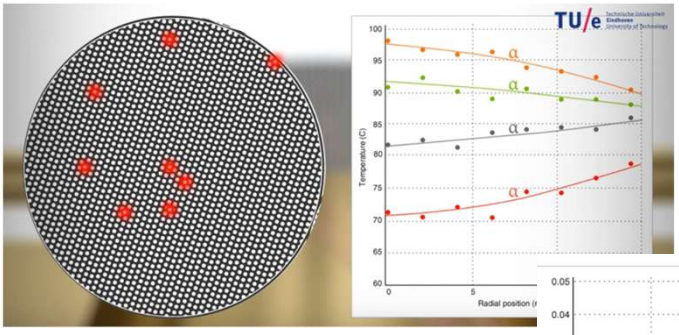

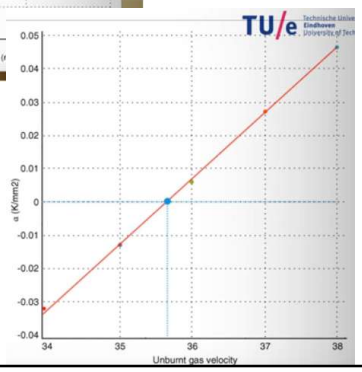

T profiles taken at various unburnt gas velocities and interpolation used to find zero gradient profile corresponding to LBV.

Counterflow flames

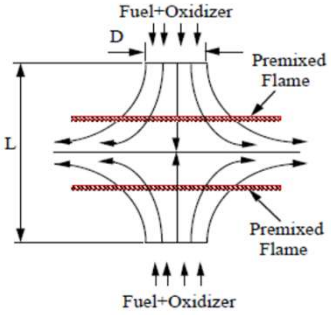

- Wu and Law, 1985 first used for LBV measurements demonstrating the influence of stretch.
- Stagnation flames achieved by:
  - impinging separate fuel and oxidizer streams
  - impinging two premixed streams
  - from a premixed stream impinging on a solid surface.
- Attractive as leads to flat flame assisting probing species and structure.
- Assumption that radial velocity varies linearly in the y or radial direction, leading to a simplification in which the fluid properties are **functions of the axial distance only**.

Uncertainties in LBV measurement

- **ALL** methods for LBV are not measuring directly & require interpretation.
- Measured values show **variability** between experiments.
- **Inherent level of uncertainty.**
- Coupling experiment with DNS may help interpretation.
- Recommend to read presentation by Egolfopoulos:

Towards Eliminating Apparatus Dependence and Approaching Extreme Engine-Relevant Conditions

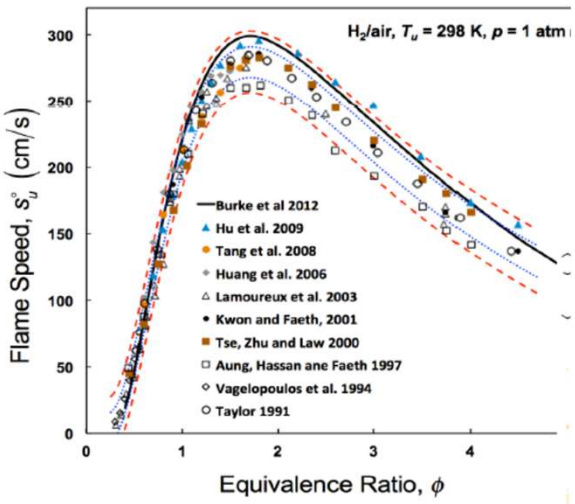

Law et al., 2015

Are the uncertainties really asymmetrical?

- Traditional use of equivalence ratio compresses data in the lean region.
- Law et al. 2015 suggested the use of a normalised equivalence ratio to better highlight the uncertainties across the range of stoichiometries.

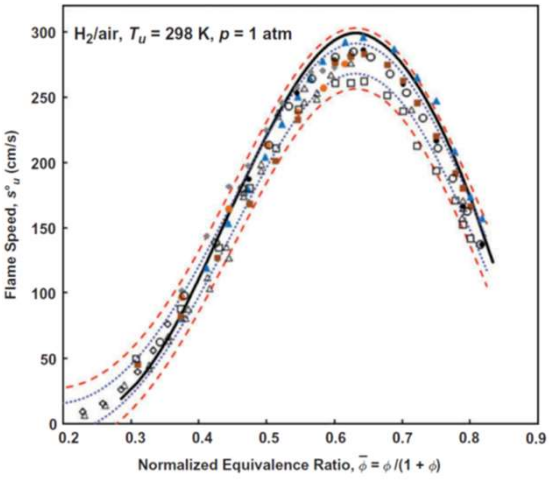

Examples of flame speed studies - butanols

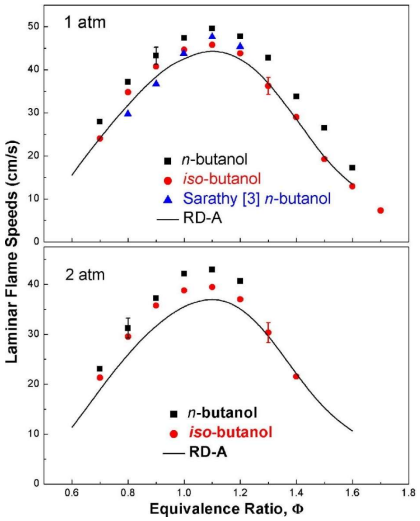

Liu et al. 2011

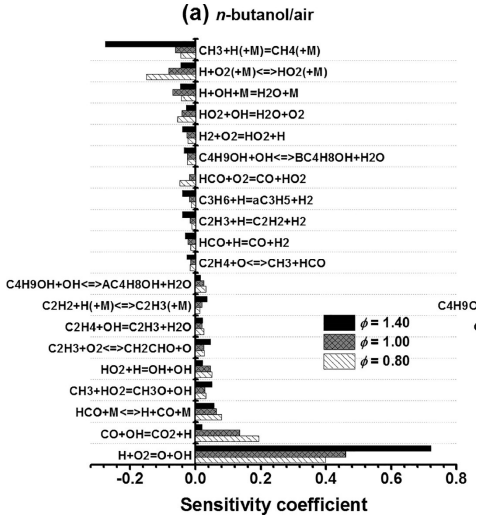

Sensitivity coefficients of LBVs for (a) n-butanol/air T = 423 K, Pu= 10 atm and ϕ = 0.80–1.40 (Wang et al., 2018).

- **Flame speed sensitivities dominated by small molecule chemistry (Li, Energies 2016, 9, 511).**

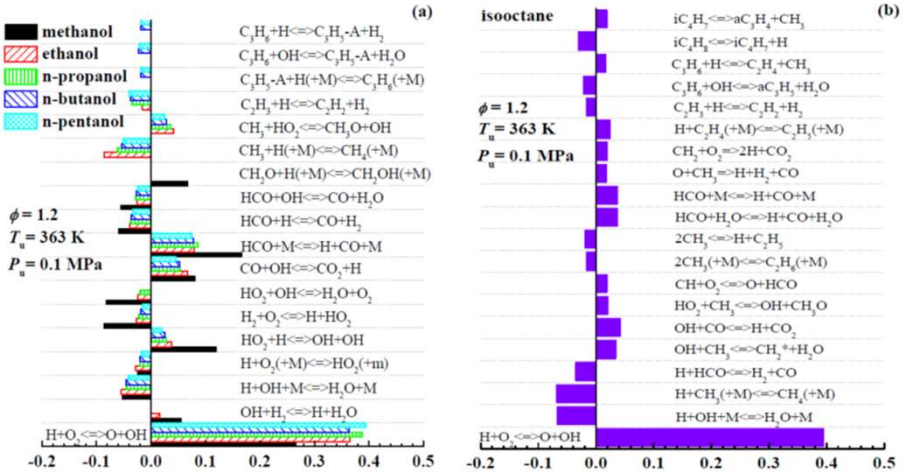

Normalized rate constant sensitivity coefficients on laminar flame speed for (**a**) pure C1–C5 primary alcohols and (**b**) pure isooctane at 363 K, 0.1 MPa and the equivalence ratio of 1.2.

Advantages of using multiple target types- n-pentane ignition and cyclic ether formation

- IDTs for n-pentane, JSR data for pentane mole fraction, well captured by previous model (dashed lines).
- Cyclic ether mole fractions very poor – requiring an update in rate constants for their formation from QOOH.
- Leads to slight increase in reactivity in NTC – due to lowering rate of propagation vs. chain branching reactions.
- Significant improvement in prediction of two major cyclic ethers formed (2-methyltetrahydrofuran and 2,4-dimethyloxetane)
- **NOTE: High level of theory required due to stated deficiencies of CBS-QB3 (Bugler, 2017).**

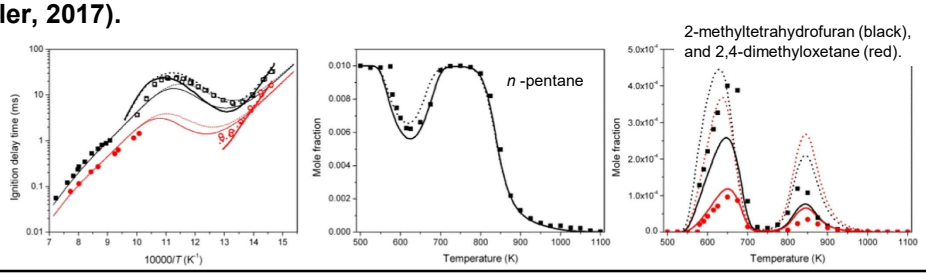

Overview of validation studies

- Each type of experiment tests a chemical model in different ways and a general model should be applicable for all scenarios.
  - **Sensitivity analysis crucial for identifying constraints offered by experiments.**
- Low *T*, **IDT** really mainly depends on predicting **relative rate of branching to termination routes**.
  - Could be predicted even with incorrect heat release or intermediate concentrations, so not a complete test.
  - However, most relevant to engine knock conditions.
  - Can add heat release rates and speciation to targets.
- **LBV measurements** add high temperature targets for models of relevance to **flame extinction** and **turbulent flame propagation** within engines.
- **Speciation measurements** in flames, STs and JSRs – particularly **intermediates** - add more stringent tests for mechanisms.
  - Often highlight missing pathways, or highly uncertain rate coefficients.
- In most cases, we are **much WORSE** at including **uncertainties for model** results than we are for experimental data.

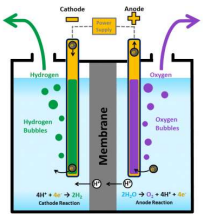

Section 4
FUTURE FUELS

Challenges of future fuels

Energy demand has grown rapidly since 1950s as economies have industrialised.

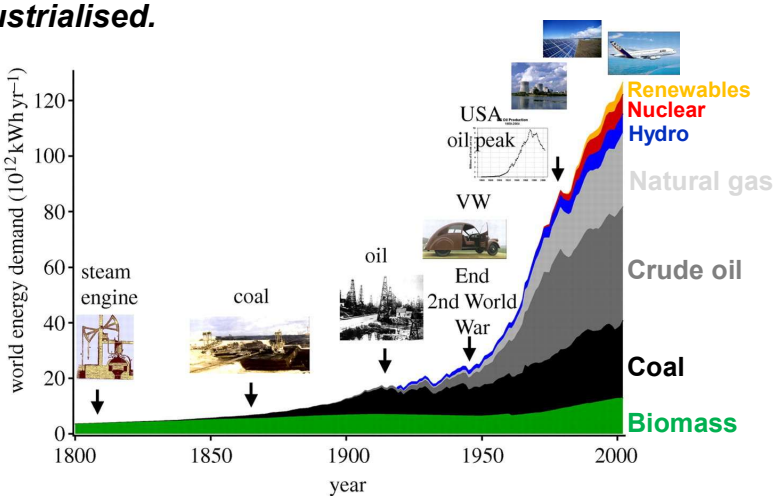

Challenges of future fuels

Solid and liquid fuels provide effective energy storage in terms of mass and volume.

Liquids good for transportation?

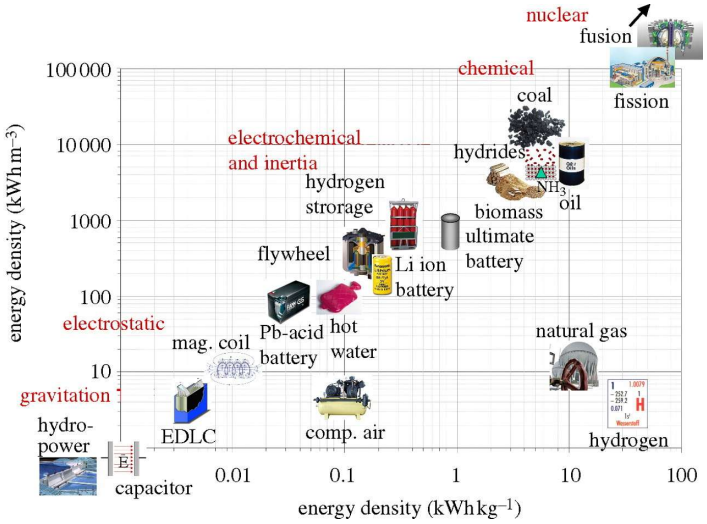

Züttel, 2010

Or do they lock us into existing technologies?

Key challenge switching transport and heat (both domestic and industrial) demand to low carbon supplies

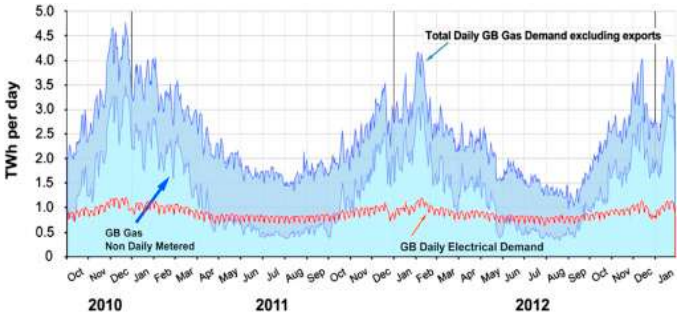

Watson, Energy Policy Volume 126, March 2019, Pages 533-544

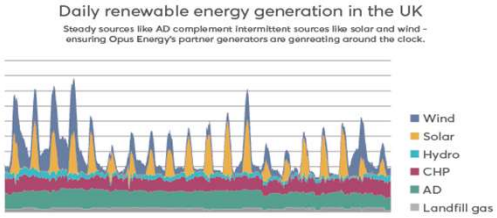

Opus Energy

Storage time-scales

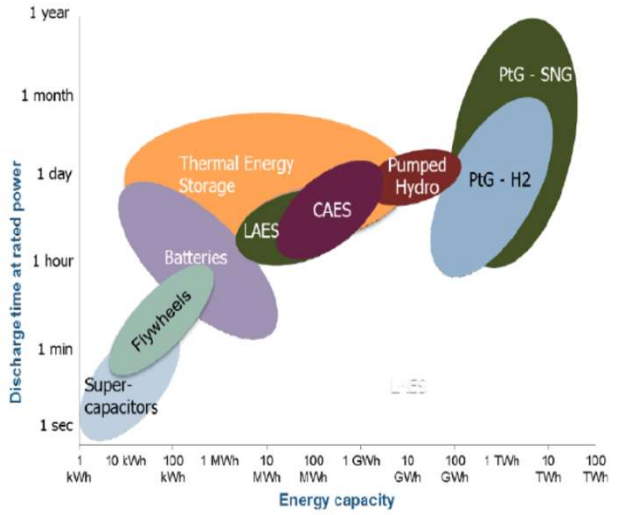

Source: World Energy Council, 2016

Long term storage needed for winter heat.

Hydrogen a possibility.

Controversial topic!

- **Question – what do you consider to the best alternative fuels for the following applications:**
  - **Aviation**
  - **Marine**
  - **Industrial heat**
  - **Peak power provision (e.g. using gas turbines, engines or fuel cells).**

Challenges of future fuels

- Change in energy economy from fossil energy carriers to renewable energy fluxes is **necessary**.
- Main challenge to efficiently convert renewable energy into electricity and store it or produce synthetic fuel.
- **Hydrogen** produced from water through electrolysis.
  - **Pros:** Novel storage methods include using hydrides and salt caverns, gas networks are existing infrastructure that could be used for heat provision, no CO_2/CO/soot emissions, low NOx strategies required.
  - **Cons:** Storage is a challenge, system energy density is significantly smaller than liquid and solid fuels.
- **Synthetic hydrocarbons** can be produced from hydrogen and CO_2 extracted from the atmosphere.
  - **Pros:** almost CO_2 neutral, energy dense, stored like fossil fuels, conventional engines and turbines can be used, suitable for hard to electrify sectors (aviation, shipping).
  - **Cons:** High cost, lack of proven Direct Air Capture (DAC) of CO_2 at scale, poor overall system efficiency.

Challenges of future fuels

Biofuels – liquid fuels generated from biomass e.g. biodiesel, ethanol, butanol, HVO, ethers, furans:

- **First generation**: corn, sugar cane and beets, soya, vegetable oils.
- **Second generation:** lignocellulosic feedstock classified as not suitable for human consumption e.g. grasses, Jatropha, seed crops, waste food & vegetable oil, municipal waste, waste wood, corn stover.
- **Third generation:** algal sources.

Pros:

- Many have similar energy densities to petroleum fuels.
- Can often be used or blended for use in engines without modifications.
- Can lead to lower particulates reducing need for after-treatment.

Cons:

- 1st gen compete with food. EU stipulating increase in 2nd gen components (RED II).
- 2nd/3rd gen more difficult and expensive to produce – breaking down complex bonds. More costly than fossil fuels. Can lead to less stable oils (algae).
- Available biomass resource is not limitless.
- Time-scales are involved in recapturing CO_2 through growth and photosynthesis.
- Potential to encourage mono-cultures.

HYDROGEN

Combustion challenges and opportunities

Opportunities

- Heat is a major sector in energy use in both domestic and industrial settings.

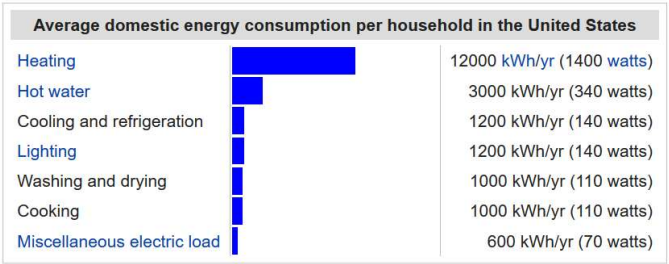

DOE, 2016

- Currently provided by natural gas, biomass, electricity (directly or via heat pumps).
- Decarbonisation of heat requires transporting more **electricity** or **carbon free or carbon neutral gas**.
- Hydrogen can be blended up to 20% by volume with NG without changing infrastructure (HyDeploy project).
- Large CO_2 reductions however, need much bigger volume fractions.

Important Combustion/ other Properties of H_2

- **High flame speeds** and **adiabatic flame temperatures**.
- **Wide flammability** limits. But long IDTs (high RON).
- Materials **embrittlement**.
- Very light/diffusive.
  - efficient storage requires high pressure cylinders or very low (below −253 °C) temperature at 1 atm.
  - Leaky, but disperses quickly if leaked.
- Odourless.
- Premixed flames have **low visibility**.
- Higher heating value (HHV) of hydrogen =13 MJ/Nm^3, whereas that of NG = 40 MJ/Nm^3.
  - To satisfy same energy demand, volume of H_2 transported 3 x that of NG.
- Differences in density result in approximately same pressure drop for H_2 and NG, a critical parameter in pipeline network.

Source: Robert Schefer, Sandia National Laboratory

Table of properties (in air, stoich)

	H_2	CH_4	Propane
Adiabatic Flame Temperature	2380 K	2226 K	2267 K
Diffusivity (m^2/s) x 10^5	6.11	1.60	1.00
Flammability limits	4-75%	5.3-15 %	2.2-9.5 %
LHV (MJ/Kg)	120	50	46.4
Energy density (MJ/m^3)	9.6	32.5	81.2
RON (with uncertainties)	130	120	
MIT	845 K	905 K	766 K
Min. Ignition Energy (10^{-5} J)	2.0	33	30.5
Fuel Volume Fraction %	29.5%	9.48%	4.03%

Combustion challenges

- Flame speeds and adiabatic flame temperatures are much higher for H_2 than NG and hydrocarbons.
- Combustors of all types will have to be redesigned for H_2.

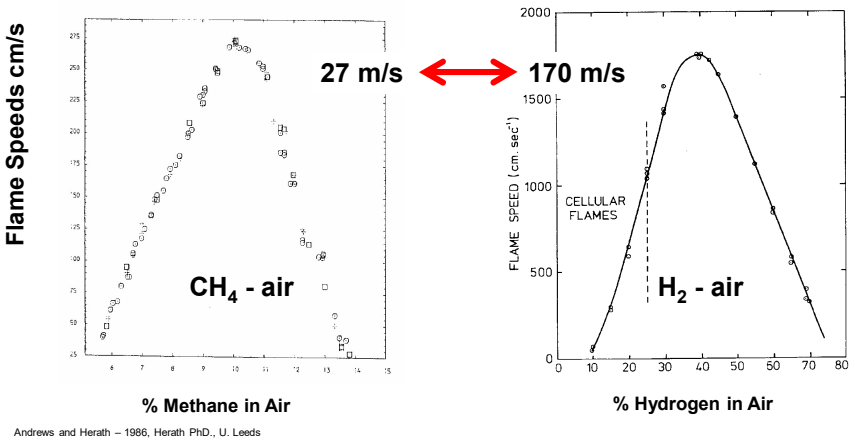

Andrews and Herath – 1986, Herath PhD., U. Leeds

Measured in a 0.5 m diameter by 0.5 m long closed vessel, 1 atm

How well can we model the mass burning rate for H_2?

- Burke (*Western States Section of the Combustion Institute Spring Technical Meeting 637-648, 2010*) showed significant variation between models.
- Updates to reaction chemistry discussed earlier need to be incorporated.
  - Models are constantly changing and being updated. If we're lucky…

Check-point. Are you still using the GRI? Are you using the most up to date mechanisms?

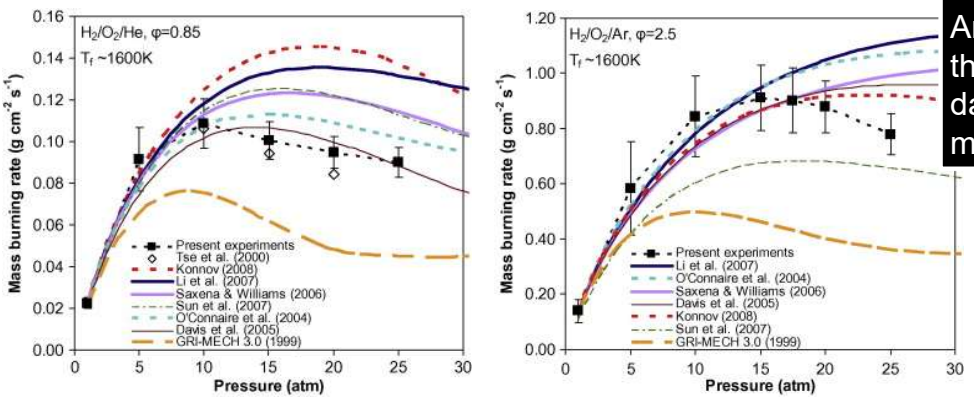

NOx formation chemistry

- **Thermal NOx** (Zeld'ovich mechanism)
  - $O + N_2 \rightarrow NO + N$, then $N + O_2$ or $N + OH$ **Highly sensitive to temperature!!**
- **Prompt:** Fenimore (1976 etc) observed NO formation in the primary reaction zone (flame front) in a flame.
- Attributed to reaction of a hydrocarbon radical with N_2.
  - $CH + N_2 \rightarrow HCN + N$
- **Fuel bound N**: Reaction of chemically bound N in fossil fuels also thought to generate HCN. Can oxidise to form NCO.
  - $NCO + O \rightarrow NO + CO$
- Route from HCN to NO discussed by Miller and Bowman (1989).
- HCN reacts with radicals (O, OH, H)
  - $HCN+O/OH/H \rightarrow CN,HNC,HNCO$ This step breaks the strong C≡N bond.
  - $CN+O_2 \rightarrow NCO+O$, $NCO+H \rightarrow NH+CO$, $NH+O \rightarrow NO+HN+OH \rightarrow NO+H$, $N+OH \rightarrow NO+H$
- NNH path: $H + N_2 = NNH$, $NNH + O = NH + NO$ (Bozzelli and Dean, 1995)

Fuel and prompt NOx formation

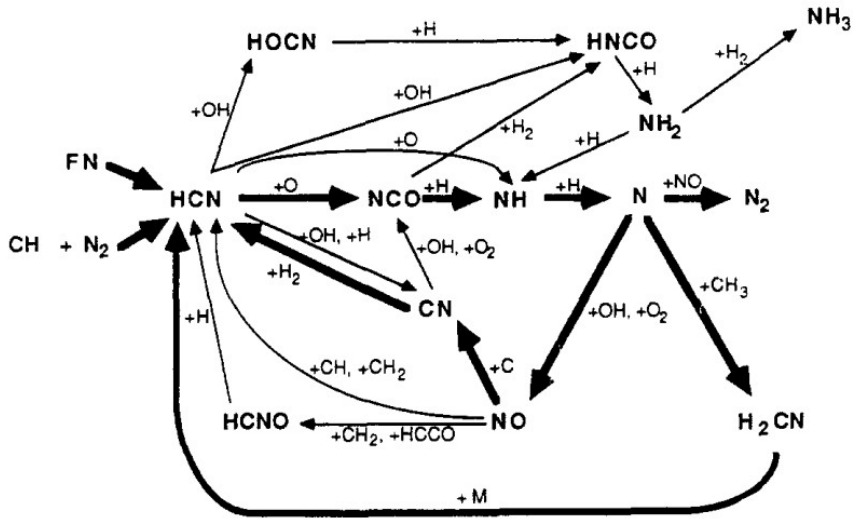

How to control for thermal NOx?

- Controlling excess air – **lean operation**.
- Reducing temperatures – **heat transfer** through impingement on surfaces: burner, coals etc..
- Affecting transit times in hot/rich zones through mixing (e.g. swirl).

- In an NG burner, **conflict** between lowering temperatures to **reduce NOx** and producing incomplete combustion (**soot and CO**).
- Hydrogen burners cannot have a CO problem. Or unburnt HC, or soot…
  - Duel fuel devices (i.e. will burn either fuel or blends) may have to deal with these issues.

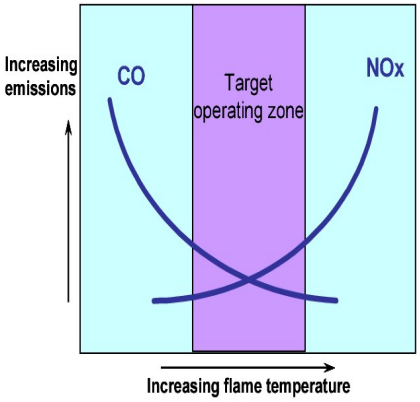

Quench distance and prevention of flashback

Quench Distance (QD) – largest characteristic distance (tube diameter *d*) that prevents the propagation of a flame**.**

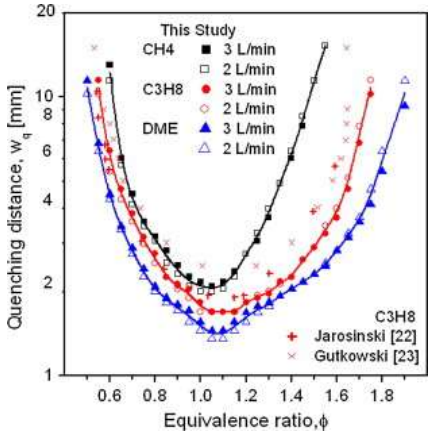

Liu and Kim 2014

QD for hydrogen ~ 10 times lower than for CH_4.

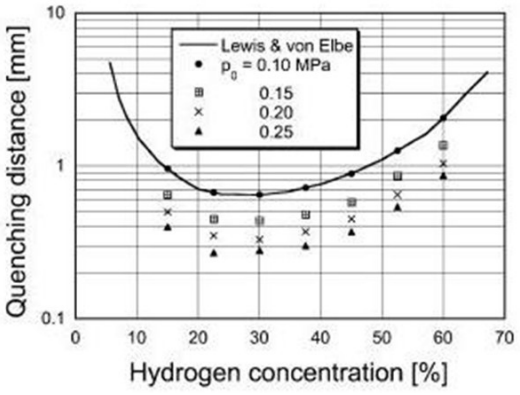

Yang et al. 2003

Flashback

- In the design of burners prevention of flashback critical.
- Ability of flame to travel back down fuel supply leads to safety risk.
- For premixed burners the risk is higher (O_2 available).
- Low QD for hydrogen requires change in design compared to methane to prevent flashback risk.
  - Smaller burner nozzles.
  - Diffusion rather than premixed flames i.e. non-aerated burners.

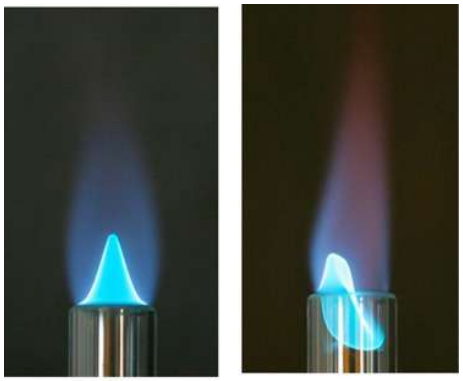

Design principles for H_2 fire

- Non-premixed
  - visibility and flash back avoidance.
- Impingement cooling
  - reducing flame temperatures and NOx.
- Balance between flame visibility and NOx emissions.
- Small burner nozzle size
  - flash back avoidance.
- Non-premixed flame was clearly visible without and additives.
- Design of NG replacement fire was entirely feasible but there is low public approval for the use of hydrogen in domestic settings.

Challenges for gas turbine operation on H_2

- Hydrogen may find more use as a storage medium – followed by use in gas turbines during periods of peak electricity demand.
  - Hydrogen peaker plant.

Challenges

- NOx emissions – high flame *T* leading to thermal NOx formation.
- Potential for oscillations – due to high flame speeds, instabilities.
- Flashback – QD and flame speed issues.

- MHPS, a joint venture between Japanese giants Mitsubishi Heavy Industries and Hitachi is addressing such problems.
  - "diffusion combustor" based on low-NO_x technology that injects fuel to air. Steam injection used to control NOx.
- GE also operating turbines with high $\%H_2$ in fuel mix.

Challenges for gas turbine operation on H_2

- NOx traditionally controlled in GTs using premixing
  - Lean operation in primary zone reducing *T*s.
- Switching to hydrogen makes premixing highly questionable
  - larger flammability limits (Chiesa et al. 2005)
  - lower ignition temperatures of hydrogen with respect to NG.
- Diffusion burners more commonly used.

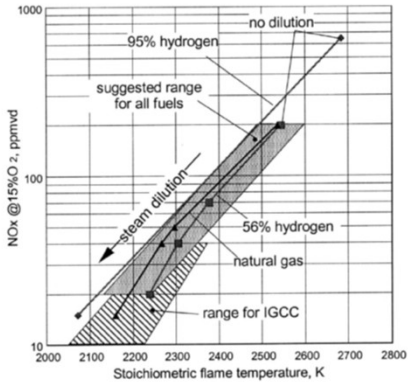

Steam supresses O radicals, inhibiting thermal NOx which normally occurs through

$N_2 + O \rightarrow NO + N$

$N + O_2 \rightarrow NO + O$

Combustion research opportunities

- Since all devices would need to be redesigned, CFD for reacting flows + NOx formation could be vital.
  - Gas turbines.
  - IC engines.
  - Boilers, fires, cooker burners.
  - H_2 injection systems.
  - Control systems.

- Rate coefficients and transport properties important.
- Mixed fuels or dual fuel systems even more challenging.

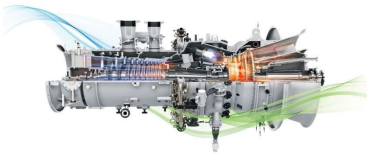

AMMONIA (Kobayashi, 2019, Glarborg, 2018)

- **Why?** Economic storage and transport of H_2 remain challenging especially in countries and regions currently lacking NG pipeline infrastructure.
- Ammonia in liquid form at room temperature (25°C) when pressurized to 9.90 atm or temperature of −33.4°C at atmospheric pressure.
  - Cf 100-300 atm or -250 °C for liquefied H_2
- Easier to transport/higher energy density than H_2. Use as a direct fuel or H_2 carrier.
  - equipment designed for the storage and transport of propane is likely applicable also for ammonia.
  - already transported for use in fertilisers.
- **Challenges:**
  - high ignition temperature and low maximum burning velocity
  - difficult to ignite and stabilise flames, may require co-firing or pre-heating
  - emissions (NOx, NH_3 slip, N_2O)
  - toxicity and odour which will impact on public acceptance
  - materials compatibility.

The vision…

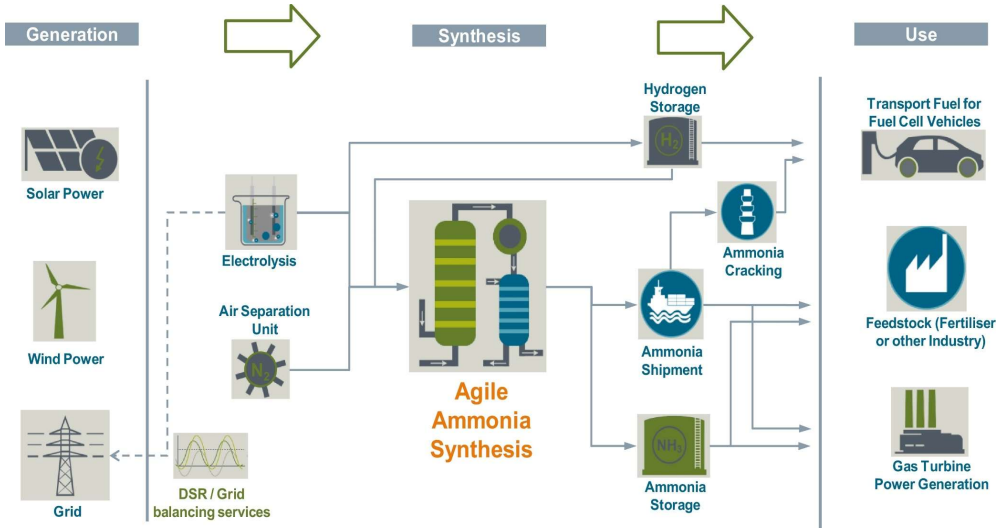

Ian Wilkinson, Siemens.

Direct ammonia formation from renewable electricity?

- The Haber Bosch process that forms ammonia from H_2 and N_2 requires high pressures and temps.
  - Energy intensive reducing overall round trip efficiency.
    - New developments attempting to produce NH_3 directly using reverse fuel cells.
    - Water reacts at anode making H+ ions which migrate to cathode where they react with N_2 to form ammonia.
    - Reaction is efficient, but slow.

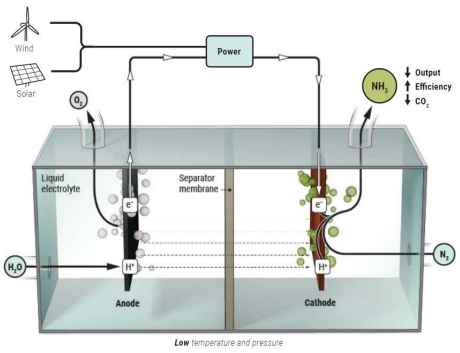

Science, 12 JUL 2018, ROBERT F. SERVICE

Features of ammonia

- Ammonia has a high N–H bond dissociation energy of ~107 kcal mol^{-1} reported via both experiments and quantum chemistry calculations (Monge-Palacios (2024))
- Generally larger than those of C–H and O–H bonds in say alcohols (other alternative fuels)
  - C–H and O–H bond dissociation energies in tert-butanol are 103.9 and 104.1 kcal mol^{-1}, respectively,
  - C–H bond of the tertiary C atom in iso-propanol is 94.1 kcal mol^{-1}.
- Low reactivity and high resistance to auto-ignition.
- Lower laminar flame speed than hydrocarbon and oxygenated fuels.

Kinetics of oxidation

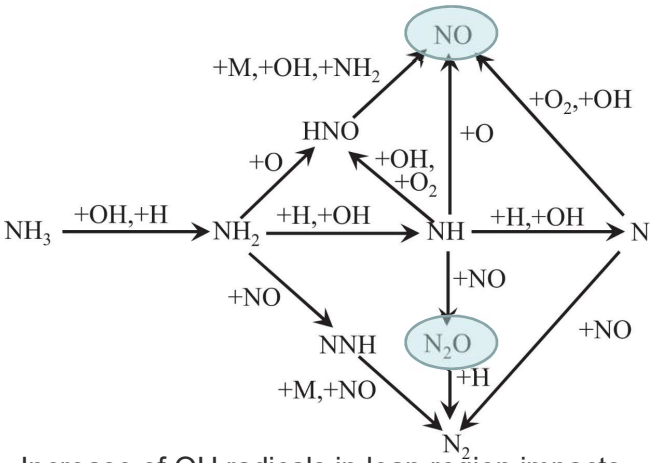

- Increase of OH radicals in lean region impacts production of HNO, thus increasing NOx.
- Stratified injection or mild combustion (Sabia et al., 2021) may offer solutions.

- Emissions of NOx and unburnt NH_3 key.
- Both contribute to atmospheric particulates and acidification.
- Reactor conditions will strongly determine selectivity of products.
- Even low concentrations of N_2O would be problematic from the climate perspective due to its high GWP and long atmospheric lifetime.

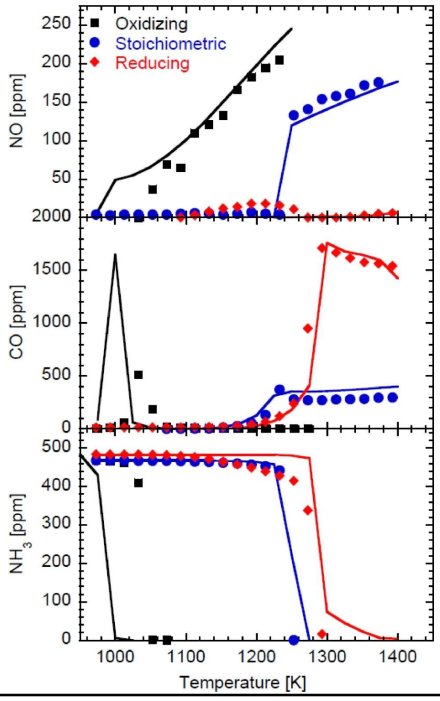

Example of model performance, (Glarborg, 2018)

- CH_4 = 2508 / 2513 / 2515 ppm, O_2 = 3480 / 5040 / 40100 ppm, NH_3 = 484 / 468 / 468 ppm; balance N_2.
- All experiments were conducted in a 12 mm inner diameter alumina reactor at 1.05 atm with a residence time in the isothermal zone of 1296/T(K).

Challenges for modelling ammonia combustion

- Historically, nitrogen chemistry has been modelled for the purpose of predicting NOx formation in H_2 and hydrocarbon flames and NOx reduction in selective non catalytic reduction (SNCR) processes.
- Need to model both cracking and oxidation
  - co-firing with more reactive fuels may be necessary.
  - some systems could be catalytically assisted processes.
- There could be missing intermediate species and pathways within our current understanding of nitrogen chemistry.
- The usual use of “typical” reaction pathways used for hydrocarbons does not apply here.
- There has been an upsurge in mechanisms for ammonia combustion from the community – with different performance for different predicted targets.
- See reviews by Monge-Palacios (2024), Valera Medina (2018), Kobayashi (2019), Sun (2025). The former paper gives a list of available mechanisms.

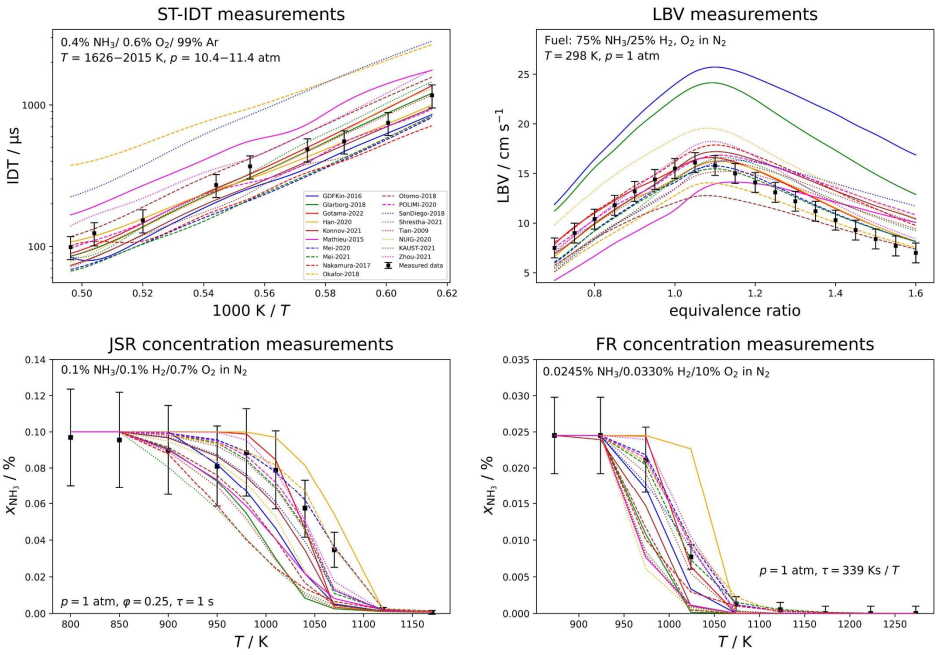

Kawka et al. (2020) and Szanthoffer et al. (2023) compared recent mechanisms and ability to reproduce IDTs and flow reactor concentrations – **see later for error analysis**.

Bar chart of frequencies of data points when the mechanisms could reproduce them within given thresholds of their standard deviations (σ). 100% means all investigated data points in the case of NH_3/H_2 fuel mixtures - 3219 data points.

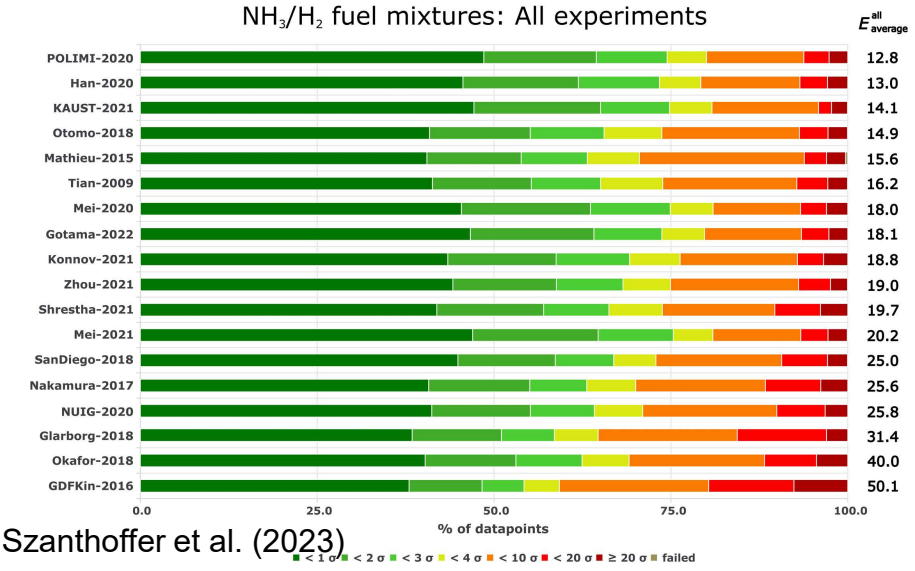

- No model is even close to perfect.
- Sensitivity analysis required to investigate causes of discrepancies and inconsistencies between models.

Szanthoffer et al. (2023)

Pyrolysis, DeNOx and NOx formation routes

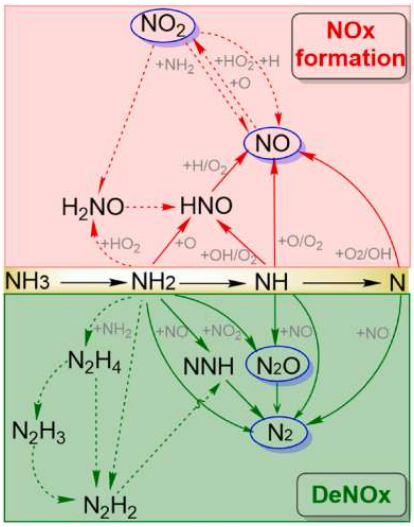

Monge-Palacios (2024)

- Important pyrolysis pathways include:
  - $NH_3 \rightarrow NH_2 + H$, $NH_3 + H \rightarrow NH_2 + H_2$.
- N_2 pathways must be incorporated via the combination of NH_i radicals
  - important under pyrolysis and rich flame conditions.
- In presence of oxygen, NH_3 can be consumed by OH, O, and HO_2 radicals via H-atom abstraction yielding NH_2.
- $NH_3 + OH \rightarrow NH_2 + H_2O$ is vital as the main chain-propagation reaction channel
- Under low- and intermediate-temperature conditions, HO_2 radical critical for oxidation chemistry of ammonia.
  - NH_2 and HO_2 combine to form H_2NO, whereas NO and HO_2 react to produce NO_2.
  - Therefore, under low- and intermediate-temperature conditions, H_2NO and NO_2-related reactions are vital for determining the ammonia oxidation chemistry

Lean vs. rich conditions (Sun et al., 2025)

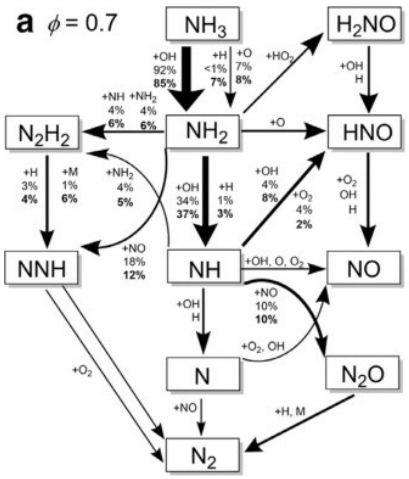

Arrow thickness indicates ratio of reaction flux to total reaction flux from fuel

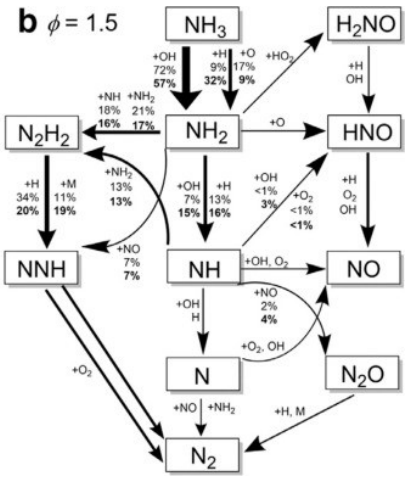

N_2O route has to be prevented due to it's high GWP!

Controlling OH concentrations e.g. by fuel staging or high pressure combustion important for controlling NOx/N_2O.

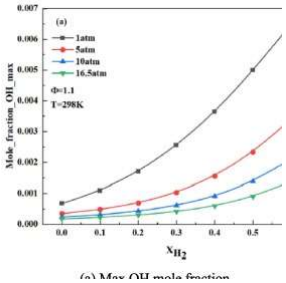

$NH_3 + OH \rightarrow NH_2 + H_2O$

- Glarborg et al. (2025) revisited this reaction using high level theory, using composite energies based on extrapolations to a complete basis set including the effects of higher order electronic excitations on the electronic energies along the variational reaction path (CCSD(T)-F12/cc-pVQZ-F12 level).
- Tested a revised model for H_2 assisted ammonia combustion in a premixed flow reactor – attempting to resolve discrepancies found in H_2 consumption found in earlier work of Alzueta et al. (2024) for reducing conditions using a laminar flow tubular reactor.

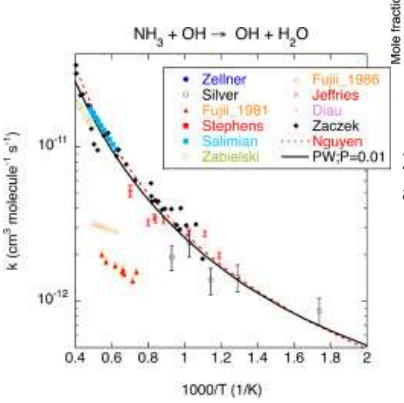

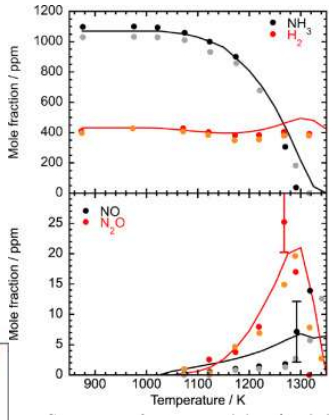

2:1 NH_3/H_2 mixture at atmospheric pressure

Renewable electricity to liquid fuels

Power to liquid fuels (PtL fuels)

- IF (big if currently…) we have abundant renewable electricity, excess can be used to create liquid fuels as storage method.
  - Create H_2 from electrolysis (TRL 5-8, depending on process type).
  - Capture CO_2 from **ambient air** (TRL 6).
  - Synthesis of liquid hydrocarbons with subsequent upgrading and refining (TRL 8-9).
- Why bother? Why not just store electricity or H_2?
  - High energy densities in terms of volume and weight.
  - Well suited to current infrastructures.
  - Long term storage.
- Applications? Aviation, heavy goods, shipping?
  - Sectors where other methods are likely to struggle due to battery weights, range etc.

Overall process

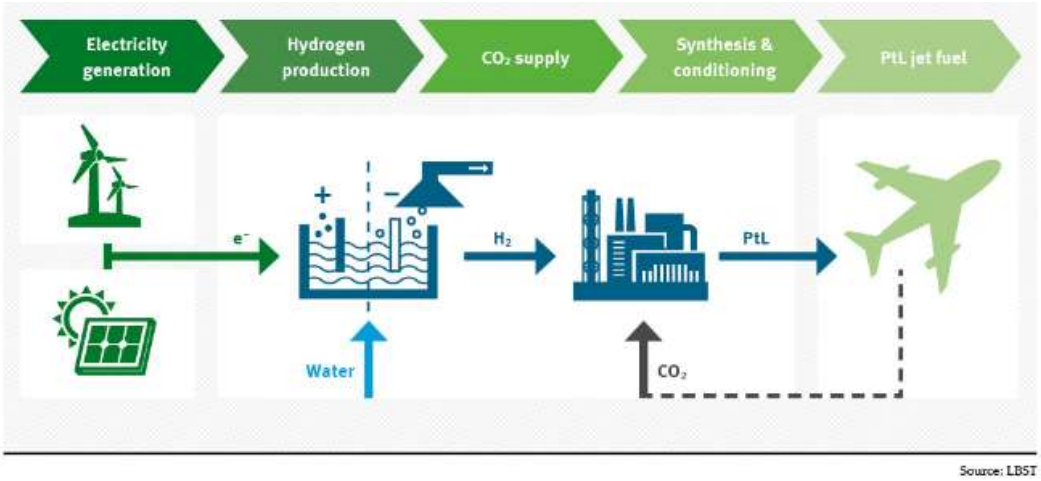

PtL vs. advanced biofuels

Advantages

- High energy density.
- Huge renewable power potential.
- Lower aromatics and zero sulphur compared to traditional fuels and cleaner to burn.
- “Drop-in” capabilities.
- Tailorable in terms of fuel structure, carbon chain length etc which means that properties can be tuned for applications.

Disadvantages

- Cost: H_2 production, Air CO_2 capture.
- Readiness of systems integration.
- Overall efficiency low – although in terms of land higher than biofuels.
- Non-zero air pollutants (NOx, PM).
- Could lead to lock in for traditional engines preventing development of zero emission innovations.

Costs

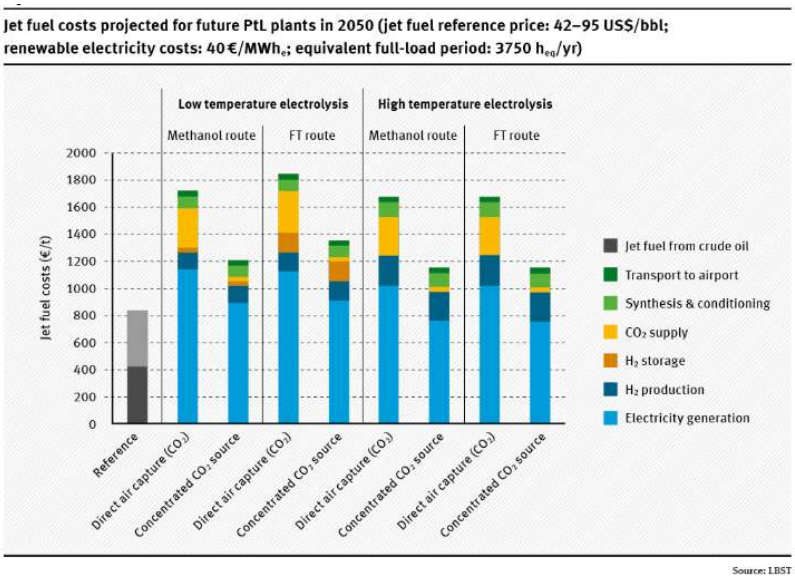

- Worth highlighting that cost estimates/forecasts are highly uncertain and will change over time and between studies.
- Without costing carbon, no renewable fuel competes easily with fossil fuel equivalents.

Production of PtL fuels

(German Environment Agency (2016))

- Two principle production pathways:
  - Fischer-Tropsch (FT) synthesis and upgrading.
  - Methanol (MeOH) synthesis and conversion.
- ASTM jet fuel standard already allows for a 50 % blend of FT synthetic fuel. PtL via the methanol pathway is not yet approved.
- It is pathways and not fuels that are approved for aviation use.

FT process

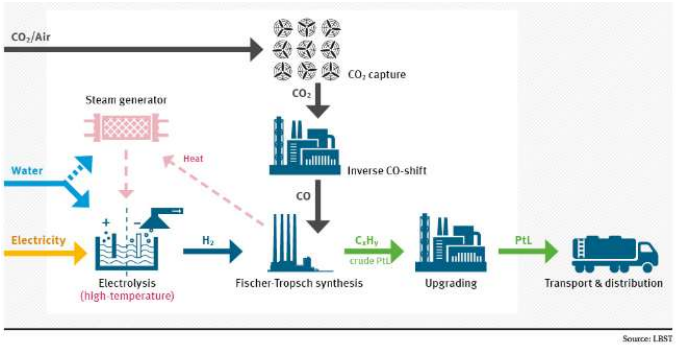

- Already commonly used in biomass-to-liquid (BtL), gas-to-liquid (GtL) and coal-to-liquid (CtL) processes.
- Requires CO which in PtL has to be obtained from CO_2.

- CO_2 converted to CO via inverse CO-shift reaction using the **reverse** water gas shift process.

  $CO + H_2O \rightleftharpoons CO_2 + H_2$

- Or, high-temperature electrolysis may allow for co-electrolysis of steam and CO_2, producing H_2 and CO in single step.

Simplified model

FTS can be simplified as a combination of the FT reaction and the WGS:

$$CO + \left(1 + \frac{m}{2n}\right) H_2 \rightarrow \frac{1}{n} C_nH_m + H_2O \quad (R_{FT})$$

$$CO + H_2O \rightleftarrows CO_2 + H_2 \quad (R_{WGS})$$

where *n* is the average carbon number and *m* is the average number of hydrogen atoms of the hydrocarbon products.

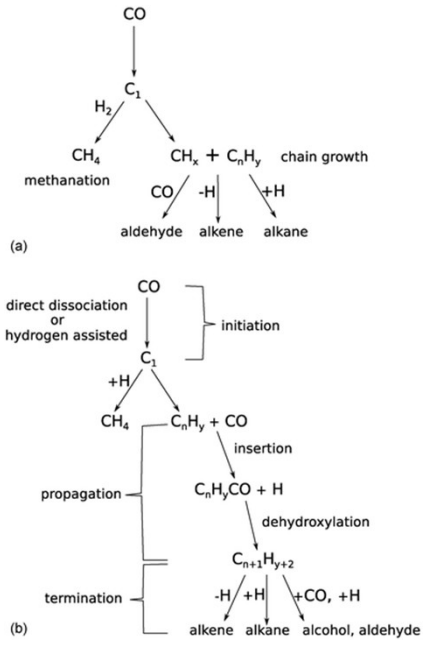

Van Santen, 2013

FT process

- Catalytic process at *T* = 200–300° C and *P* = 10–60 bars with choice of catalyst (e.g. cobalt, iron, ruthenium) depending on H_2 to CO ratios.
- Main products linear paraffins, α-olefins, alcohols.
- **Possibility for selectivity of final products based on process conditions.**
- Lack of detailed heterogeneous reaction kinetics potentially a limitation to optimal reactor design and product selectivity (Van Der Laan, 2011).

Methanol synthesis

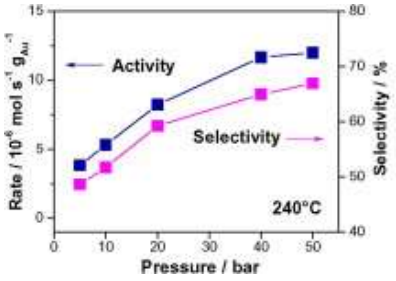

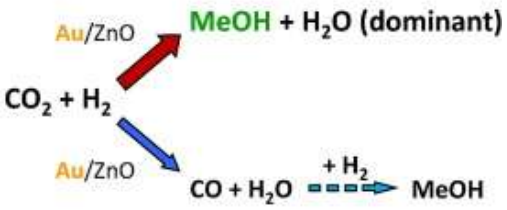

- Large number of catalytic processes developing for methanol synthesis from CO_2 + H_2.
- Methanol formation is favoured by low temperatures and elevated pressures.
- Yields can be highly dependent on process conditions and catalyst choice.
- Optimisation requires knowledge of heterogeneous kinetic processes.

Combustion of FT fuels

- Features of FT fuels:
  1. high cetane number
  2. low aromatics, C/H ratio and sulphur
  3. unwanted oxygenates can be removed through upgrading
- Advantages
  1. facilitates lower pressures and temperatures due to shorter IDTs – lowering NOx formation potential.
  2. low catalyst poisoning due to low sulphur, low soot formation due to lack of aromatics. However also leads to low lubricity which can be improved with additives.
  3. low oxygen content an advantage for aviation applications due to required energy densities.
- Overall synthetic fuels have emission benefits in the reduction of HC, CO, NO_x and PM.
- Lower volumetric energy density than diesel may require updated injection system.

Gill et al., 2011

Cetane number

- Higher cetane number means shorter IDT.
- Fraction of fuel burnt under pre-mixed conditions reduced lowering *T*s, *P*s and *P* gradients.
- Lowers production of thermal NOx.
- Shorter IDT gives more time for complete combustion and particle oxidation potentially also lowering PM.

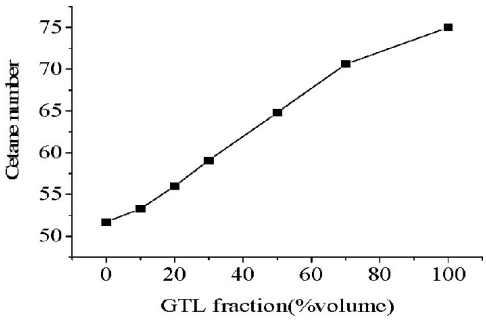

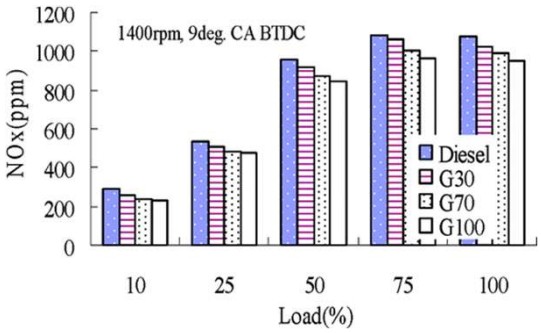

Wu et al. 2007

- Process of soot formation (Michelson 2017).

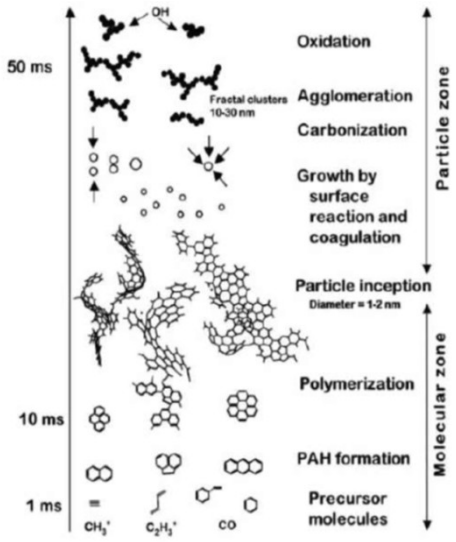

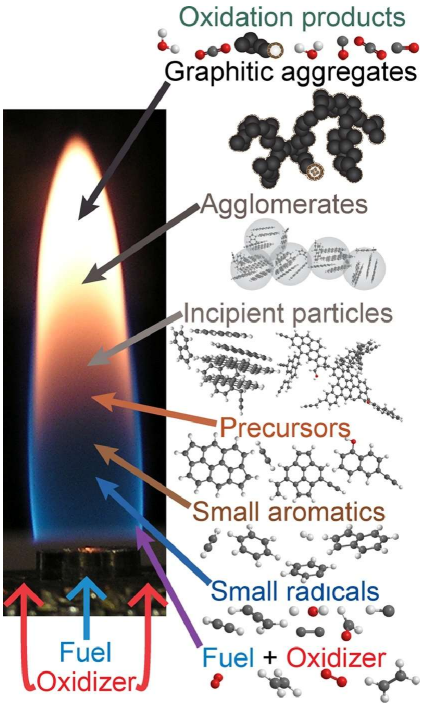

Aromatics

- Aromatics involved in early stages of soot formation.
- Lowering aromatics lowers PM formation potential.
- Aromatics also have higher adiabatic flame temperatures than paraffinic equivalents.
  - lower *T* – lower NOx.

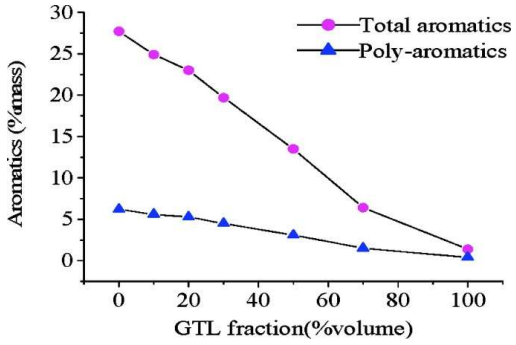

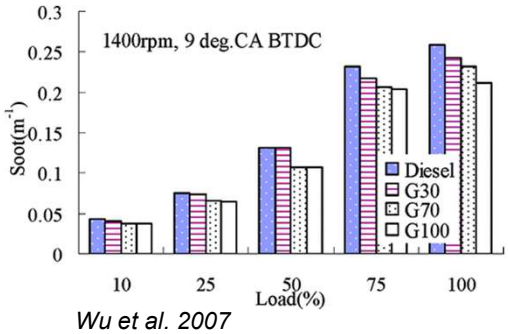

Wu et al. 2007

Biofuels

Range of biofuels

Feedstocks

- 1st generation
  - corn, wheat, sugar cane, beet
  - palm oil, rapeseed, soybean, sunflower
- 2nd generation
  - copice, forest residue, miscanthus, corn stover, bagasse.
  - jatropha, camelina, used cooking oil/tallow.
- 3rd generation
  - Algae.

Fuel

- 1st generation
  - methanol, ethanol, butanol
  - biodiesel, HVO.
- 2nd generation
  - methanol , ethanol, butanol
  - biodiesel, HVO.
  - ethers, levulinates, furans
- 3rd generation
  - range of products incl. biodiesel.

2nd Generation Biofuel Production

- Essential to avoid competition with food production.
- Mandated by EU Renewable Energy Directive II.
- BUT - more difficult to break bonds in lignocellulosic materials.

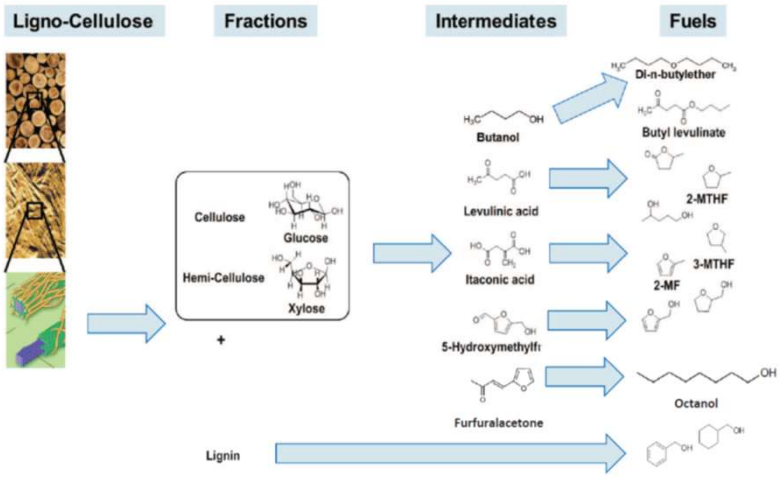

Other proposed biofuels?

- Furans e.g. from corn stover
  - 2-methylfuran (MF)
  - 2,5-Dimethylfuran (DMF)
  - tetrahydrofuran (THF)
  - 2-methyltetrahydrofuran (MTHF)
- Long chain alcohols e.g. octanol
- Ethers (DME, DEE, DBE)
- Levulinates
- Biofuel blends

Not at high TRL stage apart from DME.

Production bio-ethanol

Limayem and Ricke 2012

- Ethanol from 1st gen crops is produced via acid hydrolysis and sugar fermentation using yeast + distillation/deyhdration.
  - Conversion of lignocellulosic biomass more difficult than hydrolysis of starch due to carbohydrate polymers: **cellulose** composed of glucose molecules bonded together in long crystalline chains, **hemicellulose** consisting of a mixture of xylose, mannose, galactose, or arabinose and **lignin**.
  - Not soluble in water.
  - Currently higher production costs that could be reduced by G-engineered strains or use of thermochemical methods.

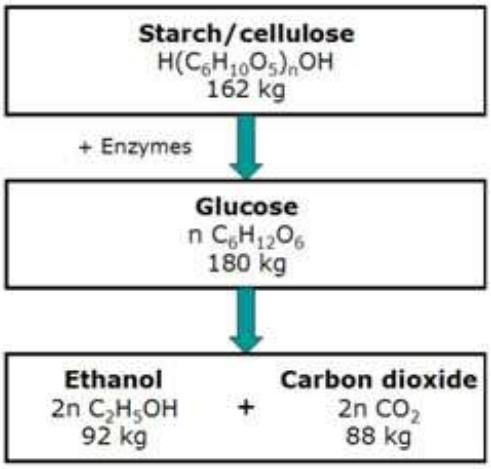

Production bio-butanol

Amiri and Karimi 2019

- Currently based on similar production process to ethanol but more costly to produce with lower yields.
- E.Coli strains developed with genes coding for 2 enzymes that converted keto-acids into aldehydes, and aldehydes into 1-butanol.
  - Able to produce butanol at much higher efficiencies.
  - Strain less sensitive to butanol concentration.
- Acetone–butanol–ethanol fermentation (ABE fermentation), also known as the Weizmann process, is a process that uses bacterial fermentation to produce acetone, n-butanol, and ethanol from carbohydrates such as starch and glucose.
  - Could be used as a blend or would require separation processes.

DME production

- Can be produced from lignocellulosic biomass.
  - Gasification to produce syngas.
  - Syngas to methanol.
  - Dehydration of methanol. 2 $CH_3OH \rightarrow (CH_3)_2O + H_2O$.
- Can also be produced from wind-based electrolytic hydrogen and captured carbon dioxide (air capture or ethanol fermentation process) .
  - Potentially lower lifecycle GHG and NOx, SOx emissions cf. biomass.

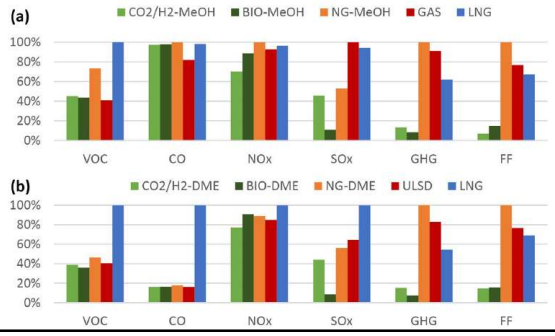

Matzen, 2016

Important properties of biofuels

- Must meet stipulated CO_2 reductions e.g. from EU Renewable Energy Directive (RED II).
- Physical properties need to be suitable for replacing or blending with petroleum derived equivalents.
  - Viscosity, flash point, density, energy density, hygroscopy, materials compatibility etc.
- Non-toxicity.
- Chemical properties need to be **suitable for replacing or blending** with petroleum derived equivalents.
  - Cetane number, octane number and sensitivity, heating value, flame speeds, NOx, PM, UHC, CO emissions. **Drop in**.
- High yields from biomass source.
- Cost competitive (controversial point since strongly affected by subsidy and taxation regimes e.g. carbon tax or FF subsidies).

Carbon footprint
Why does the generation of biofuel i.e. the feedstock matter?

Question – both FFs and biofuels produce CO_2 when burned, so why are we even considering biofuels?

Data from Royal Academy of Engineering report: Sustainability of liquid biofuels, 2017.

C foot-print bioethanol – 1st gen

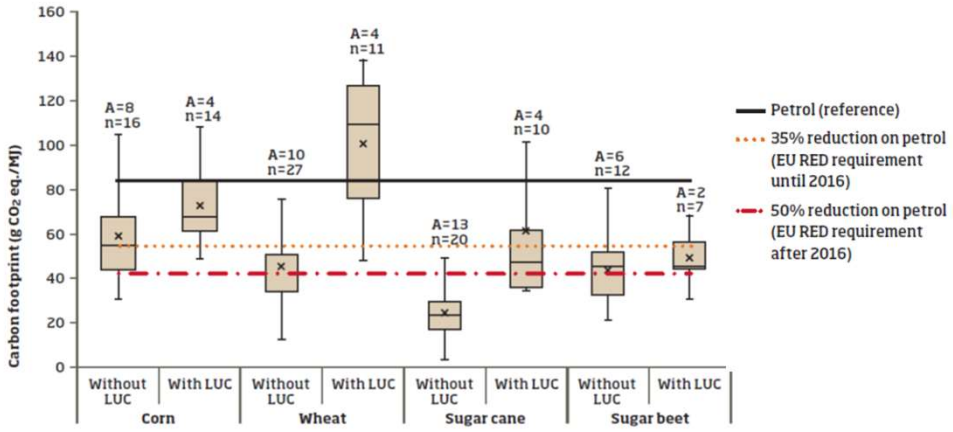

If land use change is used then no source meets the EU RED apart from sugar cane. N_2O from fertiliser and deforestation are problems.

C foot-print biodiesel – 1st gen

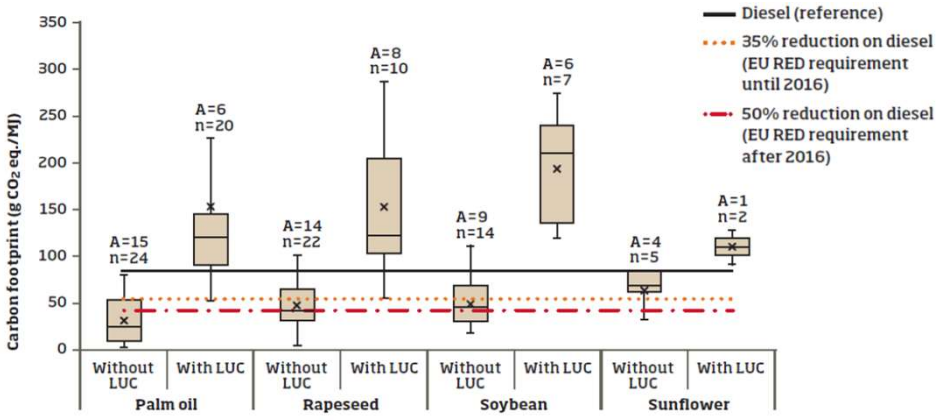

If land use change is used then no source meets the EU RED for biodiesel.

C foot-print bioethanol – 2nd gen

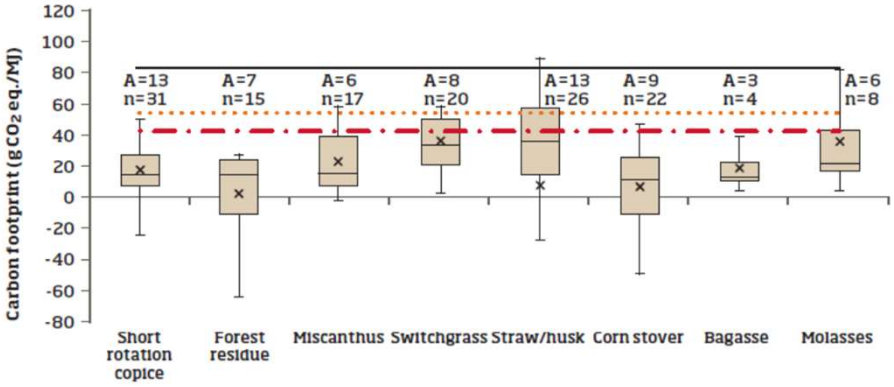

Much lower LCA CO_2 than 1st gen due to lower fertilisers and use of waste materials e.g. forest residue or co-product allocation.

Carbon footprint of fuels (Al Breiki, 2021)

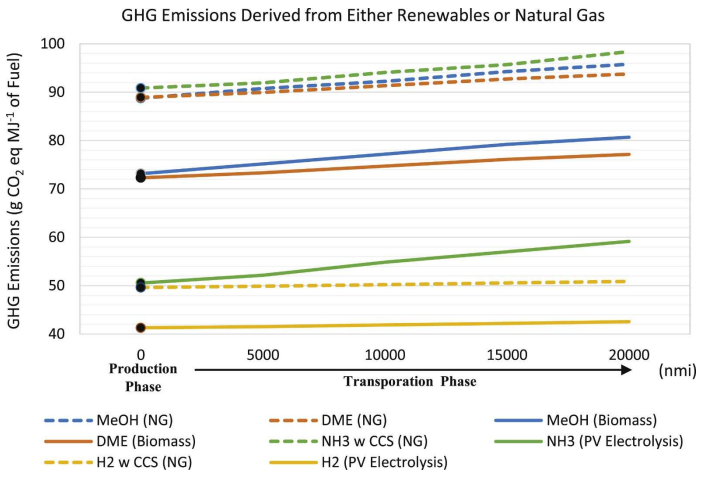

Sensitivity analysis on various distances of a full life cycle of energy carriers derived from either renewables (solar PV and biomass) or natural gas covering production, transportation, and utilization phases

Fuel properties

Wide range of physical/combustion properties to be matched for drop-in fuel, etc!

Property	Standard	Base fuel	Standard Limits
Ignition Delay Time		Gasoline	
Cetane Number	EN 590	Diesel	51
RON	EN 228	Gasoline	95
MON	EN 228	Gasoline	85
Emissions	Euro VI/VII	Both	
Viscosity at 40 C	EN 590	Diesel	2000 - 4500 mm^2/s
Density	EN 590 EN 228	Diesel	820 - 845 kg/m^3 720 - 775 kg/m^3
Cloud Point	EN 590	Diesel	-10 to -34 C depending on class
Lubricity	EN 590	Both	Wear scar diameter 460 µm
Copper Strip Corrosion	EN 590, EN 228	Both	Class 1
Materials Compatibility		Both	
Oxygen content	EN 228	Both	3.7 % m/m
Heating Values			
Toxicity ….. Etc. ↓			

Vom Lehn, 2021 - database

Property comparison

	ETHANOL	ISOBUTANOL
Blend RVP	18–22 psi	4.5–5.5 psi
Blend Octane	112	102
Energy Content (% of gasoline)	65%	82%
Water Solubility	Fully Miscible (100%)	Limited Miscibility (8.5%)
Oxygen Content	35%	22%

	OXYGEN CONTENT (%)	EV	RINS GENERATED PER 100 GALLONS FINISHED PRODUCT
12.5% Isobutanol	2.7	1.3	16.25
10% Ethanol	3.5	1.0	10.00
16.1% Isobutanol	3.5	1.3	20.93
15% Ethanol	5.2	1.0	15.00

Current limit for drop-in fuel

Properties of furans and ethanol vs. RON 95 gasoline

	RON 95 E10 Gasoline (EN51626-1)	Ethanol	MF	MTHF	DMF	TOL
Boiling T. (K)	309–463	351	337	351	367	384
Vapor P at 20 °C (kPa)	–	5.8	13.9	13.6	–	2.8
Low Heating Value (MJ/L)	30.8	21.1	27.6	28.2	30.1	35.3
RON	>95	109	103	86	119	121
Distribution Coefficient K_D[a]	–	–	–	7.2 ± 0.4	4.9 ± 0.2	4.9 ± 0.3

Gandarias 2018

Flash point of biofuels

- Typically gasoline will not form a flammable mixture until the ambient temperature is below -20°C, which is the rich limit.
- However, when ethanol is added the higher flash point and different stoichiometry make an explosion more likely at ambient temperature.
- Measurements in Sweden have recently shown that E85 has a flammable mixture at 2-5°C (rich limit) and down to -18°C (lean limit or flash point).
- **Longer carbon chains increase the flash point**, potentially making longer chain alcohols more suitable for diesel blending.

Flashpoint of example fuels

Fuel or fuel component	Flashpoint
Gasoline	~ -65° C
Diesel	>52 °C
Biodiesel	>130 °C
Jet fuel	>38 °C
Ethanol	16.6 °C
N-butanol	35 °C
Iso-butanol	28 °C
1-pentanol	49 °C
DMF	−1 °C
MF	−22 °C
DME	−41 °C

For alcohols, 5 carbons are needed to reach realm of diesel. Could affect storage, safety issues.

COMBUSTION PROPERTIES OF SELECTED ALTERNATIVE FUELS

Developing an understanding of new fuels

- Our understanding of different fuel oxidation pathways has developed over time: $H_2 \rightarrow H_2/CO \rightarrow CH_4 \rightarrow$ alkanes.
- Biofuels contain oxygen and have different functional groups (O single and double bonds, C-C double bonds etc.).
- Review from Westbrook et al. (2021) recommended reading on mechanistic development.
  - Develop key reaction pathways based on experience from well known fuels, bond energies.
  - Populate rate coefficients often using estimates.
  - Conduct fundamental experiments potentially leading to better tuning of rate constants.
  - Perform theory calculations for sensitive fuel specific reactions.
  - **ITERATE** – until some consensus emerges.
- Now we have machine learning – how/does that change things?

Effect of alcohol (OH group) addition on RON

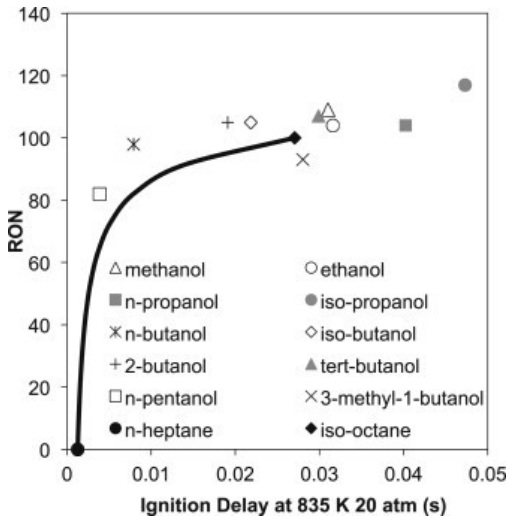

(Sarathy et al, 2014)

- Varies according to C number and bond structure with iso-propanol showing greatest knock resistance.
  - **Lower molecular weight** alcohols have highest ONs – suitable for blending with **gasoline** type fuels.
  - **C_5 and higher** have lower ONs and display significant low- and NTC-temperature reactivity, making them more suitable for **CI engine applications**.

Blends for diesel

- Longer chain alcohols likely to be more suitable for diesel blending due to higher CN.
- Octanol production process via acetone and furfural from biomass developed as part of “Tailor-Made Fuels from Biomass” program (Julis & Leitner, 2012, Heuser et al. 2013).

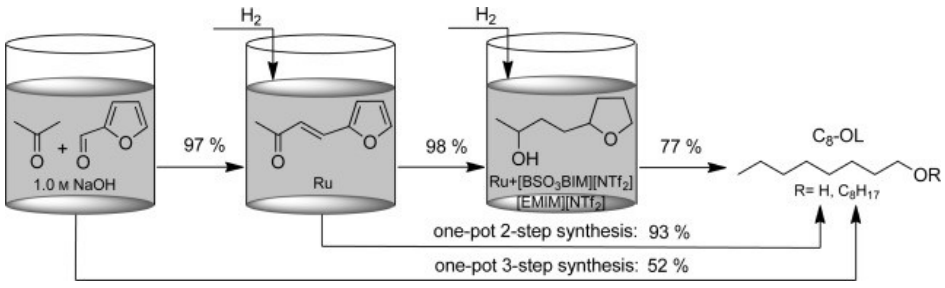

Alcohol octane numbers, (Pelucchi, 2020)

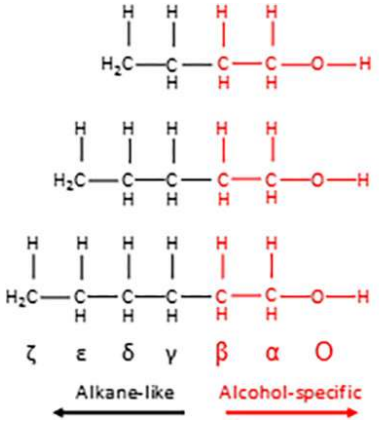

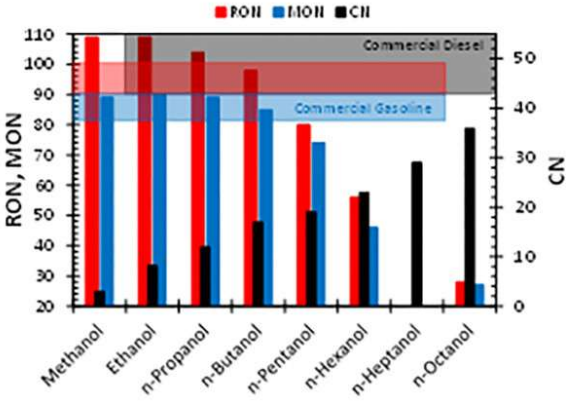

- Suggests different C number alcohols relevant for diesel vs. gasoline blending.

Effects on IDTs – alcohol blending

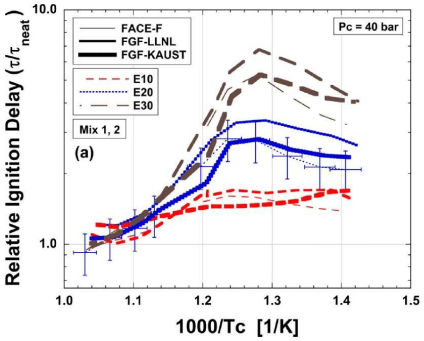

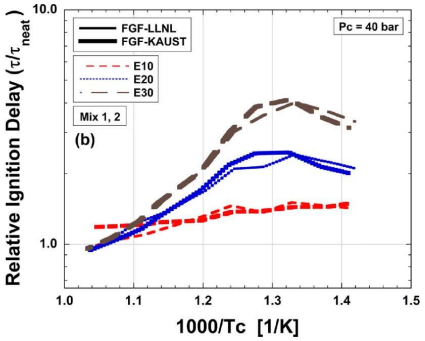

Experimental (a) and modelled (b) relative main IDTs for different blends (Cheng 2021)

- **Ethanol increases** ignition delays across all *T*, compared to RON94 FACE, although a small cross over for one surrogate.
  - On edge of NTC.

Butanols – n-butanol (Gorbatenko, 2019)

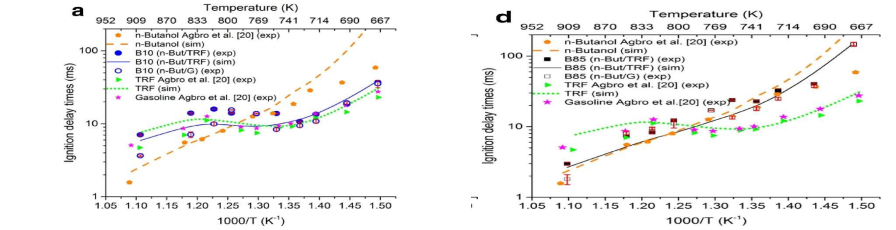

Brute force local sensitivity indices for ignition delay time for (a) 10% vol n-butanol+TRF blend and (b) 85% vol n-butanol +TRF blends

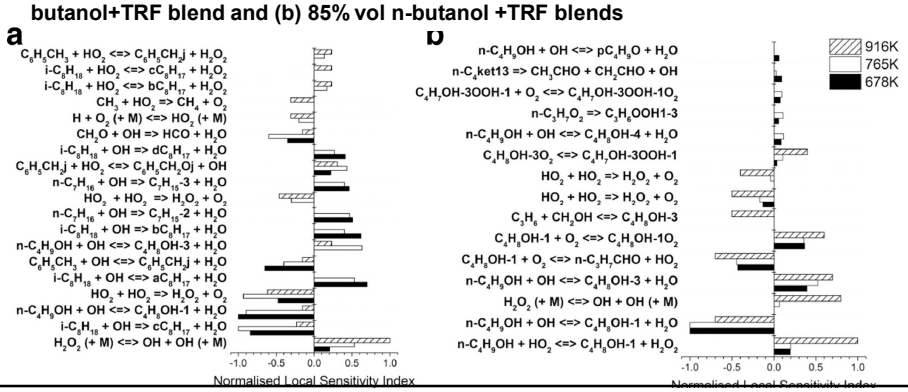

Does the use of AI mean we can predict for all fuels now?

- **No.** But…
- We know that high level theory calculations start to struggle for larger and larger molecules. We can't afford them computationally.
- We know that experiments for some types of reactions (radical-radical, +HO_2 etc.) are difficult to execute.
- Experiments are done at different conditions compared to device operation.
- But we can perform some experiments and theory calcs for small molecules and develop high quality data bases for functional groups based on this data.
- Machine learning can then help us to optimally use this data to predict rate coefficients and thermos data for larger molecules of interest if we use appropriate ways to partition available training data.

Influence of functional groups

- LT oxidation pathways depend on peroxy/QOOH radical chemistry – isomerisation to QOOH, 2nd O_2 addtition, formation of ketohydroperoxide (KHP) + OH, dissociation of KHP to give a 2nd OH.
- HT on $H_2O_2 \rightarrow OH + OH$.
  - Gap between can lead to NTC.
- **Different functional groups** on e.g. biofuels can affect the degenerate chain branching progress in different ways (Rotavera and Taatjes, 2021).
  - KHP can dissociate to give **2 stable products** and **not OH**.
  - selectivity of initial radical formation by H-abstraction from parent molecule affected by **C-H bond energy** near oxygenated group.
  - **ROO radical stabilization** and isomerization is changed by differences in relative stability created by effects of oxygenated functional group.

Influence of functional groups

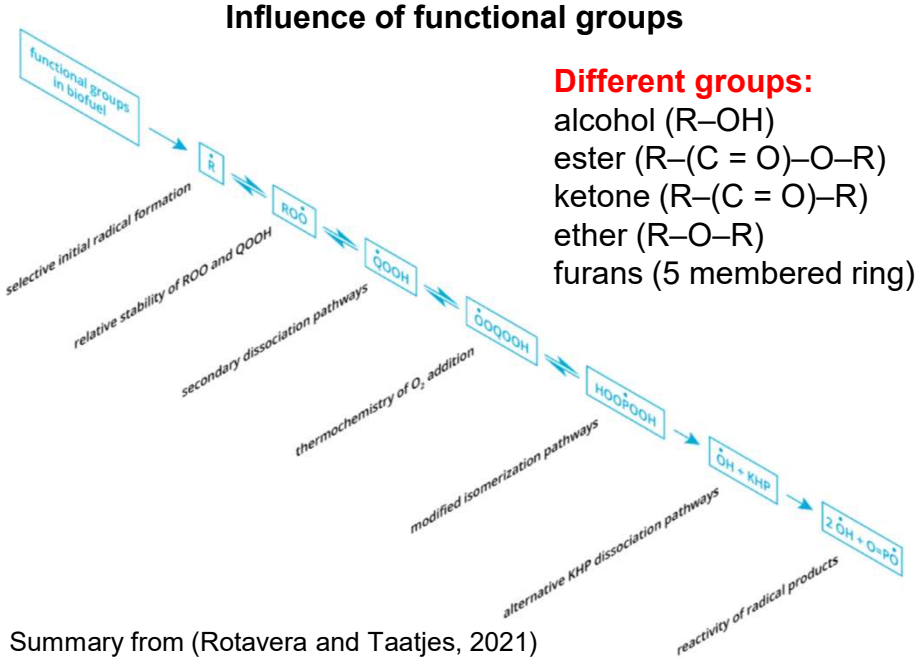

Different groups:
alcohol (R–OH)
ester (R–(C = O)–O–R)
ketone (R–(C = O)–R)
ether (R–O–R)
furans (5 membered ring)

Summary from (Rotavera and Taatjes, 2021)

General Oxygenates – thanks to Brandon Rotavera

Functional Groups Alter Chemical Mechanisms of Ignition

UNIVERSITY OF GEORGIA

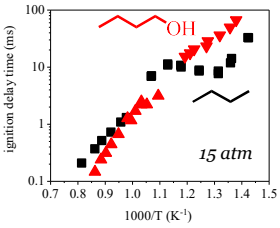

1-butanol/n-butane

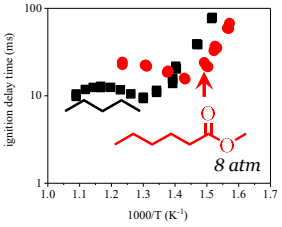

methyl hexanoate/n-pentane

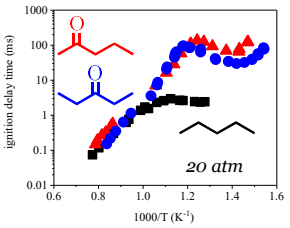

3-pentanone/2-pentanone/n-pentane

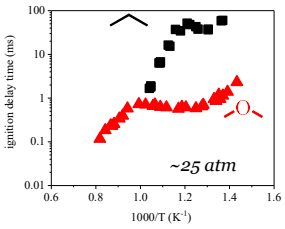

dimethyl ether/propane

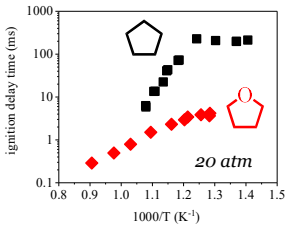

tetrahydrofuran/cyclopentane

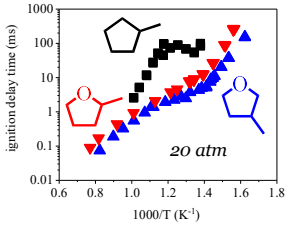

2-methyltetrahydrofuran/toluene

Emissions Characteristics

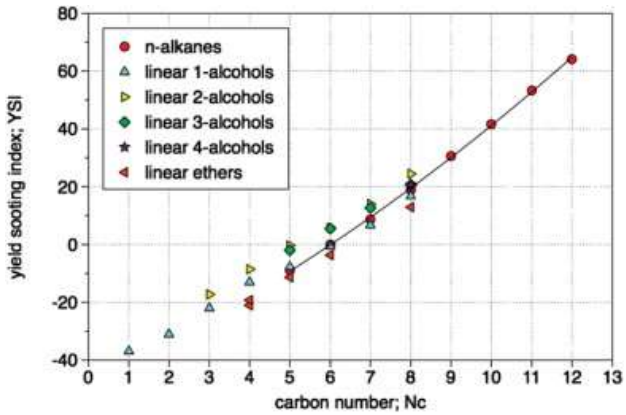

- Expect alcohol and ethers to reduce sooting tendencies compared to petroleum type fuels which contain alkanes and aromatics.
- Effects of carbon chain length and oxygen vs aromatic content.

(Sarathy, 2014)

Effects of oxygen content and dilution on TSI improvements cf diesel, (Pepiot-Desjardins, 2008)

- Smoke point measurements and modelling of n-heptane/toluene/oxygenate mixtures. Methane flames and rich homogeneous reactors.

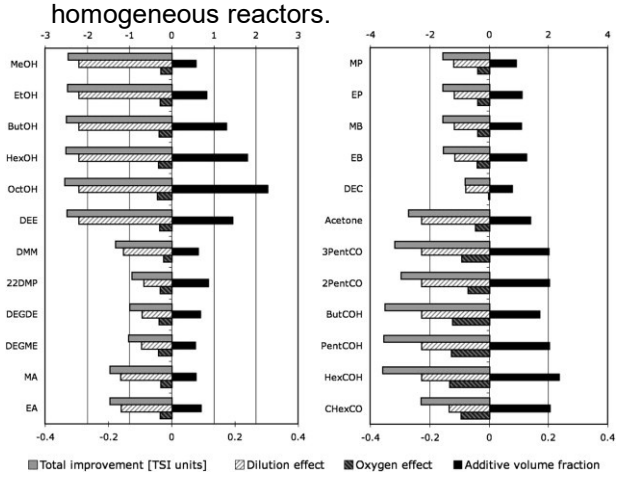

- Dilution effect depends on relative TSI of blended fuel.
  - Could be +ve or -ve
- Oxygenated groups were found to reduce sooting tendency of base fuel depending strongly on the nature of these groups.

Methyl esters

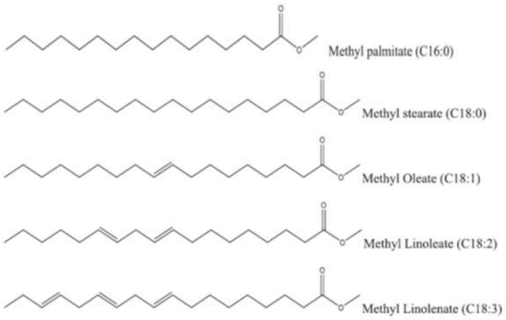

Derived from the esterification of oils – 1st generation biodiesel (Westbrook et al., 2021).

- Temperature dependence of reactivity of different components varies.
- Increasing number of C=C bonds and allylic C-H bonds decreases CN, fuel thermal stability and low-temperature reactivity.

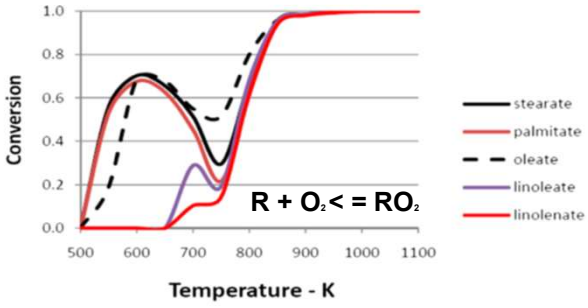

Furans

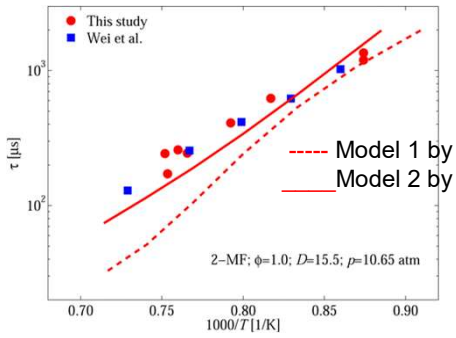

No low T chemistry

----- Model 1 by Sirjean et al.
____Model 2 by Somers et al.

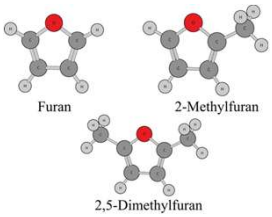

Eldeeb and Akih-Kumgeh (2014), Somers (2013)

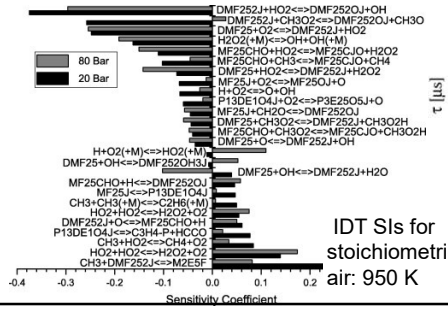

IDT SIs for stoichiometric 2,5 DMF-air: 950 K

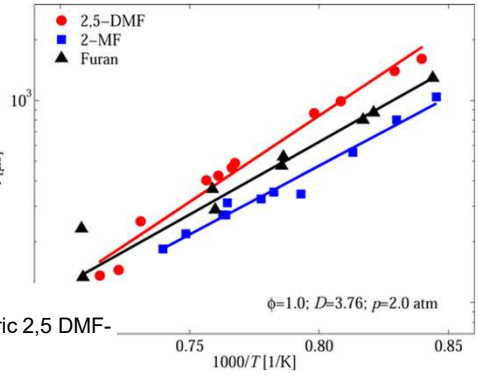

Remember earlier discussion on utility of different targets?

Somers (2013)

2,5 DMF investigation

- A single pulse shock tube to investigate the pyrolysis of 2,5 DMF.
- A low pressure shock tube to measure ignition delay times of dilute 2,5 DMF/O_2/Ar mixtures.
- A high pressure shock tube to measure ignition delay times of non-dilute 2,5 DMF/O_2/N_2 mixtures, representing “fuel in air”.
- A jet-stirred reactor to quantify mole fractions of reactants and products for the oxidation of dilute 2,5 DMF/O_2/N_2 mixtures.
- A flat-flame burner (heat-flux method) to determine laminar burning velocities of atmospheric pressure 2,5 DMF/O_2/N_2 mixtures as a function of equivalence ratio and unburnt gas temperature.

Includes new data on thermal decomposition of 25DMF2R radical from CBS-QB3 calculations and RRKM/ME modelling (Sirjean & Fournet, 2012)

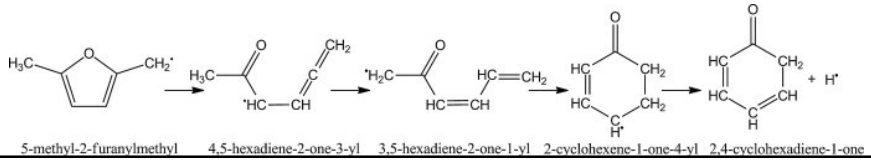

Evaluation data

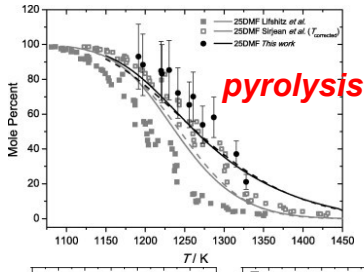

pyrolysis

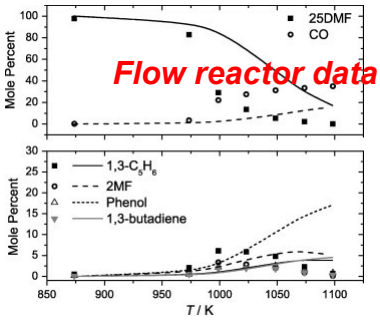

Flow reactor data

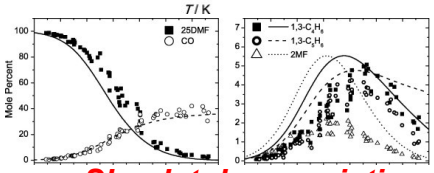

Shock tube speciation

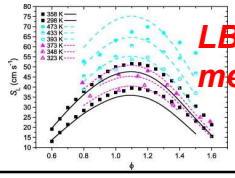

LBVs, heat flux method

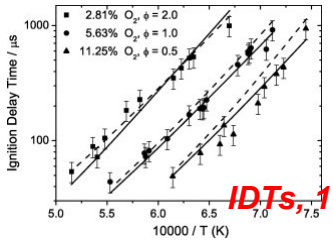

IDTs, 1 atm

Sensitivity analysis

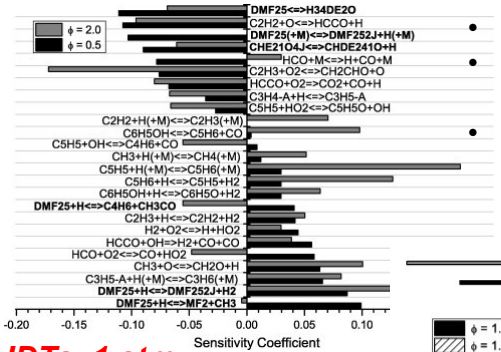

IDTs, 1 atm

- Good agreement shock tube.
- Good agreement effect of O_2 on IDT.
- LBV good except for rich conditions.

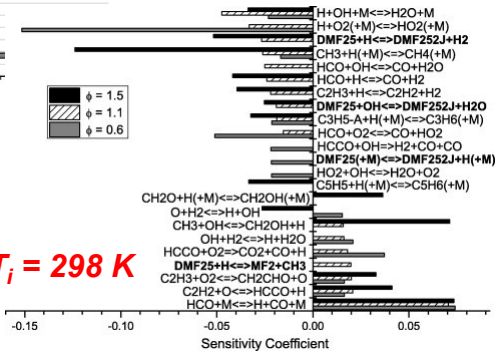

LBVs at 1.0 atm and T_i = 298 K

Remaining challenges for developing validated mechanisms

- For some complex oxygenated hydrocarbons, the data available for functional groups present is still sparse.
  - See earlier discussion about the best way to use clumpy data for parameter predictions.
- We do still need experimental data to validate models – we can't model everything without any grounding in real world data.
- The use of future fuels is likely to be as part of more complex blends (ammonia-hydrogen, methanol-hydrogen, methane-hydrogen, biofuel mixtures etc.).
  - Makes gathering validation data even more tricky.
- For non-C/H/O fuels we may not even have a complete understanding of important intermediates and reaction classes.
  - How do we estimate new species and reaction pathways?
  - Simple estimates based on collision theory coupled with sensitivity analysis?

Tailoring fuel mixtures?

- Biofuel and PTL fuel products can be selected through **optimisation of process conditions** during production process.
- Gives the opportunity to **tailor fuel mixtures** to obtain desired properties for drop in fuels/blends.
  - A lot of properties to optimise…
  - RON, CN, IDTs, flashpoints, emissions, physical properties, flame speeds etc.
- Depending on combustor and replacement fuel (gasoline, diesel, propane, jet fuel etc.) characteristics may vary. To get close to "**drop in**" characteristics:
  - Higher carbon numbers more similar to diesel.
  - Lower carbon numbers more similar to gasoline.
  - For replacement of jet fuel need mainly C8–C16 paraffins with some cycloalkanes and a small aromatic fraction.
- For ICEs adjustments of RON/OS/CN may allow **increased compression ratios.**

Biodiesel Blends

Table 2. Percentages of Methyl Esters in Each Type of Oil and Its Cetane Number CN

	sunflower	safflower	linseed	jatropha	cottonseed	corn	olive	tallow	palm	peanut	soy	rapeseed
palmitate	7	7	7	4	23	10	13	28	46	11	8	4
stearate	5	2	1	8	3	4	4	22	4	8	4	1
oleate	19	13	19	49	20	38	72	46	40	49	25	60
linoleate	68	78	19	38	53	48	10	3	10	32	55	21
linolenate	1	0	54	1	1	0	1	1	0	0	8	14
CN	49	50	39	58	51	49	55	58	62	54	47	54

- Different feed stocks lead to differing fractions of biodiesel components (Westbrook, 2021).
- Opportunity **to tailor CN** for use in unmodified engines.

*Impacts decisions on **crop choices** so that wider impacts on food production and deforestation can be minimised.*

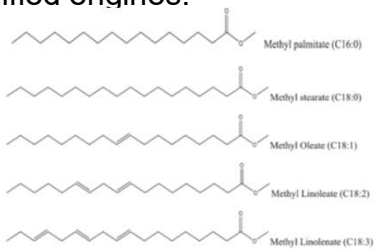

Example for ethanolic gasoline mixtures

- Biofuel blends derived from lignocellulosic biomass.
- CN and RON can be tailored (Howard, 2019).

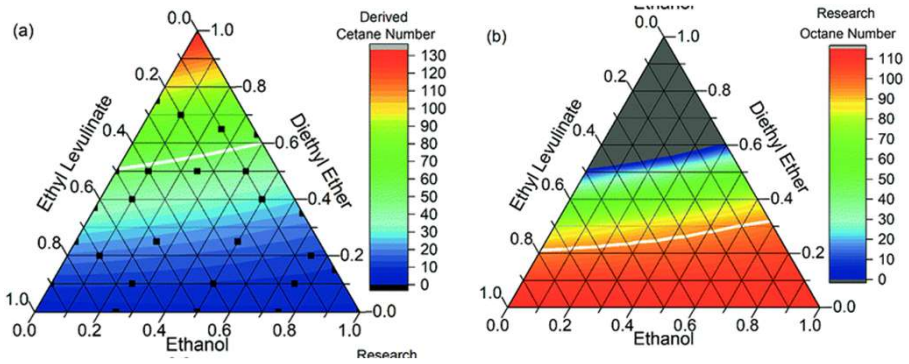

$H_2/NH_3/CH_4$ blends?

NH_3 combustion characteristics compared with other fuels, 300 K, 100 kPa.

Valero-Medina et al. 2018

	Methane (CH_4)	Hydrogen (H_2)	Methanol (CH_3OH)	Ammonia (NH_3)
Density (kg/m^3)	0.66	0.08	786	0.73
Dynamic viscosity × 10^{-5} (P)	11.0	8.80	594	9.90
Low heating value (MJ/kg)	50.05	120.00	19.92	18.80
Laminar burning velocity (m/s) – close to stoich.	0.38	3.51	0.36	0.07
Minimum ignition energy (mJ)	0.280	0.011	0.140	8.000
Auto-ignition temperature (K)	859	773–850	712	930
Octane number	120	–	119	130
Adiabatic flame temperature (with air) (K)	2223	2483	1910	1850
Heat capacity ratio, γ	1.32	1.41	1.20	1.32
Gravimetric Hydrogen density (wt%)	25.0	100.0	12.5	17.8

$H_2/NH_3/CH_4$ blends?

- Using blends of NH_3 with e.g. H_2 and or CH_4 could overcome some challenges related to **low flame speeds** (thus reduced turbulence and mixing) and **poor ignitability** (Valero-Medina et al. 2018).
- H_2 recovered from splitting NH_3 (possibly in situ).
- Blends similar to town gas.
  - Potential for use in IC engines and GTs with suitable NOx controls.
  - The ability to blend to facilitate existing infrastructure by matching combustion properties would be a **BIG advantage**.

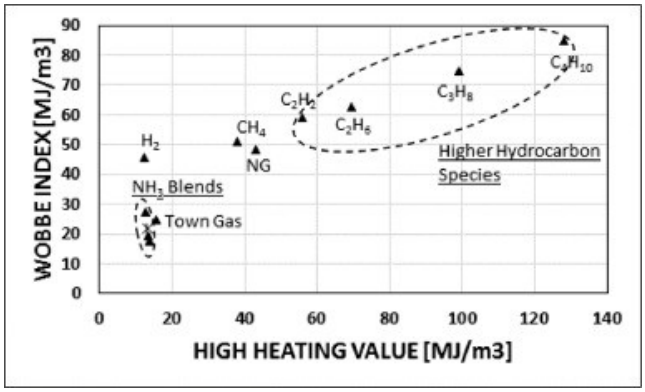

Duel fuel

- Where C is present in co-fuel (e.g. using diesel pilot for NH_3 combustion, or lubricating oil) then co-fuel can provide CO and CH_i radicals which contribute to the formation of unwanted side products such as HNCO and HCN.
- HNCO forms at intermediate temperatures (1000-1500 K) and fuel rich conditions ($\varphi > 1.2$): transition zones between diesel spray and premixed ammonia air charge.
- HCN→CN→NCO→NH→NO
- NH + CO → HNCO and NCO + H_2 → HNCO + H
- HCNO+O→NCO+OH
- This recycles NCO, feeding NO formation, and N_2O formation (via NCO + NO).
- Need to accurately represent cross reactions to design effective co-fuelling strategies.
- Adding H_2 would have HNCO reducing effect by increasing flame temperatures.

Overview of ML methods for design of fuels and mixtures (Sarathy and Eraqi, 2024)

- ML now commonly used to predict quantitative structure property relationships (QSPR).
  - Can be used to screen fuels.
- Need the inverse process – design fuel structures to target performance properties.
- Enabled by using AI/ML methods to train QSPR models using molecular graphs and NN to create differentiable mapping of molecular structure to fuel properties.
  - Gradient-based search methods then used on latent space representation to generate novel fuel components or mixtures.

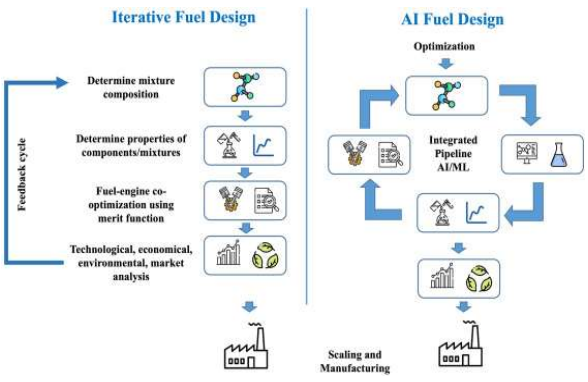

- Conclude that robust uncertainty quantification is needed for widespread adoption of machine learning techniques in fuel design.
  - techno-economic and lifecycle issues for fuel production also need to be considered.

Use of ML in fuel design for SI engines

- Chen et al. (2025) developed ANN approach for design of potential alternative fuels for applications in SI engines: targeting high efficiency and low emissions.
- Uses joint consideration of various properties estimated by ANN-based quantitative structure–property relationship models.
- Large pool of species with different structural properties and functional groups.

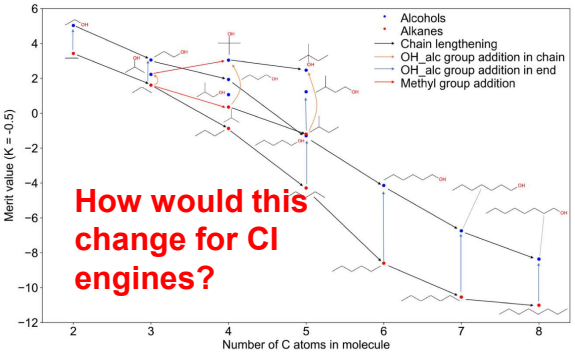

- Group contribution method used to estimate various physical and chemical properties: RON, octane sensitivity, liquid density, boiling point, melting point, and yield sooting index (YSI) using training data set.
  - 1st stage selection based on suitable physical properties.
- Remaining fuels ranked in terms of potential benefit for thermal engine efficiency.
- The results follow expected trends in terms of impact of carbon chain length and oxygen related functional groups on ONs and YSI.

Practical issues

- Changing fuels will not only require re-design of engines, but also of after-treatment systems that control their emissions.
  - Selective Catalytic Reduction (SCR) for NOx, Diesel Particle Filters (DPFs), Diesel Oxidation Catalysts (DOCs), Three Way Catalysts (TWCs).
- We must not reduce climate footprint at the expense of air quality.
- These fuels will have very different exhaust compositions compared to diesel, gasoline, jet fuels.
- This will impact on the effectiveness of after-treatment systems unless they can be re-optimised.
- Most are based on heterogeneous catalysts.

DeNOx

- Typical DeNOx systems such as **Selective Catalytic Reduction** (SCR) use chemicals that decompose to NH_3.
  - Potential for using on-board NH_3 within combustion system.

    $4NO + 4NH_3 + O_2 \rightarrow 4N_2 + 6\ H_2O$

    $2NO_2 + 4NH_3 + O_2 \rightarrow 3N_2 + 6\ H_2O$

    $NO_2 + NO + 2NH_3 \rightarrow 2N_2 + 3\ H_2O$ (fast SCR).
- Effectiveness of SCR depends on NO/NO_2 ratio which can vary within exhausts depending on fuel comustion and operation of Diesel Oxidation Catalyst (DOC).
- Care also needed to control *T* and avoid unwanted N_2O.

  $4NO + 4NH_3 + 3O_2 \rightarrow 4N_2O + 6\ H_2O$
- For Φ = 1.05-1.25 an increase in reactivity and overproduction of OH observed, suggesting recombination of molecules requiring further kinetic investigation.

Fuel tolerant after-treatment systems will be essential

- SCR systems are relatively effective for removing NOx from exhaust streams for current fuels.
- Their design and control have been optimised for diesel type fuels.
- The “fast” SCR reaction relies on **equal quantities of NO and NO_2**.
- What happens when we switch to other fuels or complex blends of methanol, hydrogen and ammonia?
- We will need to design SCR systems to work across these blends and a range of *T*’s over transient operational conditions.
  - Use of digital twin modelling for after-treatment systems?
- Catalysts can also be poisoned/blocked by hydrocarbon intermediates and oxygenated hydrocarbons for example.
- **Combined modelling of engine exhaust and catalyst chemistry** will be necessary to develop effective systems.

Why haven't I said more about soot chemistry?

- Not enough time for everything…
- Also, reality is that particle filtration methods are highly effective in treating exhaust particle emissions (efficiencies > 95 %).
- As long as they work with alternative fuels most particulates can be removed from exhausts of road vehicles, off road engines and marine applications.
- Use of SAFs should also reduce soot formation.
  - Although further research required on the production of ultra-fine particulates from SAFs and it's effects on contrail formation.
- The main source of soot exposure is likely to be indoors e.g. from cooking… This is an electrification or a ventilation problem.

Take away messages

- There are a huge number of possibilities for alternative fuels/blends that might replace FF in combustors.
- How do we make optimal choices about the best way to utilise biomass and other renewable energy sources?
  - Not clear that we yet have enough data to do that robustly but time is running out.
  - We have to work with the process of electrification and not against it.
  - Liquid fuels likely to find applications in areas such as long duration energy storage and hard to electrify sectors such as marine and aviation.
- Multiple characteristics need to be optimised in order to developed
  - Lifetime CO_2 equivalent emissions, costs of production, transportation and storage.
  - Physical properties and compatibility within existing combustors and infrastructure.
  - ON/CN matching through blending.
  - Minimising emissions from combustors.
- **To optimally use pollution control for air pollutants may benefit from digital twin type models that will require robust, yet rapid simulation tools.**

Section 5
Model uncertainties, sensitivity analysis and optimisation

Intro

- We have seen from earlier examples that presenting uncertainties in experimental data is far more common than for modelling results.
- But we need to know the **robustness** of our models to use them in design and decision making e.g. for use of new fuels.
- Need methods for **uncertainty quantification**.
  - Emerging field of UQ in combustion modelling.
  - Need first to estimate uncertainties in
    - Input parameters
    - Model structure.
  - Efficient methods for **propagating** through model to provide uncertainties on target outputs.

Sources of model input data and uncertainty information

- Kinetic evaluations (e.g. Baulch, Tsang, Atkinson).
- NIST data base.
- Output from theoretical studies.
- Trawling literature for individual papers on rate coefficients etc.….
  - ➢ Time consuming!
- Detailed statistical studies/ML
  - ➢ Active tables for thermodynamic data (Ruscic and coworkers).
  - ➢ Optimisation studies for reaction mechanisms (Nagy and coworkers).
  - ➢ New methods for mechanism generation using machine learning may at last provide automatic methods for estimating uncertainties in the fitted thermochemical parameters. 🙏
- What to do about estimated parameters using more trad methods such as reaction classes, functional groups, GA methods ?

Evaluated data (Baulch et al., 1994)

Δlogk = ±0.2 (300K) ±0.5 (2000K)

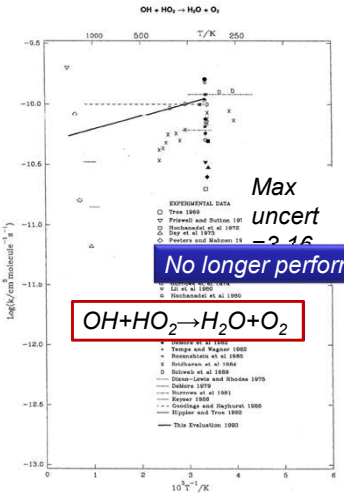

Max uncert =2.16

OH+HO₂→H₂O+O₂

Δlogk = ±0.15 (550-800K) ±0.4 (1250K)

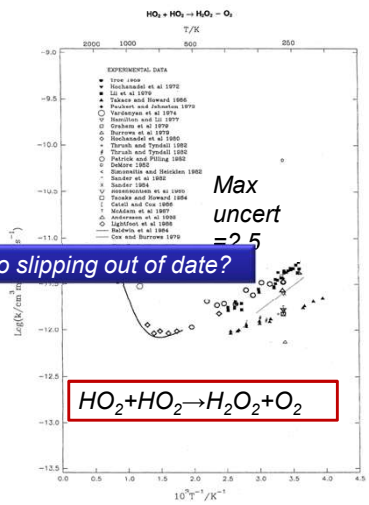

Max uncert =2.5

No longer performed so slipping out of date?

$HO_2+HO_2 \rightarrow H_2O_2+O_2$

NIST data base

$HCHO+HO_2 \rightarrow HCO+H_2O_2$

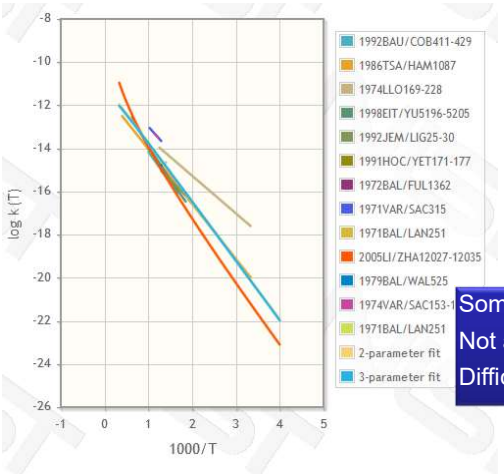

Fit of Arrhenius parameters to set:

Temperature range: 250 - 3000 K

Two-parameter fit:	**Three-parameter fit:**
$k(T) = Aexp(-E_a/RT)$	$k(T) = A(T/T_{ref})^n exp(-E_a/RT)$
A = 9.25E-12 [cm^3/molecule s]	A = 1.51E-11 [cm^3/molecule s]
E_a = 52.17 [kJ]	n = -0.3
RMSD = 4.3	T_{ref} = 298 [K]
	E_a = 53.48 [kJ]
	RMSD = 4.2

Some judgement has to be made about outliers
Not always completely up to date
Difficult to get temperature dependant uncertainties

Uncertainties from ML approaches to AMG

- Estimating uncertainties from ML approaches relies on understanding the uncertainties present in the training data (experimental or theory).
  - Relies on estimating uncertainties for different levels of theory which is not straightforward.
- RMG records such uncertainty estimates (Johnson & Green, 2024):
  - E.g. CBS-QB3 calculated rate associated with a 2.5 kcal mol^{-1} uncertainty.
  - "rule of thumb" generalization, assigned a 14 kcal mol^{-1} uncertainty.
  - Expressed as $\Delta\log(k)$ rather than Δk because $\Delta\log(k) \sim \Delta E_a$.
- Uncertainties then estimated for predicted rates at 1000 K using methods discussed in Section 3.
  - Combination of fitting error and error in underlying training data.

Comparison of accuracy of RMG rate rules (RR) and the subgraph isomorphic decision tree (SIDT) estimator for three different RMG families oxygen substitution (O-Sub), intra-molecular hydrogen transfer (intra-H), internal endocyclic radical addition (Int-Endo) and radical addition (R-Add)

Estimator	O-Sub RR	O-Sub SIDT	Intra-H RR	Intra-H SIDT	Int-Endo RR	Int-Endo SIDT	R-Add RR	R-Add SIDT	H-Abs RR	H-Abs SIDT
Median absolute error factor	10.3	5.28	8.94	3.56	9.67	1.73	2.25	1.88	5.11	4.05
MAE factor	18.5	10.1	38.1	10.9	24.7	2.95	3.07	2.34	16.4	8.02
RMSE factor	61.7	27.6	575	79.3	98.3	7.07	5.59	3.51	89.7	23.7
2-Sigma error factor	3876	770	333 000	6320	9710	50.1	31.3	12.3	8040	564

Johnson and Green, 2024

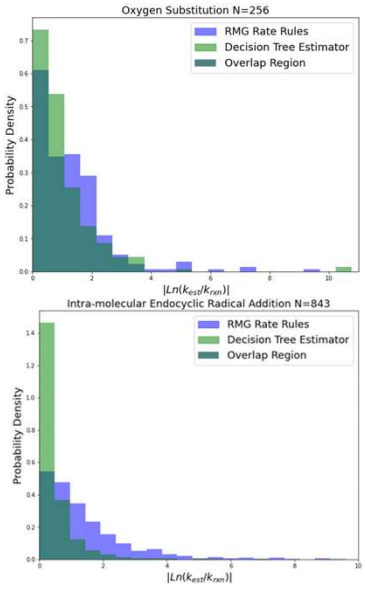

Where higher level theory available in training set – errors much reduced

Representations of Uncertainty

- Depends of level of knowledge about a particular parameter.
- If evaluation available then *f* value may be given.

$$f = \log_{10}\left(\frac{k^0}{k^{\min}}\right) = \log_{10}\left(\frac{k^{\max}}{k^0}\right) \qquad \frac{k^{\max}}{k^0} = 10^f$$

- k_0 recommended value of rate coefficient. k_{min}, k_{max} extreme values.

$$\sigma^2(\ln\{k\}) = ((f\ \ln 10)/m)^2$$

where m is the level of uncertainty suggested.
m = 2, 2σ deviation or 95 %ile,
m= 3, 3σ deviation or 99.7 %ile

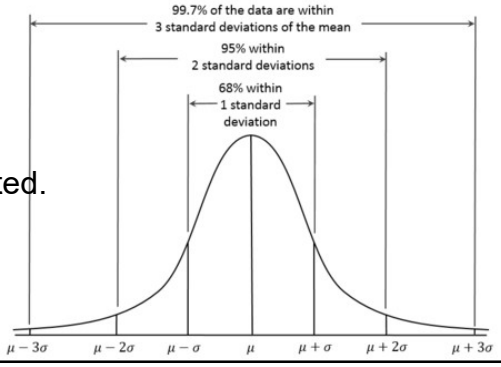

Examples of levels of uncertainty

uncertainty parameter *f*	multiplication factor of 3σ uncertainty limits	σ($\log_{10}$ k)	σ(ln k)	multiplication factor of 1σ	multiplication factor of 2σ
0.1	1.26	0.03	0.08	1.09 (9%)	1.17
0.3	2.00	0.10	0.23	1.33 (33%)	1.67
0.5	3.16	0.17	0.38	1.72	2.44
0.7	5.01	0.23	0.54	2.34	3.67
0.9	7.94	0.30	0.69	3.31	5.63
1.0	10.00	0.33	0.77	4.00	7.00

Statistical methods

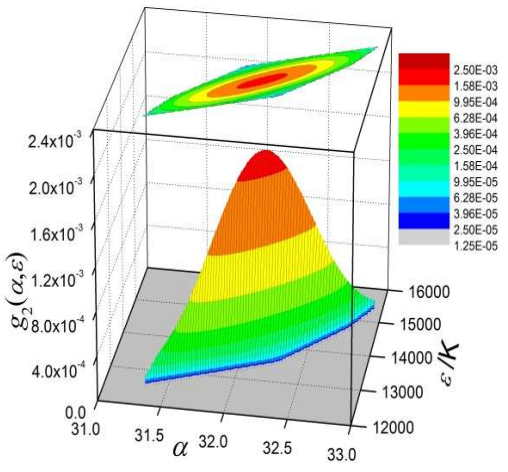

- All available current information on a system is used to fit a joint pdf of parameters.
- (see work of Turanyi, Nagy, Li et al. 2025)
  - ➢e.g. 2,3 parameter Arrhenius
- Provides highly detailed data on parameter correlations etc.

For reaction kinetics has been carried out for only a few simple systems e.g. H_2, wet CO oxidation, methanol (Nagy et al., 2011).

Estimated parameters

- For estimated parameters 10^f is likely to be a **guestimate** e.g. factor of 2 or a factor of 5.
- A **uniform distribution** used since no probabilistic information likely to be available.
- Estimates could be based on **reaction classes and rate rules** from AMG packages like RMG etc.
  - What is the uncertainty for a particular reaction class based on available data?
  - How does the uncertainty change as e.g. the number of carbons grows?
  - Likely in the near future to be replaced with ML estimates.

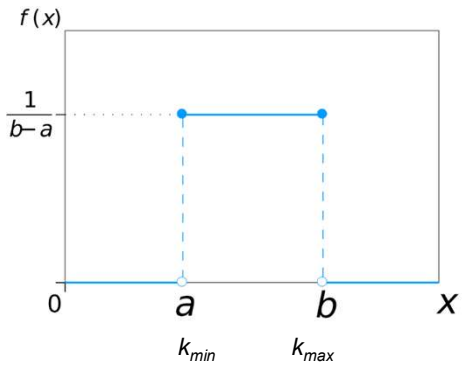

Active Tables

- New paradigm to develop accurate, reliable, and internally consistent thermochemical values for stable, reactive, and transient chemical species by utilizing to the fullest all available experimental measurements as well as state-of-the art theoretical data.
- **ATcT** is based on constructing, analysing, and solving the underlying Thermochemical Network (TN).
- Brings together both experimental and theoretical studies (**see earlier**) to reduce uncertainties in data (Burcat & Ruscic, 2005).
- Network of Computed Reaction Enthalpies to Atom-Based thermochemistry **(NEAT)** (*Csaszar and Furtenbacher, 2010)*
- **Results in highly correlated parameters – be careful of the effects of neglecting such correlations!**

Species Name	Formula	$\Delta_f H°(0\ K)$	$\Delta_f H°(298.15\ K)$	Uncertainty	Units	Relative Molecular Mass	ATcT ID
Dihydrogen	H2 (g)	0	0	exact		2.01588 ± 0.00014	1333-74-0*0
Helium	He (g)	0	0	exact		4.0026020 ± 0.0000020	7440-59-7*0
Heptane	C7H16 (l)	-201.46	-223.91	± 0.74	kJ/mol	100.2019 ± 0.0057	142-82-5*500
Octane	C8H18 (l)	-226.61	-249.73	± 0.79	kJ/mol	114.2285 ± 0.0065	111-65-9*500
2,2,4-Trimethylpentane	(CH3)2CHCH2C(CH3)3 (l)	-224.4	-258.9	± 1.5	kJ/mol	114.2285 ± 0.0065	540-84-1*500

Part of a thermo-chemical network showing the basic ideas

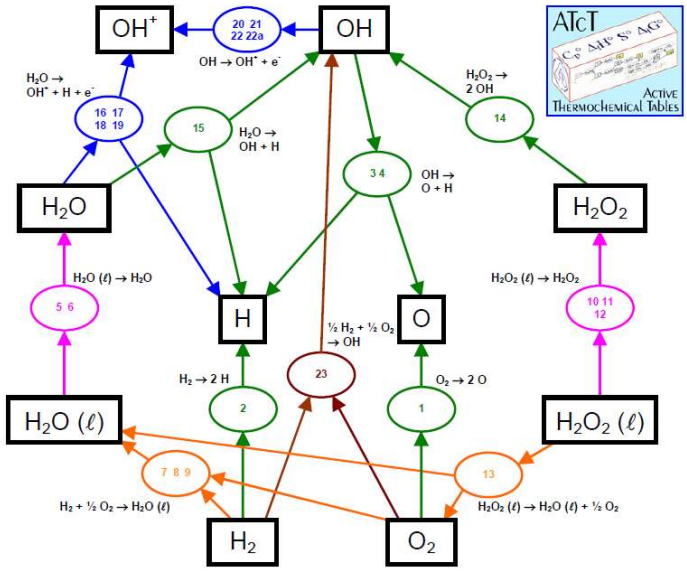

Figure 1. A small subsection of the current Core (Argonne) Thermochemical Network. The full network currently contains >600 primary vertices and >3200 secondary vertices. See text for further details

417

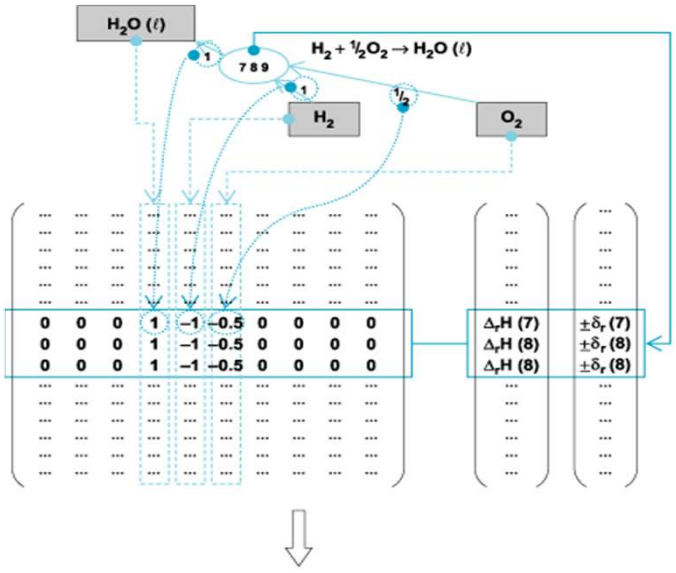

Eq. (7): $\Delta_f H(H_2O <\ell>) - \Delta_f H(H_2) - 0.5\ \Delta_f H(O_2) = \Delta_r H\ (7) \pm \delta_r\ (7)$

Eq. (8): $\Delta_f H(H_2O <\ell>) - \Delta_f H(H_2) - 0.5\ \Delta_f H(O_2) = \Delta_r H\ (8) \pm \delta_r\ (8)$

Eq. (9): $\Delta_f H(H_2O <\ell>) - \Delta_f H(H_2) - 0.5\ \Delta_f H(O_2) = \Delta_r H\ (9) \pm \delta_r\ (9)$

418

Example: CH_3

Formula	$\Delta_f H^{\ominus}$(0 K)	$\Delta_f H^{\ominus}$(298K)	Uncertainty	Units
CH_3(g)	149.788	146.374	± 0.08	kJ mol^{-1}

95% uncertainty limits

- **Top contributors to the provenance of $\Delta_f H°$ of CH_3 (g):** The top **20** contributors account only for **72.5%** of the provenance of $\Delta_f H°$ of CH_3 (g). A total of **99** contributors would be needed to account for **90%** of the provenance.
- Link to latest version of ATcT: https://atct.anl.gov/Thermochemical%20Data/version%201.122/index.php

Ab Initio Computations and Active Thermochemical Tables Hand in Hand: Heats of Formation of Core Combustion Species

Klippenstein, 2017

- **High level ab initio electronic structure** based predictions of $\Delta_f H^{\ominus}$(0 K) for 348 C, N, O, and H containing species - essentially all core combustion species with 34 or fewer electrons.

- Accuracy of theoretical predictions is explored through

(i) examination of the magnitudes of the various corrections,
(ii) comparisons with other high level calculations, and
(iii) through comparison with the ATcT values.

- Inclusion of theoretical results into ATcT thermochemical network expected to significantly improve the thermochemical knowledge base for less-well studied species.

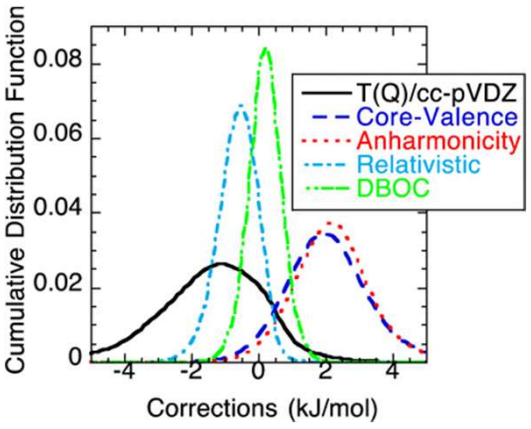

RESPECTH
Reaction Kinetics, Spectroscopy, Thermodynamics database

- http://respecth.chem.elte.hu/respecth/
- Thermodynamics section:
  - Thermochemical data calculated by the method NEAT;
  - High-accuracy thermochemical data for $H_2^{(16)}O$;
  - A mirror of Burcat's thermochemistry database – which incorporates ATcT values where available. .
  - **Always check your data sources and uncertainties!**

```
CH2O  FORMALDEHYDE  SIGMA=2 A0=9.40546 B0=1.295407 C0=1.134216
NU=2782.4,1746.1,
1500.1,1167.2,2843.2,1249.1   HF298=-109.164+/-0.1 kJ     REF=ATcT C
2011.
C4H10O-N 1-BUTANOL SIGMA=1  STATWT=1 IA=4.4899  IB=42.7094  IC=45.1130
NU=3300,2950(9),1470,1450(4),1294(7),1250,1070,1050,955(4),890(3),446,3
92,350
REF=Chao et. al, JPCRD 15,(1986),1369  HF298=-275.981+/-8. kJ
REF=Burcat G3B3
```

Sensitivity and uncertainty analysis

• **Uncertainty quantification (UQ)** estimates the overall predictive uncertainty of a model given the state/or lack of knowledge about its input parameters.

• UQ puts error bars on predictions.

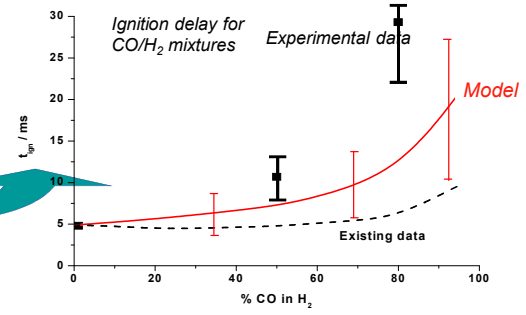

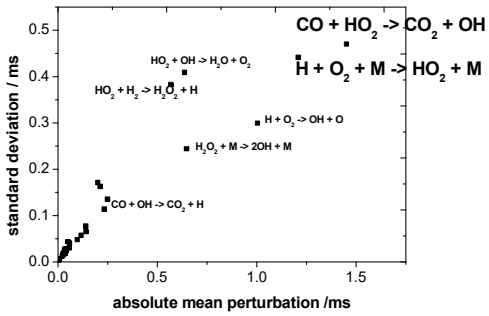

Sensitivity analysis (SA) determines how much each input parameter contributes to the output uncertainty (usually variance).

Local sensitivity coefficients

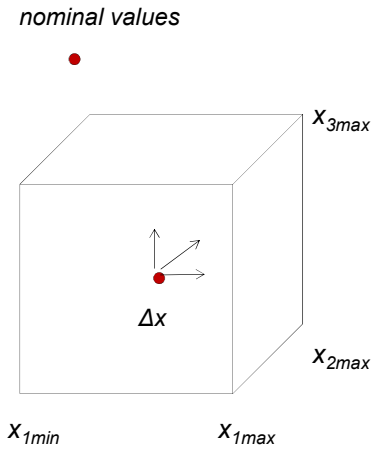

Local first-order sensitivity coefficient

$$S_{ij} = \frac{\partial Y_i}{\partial x_j}$$

Normalised first-order sensitivity coefficient

$$S'_{ij} = \frac{x_j}{Y_i}\frac{\partial Y_i}{\partial x_j}$$

Commonly incorporated into codes such as Chemkin, Cantera using finite difference methods.

Contributions to uncertainty?

- Really we want to know, not just sensitivity, but also how much a parameter contributes to model uncertainty.
- Some parameters have **high sensitivity**, but are very **well quantified**.
- Others may have **lower sensitivity** but are **poorly known** and therefore drive potential errors in models.
- If $\sigma(x_j)$ are known – or estimated - then we can estimate overall uncertainty:

$$\sigma^2(\mathbf{Y}) = \sum_j \left(\mathbf{S}'_j\right)^2 \frac{\sigma^2\left(x_j\right)}{x^2{}_j}$$

- The **fractional contribution** of each parameter to this **uncertainty** can be estimated.
- Gives a better measure of parameter importance than S'_{ij} alone.
- Tells us how better quantification of each parameter could reduce overall modelling uncertainty.

Local vs global methods

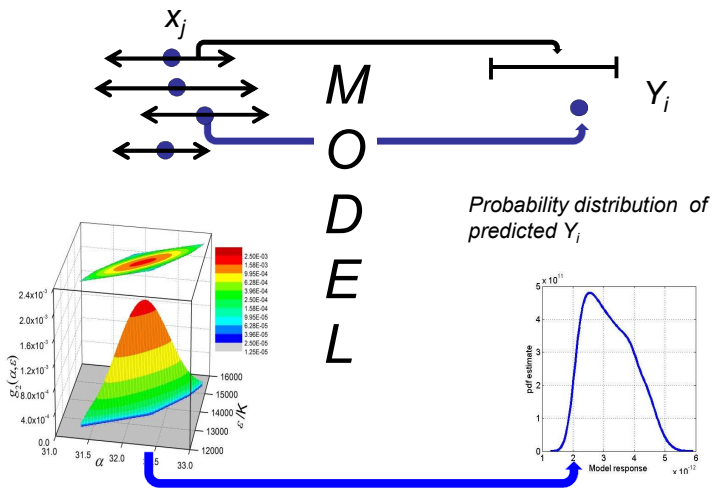

Global sensitivity/uncertainty methods

Global - attempts to cover whole input space using a sampling method.

Najm, Wang, Frenklach, Sheen, Tomlin, Turányi etc.

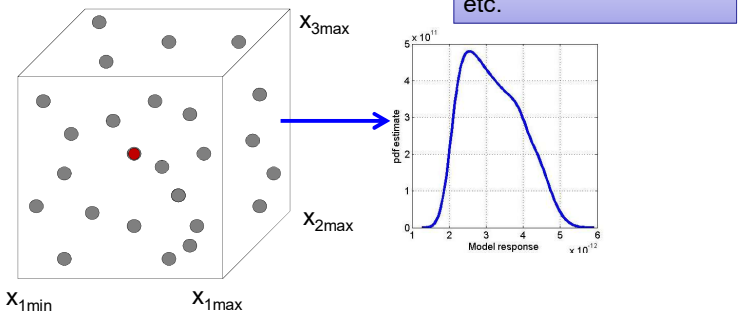

Why use global methods?

- Local sensitivity and uncertainty methods are usually based on a single (best estimate) value of the parameters.
- If the sensitivity of the output changes depending on the values of the parameters then local methods could be inaccurate.
- Particularly important for **non-linear models** and models with **large uncertainties**.

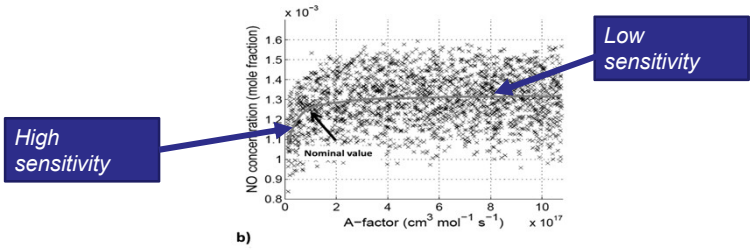

Disadvantages of global methods

- In order to cover the regions of parameter uncertainty, ***sampling based methods*** need to be used and therefore a ***large number of model runs*** is needed instead of the single run required for local sensitivity analysis using e.g. finite difference methods.
- The methods also require **prior knowledge of the input parameter distributions**.
- Methods are then required to interpret the data from a large number of samples to determine the sensitivity indices.
- For large parameter systems sample sparsity can be an issue.
- Screening methods are therefore often first applied to identify **unimportant** parameters which do not need to be varied in the full global approach.

Screening methods.

- Can be based on **local sensitivity coefficients**.
- Problematic unless it is applied at various values of the nominal parameters e.g. recommended value, rv, rv x 2, rv x 0.5.
- Can be automatically calculated using simple finite differences approaches in Chemkin/Cantera for simple outputs such as peak *T*, peak [OH].
  - Adds to model run time but not significantly.
- Can be run as **Brute Force Method**, changing each parameter in scheme once and assessing sensitivity of target outputs.
  - Very expensive for large models, useful for targets such as IDTs.
- **Morris method** also used for screening and applies a one at a time method, changing one parameter by a fixed amount for each run of the model starting with a random seed.
- Several random seeds used at different points in parameter space.
  - Probably 10 times more expensive than even the Brute Force Method.

Brute Force Methods

- Useful for target outputs which do not have an obvious functional relationship to inputs e.g. ignition delay times.
- Each parameter of interest is modified in turn from the chosen nominal value by a small %, the model is re-run and the % change in output calculated.
- The relative output change gives a ranking of parameter importance.
- Cost is proportional to number of parameters *n*.
- Can be run for different chosen nominal values – pushing cost to 2*n*, 3*n* etc.
- Method **does not consider non-linear interactions** between parameters.
- Still, a straightforward way to screen out unimportant parameters before full global study.

Example

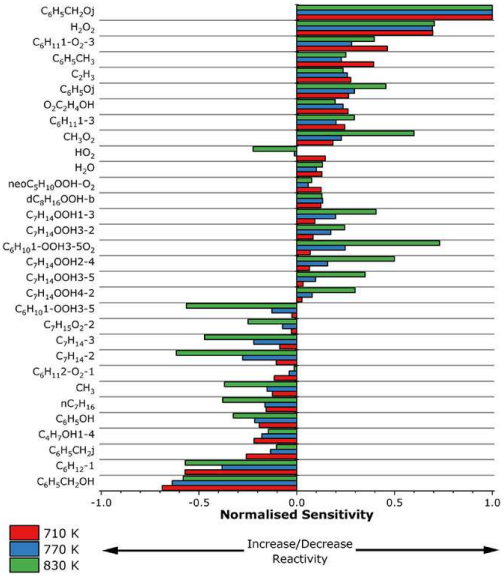

- Normalized sensitivity coefficients of IDTs on species enthalpy of formation, for a 5-component gasoline surrogate. Rapid compression machine, P_C = 20 bar, Φ = 1

Morris Method

- A series of parameter sets are generated so that the next one differs from the previous in the value of a single parameter only, which is randomly chosen.
- The value of each parameter x_j is modified within the range $[x_j^{min}, x_j^{max}]$ by a fixed amount Δ determined as follows.
- A vector $\left\{0, \frac{1}{q-1}, \frac{2}{q-1}, \frac{3}{q-1}, \ldots, 1\right\}$ is generated using a small even number q selected by user.
- 0 and 1 are assigned to x_j^{min}, x_j^{max} respectively.
- All other parameter values are scaled according to the vector above.
- The first parameter set is randomly selected from the values determined by the vector.
- The next parameter set is identical to the previous one, except for the value of a single parameter which is moved randomly to another possible value.

MM cont.

- Next parameter set obtained by changing another parameter etc. with a random order of parameter selection.
- By the end, the algorithm has changed the value of each parameter exactly once, and hence m + 1 parameter sets are generated.
- The method is also a **one-at-a-time** method together with brute force linear sensitivity analysis.
- However, here, the full uncertainty range of the input parameters can be covered, whereas in the BF method, all parameters were each changed from their nominal values.

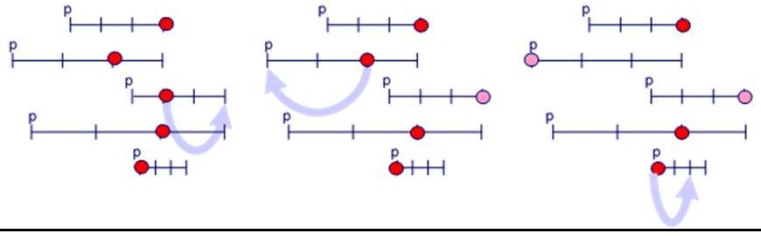

MM continued

- Measure d_{ij} shows the effect of changing parameter x_j on model result Y_i at arbitrary values of all other parameters:

$$d_{ij} = \frac{Y_i\left(x_1^z, x_2^z, \ldots, x_j^z + \Delta, \ldots, x_m^z\right) - Y_i\left(\mathbf{x}^{z-1}\right)}{|\Delta|}$$

- In the z-th parameter set, the value of parameter x_j was changed by Δ.
- The calculation above is repeated several (r=10-20) times, always starting from randomly selected different parameter sets.
- The total computational effort required is therefore $r(m + 1)$, where r is the number of repeated parameter sets.

Examples of application of Morris screening method

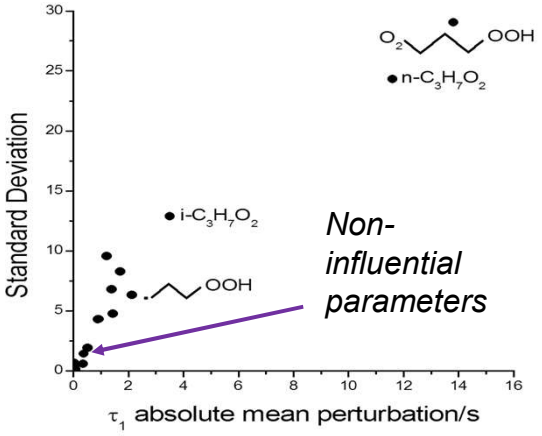

*Morris analysis for species ΔH_f^o with respect to **time to cool flame for propane oxidation**. T= 593 K, equimolar C_3H_8+O_2 at 53.4 kPa, diluted by N_2 to 101.3 kPa (Hughes et al., 2006)*

- *Note the high standard deviation of the outputs compared to the mean.*
- *Very nonlinear responses requiring large sample size to converge.*
- *High and linear influence would be in the lower right corner of the plot.*

Global sampling methods Monte Carlo

- For a global sampling method it is important to get good coverage of the input parameter space – which may be high dimensional.
- Typical random sampling methods can lead to clustering and holes.

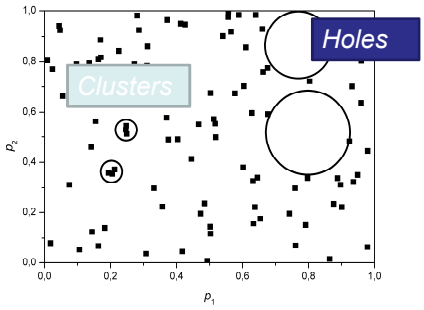

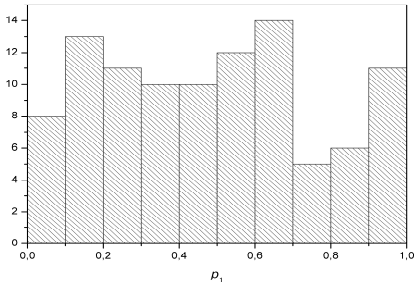

100 numbers – 2 parameters

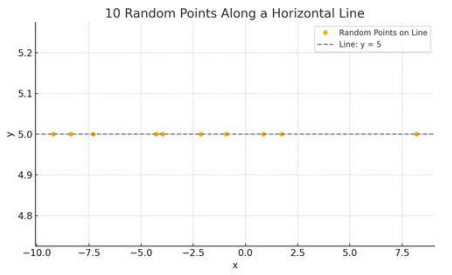

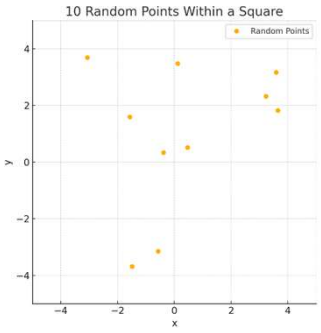

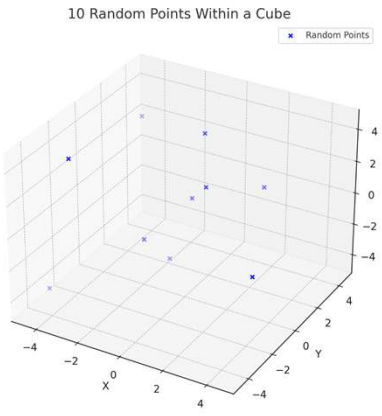

As the dimension goes up the sparsity increases massively!

Structured sampling

Latin Hypercube

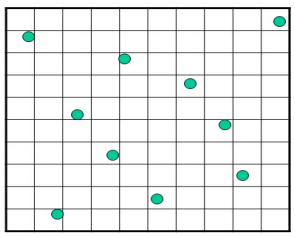

- Points generated by Latin hypercube sampling according to a uniform distribution.
- Each horizontal and vertical stratus contains a single point, while the location of the point is random in the corresponding small square.

Low discrepancy sequences

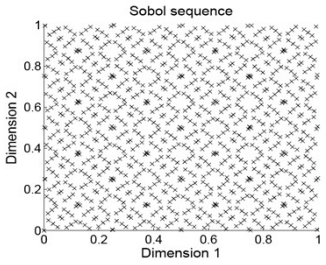

d)

Successive sample points are added to positions as far away as possible from existing sample points so that clustering can be avoided.

Sobol sequence

Sobol sequences use a base of two to form successively finer uniform partitions of the unit interval and then reorder the coordinates in each dimension.

0.000e+00	0.000e+00	0.000e+00
5.000e-01	5.000e-01	5.000e-01
7.500e-01	2.500e-01	7.500e-01
2.500e-01	7.500e-01	2.500e-01
3.750e-01	3.750e-01	6.250e-01
8.750e-01	8.750e-01	1.250e-01
6.250e-01	1.250e-01	3.750e-01
1.250e-01	6.250e-01	8.750e-01
1.875e-01	3.125e-01	3.125e-01
6.875e-01	8.125e-01	8.125e-01
9.375e-01	6.250e-02	5.625e-01
4.375e-01	5.625e-01	6.250e-02
3.125e-01	1.875e-01	9.375e-01
8.125e-01	6.875e-01	4.375e-01
5.625e-01	4.375e-01	1.875e-01
6.250e-02	9.375e-01	6.875e-01

The Sobol sequence is designed to have the best convergence properties and hence can lead to savings in sampling based sensitivity and uncertainty analysis because smaller sample sizes are needed to get equivalent accuracy in the results.

Comparison of convergence properties of different sampling strategies for a simple test model: $f(x) = x_1 + x_2^4$

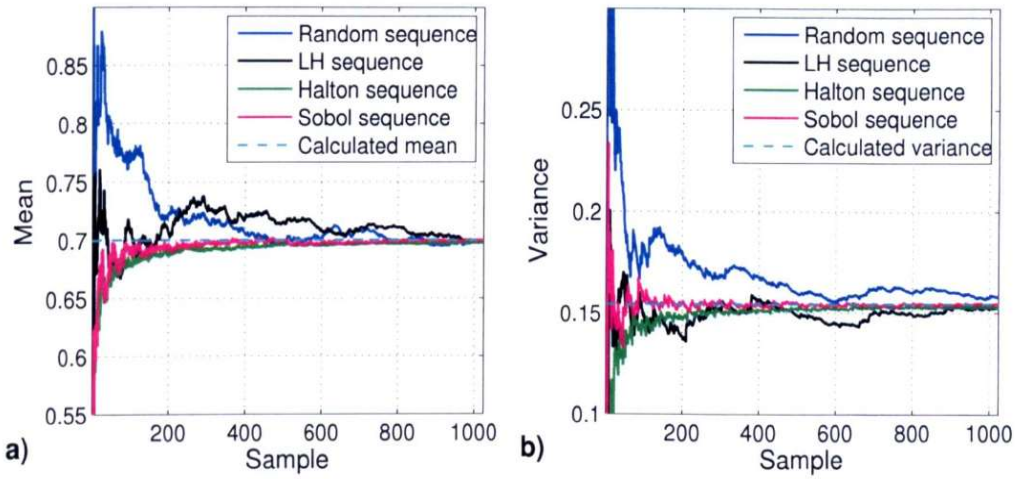

Probabilistic sampling

If probabilistic information known then we may wish to sample from this distribution e.g. **a normal distribution** based on 2σ uncertainties (Hébrard et al., 2015)

- 2-parameter samples, N = 1000.
- Box-Muller transformation applied to an uniform pseudo-random sample (bottom left)
- Normal inverse cumulative function of a Sobol's quasi-random sequence sample (bottom right).

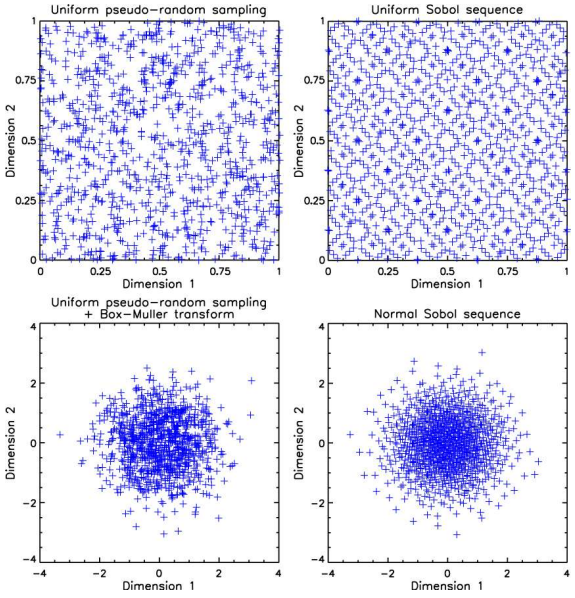

What parameters to include in UQ?

- ***In an ideal world, just for fundamental devices:***
  - All Arrhenius parameters
  - Thermodynamic parameters - used to calculate reverse reaction rates
  - Species transport data
  - Other potential model errors
    - Temperature profile
    - Heat transfer coefficients
    - Residence times
    - Loss rates to the walls of the reactor vessel
- In reality many of these are often ignored and a most common approach is to simply look at the *A*-factors for each forward reaction.
  - **Tells us something about the important reactions but does not give a full picture of uncertainties.**

Examples of outputs

Ignition delays:
Predicted output distributions (butane model)

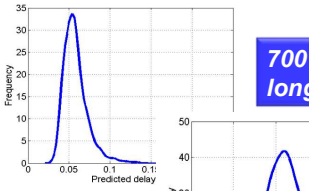

700 K – narrow distribution but long tail

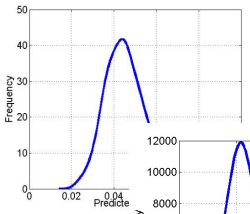

900 K - factor of 2 uncertainty

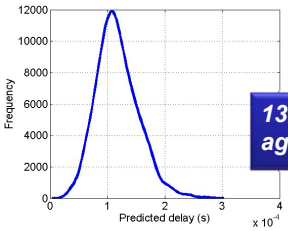

1300 K – narrows again

- *1σ used to represent output error bars.*

(Hébrard et al., 2015)

Interpreting output distributions

- Example from simulations of ignition delay time for a butane oxidation system.
- The blue shaded area represents 1σ of the outputs based on a sampled normal distribution of the input rate parameters.
- Hébrard et al. (2015)

Reasonable agreement between model and shock tube and RCM data if uncertainties are taken into account.

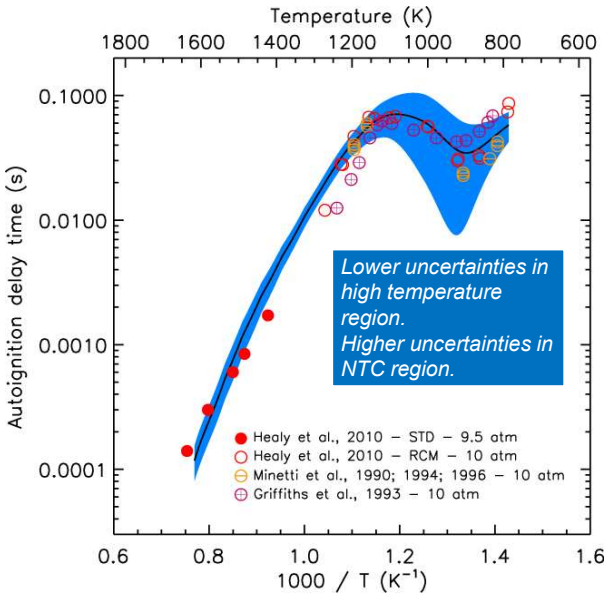

JSR data

Some discrepancies between model and experimental data even when accounting for estimated uncertainties.

Missing reaction steps?

Other uncertainties not identified?

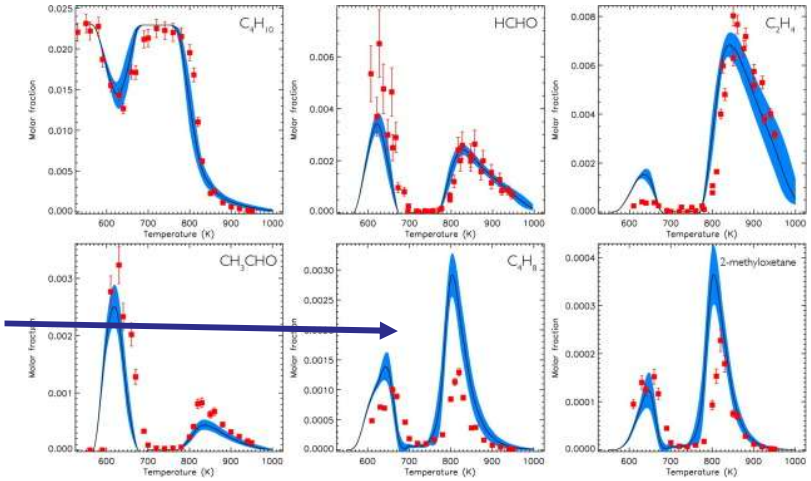

We learn about missing parts of the model.

(Hébrard et al., 2015)

CALCULATING SENSITIVITY INDICES FROM SAMPLING METHODS

Sobol's method

- Is a sampling based method to calculate fraction of total variance that can be attributed to each parameter in a joint pdf distribution.
- If the model result $Y_i = f_i(x_1, x_2, \ldots, x_N)$ is influenced by independent random parameters, then the joint pdf of the parameters $P(x_1, x_2, \ldots, x_N) = \prod_{j=1}^{N} p_j(x_j)$.
- The mean or expected value $E(Y_i)$ of the calculated result Y_i is then given by:

$$E(Y_i) = \iint \ldots \int f_i(x_1, x_2, \ldots, x_N) \prod_{j=1}^{N} p_j(x_j)\, \mathrm{d}x_j$$

- while the variance $V(Y_i)$ of the calculated result Y_i is specified as:

$$V(Y_i) = \iint \ldots \int (f_i(x_1, x_2, \ldots, x_N) - E(Y_i))^2 \prod_{j=1}^{N} p_j(x_j)\, \mathrm{d}x_j$$

$$= \iint \ldots \int f_i^2(x_1, x_2, \ldots, x_N) \prod_{j=1}^{N} p_j(x_j)\, \mathrm{d}x_j - E^2(Y_i)$$

- If integral calculated with **fixed value of parameter x_j**, variance caused by all other parameters except for x_j , (Y_i/x_j) obtained.
- If $V(Y_i/x_j)$ calculated for many values of x_j, selected according to its pdf, then expected value $E(V(Y_i/x_j))$ can be calculated.
- Requires integration of $V(Y_i/x_j)$ over pdf of x_j (Saltelli et al., 2002).
- $V(Y_i) - E(V(Y_i/x_j))$ equal to reduced variance of Y_i caused by fixing value of x_j , and is equal to $V(E(Y_i/x_j))$.
- By dividing this **conditional variance** by **unconditional variance**, the first-order sensitivity index for parameter x_j can be calculated:

$$S_{j(i)} = \frac{V\left(E\left(Y_i \middle| x_j\right)\right)}{V\left(Y_i\right)}$$

- Shows **the fraction of the total variance of Y_i which is reduced when the value of x_j is held at a fixed value** – a measure of the influence of uncertainty in x_j.
- The calculation of integrals is non-trivial and the use of a Monte Carlo sampling method (Saltelli et al., 2002) requires ***N*(2*m*+1) model runs for first-order indices** where N is the sample size chosen for the Monte Carlo estimates.

Response Surface Methods, RSM

- RSM based methods attempt to reduce computational cost of Variance based sensitivity methods by first developing a fitted ***meta-model*** accurately representing **relationship between model parameters and outputs**.
- If ***meta-model*** can be fitted with a lower number of model runs then it can be used to calculate variance based indices at lower cost.
- Some similarities with Monte Carlo approaches:
  - first input parameter ranges must be selected
  - then a **suitable sampling approach** taken so that full model runs are obtained across a design suitable for development of accurate meta-model.
- Cost of method driven by cost of providing accurate surrogate model.
- This is not always dependant on size of scheme but is **driven by the complexity of the response surface**.
  - Could be cheaper than Brute Force.

Polynomial chaos expansion, PCE methods (Najm et al., 2009)

- Here an uncertainty factor u_i is first assigned to each input variable.
  - Note that this uncertainty parameter u_i is related to uncertainty parameter f by $u_i = 10^f$.
- Taking the example of rate coefficients, they are then normalised into factorial variables **x** as follows:

$$x_i = \frac{\ln k_i / k_{i,0}}{\ln u_i}$$

Nominal value

- Hence $x_i = 0$ gives the nominal value of the rate coefficient, and -1 and +1 represent the upper and lower bounds.
- A response surface of the predicted combustion properties is then generated with respect to **x**.

- Often restricted to a 2nd order polynomial expansion which for the r'th model response $\eta_r(\mathbf{x})$ can be written as:

$$\eta_r(\mathbf{x}) = \eta_{r,0} + \sum_{i=1}^{m} a_{r,i} x_i + \sum_{i=1}^{m} \sum_{j \geq i}^{m} b_{r,i,j} x_i x_j$$

- The uncertainty in **x** may be expressed as a polynomial expansion of basis random variables $\boldsymbol{\xi}$:

$$\mathbf{x} = \mathbf{x}^{(0)} + \sum_{i=1}^{m} \boldsymbol{\alpha}_i \xi_i + \sum_{i=1}^{m} \sum_{j \geq i}^{m} \boldsymbol{\beta}_{ij} \xi_i \xi_j + \ldots,$$

where **α** and **β** are column vectors of expansion coefficients, *m* is the number of rate coefficients under consideration and $\mathbf{x}^{(0)}$ is a column vector of normalised rate coefficients which is a zero vector for the nominal reaction model.

- If the **x**'s are independent of each other and normally distributed, then ξ would be a set of unit-normal random variables. Uncertainty decomposes as:

$$\sigma_r(\xi)^2 = \sum_{i=1}^{m} \hat{\boldsymbol{\alpha}}^2{}_{r,i} + 2\sum_{i=1}^{m} \hat{\boldsymbol{\beta}}^2{}_{r,ij} + \sum_{i=1}^{m} \sum_{j>i}^{m} \hat{\boldsymbol{\beta}}^2{}_{r,ij}$$

Examples of application

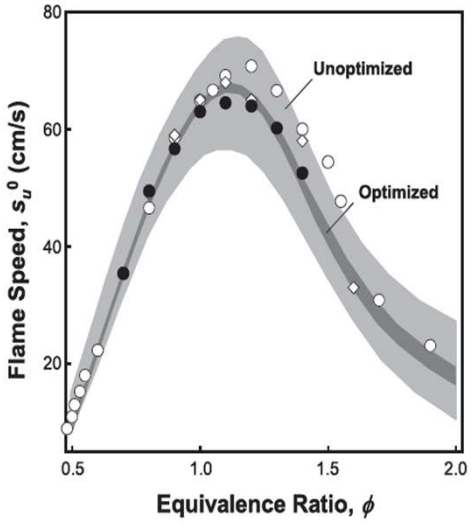

- Experimental data and computed 2σ uncertainty bands for the laminar flame speed of ethylene-air mixtures at *p* = 1 atm. (Sheen et al., 2009).
- Note that following the application of an optimization procedure, the uncertainty bounds are much narrower.
- The polynomial chaos expansion is used within the optimisation procedure.

Method is included in Chemkin but if you use it watch out for accuracy of fits. The sample used is sparse!

ANOVA (Analysis Of Variances) Variance decomposition

- For independent inputs (i.e. no correlations exist between inputs), a unique decomposition of the unconditional variance *V(Y)* can be obtained (Li et al., 2010):

$$V(Y) = \sum_{i=1}^{n} V_i + \sum_{1 \le i < j \le n} V_{ij} + \ldots + V_{12\ldots n} = \sum_{j=1}^{2^n-1} V_{x_j}$$

$$\sum_{j=1}^{2^n-1} \frac{V_{x_j}}{V(Y)} = \sum_{j=1}^{2^n-1} S_{x_j} = 1$$

- The approach is therefore analogous to the classical approaches described above but instead of directly calculating the conditional variances using e.g. Monte Carlo samples, now a meta-model is developed first and the sensitivity indices are calculated using the meta-model.

RSM approaches to ANOVA decomposition

- Polynomial chaos expansions are one method to achieve this ANOVA decomposition.
- Other methods are based on **High Dimensional Model Representations** (HDMR).
- HDMR originally developed to provide a straightforward approach to explore input-output mapping of models without requiring large numbers of runs (Sobol', 1990; Rabitz et al., 1999; Li et al., 2001).
- The use of truncated expansions is possible because usually only low-order correlations between inputs have a significant effect on the outputs.
- Because of the ***hierarchical form*** of HDMR component functions, sensitivity indices can be determined from them in an automatic way in order to rank the importance of input parameters and to explore the influence of parameter interactions.

Basic mapping

- The mapping between the inputs $x_1,\ldots, x_n$ and the output variable $Y(\mathbf{x}) = f(x_1,\ldots,x_n)$ can be written in the following hierarchical form:

$$Y(\mathbf{x}) = f_0 + \sum_{i=1}^{n} f_i(x_i) + \sum_{1\le i<j\le n} f_{ij}(x_i, x_j) + \ldots + f_{12\ldots n}(x_1, x_2, \ldots, x_n)$$

- Here the zeroth-order component f_0 denotes the mean effect, which is the expected value of the model output $f_0 = E(Y)$.
- The first-order component functions $f_i(x_i)$ give the effect of variable x_i acting independently (although generally nonlinearly) upon the output $Y(\mathbf{x})$:

$$f_i(x_i) = E(Y|x_i) - f_0$$

- The function $f_{ij}(x_i,x_j)$ is a second-order term describing the cooperative effects of the variables x_i and x_j upon the output $Y(\mathbf{x})$:

$$f_{ij}(x_i, x_j) = E(Y|x_{i,}, x_j) - f_i - f_j - f_0$$

If we find an **accurate meta-model** with which to represent the HDMR expansion, we can provide an accurate estimate of the partial variances and therefore the global sensitivity indices.

Calculation of sensitivity indices

- The HDMR expansion is analogous to the variance decomposition:

$$V(Y) = \sum_{i=1}^{n} V_i + \sum_{1\le i<j\le n} V_{ij} + \ldots + V_{12\ldots n} = \sum_{j=1}^{2^n-1} V_{p_j}$$

And the coefficients of the expansion can be used to calculate the sensitivity indices.

$$V_{p_j} = V(f_{p_j}(\mathbf{x}_{p_j}))$$

$$\sum_{j=1}^{2^n-1} \frac{V_{p_j}}{V(Y)} = \sum_{j=1}^{2^n-1} S_{p_j} = 1$$

QRS-HDMR

- **Quasi-random sequences** such as a **Sobol sequence** have **better convergence** properties than other sampling approaches.
- Therefore we expect the Sobol' sequence to be a good choice of sampling strategy for fitting an HDMR meta model.
  1. A quasi-random sample is developed for chosen input parameter space.
  2. The full model would be run for each sample (e.g. 1024, 2048, etc) and target outputs stored.
  3. A meta-model would be fitted to the input-output relationships for each target output. **Orthonormal polynomials** are generally used.
  4. The fitted HDMR meta-model would be used to derive global sensitivity indices.
- The accuracy of the meta-model determines the accuracy of the calculated indices and needs to be checked carefully.

Sample size

- The coefficients are determined using Monte Carlo integration over the chosen input sample (Li et al., 2002).
- The approximation of the component functions reduces the sampling effort dramatically so that only one set of quasi-random samples *N* is necessary in order to determine all RS-HDMR component functions and subsequently the sensitivity indices.
- For first-order indices this sample can usually be quite small (e.g. 1024).
- If significant **second-order effects** are present then the **sample size** will need to be **bigger**.

- **Remember – base 2 system so sample size increases as 2^{Ns}**
  - **2, 4, 8, 16, 32, 64, 128, 256, 512, 1024, 2048 etc!**

Example: Ignition delays of butane: sources of uncertainties

Uncertainties lowest at higher temperatures.

Dominated by sensitivity to reactions in C0-C2 base scheme

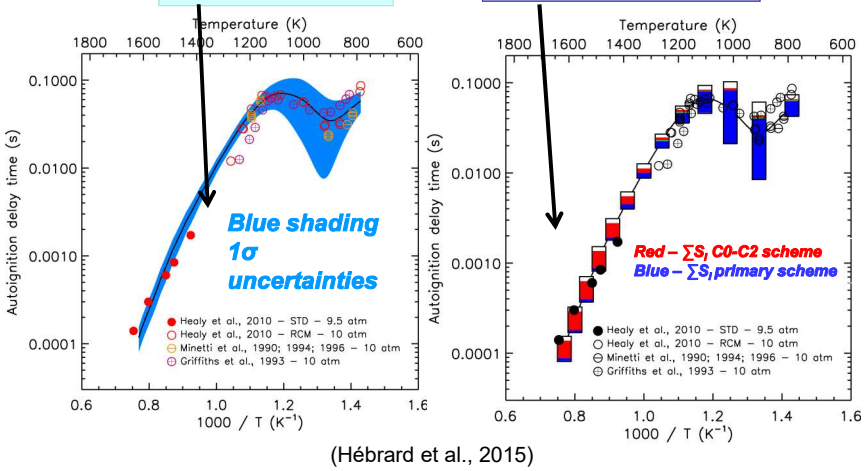

(Hébrard et al., 2015)

(Hébrard et al., 2015)

Ignition delays: 1st-order global sensitivities

Key reactions at low temperatures

$C_4H_9\text{-}1\text{-}OO \rightarrow C_4H_8\text{-}1\text{-}OOH$

$C_4H_9\text{-}1\text{-}OO \rightarrow C_4H_8\text{-}2\text{-}OOH$

$1\text{-}C_4H_9+O_2 \rightarrow 1\text{-}C_4H_8+HO_2$

$2\text{-}C_4H_9+O_2 \rightarrow 1\text{-}C_4H_8+HO_2$

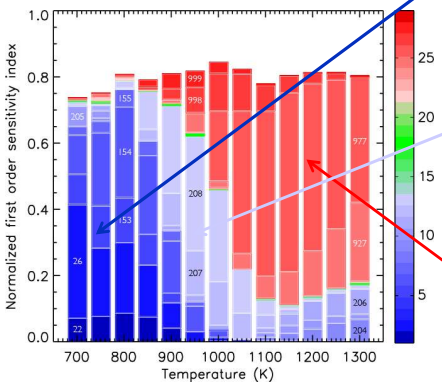

Key reactions at intermediate temperatures

$C_4H_{10}+HO_2 \rightarrow H_2O_2+1\text{-}C_4H_9$

$C_4H_{10}+HO_2 \rightarrow H_2O_2+2\text{-}C_4H_9$

Key reactions at high temperatures

$HO_2+CH_3 \rightarrow CH_3O+OH$

$O_2+H \rightarrow OH+O$

$C_4H_{10}+H \rightarrow H_2+2\text{-}C_4H_9$

$C_4H_{10}+OH \rightarrow H_2O+2\text{-}C_4H_9$

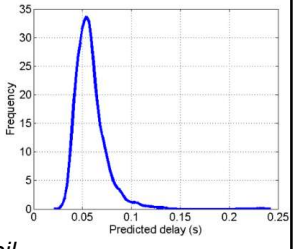

White space are higher order effects not shown - lead to the tail

Importance of uncertainties in thermodynamic data

- Many sensitivity studies focus only on a local analysis of A factors for reactions.
  - Tells us about importance of different reaction steps but not really sufficient for full uncertainty propagation.
- Effects of thermo data often ignored but can be critical for predicting e.g.
  - Heat release
  - Equilibrium between important species in low T reactions such as RO_2, QOOH
- At simplest level **should involve variability in heats of formation**.
- In reality where data from ATChT – data is highly correlated.

Some examples

- 2 stage ignition delay times for **stoichiometric propane oxidation**.
- Morris method (Hughes, 2006).
- Variations in ΔH_{f° from NIST Chemistry WebBook where possible.
- Where no quoted error, ±5, +10 or +15 kJ mol^{-1}, used depending on complexity of species.

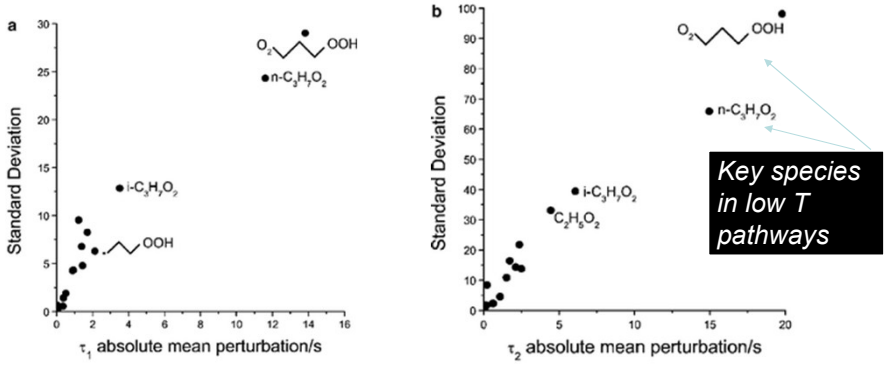

Impact of thermo uncertainties on diethyl ether oxidation (Vom Lehn, 2019)

- Highest prediction uncertainty observed in the NTC regime.

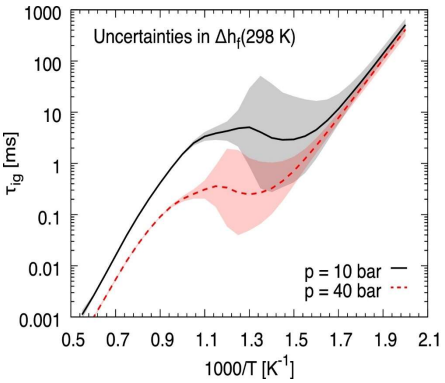

Optimization potential of τ_{ign} for uncertainties in Δh_f(298 K), s^0(298 K), and c_p for a stoichiometric DEE/air mixture at T=769 K and 10 bar.

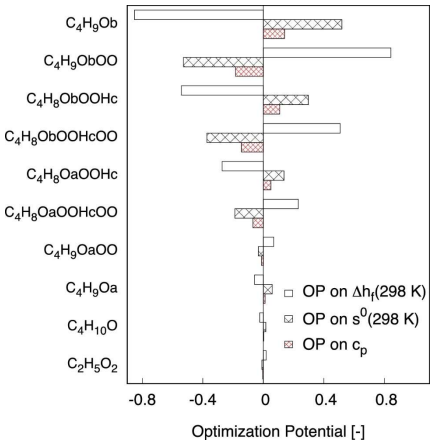

Impacts of group additivity values on kinetic model predictions (vom Lehn, 2020)

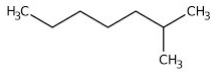

- 2 methyl heptane, shock tube ignition delays.
- Non-dimensionalized sensitivity coefficients of ignition delay time with respect to group parameters ψ_j defined as:
- $SC_j^{\psi} = \frac{\partial \tau_{ign}}{\psi_j} \frac{\psi_{norm}}{\tau_0}$

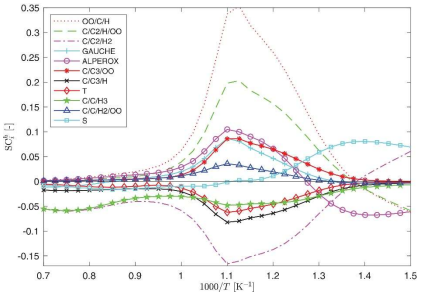

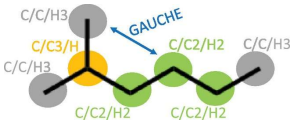

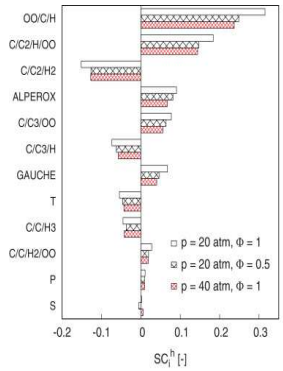

Sensitivity coefficients of ignition delay time on the group values of Δh_f(298 K)

Optimisation methods for constraining model uncertainties.

Range of data types available:

Direct measurements:

- Determination of the rate coefficient of a single elementary reaction.
- Rate coefficients are published at a given temperature, pressure, and bath gas. Sometimes Arrhenius expressions developed.

Theoretical (direct) determinations:

- TST/master equation calculations.
- The rate coefficients are published at given *T*, *P.*
- Parameterized *T*, *P* dependence of rate coefficient *k.*

Indirect measurements:

- A property of the whole combustion system is measured.
- Interpretation is based on a detailed mechanism.
- *Examples:* Laminar burning velocities, ignition delays, concentration profiles.

Traditional approach is to develop *k(T,P)* using first two methods and evaluate using third.

Evaluation

- More effective to automate mechanism evaluation via codes that perform many simulations over all available indirect experiments.
- Normalised error measures needed to rank accuracy of mechanisms and to evaluate which are the key reactions and species within them.
  - i.e. not just eyeballing results.
- Examples from Eötvos group:

Absolute deviation of a single data point

$$D = \frac{1}{N}\sum_{i=1}^{N}\frac{1}{N_i}\sum_{j=1}^{N_i}\left(\frac{Y_{ij}^{sim} - Y_{ij}^{exp}}{\sigma(Y_{ij}^{exp})}\right)$$

$$E = \frac{1}{N}\sum_{i=1}^{N}\frac{1}{N_i}\sum_{j=1}^{N_i}\left(\frac{Y_{ij}^{sim} - Y_{ij}^{exp}}{\sigma(Y_{ij}^{exp})}\right)^2$$

Difference of simulated and experimental value
(characterized the prediction of one measured value)

$$Y_{ij} = \begin{cases} y_{ij} & \text{if } \sigma(y_{ij}^{exp}) \approx \text{constant} \\ \ln y_{ij} & \text{if } \sigma(\ln y_{ij}^{exp}) \approx \text{constant} \end{cases}$$

Number of data series
(reduction to a single value)

Number of points
(division makes data series differing in size comparable)

Estimated standard deviation / scatter
(makes different types of experiments comparable, accounts for different reliability of data)

Zsely (2022)

Example

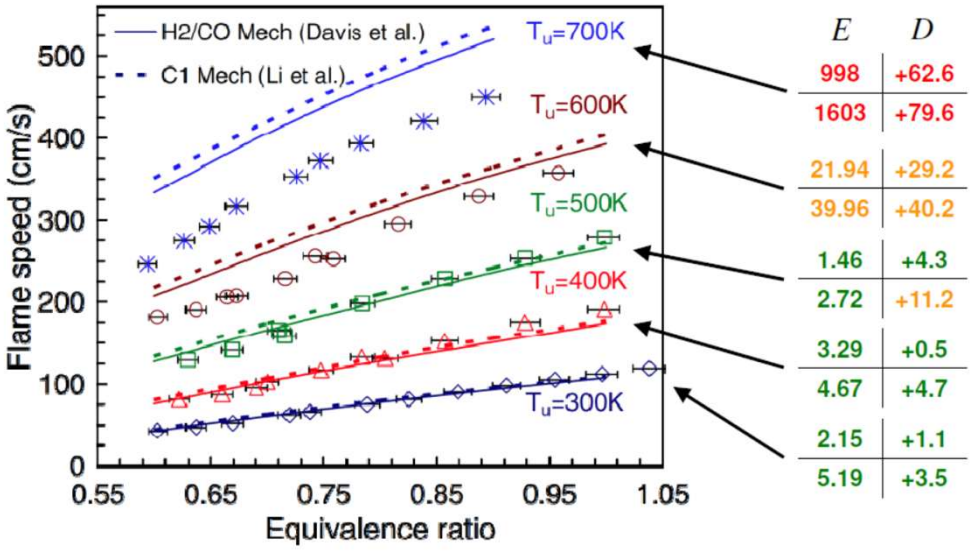

Ammonia example (Kawka, 2020)

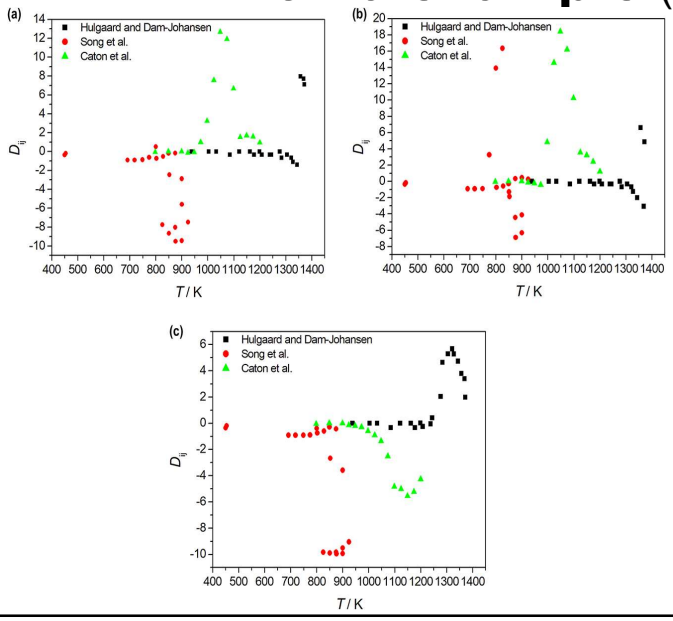

- Plot of the $\boldsymbol{D}_{ij}$ values versus temperature calculated by mechanisms Klippenstein-2011 (a), Glarborg-2018 (b) and Song-2019 (c) for the N_2O concentration measurements.

Optimisation

- What then if we can **vary the parameters** within **uncertainty bounds** to **minimise** such **error functions** and improve overall fit with available data:
  - Optimisation.
  - Error function used as objective function in minimisation process.
- First used for development of GRI mech for methane combustion (Frenklach and co-workers).
- BUT available data sets grow in size over time, new parameter estimations developed, uncertainties change.
- **Mechanisms are not static** and we shouldn't get stuck with old mechanisms out of convenience.

Example for hydrogen combustion

- First: comparison of mechanisms using available data..

• Ignition delays – shock tube	770 data points in 53 datasets
• Ignition delays – RCM	229 data points in 20 datasets
• Laminar burning velocities	631 data points in 73 datasets
• Species profiles – JSR	152 data points in 9 datasets
• Species profiles – flow reactor	389 data points in 17 datasets

Wide range of conditions

• Temperature:	800 K – 2300 K	Pressure	0.1 bar – 65 bar
• Equivalence ratio	0.2 – 5.0		

C. Olm, I. Gy. Zsély, R. Pálvölgyi, T. Varga, T. Nagy, H. J. Curran, T. Turányi
Comparison of the performance of several recent hydrogen combustion mechanisms
Combustion and Flame, **161**, 2219-2234 (2014)

Methods used for optimisation

- Frenklach and co-workers
  - Most influential (**active**) parameters identified via sensitivity analysis (often local method).
  - **Response surfaces models** used for each optimization target to express the simulation result as a function of values of active parameters.
  - Minimise error function by varying active parameters.
  - **LATER** with penalties for distance from evaluated nominal values - MUM-PCE. $\Phi = \sum_r [(\mu_{r,expt} - \mu_{r,calc})/\sigma_r]^2 + \sum_k 2xk^2$
  -
- Wang and co-workers
  - Use of polynomial chaos expansions to provide covariance matrix of fitted parameters.

Validity of optimised mechanism

- Limited set of targets makes **extrapolation** of mechanism to new conditions dangerous.
- **Must be based on sensitive parameters** or others will be changed with no basis.
- Sets of targets can in principle include:
  - Direct measurements
  - Theory
  - Indirect measurements
- Very large number of simulations required hence use of surrogate models – see later.
- Can also use **hierarchical approach**:
  - First, most influential parameters optimized roughly.
  - Reactions (and corresponding experiments) added one by one and optimized first separately, later altogether.

Example: Keromnes mechanism

- Thousands of samples required.
- Orthonormal polynomial response surface used.

Final set of optimization targets

• Ignition measurements in shock tubes	566 data points in 43 datasets
• Rapid compression machines	219 data points in 19 datasets
• Burning velocity measurements	364 data points in 59 datasets
• Direct rate coefficient measurements	1749 data points in 59 datasets

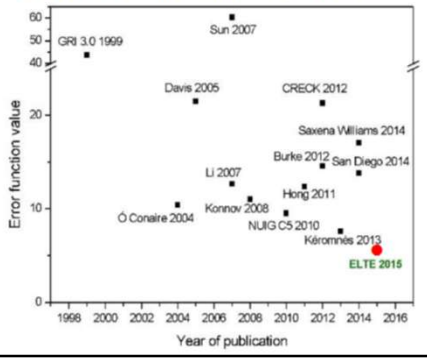

Measurement type	Kéromnès mechanism	Optimized mechanism
Shock tube	1.081	1.043
RCM	1.400	0.600
Burning velocities	3.115	1.770
Direct measurements	2.254	0.924
Total	7.851	4.338

Prior and posterior uncertainties

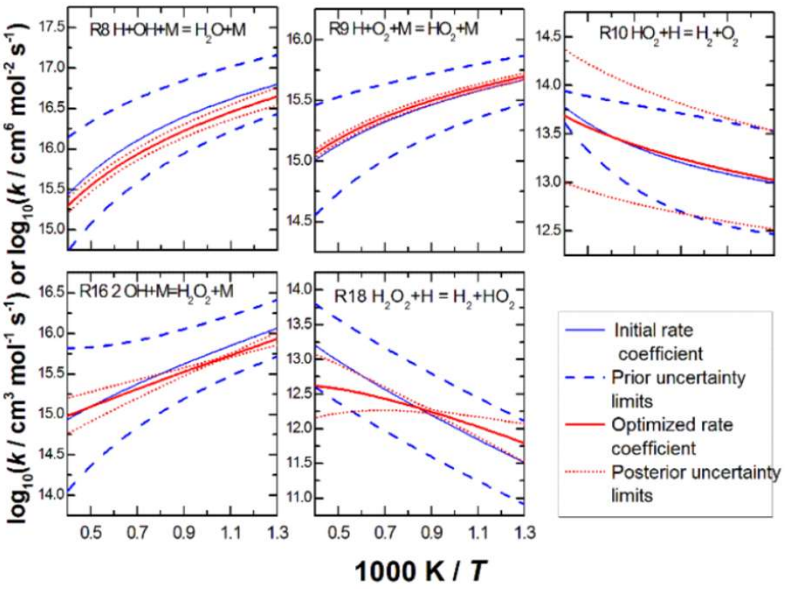

Correlated sensitivities

- The result of optimisation of reaction/thermodynamic networks is a joint probability distribution of parameters.
- Correlations must be accounted for when propagating uncertainties or final predictive uncertainties will be overestimated.

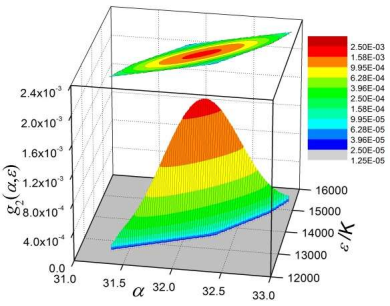

- Straightforward for uncertainty propagation – just sample from **joint probability distribution**.
- Need a way to account for correlations in sensitivity analysis.
  - Trickier.

Information content and design of experiments (DoE)

- High correlations perhaps suggests a different approach for determining new experiments of value.
- Instead of designing experiments to isolate and improve accuracy of individual reactions, need to think about **minimising uncertainty of system as a whole through optimisation.**
- Methods from information theory useful.
  - Particularly for alternative fuels where little data exists and species are large (limiting application of high level theory).
- Optimal experiments are chosen iteratively one by one.
  - Giving high priority experiments and their order.
- Or through genetic algorithm type approaches based on sensitivity entropies (Zhou et al., 2023).

We are not used to simulating experiments before we perform them but we should do it!

Example for DME combustion (Vom Lehn, 2021)

- Assuming a multivariate normal distribution for optimized parameters in model, posterior covariance matrix **Σ*** of **x** is estimated based on linearization of response surface in neighbourhood of posterior values **x*** where $\mathbf{J}_r^*$ is local gradient of model response r with respect to **x**, evaluated at **x*.**

$$\boldsymbol{\Sigma}^* = \left[\sum_{r=1}^{n} \frac{\mathbf{J}_r^* \mathbf{J}_r^{*\mathrm{T}}}{\left(\sigma_r^{\mathrm{obs}}\right)^2} + 4\mathbf{I} \right]^{-1}.$$

contains the important information about the joint uncertainty space of the optimized parameters

Aim: *efficient minimization of joint parameter uncertainties.*

- Each iteration starts with evaluation of all not yet selected conditions *p* in terms of covariance matrices that would result if the experiment *p* were selected.
- Nominal model prediction from previous iteration assumed as hypothetical experimental value of experiment *p* to determine Σ*p**. Sum includes all previous exp.

Example for DME combustion (Vom Lehn, 2021)

- Equivalent to D-optimal design.
  - select the experiment which minimizes the Shannon entropy of the multivariate normal distribution of model parameters in each step.

- Shannon entropy in this context measures the variability of the multivariate normal distribution of the model parameters.
- Minimization is equivalent to minimizing the determinant of the expected covariance matrix after inclusion of the new experiment:

$$\Psi(p) = \min_{p} \left(\det \left(\boldsymbol{\Sigma}_p^* \right) \right)$$

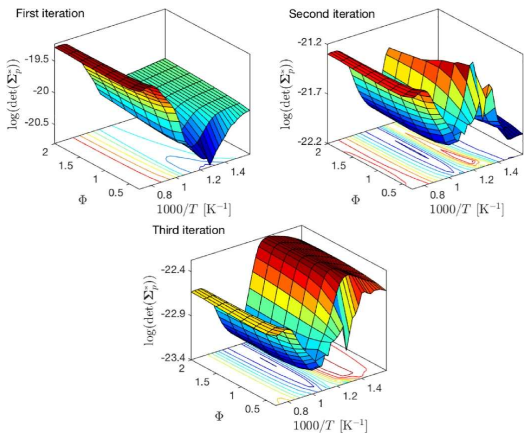

Example for DME combustion (Vom Lehn, 2021)

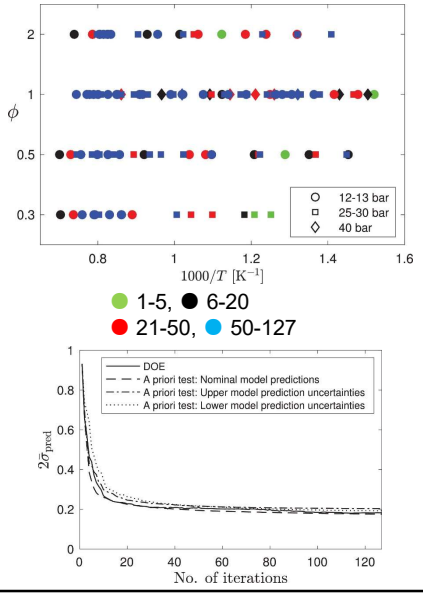

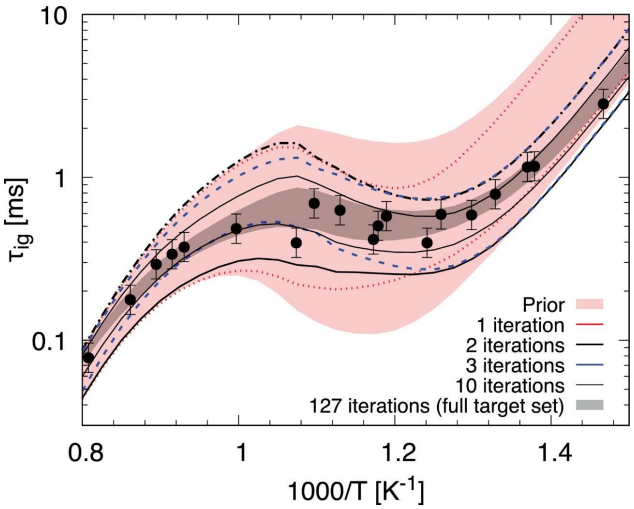

2σ prediction uncertainties after different DOE iteration steps

Doing things optimally

- There are other methods based on the use of ML (e.g. Li et al., 2025).
- All methods require collated data sets - requires collaboration as a community!
  - To combine modelling, experimental design and expertise, statistical methods and ML.
  - To think about what experiments/theory calcs are required to reduce system uncertainty and not just what we fancy/might be easiest…

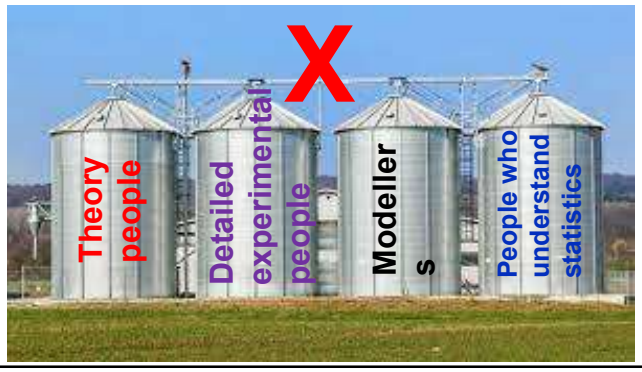

SECTION 6
CHEMICAL MODEL REDUCTION

Why is it necessary?

- Reactive flow models may involve resolving complex 3D turbulent flows within complex geometries.
- In order to achieve realistic computational times something has to be sacrificed:
  - **Spatial resolution**
  - **Highly averaged turbulence models**
  - **Use of simplified chemistry.**
- Detailed chemistry is often sacrificed but some phenomena require models that couple turbulent mixing and chemical processes in a resolved way.
- **Can we simplify detailed chemistry in such a way that we do not loose the important chemical information?**

Types of chemical model reduction

- **Skeletal model reduction – usually local i.e. specific C, *P, T***
  - Methods for removing species and reactions that are not required to accurately simulate the desired target quantities or phenomena.
  - Sensitivity or graph theory based.
- **Time-scale based methods**
  - Rely on the fact that chemical processes take place on a wide range of time-scales and both SLOW and FAST processes can be simplified.
  - Usually processes faster than the mixing time-scales can be assumed to locally equilibrate, a kind of quasi-steady-state, QSS.
  - Simplified expressions then found for QSS species so that their rate equations need not be solved.
- **Lumping**
  - Can be applied to reactions or species based on different principles.
  - Reaction lumping based on QSS arguments.
  - Species lumping based on reactive or structural similarities of species.
- **Tabulated or functional representations of chemistry**
  - Pre-solve chemical problem in someway and store the results for use in CFD – or do on the fly.

Skeletal reduction

- Species and reactions that are redundant over wide ranges of conditions (*T*, *P*, composition) can be removed from the scheme.
- IMPORTANT to ensure that reduced model has been developed over conditions covering final application – wide **C**, *P*, *T*.

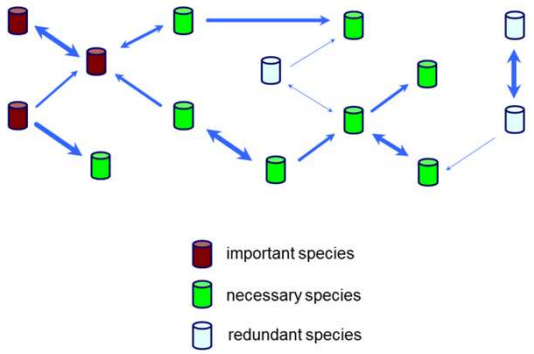

Important species identified by user. Methods find *Necessary* species and reactions required. *Redundant* species removed.

Directed relation graph based methods

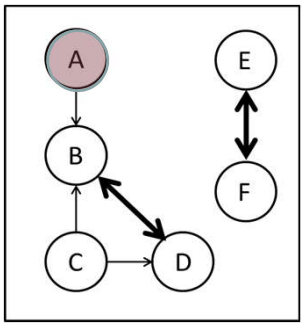

$$R_{i\to j}^{(\mathrm{Lu})} = \frac{\sum_{\alpha\in C(i,j)} \left|\nu_{i\alpha} r_\alpha\right|}{\sum_{\alpha\in R(i)} \left|\nu_{i\alpha} r_\alpha\right|}$$

- Lu & Law (2005) suggested graph based methods for exploring couplings between species.
- Such methods applied to remove groups of species that can be internally coupled, through e.g. fast reactions, but are not strongly coupled to important processes: **species E, F**
- Each node in DRG represents a species and an edge from vertex A to B exists *if and only if* the removal of species B directly induces significant error to the production rate of species A.
- An edge from A -> B means B has to be kept to correctly evaluate the production rate of A.

threshold

$$I_i^{(\mathrm{DRG})} = \begin{cases} 1 & \text{if species } i \text{ is a target species} \\ \max_{j\in S}\left(\min\left(R_{j\to i}, I_j^{(DRG)}\right)\right) & \text{otherwise} \end{cases} < \varepsilon$$

Connection weight: R_i - set of reactions related to species *i*; $C_{i,j}$ set of reactions in which both species *i* and *j* participate, $\nu_{i\alpha}$ is the stoichiometric coefficient of species *i* in reaction *α*, and r_α is the net reaction rate

Examples of variants of DRG

$$R_{i\to j}^{(\mathrm{Luo})} = \frac{\max_{\alpha\in C(i,j)} \left|\nu_{i\alpha} r_\alpha\right|}{\max_{\alpha\in R(i)} \left|\nu_{i\alpha} r_\alpha\right|}$$

- Use of maximum norm (Luo et al., 2010).
- **DRG with restart**, two-stage reduction where the DRG procedure is repeated on the DRG-reduced mechanism (Lu & Law, 2006).
  - Graph structure likely will change on first reduction step.
- **Flux-based DRG** (Tosatto et al., 2011), considers effects of transport fluxes in flames.
- **DRG-aided sensitivity analysis (DRGASA)**, (Nieymeyer et al., 2010)
  - Not as name suggests a sensitivity method, but a method that includes testing simulation error of proposed mechanisms with tighter and tighter thresholds.
- **DRG with error propagation (DRGEP),** (Pepiot & Pitsch, 2008)
  - Errors are damped as they propagate along the graph from the initially selected important species.
- **Factor of 3 reduction** in species and reactions is typical when starting with comprehensive mechanisms.

Simulation Error Minimization Connectivity Method (SEM-CM)

- Connectivity determined iteratively using: $B_i = \sum_j \left(\left(y_i / f_j \right) \left(\partial f_j / \partial y_i \right) \right)^2$
- Shows % change of production rate of species *j* due to small change in concentration of species *i*. If square is summed over all important species, B_i shows effect of a change in concentration of each species on the concentrations of all **important + necessary** species, *j*.
- Gaps in B_i values show groups of un-connected species in a similar way to un-connected groups in the DRG.
- Several trial reduced mechanisms are created, and the simulation results obtained guide the further search for the nearly optimal reduced mechanism (Nagy & Turányi, 2009).
  - Adds to computational expense.

- **ALL THESE METHODS** should be applied over many pre-simulations to ensure all conditions covered in a reactive flow simulation will be included in reduction process.

Comparison of methods (Nagy &Turányi, 2009)

methane partial oxidation mechanism

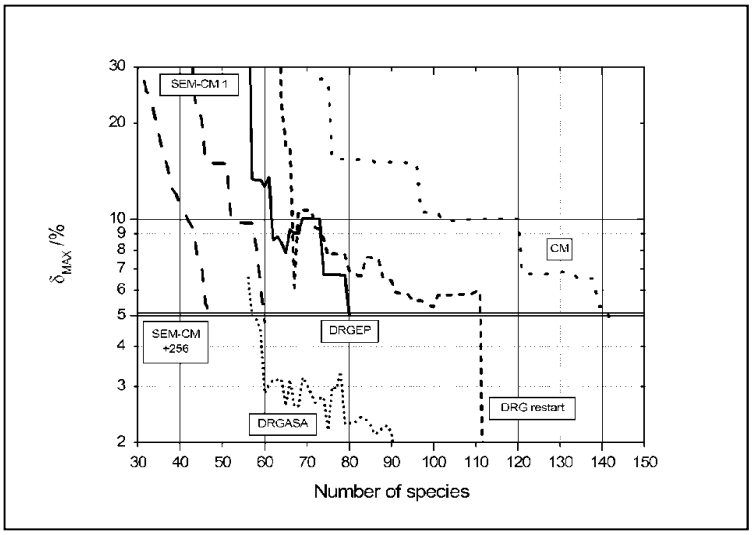

Time-scale based methods

- Chemical systems contain a large range of time-scales due to the differing behaviour of highly reactive radicals, slower intermediates, initial reactants and products.
- Creates problems for numerical methods since the eigenvalues of the Jacobian can span many orders of magnitude creating ***stiffness***.
- Very small time-steps are then required for standard methods hugely adding to the computational costs.
- **On the other hand….**
- This range of time-scales can be exploited within chemical model reduction by assuming that very fast time-scales are in **local equilibrium with the slower variables**.
- Allows a range of different methods to be used to limit the solution of chemical rate equations to only slower species.

Collapse of system dimension

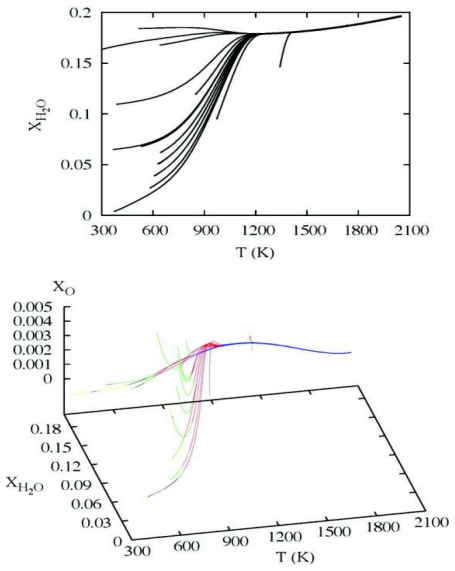

- Example of premixed laminar hydrogen oxygen flame.
- In phase space trajectories converge from all boundary conditions to final equilibrium point.
- Colours show underlying system dimension as the time-scales collapse.
- n = 1 (blue), n = 2 (red), n = 3 (green), n = 4 (black), and n = 5 (yellow).
- Depending on temperature space the model is trying to predict, different reduced models could be developed.
- HOW??

Davis & Tomlin, 2008

Quasi-steady-state assumption QSSA

- Goes all the way back to Bodenstein (1913)
- Here **time-scales are associated with species directly**.
- Error induced by assuming QSSA for a species relates to its chemical lifetime within the system – 1/diagonal Jacobian element and its net production rate (Turányi et al., 1993).

$$\Delta Y_i = \left(-\frac{\mathrm{d}Y_i}{\mathrm{d}t}\right)\left(-\frac{1}{J_{ii}}\right)$$

- Or for coupled groups of QSS species: $\frac{\mathrm{d}\mathbf{Y}^{(QSS)}}{\mathrm{d}t} = \mathbf{J}^{(QSS)}\Delta\mathbf{Y}^{(QSS)}$
- Consistent with ***small local error for species consumed in fast reactions*** and in such cases the local production rate of the QSS species can be large - counter intuitive.
- Term quasi-steady state means that concentrations do not change significantly ***with respect to the slow species*** which may exhibit steep concentration gradients in time.

How to apply QSSA

- Set right hand side of rate equation to zero and solve algebraically.
- Some times this can be done using symbolic algebra and a lumped reaction can be formed completely removing QSS species.

$$\mathrm{A} \underset{k_{-1}}{\overset{k_1}{\rightleftharpoons}} B \xrightarrow{k_2} \mathrm{C}\,. \quad d[\mathrm{B}]/dt = k_1[\mathrm{A}] - k_{-1}[\mathrm{B}] - k_2[\mathrm{B}]$$

- If QSSA applied to B $\quad \frac{d[B]}{dt} = 0, \qquad [B] = \frac{k_1}{k_{-1}+k_2}[A]$

$$\frac{d[C]}{dt} = k_2[B] = \frac{k_1 k_2[A]}{k_{-1}+k_2} \text{ and}$$

B can be removed providing the global reaction step: A → C

with $\quad k' = \frac{k_1 k_2}{k_{-1}+k_2}$

- In other cases numerical iteration methods are needed.

Global reaction schemes

- Global reaction schemes often used in complex reacting flows are usually generated using similar approaches to this e.g. (Peters & Rogg, 1993).
- Few species may be contained in the global schemes but the reaction rates contain complex expressions due to the lumping.
- Or they can be fitted as Arrhenius expressions to e.g. full model or experimental data.
  WARNING – such expressions are often out of date from a kinetics perspective.

Example from CERFACS – **note non-integer stoichiometries**:
Reaction 1 reaction("C3H8 + 3.5 O2 => 3 CO + 4 H2O", [5.82320E+12, 0, 34000], order = " C3H8:0.8 O2:0.86 ")
Reaction 2 reaction("CO + 0.5 O2 <=> CO2", [2.00000E+09, 0, 12000])

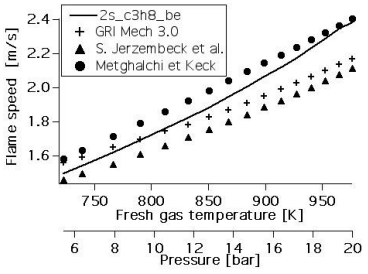

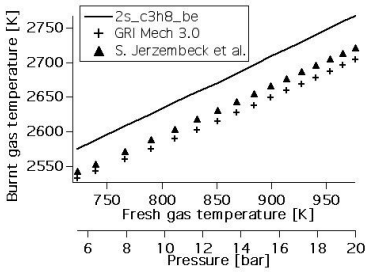

Intrinsic low dimensional manifolds (ILDM)

- The **QSSA** is restrictive in the sense that it **associates time-scales with specific species concentrations**.
- More general formulations look for intrinsic low dimensional hyper-surfaces with the phase space that exist when the fast time scales have collapsed – low dimensional or **slow manifolds**.
  - By restricting the chemical changes to such ILDMs the dimensionality of the problem can be vastly reduced.
  - **Hard part:** defining the dynamic chemical changes within the manifold.

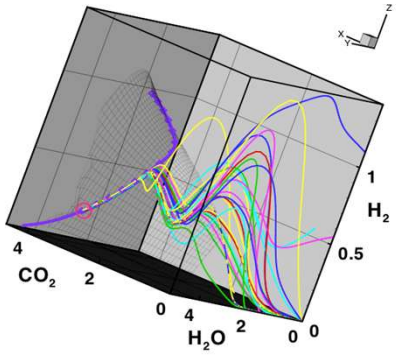

ILDM (black mesh) for iso-octane-air system 1D ILDM (purple symbols), 0D ILDM (equilibrium, red circle). Lines - homogeneous reactor calculations for different fuels using different reaction mechanisms. (Blasenbrey & Maas, 2000)

Formulation of ILDM

General reaction diffusion system:

$$\frac{\partial \psi}{\partial t} = F(\psi) - \vec{v} \cdot \mathrm{grad}\psi + \frac{1}{\rho}\mathrm{div}D\ \mathrm{grad}\psi$$

where $\psi = (\psi_1, \psi_2, \ldots, \psi_{S+2})^T$ is the thermokinetic state, $\psi = (h, p, w_1, \ldots, w_S)^T$, F the chemical source term, $\vec{v}$ the velocity, ρ the density and D the matrix of transport coefficients.

Using operator splitting the chemical source term can be separated: $\frac{\partial \psi}{\partial t} = F(\psi)$

System is then separated into three parts representing conserved, slow and fast subspaces:

$$\left(Z_c\ Z_s\ Z_f\right) \cdot \begin{pmatrix} \tilde{Z}_c \\ \tilde{Z}_s \\ \tilde{Z}_f \end{pmatrix} = I$$

$$\tilde{Z}_c \frac{\partial \psi}{\partial t} = \tilde{Z}_c F(\psi)$$
$$\tilde{Z}_s \frac{\partial \psi}{\partial t} = \tilde{Z}_s F(\psi)$$
$$\tilde{Z}_f \frac{\partial \psi}{\partial t} = \tilde{Z}_f F(\psi)$$

Equilibrate fast time-scales

$$\tilde{Z}_f F(\psi) = 0$$

Project onto slow subspace

$$\frac{\partial \psi}{\partial t} = \left(I - \tilde{Z}_f Z_f\right) F(\psi)$$

(Maas & Pope, 1992; Lam & Goussis, 1994)

Intrinsic dimensionality

- Two key aspects to using ILDMs/slow manifolds:
  - What is the **required dimension** of manifold to get desired accuracy?
  - How are the **chemical changes** along the **manifold defined**.

Z_s and Z_f *are* defined via invariant subspaces associated with the local Jacobian of the chemical source term according to:

$$F_\psi = \left(Z_c\ Z_s\ Z_f\right) \cdot \begin{pmatrix} N_c & & \\ & N_s & \\ & & N_f \end{pmatrix} \cdot \begin{pmatrix} \tilde{Z}_c \\ \tilde{Z}_s \\ \tilde{Z}_f \end{pmatrix},$$

$$|\lambda_i(N_c)| < \tau_c, \quad \lambda_i^{\mathrm{real}}(N_f) < \tau_s < \lambda_i^{\mathrm{real}}(N_s)$$

τ_c is upper limit for the λ*s* associated with very slow processes ("almost conserved scalars"), and τ_s is upper limit for λ*s* associated with fast relaxing (-ve) time-scales.

By an eigenvalue analysis gaps in the time-scale spectrum can be found and a dimension defined.

Computational Singular Perturbation (CSP) Theory uses a similar approach with slightly different formulation (Lam & Goussis, 1994):

Operator splitting

- For many models of reacting flows, the **chemistry equations can dominate the CPU usage**.
- Stiffness adds further issues.
- Using operator splitting the chemical part can be separated from the solution of the flow terms, allowing reduction or special numerical strategies to be applied to chemical source term rather than having to apply them everywhere.
- Sportisse, 2000, suggests that the **stiff terms** should be **solved last** within each time-step.
  - Advection due to mean flow → diffusion, turbulent mixing → chemistry
  - Allows system to relax back onto slow manifold.
- Representation of chemical changes on the slow manifold e.g. using **tabulation** or **fitting** can overcome some of these problems (Pope, 1997).
  See later for these methods.

LUMPING

What does lumping mean?

- Combining information into “lumps” in such a way that we can still represent detailed kinetics but with fewer species or equations.
- Can take two forms:
  - Reaction Lumping $A \rightarrow B \rightarrow C$ becomes: $A \rightarrow C$ *Vertical*
  - Species Lumping [Y] = [A] + [B] + [C] *Horizontal*
- **WHY?**
  - Skeletal mechanism reduction methods are useful but sometimes not sufficient to make the mechanism small enough for use in e.g. CFD codes.
  - By combining species or reactions we can compress the mechanism further and potentially reduce the number of equations we need to solve.

Advantages and Disadvantages

Advantages

- Reduction in number of variables and therefore equations to solve.
- When combined with time-scale analysis a reduction in system stiffness.
- Computational speed-up.
- Less species to “transport” in CFD code.

Disadvantages

- Lumped model cannot always be expressed as a kinetic scheme.
- Lumped scheme may “loose” information that was contained in full scheme.
- Cannot always recover original species concentrations.
- Need a method to define lumped reaction rates.

Crucial issues for successful species lumping

1. To determine which species are to be lumped;
2. To classify how the selected species should contribute to the lumped species, *i.e.* define the **lumping transformation**;
   - could also require defining the **inverse transformation** i.e. how to get back to the original species from the lump;
3. To estimate kinetic parameters for the reactions of the lumped species.

Two types of methodology are commonly used:

i) ***Chemical Lumping*****:** based on chemical knowledge of species involved e.g. structural similarities.

ii) ***Mathematical Lumping*****:** based on looking for similar mathematical quantities or applying mathematical rules.

The two can often be equivalent since species with the same reaction steps and rate constants will lead to mathematical similarities within the equations.

Using mathematical approaches does not usually rely on chemical knowledge/intuition.

Chemical Lumping

- Has some commonality with topics on automatic mechanism generation since often based on ***isomers*** being involved in the same ***reaction classes***.
- For *n*-heptane the classes of propagation routes are defined as:
  1. Decomposition and isomerization of alkyl radicals R.
  2. H-abstraction with O_2 to form HO_2 and conjugate olefins.
  3. Direct and reverse O_2 addition to R to form peroxy radicals ROO.
  4. Internal isomerisation between ROO and hydroperoxyalkyl radicals QOOH.
  5. Decomposition of QOOH radicals to form olefins.
  6. Decomposition of QOOH radicals to form HO_2 and conjugate olefins. etc.
- Reference rate parameters defined for each reaction class based on literature data or **similarity rules**.
- The **pathways for each isomer** and the resulting intermediate radicals can then potentially be **lumped** to give a simplified scheme with only a single pathway representing degradation to the average products of all the isomers (Ranzi et al., 1995).
  - Commonly used by Polimi in their mechanism generation.

***n*-heptane** scheme - 4 alkyl radicals noted by R_1, R_2, R_3, R_4 giving rise to 4 reactions involving the addition of O_2.

$R_1 + O_2 \rightarrow R_1OO$ $\quad k_1$

$R_2 + O_2 \rightarrow R_2OO$ $\quad k_2$

$R_3 + O_2 \rightarrow R_3OO$ $\quad k_3$

$R_4 + O_2 \rightarrow R_4OO$ $\quad k_4$

The lumped alkyl radical is then defined by:

$[R] = [R_1] + [R_2] + [R_3] + [R_4]$,

with the corresponding lumped reaction given by: $R + O_2 \rightarrow ROO$ $\quad k_5$

Lumped rates defined by **fitting** with respect to experimental data or with respect to the complex full model (MAMOX, Milan) or **weighted averages** for the different component isomers depending on the relative **weights** within the initial fuel or from the **weighted mean of the elementary rate coefficient** for the individual isomers (Fournet et al., 2000):

$$k_5 = \frac{k_1[R^\bullet_1] + k_2[R^\bullet_2] + k_3[R^\bullet_3] + k_4[R^\bullet_4]}{[R^\bullet]}$$

Much easier if all the rate constants are the same!

Applications of Chemical Lumping

- Mechanisms developed in Milan tend to incorporate lumping and have now addressed a large number of parent fuel compounds.
- Key example is that for *n*-heptane which contains only 4 lumped radicals.
- High degree of lumping leads to reactions with non-integer stoichiometries which represent the relative weights of the different product channels.
- $Q7OOH \rightarrow OH + 0.3HCHO + 0.32C_5H_{10} + 0.3C_4H_8 + 0.35CH_3CHO + 0.31C_3H_6 + 0.35C_2H_5CHO + 0.4C_2H_4 + 0.06C_7H_{14}$

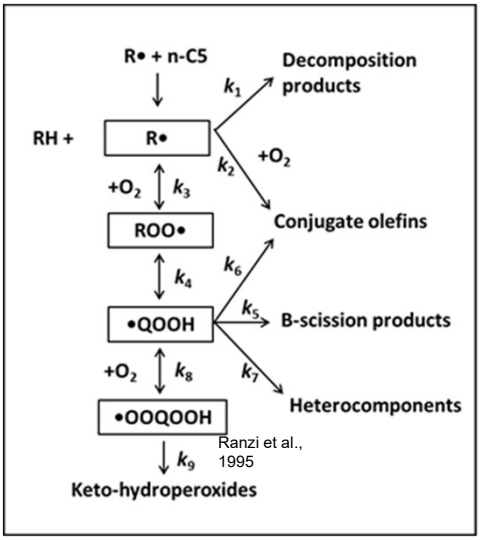

Mathematical Approaches: linear lumping

- The previous example showed that a simple linear transformation could be applied to define new lumped variables that were weighted sums of the original species.
- This type of lumping can be written in a more formal way.
- The formal definition of lumping is the transformation of the original vector of variables **Y** to a new transformed variable vector $\hat{\mathbf{Y}}$ using the transformation function **h**:

$$\hat{\mathbf{Y}} = \mathbf{h}\left(\mathbf{Y}\right)$$

- The dimension $\hat{n}$ of the new variable vector $\hat{\mathbf{Y}}$ is smaller than that of the original concentration vector. A new kinetic system of ODEs is formed:

$$\frac{\mathrm{d}\hat{\mathbf{Y}}}{\mathrm{d}t} = \hat{\mathbf{f}}\left(\hat{\mathbf{Y}}, \hat{\mathbf{k}}\right) \qquad \hat{\mathbf{Y}}(t_0) = \hat{\mathbf{Y}}_0$$

Linear Lumping

In the linear case the transformation is simply a matrix multiplication operation:

$$\hat{\mathbf{Y}} = \mathbf{M}\mathbf{Y}$$

where **M** is a matrix of size $\hat{n} \times N_S$. Consider for example:

$$\mathbf{M} = \begin{pmatrix} 1 & 0 & 0 & 0 \\ 0 & 1 & 1 & 1 \end{pmatrix}$$

Lumping matrix transforms original concentration vector (Y_1, Y_2, Y_3, Y_4) to the concentration vector *of lumped species,* $(\hat{Y}_1, \hat{Y}_2)$

where $\hat{Y}_1 = Y_1$

$$\hat{Y}_2 = Y_2 + Y_3 + Y_4$$

Soot modelling – the HACA Reaction Sequence as an Example of Linear Lumping

- Chemical reactions describing polymer growth are of the same type, **rate parameters and thermodynamic data vary only slightly with polymer size**.
- Reaction described by distribution function for degree of polymerization, and repeating reaction cycle for particle growth with structure and rate coefficients for each cycle treated as the same.
- Lumping guided by similarities in structure of hydrocarbon species (Frenklach, 1990).

(*i*,1)	$A_i + H \leftrightarrow A_i^{\cdot} + H_2$
(*i*,2)	$A_i^{\cdot} + C_2H_2 \leftrightarrow A_iCHCH^{\cdot}$
(*i*,3)	$A_iCHCH^{\cdot} + C_2H_2 \rightarrow A_{i+1} + H$
(*i*+1,1)	$A_{i+1} + H \leftrightarrow A_{i+1}^{\cdot} + H_2$
(*i*+1,2)	$A_{i+1}^{\cdot} + C_2H_2 \leftrightarrow A_{i+1}CHCH^{\cdot}$
(*i*+1,3)	$A_{i+1}CHCH^{\cdot} + C_2H_2 \rightarrow A_{i+2} + H$

(*i*+2, *i*+3, …, *n*) … etc.

where A_i is an aromatic molecule containing *i* fused aromatic rings, $A_i^{\cdot}$ is an aromatic radical formed by H abstraction and $A_iCHCH^{\cdot}$ is a radical formed by adding C_2H_2 to $A_i^{\cdot}$

$$\frac{dM_1}{dt} = \left(m_o \frac{d[A_i]}{dt} + m_o \frac{d[A_i^{\cdot}]}{dt} + (m_o + 2) \frac{d[A_iCHCH^{\cdot}]}{dt} + (m_o + 4) \frac{d[A_{i+1}]}{dt} + \cdots \right)$$

$$= m_o r_o + 2k_2[C_2H_2] \sum_i [A_i^{\cdot}] - 2k_{-2} \sum_i [A_iCHCH^{\cdot}] + 2k_3[C_2H_2] \sum_i [A_iCHCH^{\cdot}]$$

where $M_1 = m_o[A_i] + m_o[A_i^{\cdot}] + (m_o + 2)[A_iCHCH^{\cdot}] + (m_o + 4)[A_{i+1}] + (m_o + 4)[A_{i+1}^{\cdot}] + \cdots$,

is the total number of carbon atoms accumulated in the PAHs *i.e.* **the first moment of the PAH distribution.**

- In terms of species lumping we can now see that it is possible to define a new set of variables which define the lumped species:

$$\hat{c}_1 = \sum_i [A_i]$$

$$\hat{c}_2 = \sum_i [A_i^{\cdot}]$$

$$\hat{c}_3 = \sum_i [A_iCHCH^{\cdot}]$$

With corresponding lumped equation system :

$$\frac{d\hat{c}_1}{dt} = r_o - k_1[H]\hat{c}_1 + k_{-1}[H_2]\hat{c}_2 + k_3[C_2H_2]\hat{c}_3$$

$$\frac{d\hat{c}_2}{dt} = k_1[H]\hat{c}_1 - k_{-1}[H_2]\hat{c}_2 - k_{-2}\hat{c}_3$$

$$\frac{d\hat{c}_3}{dt} = k_2[C_2H_2]\hat{c}_2 - k_{-2}\hat{c}_3 - k_3[C_2H_2]\hat{c}_3$$

Fitted models

- Sometimes e.g. in repeated design calculations, it is possible to solve the chemical source terms and **store** the **information** for use in more complex reactive flow simulations.
- Methods based on e.g.:
  1. Fitting a functional equation e.g. polynomial
  2. Look-up tables
  3. Flamelets
- If not specifically probing kinetics can be useful.
- **Caution:** if chemical scheme updated, stored data can easily go out of date unless in situ methods are used.

Use of difference equations for time dependent models – repro-modelling

- For chemical kinetic systems we **usually solve differential equations** to determine the change in species concentrations over time.
- For large, complex, nonlinear systems requires sophisticated numerical integration techniques.
- For repeated calculations (e.g. in CFD codes) the **same conditions of composition, temperature, pressure may be revisited many times**.
- May be quicker to **store** the model results to **reuse** later.
- This can be achieved via the tabulation of model quantities (see later) or by the use of fitted difference equations.

1. Δt is selected to achieve good resolution of the characteristic system time-scale.
2. Several thousand, spatially homogeneous simulations carried out with series of initial concentrations and/or T, representative of circumstances of final applications.
3. $\mathbf{Y}(t)$, $\mathbf{Y}(t+\Delta t)$ concentration vector pairs are stored in a database.
4. Function **G** is fitted to data and to predict change in concentration after time step

$$\Delta t : \mathbf{Y}(t+\Delta t) = \mathbf{G}(\mathbf{Y}(t)).$$

Operator splitting allows difference equation to be applied to only chemical time-step.

Different approaches

- The application of ***orthonormal polynomials*** (Turányi, 1994) can be advantageous for this task, since their ***coefficients can be determined independently*** from each other.
- Overall aim is to get a good fit using as few monomials as possible.
- For large complex systems, rapidly convergent hierarchical correlated function expansions in the input variables, or HDMR, can be used (as in global sensitivity analysis section).
  - Applied in Li et al. (2008) to the simulation of ignition within homogeneous H_2/air mixtures over wide ranges of temperatures and pressures (1000 < T0 < 1500 K, 0.1 < P < 100 atm)
- Artificial Neural Networks, ANNs, have also been used for this purpose (Christo et al., 1996; Blasco et al., 2000).
- Fitted models can be used to represent dynamics within the slow low dimensional manifold.
- Reduces dimension and stiffness and uses less memory than look-up tables.

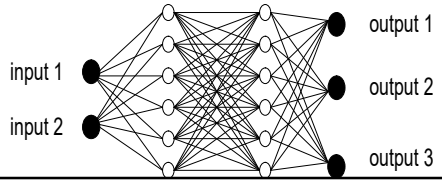

Oscillatory ignition example

- Orthonormal polynomials used for generation of repro-model describing **oscillatory ignition of CO-H_2 mixtures** in a continuously stirred tank reactor (CSTR) at very low pressures (Brad et al., 2007).
- **4-variable repro-model based on 6th order polynomials**, successful representation of regions of steady state, cool flames and large temperature oscillations achieved based on fits to a 14-variable full model.
- $[H_2]$, $[O_2]$, [CO] and *T* used for fitted model.
- Dynamically complex system.
- Regions of high accuracy were required during oscillatory ignition.
  - Diverging trajectories in phase space.
- Whole composition space was partitioned to achieve accurate fits.

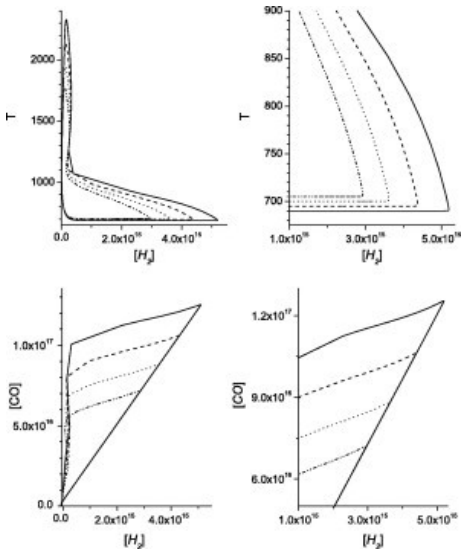

PRISM (Piecewise Reusable Maps)

- Polynomial approach (Tonse et al., 1999) whereby fitted polynomial functions are ***developed during the calculation***, and then ***reused*** when the region of composition space is revisited in subsequent time steps or different spatial regions (c.f. ISAT later).
- Uses **second-order polynomials** so that in order to cover the realisable region, multiple expressions are used, each valid over a different portion of composition space.
- Integration of full kinetic equations provides the solution at selected points throughout a hypercube, in order to determine the polynomial coefficients.
  - Increase in accuracy with reduced hypercube size.
- Trade-off between accuracy and the efficiency of polynomial generation as well as storage and retrieval.
  - **Polynomial construction only allowed for those hypercubes that are revisited enough times to make the construction worthwhile.**
- Successful application to hydrogen ignition, a 1D laminar hydrogen flame, a 2D axisymmetric turbulent jet (Tonse et al., 1999; Tonse et al., 2003) and a turbulent premixed hydrogen flame (Bell et al., 2000).

The use of look-up tables

- Key quantities of chemical changes e.g. species concentrations and rates of change calculated using simple models:
  - Perfectly stirred reactors, laminar flames
- Stored as a function of key quantities:
  - *T*, concentrations, reaction progress variable.
- Key aspect is coverage of **appropriate phase space** that will be encountered in CFD model.
- When CFD code receives input vector, it locates points within table close to input point. Output vector is composed using linear interpolation between output vector elements at the storage points.
- Critical aspects are **accuracy**, **storage** and **efficiency** of retrieval.
- Latter two can be vastly improved by tabulating on ILDMs which are much lower dimensional than the full composition space.
  - **Use of full mechanism and tabulation gives improvement compared to creating table from global mechanism**.

In situ adaptive tabulation (ISAT), (Pope, 1997)

- Exploits the fact that during reactive flow calculations, regions of composition space may be **revisited many times**.
- Calculate the first time and then **store and retrieve** in subsequent requests.
- Since systems naturally **relax to low dimensional manifolds** over time, creating tables on the fly automatically requires les variables and hence much smaller tables.
- Storage within a **binary tree structure**.
- Interpolation error controlled by adaptive refinement of mesh.
- Error controlled using ellipsoid of accuracy for stored points – as new points are tabulated ellipsoid grows.
- Many examples of use in turbulent reacting flows by incorporating operator splitting.

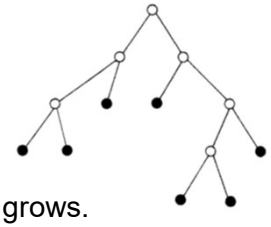

Offline training vs. On-the-fly

- There have been a number of applications of fitted/trained kinetic models within combustion models including for simulations of turbulent flames.
- Earlier examples used offline training.
- Disadvantages
  - If a regime is encountered which is outside the training data.
  - Many chemical mechanisms are regularly updated, which would mean re-training an ANN for example.
- More recent methods include on-the-fly training, in common with PRISM, ISAT and other in-situ methods.
  - Disadvantage here may be that the ANN would be less general overall.

- **On-the-fly ANN method** developed in Chi et al. (2021) for Direct Numerical Simulation (DNS) predictions of hot spot ignition in turbulent flames.

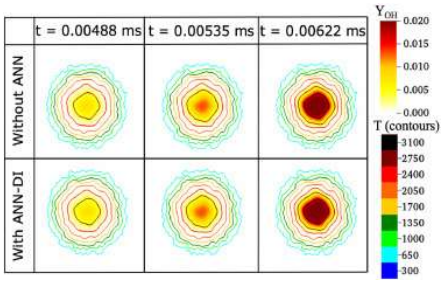

- ANN regression is achieved through a multilayer (4 layers) perceptron (MLP), involving sum of non-linear basis functions and coefficients (biases and weights) to fit input-output training dataset.
- Biases and weights adjusted for each layer of the MLP to obtain a minimal error at the output layer compared to full integration.
- Data clustering used for 1) burned-gas zone, 2) reaction zone, 3) preheated zone, and 4) unburned zone (fresh gas region).
- Stored ANN models are created during simulation and used to replace the expensive ODE integrations in later simulation steps.
  - Retrained and updated throughout simulation.
- Speed up factor of 3.5 but memory requirements very low compared to say ISAT.

Flamelets (Bray, 2016)

- Used to approximate the edge of a turbulent flame by an **ensemble of discrete, steady laminar flames**, called flamelets.
- Individual flamelets assumed to have a similar structure to laminar flames for the same concentration, T conditions.

– Detailed calculations of flamelet chemistry obtained from lower dimensional numerical calculations and potentially stored as **look-up tables** of species compositions and reaction rates in terms of suitably chosen reaction progress variable.
– Coupling with assumed probability density function (PDF) for this variable then provides an estimate for mean properties.
– Alternative is to provide a laminar flamelet expression for the PDF, $P(c;\mathbf{x})$.

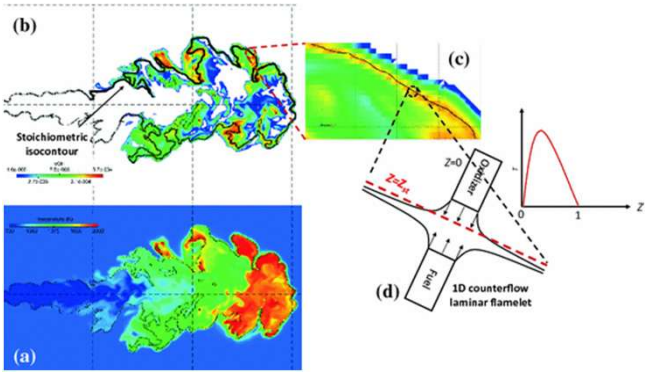

Kundu et al, 2018

Flamelets (Bray, 2016)

Advantages:

- Rapid and usually low dimensional in terms of numbers of state variables.
- Commonly used in CFD packages using RANs and LES approaches.
- Detailed chemistry can be used in developing flamelet tables and hence problems with using global reactions can be avoided.

Disadvantages:

- Can fail in situations of significant flame stretch, intense small-scale turbulence, and flame-flame interactions.
- Difficult to estimate errors induced by assumption except by comparison with DNS.
- DNS data suggests that preheat zone structure differs from that of an unstretched laminar flame much more strongly than the high temperature side.

YOU NEED TO KNOW FROM WHAT CHEMISTRY THE FLAMELET WAS GENERATED… or generate your own using up to date kinetics.

Final Considerations on reduction methods

- The level of detail you decide to use to represent chemistry depends on your research goals.
- If you are probing kinetics, then a skeletal model may be ideal, so that elementary reactions can be retained and explored.
- To simulate turbulent combustion, tabulation/fitting may be only way to gain enough speed to incorporate detailed chemistry.

- Check-point - Should always be aware of underlying chemistry:
  If using a table/flamelet when was it created and using which detailed scheme? **Is it up to date?**
  If using global reaction scheme, **are sufficient intermediates retained**, are underlying rate constants up to date?
- **Always be wary of over-extrapolation.**
- **Tracking uncertainties always useful** if affordable.
  Tells us whether our model is likely to be robust or if process may be missing.
  With SA tells us areas of model to focus on to improve the models predictive capabilities.

Final overall considerations

- All this work has required an enormous human effort.
- New fuels are likely to be more complex/varied than the ones we know.
- Devices will need to be redesigned and optimised to work with new fuels/blends.
- We should work in collaboration with other sectors (electrification, carbon capture, H_2 production) and not against them.
- We need to get a move on to be relevant.
  - ➢ net zero by 2050!

Fully automated process for kinetics?

- Automated laboratories.
  - High throughput/accuracy.
  - Conditions chosen by DOE.
- Automated big data analysis.
  - For evaluation of mechanisms, optimisation.
  - **Effective sharing** of data, including raw.
- Automated theory calculations (Elliot, 2021).
  - Large number of reactions for new fuels.
  - Hierarchical approach in terms of level of accuracy.
- Machine learning for AMG and parameter estimation.
- Automated uncertainty quantification and model optimisation.
- Automated model reduction for inclusion into CFD design codes.

➢ **SOLVE GRAND CHALLENGE PROBLEMS.**

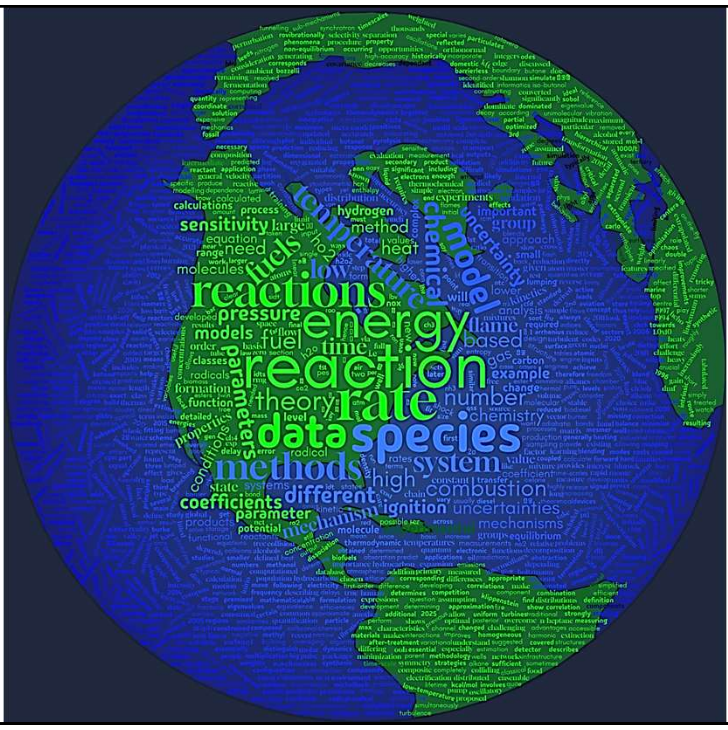

Thanks for listening!

Reference List for Tomlin Lectures 2026 Summer School, Tsinghua.

1. Agbro, E., Zhang, W., Tomlin, A.S., Burluka, A., 2018. Experimental Study on the Influence of n-Butanol Blending on the Combustion, Autoignition, and Knock Properties of Gasoline and Its Surrogate in a Spark-Ignition Engine. Energy Fuels 32, 10052–10064.
2. Agbro, E., A. S. Tomlin, M. Lawes, S. Park and S. M. Sarathy (2017). The influence of n-butanol blending on the ignition delay times of gasoline and its surrogate at high pressures. Fuel 187: 211-219.
3. Aguilera-Iparraguirre, J., Curran, H.J., Klopper, W., Simmie, J.M., 2008. Accurate Benchmark Calculation of the Reaction Barrier Height for Hydrogen Abstraction by the Hydroperoxyl Radical from Methane. Implications for CnH2n+2 where n = 2 → 4. J. Phys. Chem. A 112, 7047–7054.
4. Al-Breiki, M., Bicer, Y., 2021. Comparative life cycle assessment of sustainable energy carriers including production, storage, overseas transport and utilization. Journal of Cleaner Production 279, 123481. https://doi.org/10.1016/j.jclepro.2020.123481
5. Alzueta, M.U., Mercader, V., Cuoci, A., Gersen, S., Hashemi, H., Glarborg, P., 2024. Flow Reactor Oxidation of Ammonia–Hydrogen Fuel Mixtures. Energy Fuels 38, 3369–3381.
6. Amiri, H. and K. Karimi (2019). Chapter 6 - Biobutanol Production. Advanced Bioprocessing for Alternative Fuels, Biobased Chemicals, and Bioproducts. M. Hosseini, Woodhead Publishing: 109-133.
7. Andrews, G. E. and D. Bradley (1972). The burning velocity of methane-air mixtures. Combustion and Flame 19(2): 275-288.
8. Andrews, G. E. and D. Bradley (1972). Determination of burning velocities: A critical review. Combustion and Flame 18(1): 133-153.
9. Atkinson, R., D. L. Baulch, R. A. Cox, J. N. Crowley, R. F. Hampson, R. G. Hynes, M. E. Jenkin, M. J. Rossi, J. Troe and T. J. Wallington (2008). Evaluated kinetic and photochemical data for atmospheric chemistry: Volume IV – gas phase reactions of organic halogen species. Atmos. Chem. Phys. 8: 4141-4496.
10. Barbet, M. C., K. McCullough and M. P. Burke (2019). A framework for automatic discovery of chemically termolecular reactions. Proceedings of the Combustion Institute 37(1): 347-354.
11. Battin-Leclerc, F. (2008). Detailed chemical kinetic models for the low-temperature combustion of hydrocarbons with application to gasoline and diesel fuel surrogates. Progress in Energy and Combustion Science 34(4): 440-498.
12. Battin-Leclerc, F., E. Blurock, R. Bounaceur, R. Fournet, P. A. Glaude, O. Herbinet, B. Sirjean and V. Warth (2011). Towards cleaner combustion engines through groundbreaking detailed chemical kinetic models. Chemical Society Reviews 40(9): 4762-4782.
13. Battin–Leclerc, F., P. A. Glaude, V. Warth, R. Fournet, G. Scacchi and G. M. Côme (2000). Computer tools for modelling the chemical phenomena related to combustion. Chemical Engineering Science 55(15): 2883-2893.
14. Baulch, D. L., C. T. Bowman, C. J. Cobos, R. A. Cox, T. Just, J. A. Kerr, M. J. Pilling, D. Stocker, J. Troe, W. Tsang, R. W. Walker and J. Warnatz (2005). Evaluated Kinetic Data for Combustion Modeling: Supplement II. Journal of Physical and Chemical Reference Data 34(3): 757-1397.
15. Baulch, D. L., C. J. Cobos, R. A. Cox, J. H. Frank, G. Hayman, T. H. Just, J. A. Kerr, T. Murrels, M. J. Pilling, J. Troe, B. F. Walker and J. Warnatz (1994). Summary table of evaluated kinetic data for combustion modeling - Supplement-1. Combust. Flame 98: 59-79.
16. Bell, J. B., N. J. Brown, M. S. Day, M. Frenklach, J. F. Grcar, R. M. Propp, S. R. Tonse and A. Wagner (2000). Scaling and efficiency of prism in adaptive simulations of turbulent premixed flames. Proceedings of the Combustion Institute 28: 107-113.
17. Biswas, P., Boddapati, V., Klingberg, A., Panda, A., Wang, H., Hanson, R., 2025a. IR-HyChem: Towards modeling the high-T combustion behavior of aviation fuels using infrared spectra.

18. Biswas, P., Boddapati, V., Klingberg, A.R., Panda, A., Wang, H., Hanson, R.K., 2025b. IR-HyChem: Towards modeling the high-T combustion behavior of aviation fuels using infrared spectra. Proceedings of the Combustion Institute 41, 105792.
19. Blasco, J. A., N. Fueyo, C. C Dopazo and J.-Y. Chen (2000). A self-organizing-map approach to chemistry representation in combustion applications. Combust. Theory Modelling 4: 61-76.
20. Blasenbrey, T. and U. Maas (2000). ILDMs of higher hydrocarbons and the hierarchy of chemical kinetics. Proceedings of the Combustion Institute 28(2): 1623-1630.
21. Blitz, M.A., Goddard, A., Ingham, T., Pilling, M.J., 2007. Time-of-flight mass spectrometry for time-resolved measurements. Review of Scientific Instruments 78, 034103. https://doi.org/10.1063/1.2712797
22. Blurock, E. S. (1995). Reaction: System for Modeling Chemical Reactions. Journal of Chemical Information and Computer Sciences 35(3): 607-616.
23. Bodenstein, M. (1913). Eine Theorie der photochemischen Reaktionsgeschwindigkeiten. Z. Phys. Chem. 85: 329-397.
24. Bozzelli, J.W., Dean, A.M., 1995. O + NNH: A possible new route for NOX formation in flames. International Journal of Chemical Kinetics 27, 1097–1109.
25. Brad, R. B., A. S. Tomlin, M. Fairweather and J. F. Griffiths (2007). The application of chemical reduction methods to a combustion system exhibiting complex dynamics. Proc. Combust. Inst. 31: 455-463.
26. Bray, K. (2016). Laminar Flamelets in Turbulent Combustion Modeling. Combustion Science and Technology 188(9): 1372-1375.
27. Bugler, J., Power, J., Curran, H.J., 2017. A theoretical study of cyclic ether formation reactions. Proceedings of the Combustion Institute 36, 161–167.
28. Bugler, J., B. Marks, O. Mathieu, R. Archuleta, A. Camou, C. Grégoire, K. A. Heufer, E. L. Petersen and H. J. Curran (2016). An ignition delay time and chemical kinetic modeling study of the pentane isomers. Combustion and Flame 163: 138-156.
29. Burcat, A., B. Ruscic, Chemistry and T. Technion - Israel Inst. of (2005). Third millenium ideal gas and condensed phase thermochemical database for combustion (with update from active thermochemical tables). United States.
30. Burke, M. P., M. Chaos, Y. Ju, F. L. Dryer and S. J. Klippenstein (2012). Comprehensive H2/O2 kinetic model for high-pressure combustion. International Journal of Chemical Kinetics 44(7): 444-474.
31. Burke, M. P. and S. J. Klippenstein (2017). Ephemeral collision complexes mediate chemically termolecular transformations that affect system chemistry. Nature Chemistry 9: 1078.
32. Burke, M. P., S. J. Klippenstein and L. B. Harding (2013). A quantitative explanation for the apparent anomalous temperature dependence of OH+HO2=H2O+O2 through multi-scale modeling. Proceedings of the Combustion Institute 34(1): 547-555.
33. Cai, L., vom Lehn, F., Pitsch, H., 2021. Higher Alcohol and Ether Biofuels for Compression-Ignition Engine Application: A Review with Emphasis on Combustion Kinetics. Energy Fuels 35, 1890–1917.
34. Cai, J., Zhang, L., Zhang, F., Wang, Z., Cheng, Z., Yuan, W., Qi, F., 2012. Experimental and Kinetic Modeling Study of n-Butanol Pyrolysis and Combustion. Energy Fuels 26, 5550–5568. https://doi.org/10.1021/ef3011965
35. Cheng, S., Saggese, C., Kang, D., Goldsborough, S.S., Wagnon, S.W., Kukkadapu, G., Zhang, K., Mehl, M., Pitz, W.J., 2021. Autoignition and preliminary heat release of gasoline surrogates and their blends with ethanol at engine-relevant conditions: Experiments and comprehensive kinetic modeling. Combustion and Flame 228, 57–77.
36. Chen, Z., vom Lehn, F., Pitsch, H., Cai, L., 2025. Design of novel high-performance fuels with artificial intelligence: Case study for spark-ignition engine applications. Applications in Energy and Combustion Science 23, 100341.

37. Chi, C., Janiga, G., Thévenin, D., 2021. On-the-fly artificial neural network for chemical kinetics in direct numerical simulations of premixed combustion. Combustion and Flame 226, 467–477.
38. Chiesa, P., G. Lozza and L. Mazzocchi (2005). Using Hydrogen as Gas Turbine Fuel. Journal of Engineering for Gas Turbines and Power 127(1): 73-80.
39. Choudhary, R., Biswas, P., Boddapati, V., Wang, H., Hanson, R.K., 2025. LT-HyChem - A physics-based chemical kinetic modeling approach for low-temperature oxidation of real fuels I: Rationale, methodology, and application to a simple fuel mixture. Combustion and Flame 271, 113852.
40. Christo, F. C., A. R. Masri and E. M. Nebot (1996). Artificial neural network implementation of chemistry with *pdf* Simulation of H_2 / CO_2 flames. Combust. Flame 106: 406-427.
41. Côme, G. M., V. Warth, P. A. Glaude, R. Fournet, F. Battin-Leclerc and G. Scacchi (1996). Computer-aided design of gas-phase oxidation mechanisms—Application to the modeling of n-heptane and iso-octane oxidation. Symposium (International) on Combustion 26(1): 755-762.
42. Császár, A.G., Furtenbacher, T., 2010. From a Network of Computed Reaction Enthalpies to Atom-Based Thermochemistry (NEAT). Chemistry – A European Journal 16, 4826–4835. https://doi.org/10.1002/chem.200903252
43. Curran, H. J. (2019). Developing detailed chemical kinetic mechanisms for fuel combustion. Proceedings of the Combustion Institute 37(1): 57-81.
44. Curran, H.J., Gaffuri, P., Pitz, W.J., Westbrook, C.K., 1998. A Comprehensive Modeling Study of n-Heptane Oxidation. Combustion and Flame 114, 149–177. https://doi.org/10.1016/S0010-2180(97)00282-4
45. Davidson, D. F., D. R. Haylett and R. K. Hanson (2008). Development of an aerosol shock tube for kinetic studies of low-vapor-pressure fuels. Combustion and Flame 155(1): 108-117.
46. Davidson, D.F., Hanson, R.K., 1990. A direct comparison of shock tube photolysis and pyrolysis methods in the determination of the rate coefficient for O + H2 → OH + H. Combustion and Flame 82, 445–447. https://doi.org/10.1016/0010-2180(90)90014-I
47. Davis, M. J. and A. S. Tomlin (2008). Spatial dynamics of steady flames 1. Phase space structure and the dynamics of individual trajectories. J. Phys. Chem. A 112: 7768-7783.
48. Driscoll, J. F. (2008). Turbulent premixed combustion: Flamelet structure and its effect on turbulent burning velocities. Progress in Energy and Combustion Science 34(1): 91-134.
49. Elliott, S.N., Moore, K.B., Copan, A.V., Keçeli, M., Cavallotti, C., Georgievskii, Y., Schaefer, H.F., Klippenstein, S.J., 2021. Automated theoretical chemical kinetics: Predicting the kinetics for the initial stages of pyrolysis. Proceedings of the Combustion Institute 38, 375–384. https://doi.org/10.1016/j.proci.2020.06.019
50. Fenimore, C.P., 1976. Reactions of fuel-nitrogen in rich flame gases. Combustion and Flame 26, 249–256.
51. Fernandes, R.X., Luther, K., Troe, J., Ushakov, V.G., 2008. Experimental and modelling study of the recombination reaction H + O2 (+M) → HO2 (+M) between 300 and 900 K, 1.5 and 950 bar, and in the bath gases M = He, Ar, and N2. Phys. Chem. Chem. Phys. 10, 4313–4321. https://doi.org/10.1039/B804553D
52. Fournet, R., V. Warth, P. A. Glaude, F. Battin-Leclerc, G. Scacchi and G. M. Côme (2000). Automatic reduction of detailed mechanisms of combustion of alkanes by chemical lumping. Int. J. Chem. Kinet. 32: 36-51.
53. Frassoldati, A., R. Grana, T. Faravelli, E. Ranzi, P. Oßwald and K. Kohse-Höinghaus (2012). Detailed kinetic modeling of the combustion of the four butanol isomers in premixed low-pressure flames. Combustion and Flame 159(7): 2295-2311.
54. Frenklach, M. (1990). Reduction of chemical reaction models. Numerical approaches to combustion modelling. Washington, AIAA. 135.

55. Gandarias, I., S. García-Fernández, I. Obregón, I. Agirrezabal-Telleria and P. L. Arias (2018). Production of 2-methylfuran from biomass through an integrated biorefinery approach. Fuel Processing Technology 178: 336-343.
56. Gauthier, B. M., D. F. Davidson and R. K. Hanson (2004). Shock tube determination of ignition delay times in full-blend and surrogate fuel mixtures. Combustion and Flame 139(4): 300-311.
57. Gilbert, R. G., K. Luther and J. Troe (1983). Theory of Thermal Unimolecular Reactions in the Fall-off Range. II. Weak Collision Rate Constants. Berichte der Bunsengesellschaft für physikalische Chemie 87(2): 169-177.
58. Gill, S. S., A. Tsolakis, K. D. Dearn and J. Rodríguez-Fernández (2011). Combustion characteristics and emissions of Fischer–Tropsch diesel fuels in IC engines. Progress in Energy and Combustion Science 37(4): 503-523.
59. Glarborg, P., Miller, J.A., Ruscic, B., Klippenstein, S.J., 2018. Modeling nitrogen chemistry in combustion. Progress in Energy and Combustion Science 67, 31–68. https://doi.org/10.1016/j.pecs.2018.01.002
60. Glarborg, P., Brodersen, A.R.N., Jian, J., Hashemi, H., Sivaramakrishnan, R., Klippenstein, S.J., 2025. Progress in modeling hydrogen assisted ammonia oxidation with new experiments and a further reconciliation of the NH_3+ OH rate constant. Proceedings of the Combustion Institute 41, 105942.
61. Goldsborough, S.S., Hochgreb, S., Vanhove, G., Wooldridge, M.S., Curran, H.J., Sung, C.-J., 2017. Advances in rapid compression machine studies of low- and intermediate-temperature autoignition phenomena. Progress in Energy and Combustion Science 63, 1–78. https://doi.org/10.1016/j.pecs.2017.05.002
62. Goldsborough, S.S., Santner, J., Kang, D., Fridlyand, A., Rockstroh, T., Jespersen, M.C., 2019. Heat release analysis for rapid compression machines: Challenges and opportunities. Proceedings of the Combustion Institute 37, 603–611. https://doi.org/10.1016/j.proci.2018.05.128
63. Goldsmith, C.F., Magoon, G.R., Green, W.H., 2012. Database of Small Molecule Thermochemistry for Combustion. J. Phys. Chem. A 116, 9033–9057. https://doi.org/10.1021/jp303819e
64. Goldsmith, C. F., A. S. Tomlin and S. J. Klippenstein (2013). Uncertainty propagation in the derivation of phenomenological rate coefficients from theory: A case study of n-propyl radical oxidation. Proceedings of the Combustion Institute 34(1): 177-185.
65. Goldsmith, C.F., Green, W.H., Klippenstein, S.J., 2012. Role of O2 + QOOH in Low-Temperature Ignition of Propane. 1. Temperature and Pressure Dependent Rate Coefficients. J. Phys. Chem. A 116, 3325–3346. https://doi.org/10.1021/jp210722w
66. Gorbatenko, I., Tomlin, A.S., Lawes, M., Cracknell, R.F., 2019. Experimental and modelling study of the impacts of n-butanol blending on the auto-ignition behaviour of gasoline and its surrogate at low temperatures. Proceedings of the Combustion Institute 37, 501–509. https://doi.org/10.1016/j.proci.2018.05.089
67. Green, W. H., P. I. Barton, B. Bhattacharjee, D. M. Matheu, D. A. Schwer, J. Song, R. Sumathi, H. H. Carstensen, A. M. Dean and J. M. Grenda (2001). Computer Construction of Detailed Chemical Kinetic Models for Gas-Phase Reactors. Industrial & Engineering Chemistry Research 40(23): 5362-5370.
68. Green, W.H., 2024. Perspective on automated predictive kinetics using estimates derived from large datasets. Int J of Chemical Kinetics kin.21744.
69. Guo, H., W. Sun, F. M. Haas, T. Farouk, F. L. Dryer and Y. Ju (2013). Measurements of H2O2 in low temperature dimethyl ether oxidation. Proceedings of the Combustion Institute 34(1): 573-581.
70. Haeseldonckx, D. and W. D'haeseleer (2007). The use of the natural-gas pipeline infrastructure for hydrogen transport in a changing market structure. International Journal of Hydrogen Energy 32(10): 1381-1386.

71. Hébrard, É., A. S. Tomlin, R. Bounaceur and F. Battin-Leclerc (2015). Determining predictive uncertainties and global sensitivities for large parameter systems: A case study for n-butane oxidation. Proceedings of the Combustion Institute 35(1): 607-616.
72. Heuser, B., Jakob, M., Kremer, F., Pischinger, S., Kerschgens, B., Pitsch, H., 2013. Tailor-Made Fuels from Biomass: Influence of Molecular Structures on the Exhaust Gas Emissions of Compression Ignition Engines. Presented at the 22nd SAE Brasil International Congress and Display, pp. 2013-36–0571. https://doi.org/10.4271/2013-36-0571
73. Hong, Z., Davidson, D.F., Hanson, R.K., 2011. An improved H2/O2 mechanism based on recent shock tube/laser absorption measurements. Combustion and Flame, Special Issue on Kinetics 158, 633–644. https://doi.org/10.1016/j.combustflame.2010.10.002
74. Howard, M.J., Smith, I.W.M., 1981. Direct rate measurements on the reactions N + OH → NO + H and O + OH → O2+ H from 250 to 515 K. J. Chem. Soc., Faraday Trans. 2 77, 997–1008. https://doi.org/10.1039/F29817700997
75. Howard, M.S., Issayev, G., Naser, N., Sarathy, S.M., Farooq, A., Dooley, S., 2019. Ethanolic gasoline, a lignocellulosic advanced biofuel. Sustainable Energy Fuels 3, 409–421. https://doi.org/10.1039/C8SE00378E
76. Hughes, K. J., J. F. Griffiths, M. Fairweather and A. S. Tomlin (2006). Evaluation of models for the low temperature combustion of alkanes through interpretation of pressure-temperature ignition diagrams. Phys. Chem. Chem. Phys. 8(27): 3197-3210.
77. Jasper, A. W., C. M. Oana and J. A. Miller (2015). Third-Body collision efficiencies for combustion modeling: Hydrocarbons in atomic and diatomic baths. Proceedings of the Combustion Institute 35(1): 197-204.
78. Javoy, S., Naudet, V., Abid, S., Paillard, C.E., 2000. Rate constant for the reaction of O with H2 at high temperature by resonance absorption measurements of O atoms. International Journal of Chemical Kinetics 32, 686–695. https://doi.org/10.1002/1097-4601(2000)32:11<686::AID-KIN4>3.0.CO;2-R
79. Ji, W., Zhang, P., He, T., Wang, Z., Tao, L., He, X., Law, C.K., 2015. Intermediate species measurement during iso-butanol auto-ignition. Combustion and Flame 162, 3541–3553. https://doi.org/10.1016/j.combustflame.2015.06.010
80. Johnson, M.S., Green, W.H., 2024. A machine learning based approach to reaction rate estimation. Reaction Chemistry & Engineering 9, 1364–1380.
81. Johnson, M.S., Pang, H.-W., Doner, A.C., Green, W.H., Zádor, J., 2025. PySIDT: Subgraph Isomorphic Decision Trees for Molecular Property Prediction. J. Phys. Chem. A 129, 10228–10239.
82. Julis, J., Leitner, W., 2012. Synthesis of 1-Octanol and 1,1-Dioctyl Ether from Biomass-Derived Platform Chemicals. Angewandte Chemie International Edition 51, 8615–8619. https://doi.org/10.1002/anie.201203669
83. Kaiser, E.W., Siegl, W.O., Cotton, D.F., Anderson, R.W., 1992. Effect of fuel structure on emissions from a spark-ignited engine. 2. Naphthene and aromatic fuels. Environ. Sci. Technol. 26, 1581–1586.
84. Kalghatgi, G. T. (2001). Fuel Anti-Knock Quality - Part I. Engine Studies, SAE International.
85. Kawka, L., Juhász, G., Papp, M., Nagy, T., Zsély, I.G., Turányi, T., 2020. Comparison of detailed reaction mechanisms for homogeneous ammonia combustion. Zeitschrift für Physikalische Chemie 234, 1329–1357.
86. Keçeli, M., Elliott, S.N., Li, Y.-P., Johnson, M.S., Cavallotti, C., Georgievskii, Y., Green, W.H., Pelucchi, M., Wozniak, J.M., Jasper, A.W., Klippenstein, S.J., 2019. Automated computational thermochemistry for butane oxidation: A prelude to predictive automated combustion kinetics. Proceedings of the Combustion Institute 37, 363–371.
87. Kéromnès, A., W. K. Metcalfe, K. A. Heufer, N. Donohoe, A. K. Das, C.-J. Sung, J. Herzler, C. Naumann, P. Griebel, O. Mathieu, M. C. Krejci, E. L. Petersen, W. J. Pitz and H. J. Curran (2013). An

experimental and detailed chemical kinetic modeling study of hydrogen and syngas mixture oxidation at elevated pressures. Combustion and Flame 160(6): 995-1011.
88. Klippenstein, S. J. (2017). From theoretical reaction dynamics to chemical modeling of combustion. Proceedings of the Combustion Institute 36(1): 77-111.
89. Klippenstein, S.J., Harding, L.B., Ruscic, B., 2017. Ab Initio Computations and Active Thermochemical Tables Hand in Hand: Heats of Formation of Core Combustion Species. J. Phys. Chem. A 121, 6580–6602. https://doi.org/10.1021/acs.jpca.7b05945
90. Klippenstein, S.J., Sivaramakrishnan, R., Burke, U., Somers, K.P., Curran, H.J., Cai, L., Pitsch, H., Pelucchi, M., Faravelli, T., Glarborg, P., 2022. HȮ2 + HȮ2: High level theory and the role of singlet channels. Combustion and Flame 111975.
91. Klippenstein, S.J., Sivaramakrishnan, R., Labbe, N.J., Tao, Y., Burke, M.P., Elliott, S.N., Goldsmith, C.F., Mulvihill, C.R., Jasper, A.W., Ruscic, B., Bross, D.H., Glarborg, P., Hansen, N., Zádor, J., Miller, J.A., 2025. Theoretically Informed Kinetics (ThInK): Establishing a modern C0-C3 mechanism for combustion modeling. Combustion and Flame 282, 114501.
92. Kobayashi, H., Hayakawa, A., Somarathne, K.D.K.A., Okafor, E.C., 2019. Science and technology of ammonia combustion. Proceedings of the Combustion Institute 37, 109–133.
93. Kumamoto, A., H. Iseki, R. Ono and T. Oda (2011). Measurement of minimum ignition energy in hydrogen-oxygen-nitrogen premixed gas by spark discharge. Journal of Physics: Conference Series 301: 012039.
94. Kundu, P., M. M. Ameen and S. Som (2018). Recent Progress in Turbulent Combustion Modeling of Spray Flames Using Flamelet Models. Modeling and Simulation of Turbulent Combustion. S. De, A. K. Agarwal, S. Chaudhuri and S. Sen. Singapore, Springer Singapore: 477-512.
95. Lam, S. H. and D. A. Goussis (1994). The CSP method for simplifying kinetics. Int. J. Chem. Kinet. 26: 461-486.
96. Law, C. K., T. F. Lu and A. Makino (2006). On the off-stoichiometric peaking of adiabatic flame temperature.
97. Law, C.K., Wu, F., Egolfopoulos, F.N., Gururajan, V., Wang, H., 2015. On the Rational Interpretation of Data on Laminar Flame Speeds and Ignition Delay Times. Combustion Science and Technology 187, 27–36. https://doi.org/10.1080/00102202.2014.970686
98. Li, S., Tao, T., Wang, J., Yang, B., Law, C.K., Qi, F., 2017. Using sensitivity entropy in experimental design for uncertainty minimization of combustion kinetic models. Proceedings of the Combustion Institute 36, 709–716. https://doi.org/10.1016/j.proci.2016.07.102
99. Li, G., H. Rabitz, J. Hu, Z. Chen and Y. Ju (2008). Regularized random-sampling high dimensional model representation (RS-HDMR). Journal of Mathematical Chemistry 43(3): 1207-1232.
100. Li, G., C. Rosenthal and H. Rabitz (2001). High dimensional model representations. J. Phys. Chem. A 105: 7765 -7777.
101. Li, G., S.-W. Wang and H. Rabitz (2002). Practical approaches to construct RS-HDMR component functions. J. Phys. Chem. A 106: 8721-8733.
102. Li, G. Y., H. Rabitz, P. E. Yelvington, O. O. Oluwole, F. Bacon, C. E. Kolb and J. Schoendorf (2010). Global Sensitivity Analysis for Systems with Independent and/or Correlated Inputs. Journal of Physical Chemistry A 114(19): 6022-6032.
103. Li, B., Su, S., Zhu, C., Lin, J., Hu, X., Su, L., Yu, Z., Liao, K., Chen, H., 2023. A deep learning framework for accurate reaction prediction and its application on high-throughput experimentation data. J Cheminform 15, 72.
104. Li, N., Girhe, S., Zhang, M., Chen, B., Zhang, Y., Liu, S., Pitsch, H., 2024. A machine learning method to predict rate constants for various reactions in combustion kinetic models. Combustion and Flame 263, 113375.

105. Li, Q., Chen, H., Koenig, B.C., Deng, S., 2023. Bayesian chemical reaction neural network for autonomous kinetic uncertainty quantification. Phys. Chem. Chem. Phys. 25, 3707–3717.
106. Libby, P. A. and K. N. C. Bray (1980). IMPLICATIONS OF THE LAMINAR FLAMELET MODEL IN PREMIXED TURBULENT COMBUSTION. Combustion and Flame 39(1): 33-41.
107. Limayem, A. and S. C. Ricke (2012). Lignocellulosic biomass for bioethanol production: Current perspectives, potential issues and future prospects. Progress in Energy and Combustion Science 38(4): 449-467.
108. Lindemann, F. A., S. Arrhenius, I. Langmuir, N. R. Dhar, J. Perrin and W. C. McC. Lewis (1922). Discussion on the radiation theory of chemical action. Transactions of the Faraday Society 17(0): 598-606.
109. Liu, W., Kelley, A.P., Law, C.K., 2011. Non-premixed ignition, laminar flame propagation, and mechanism reduction of n-butanol, iso-butanol, and methyl butanoate. Proceedings of the Combustion Institute 33, 995–1002. https://doi.org/10.1016/j.proci.2010.05.084
110. Liu, Z. and N. I. Kim (2014). An assembled annular stepwise diverging tube for the measurement of laminar burning velocity and quenching distance. Combustion and Flame 161(6): 1499-1506.
111. Liu, Y., Bai, M., Song, H., Xie, D., Li, J., 2019. Anomalous kinetics of the reaction between OH and HO2 on an accurate triplet state potential energy surface. Phys. Chem. Chem. Phys. 21, 12667–12675. https://doi.org/10.1039/C9CP01553A
112. Lu, T. and C. K. Law (2005). A directed relation graph method for mechanism reduction. Proc. Comb. Inst. 30: 1333–1341.
113. Lu, T. and C. K. Law (2006). On the applicability of directed relation graphs to the reduction of reaction mechanisms. Combust. Flame(146): 472–483.
114. Lu, T. and C. K. Law (2009). Toward accommodating realistic fuel chemistry in large-scale computations. Progress in Energy and Combustion Science 35(2): 192-215.
115. Luo, Z. Y., T. F. Lu, M. J. Maciaszek, S. Som and D. E. Longman (2010). A Reduced Mechanism for High-Temperature Oxidation of Biodiesel Surrogates. Energy & Fuels 24: 6283-6293.
116. Maas, U. and S. B. Pope (1992). Simplifying chemical kinetics:Intrinsic low-dimensional manifolds in composition space. Combust. Flame 88: 239-264.
117. Macpherson, M.T., Pilling, M.J., Smith, M.J.C., 1985. Determination of the absorption cross section for methyl at 216.36 nm and the absolute rate constant for methyl radical recombination over the temperature range 296-577 K. J. Phys. Chem. 89, 2268–2274. https://doi.org/10.1021/j100257a024
118. Matzen, M., Demirel, Y., 2016. Methanol and dimethyl ether from renewable hydrogen and carbon dioxide: Alternative fuels production and life-cycle assessment. Journal of Cleaner Production 139, 1068–1077.
119. McKee, K.W., Blitz, M.A., Cleary, P.A., Glowacki, D.R., Pilling, M.J., Seakins, P.W., Wang, L., 2007. Experimental and Master Equation Study of the Kinetics of OH + C2H2: Temperature Dependence of the Limiting High Pressure and Pressure Dependent Rate Coefficients. J. Phys. Chem. A 111, 4043–4055. https://doi.org/10.1021/jp067594y
120. Metcalfe, W.K., Burke, S.M., Ahmed, S.S., Curran, H.J., 2013. A Hierarchical and Comparative Kinetic Modeling Study of C1 − C2 Hydrocarbon and Oxygenated Fuels. International Journal of Chemical Kinetics 45, 638–675. https://doi.org/10.1002/kin.20802
121. Michael, J.V., Su, M.-C., Sutherland, J.W., Carroll, J.J., Wagner, A.F., 2002. Rate Constants For H + O2 + M → HO2 + M in Seven Bath Gases. J. Phys. Chem. A 106, 5297–5313. https://doi.org/10.1021/jp020229w
122. Michelbach, C., Hakimov, K., Farooq, A., Tomlin, A.S., 2024. Predicting the autoignition behaviour of tailorable advanced biofuel blends using automatically generated mechanisms. Proceedings of the Combustion Institute 40, 105667.

123. Michelbach, C.A., Tomlin, A.S., 2024. Automatic mechanism generation for the combustion of advanced biofuels: A case study for diethyl ether. Int J of Chemical Kinetics 56, 233–262.
124. Michelbach, C., Tomlin, A., 2021. An experimental and kinetic modeling study of the ignition delay and heat release characteristics of a five component gasoline surrogate and its blends with iso-butanol within a rapid compression machine. International Journal of Chemical Kinetics 53, 787–808. https://doi.org/10.1002/kin.21483
125. Michelsen, H.A., 2017. Probing soot formation, chemical and physical evolution, and oxidation: A review of in situ diagnostic techniques and needs. Proceedings of the Combustion Institute 36, 717–735. https://doi.org/10.1016/j.proci.2016.08.027
126. Miller, J.A., Bowman, C.T., 1989. Mechanism and modeling of nitrogen chemistry in combustion. Progress in Energy and Combustion Science 15, 287–338.
127. Westbrook, C., Heufer, K.A., Wildenberg, A., 2021. Key Chemical Kinetic Steps in Reaction Mechanisms for Fuels from Biomass: A Perspective. Energy Fuels 35, 15339–15359. https://doi.org/10.1021/acs.energyfuels.1c02210Lee, D. and S. Hochgreb (1998). Rapid Compression Machines: Heat Transfer and Suppression of Corner Vortex. Combustion and Flame 114(3): 531-545.
128. Miller, J.A., Sivaramakrishnan, R., Tao, Y., Goldsmith, C.F., Burke, M.P., Jasper, A.W., Hansen, N., Labbe, N.J., Glarborg, P., Zádor, J., 2021. Combustion chemistry in the twenty-first century: Developing theory-informed chemical kinetics models. Progress in Energy and Combustion Science 83, 100886. https://doi.org/10.1016/j.pecs.2020.100886
129. Monge-Palacios, M., Sarathy, S.M., 2018. Ab initio and transition state theory study of the OH + HO2 → H2O + O2(3Σg−)/O2(1Δg) reactions: yield and role of O2(1Δg) in H2O2 decomposition and in combustion of H2. Phys. Chem. Chem. Phys. 20, 4478–4489. https://doi.org/10.1039/C7CP05850K
130. Monge-Palacios, M., Zhang, X., Morlanes, N., Nakamura, H., Pezzella, G., Sarathy, S.M., 2024. Ammonia pyrolysis and oxidation chemistry. Progress in Energy and Combustion Science 105, 101177.
131. MorÉAc, G., E. S. Blurock and F. Mauss (2006). AUTOMATIC GENERATION OF A DETAILED MECHANISM FOR THE OXIDATION OF n-DECANE. Combustion Science and Technology 178(10-11): 2025-2038.
132. Moshammer, K., A. W. Jasper, D. M. Popolan-Vaida, Z. Wang, V. S. Bhavani Shankar, L. Ruwe, C. A. Taatjes, P. Dagaut and N. Hansen (2016). Quantification of the Keto-Hydroperoxide (HOOCH2OCHO) and Other Elusive Intermediates during Low-Temperature Oxidation of Dimethyl Ether. The Journal of Physical Chemistry A 120(40): 7890-7901.
133. Nagy, T. and T. Turányi (2009). Reduction of very large reaction mechanisms using methods based on simulation error minimization. Combust. Flame 156: 417–428.
134. Nagy, T. and T. Turányi (2011). Uncertainty of Arrhenius parameters. Int.J.Chem.Kinet. 43: 359-378.
135. Najm, H., B. J. Debusschere, Y. M. Marzouk, S. Widmer and O. P. Le Maître (2009). Uncertainty quantification in chemical systems. Int. J. Numer. Meth. Eng. 80: 789-814.
136. Németh, A., T. Vidóczy, K. Héberger, Z. Kúti and J. Wágner (2002). MECHGEN: Computer aided generation and reduction of reaction mechanisms. J. Chem. Inf. Comput. Sci. 42: 208-214.
137. Niemeyer, K. E., C.-J. Sung and M. P. Raju (2010). Skeletal mechanism generation for surrogate fuels using directed relation graph with error propagation and sensitivity analysis. Combustion and Flame 157(9): 1760-1770.
138. Olm, C., Zsély, I.Gy., Pálvölgyi, R., Varga, T., Nagy, T., Curran, H.J., Turányi, T., 2014. Comparison of the performance of several recent hydrogen combustion mechanisms. Combustion and Flame 161, 2219–2234. https://doi.org/10.1016/j.combustflame.2014.03.006
139. Pelucchi, M., Namysl, S., Ranzi, E., Rodriguez, A., Rizzo, C., Somers, K.P., Zhang, Y., Herbinet, O., Curran, H.J., Battin-Leclerc, F., Faravelli, T., 2020. Combustion of n-C3–C6 Linear Alcohols: An

Experimental and Kinetic Modeling Study. Part I: Reaction Classes, Rate Rules, Model Lumping, and Validation. Energy Fuels 34, 14688–14707.
140. Pepiot-Desjardins, P. and H. Pitsch (2008). An efficient error-propagation-based reduction method for large chemical kinetic mechanisms. Combust. Flame 154: 67-81.
141. Pepiot-Desjardins, P., Pitsch, H., Malhotra, R., Kirby, S.R., Boehman, A.L., 2008. Structural group analysis for soot reduction tendency of oxygenated fuels. Combustion and Flame 154, 191–205.
142. Peters, N. and B. Rogg, Eds. (1993). Reduced kinetic mechanisms for applications in combustion systems. Berlin, Springer.
143. Pope, S. B. (1997). Computationally efficient implementation of combustion chemistry using *in situ* adaptive tabulation. Combust. Theory Modell. 1(1): 41-63.
144. Prager, J., Najm, H.N., Zádor, J., 2013. Uncertainty quantification in the ab initio rate-coefficient calculation for the CH3CH(OH)CH3+OH→CH3C(OH)CH3+H2O reaction. Proceedings of the Combustion Institute 34, 583–590.
145. Rabitz, H., Ö. F. Aliu, J. Shorter and K. Shim (1999). Efficient input-output model representations. Comput. Phys. Commun. 117: 11-20.
146. Ramalingam, A., Fenard, Y., Heufer, A., 2020. Ignition delay time and species measurement in a rapid compression machine: A case study on high-pressure oxidation of propane. Combustion and Flame 211, 392–405.
147. Ranzi, E., T. Faravelli, P. Gaffuri and A. Sogaro (1995). Low-temperature combustion: Automatic generation of primary oxidation reactions and lumping procedures. Combustion and Flame 102(1): 179-192.
148. Ranzi, E., P. Gaffuri, T. Faravelli and P. Dagaut (1995). A wide-range modeling study of n-heptane oxidation. Combustion and Flame 103(1): 91-106.
149. Rotavera, B., Taatjes, C.A., 2021. Influence of functional groups on low-temperature combustion chemistry of biofuels. Progress in Energy and Combustion Science 86, 100925. https://doi.org/10.1016/j.pecs.2021.100925
150. Sabia, P., Sorrentino, G., Ariemma, G.B., Manna, M.V., Ragucci, R., de Joannon, M., 2021. MILD Combustion and Biofuels: A Minireview. Energy Fuels 35, 19901–19919. https://doi.org/10.1021/acs.energyfuels.1c02973
151. Saltelli, A. (2002). Making best use of model evaluations to compute sensitivity indices. Computer Physics Communications 145(2): 280-297.
152. Sarathy, S. M., P. Oßwald, N. Hansen and K. Kohse-Höinghaus (2014). Alcohol combustion chemistry. Progress in Energy and Combustion Science 44: 40-102.
153. Sarathy, S. M., E.-A. Tingas, E. F. Nasir, A. Detogni, Z. Wang, A. Farooq and H. Im (2019). Three-stage heat release in n-heptane auto-ignition. Proceedings of the Combustion Institute 37(1): 485-492.
154. Sarathy, S. M., C. K. Westbrook, M. Mehl, W. J. Pitz, C. Togbe, P. Dagaut, H. Wang, M. A. Oehlschlaeger, U. Niemann, K. Seshadri, P. S. Veloo, C. Ji, F. N. Egolfopoulos and T. Lu (2011). Comprehensive chemical kinetic modeling of the oxidation of 2-methylalkanes from C7 to C20. Combustion and Flame 158(12): 2338-2357.
155. Sarathy, S.M., Eraqi, B.A., 2024. Artificial intelligence for novel fuel design. Proceedings of the Combustion Institute 40, 105630.
156. Saunders, S. M., M. E. Jenkin, R. G. Derwent and M. J. Pilling (2003). Protocol for the development of the Master Chemical Mechanism, MCM V3: tropospheric degradation of non-aromatic VOC. Atmospheric Chemistry and Physics 3: 161-180.
157. Shannon, R.J., Tomlin, A.S., Robertson, S.H., Blitz, M.A., Pilling, M.J., Seakins, P.W., 2015. Global Uncertainty Propagation and Sensitivity Analysis in the CH3OCH2 + O2 System: Combining Experiment and Theory To Constrain Key Rate Coefficients in DME Combustion. J. Phys. Chem. A 119, 7430–7438.

158. Schefer, R. W., W. D. Kulatilaka, B. D. Patterson and T. B. Settersten (2009). Visible emission of hydrogen flames. Combustion and Flame 156(6): 1234-1241.
159. Sheen, D. A., X. You, H. Wang and T. Løvås (2009). Spectral uncertainty quantification, propagation and optimization of a detailed kinetic model for ethylene combustion. Proc. Combust. Inst. 32: 535-542.
160. Sobol', I. M. (1990). Sensitivity estimates for nonlinear mathematical models. Mat. Model 2: 112-118.
161. Sobol', I. M. (1967). On the distribution of points in a cube and the approximate evaluation of integrals. *USSR Comput. Math. Math. Phys.* 7(4): 86-112.
162. Somers, K.P., Simmie, J.M., 2015. Benchmarking Compound Methods (CBS-QB3, CBS-APNO, G3, G4, W1BD) against the Active Thermochemical Tables: Formation Enthalpies of Radicals. J. Phys. Chem. A 119, 8922–8933. https://doi.org/10.1021/acs.jpca.5b05448
163. Somers, K.P., Simmie, J.M., Gillespie, F., Conroy, C., Black, G., Metcalfe, W.K., Battin-Leclerc, F., Dirrenberger, P., Herbinet, O., Glaude, P.-A., Dagaut, P., Togbé, C., Yasunaga, K., Fernandes, R.X., Lee, C., Tripathi, R., Curran, H.J., 2013. A comprehensive experimental and detailed chemical kinetic modelling study of 2,5-dimethylfuran pyrolysis and oxidation. Combustion and Flame 160, 2291–2318.
164. Song, Y., Marrodán, L., Vin, N., Herbinet, O., Assaf, E., Fittschen, C., Stagni, A., Faravelli, T., Alzueta, M.U., Battin-Leclerc, F., 2019. The sensitizing effects of NO2 and NO on methane low temperature oxidation in a jet stirred reactor. Proceedings of the Combustion Institute 37, 667–675. https://doi.org/10.1016/j.proci.2018.06.115
165. Sun, J., Zhao, N., Zheng, H., 2025. A comprehensive review of ammonia combustion: Fundamental characteristics, chemical kinetics, and applications in energy systems. Fuel 394, 135135.
166. Sung, C.-J. and H. J. Curran (2014). Using rapid compression machines for chemical kinetics studies. Progress in Energy and Combustion Science 44: 1-18.
167. Taatjes, C.A., Hansen, N., McIlroy, A., Miller, J.A., Senosiain, J.P., Klippenstein, S.J., Qi, F., Sheng, L., Zhang, Y., Cool, T.A., Wang, J., Westmoreland, P.R., Law, M.E., Kasper, T., Kohse-Höinghaus, K., 2005. Enols are common intermediates in hydrocarbon oxidation. Science 308, 1887–1889. https://doi.org/10.1126/science.1112532
168. Tomlin, A. S., E. Agbro, V. Nevrlý, J. Dlabka and M. Vašinek (2014). Evaluation of Combustion Mechanisms Using Global Uncertainty and Sensitivity Analyses: A Case Study for Low-Temperature Dimethyl Ether Oxidation. International Journal of Chemical Kinetics 46(11): 662-682.
169. Tonse, S. R., N. W. Moriarty, N. J. Brown and M. Frenklach (1999). PRISM: Piece-wise reusable implementation of solution mapping. An economical strategy for chemical kinetics. Israel J. Chem. 39: 97–106.
170. Tonse, S. R., N. W. Moriarty, M. Frenklach and N. J. Brown (2003). Computational economy improvements in PRISM. Int J Chem Kinet. 35: 438-452.
171. Tosatto, L., B. A. V. Bennett and M. D. Smooke (2011). A transport-flux-based directed relation graph method for the spatially inhomogeneous instantaneous reduction of chemical kinetic mechanisms. Combustion and Flame 158(5): 820-835.
172. Troe, J. (2011). The thermal dissociation/recombination reaction of hydrogen peroxide H2O2(+M)⇔2OH(+M) III.: Analysis and representation of the temperature and pressure dependence over wide ranges. Combustion and Flame 158(4): 594-601.
173. Turányi, T. (1994). Parametrization of reaction mechanisms using orthonormal polynomials. Comput. Chem. 18(1): 45-54.
174. Turányi, T., A. S. Tomlin and M. J. Pilling (1993). On the error of the quasi-steady-state approximation. J. Phys. Chem. 97: 163-172.
175. Ureel, Y., Vermeire, F.H., Sabbe, M.K., Van Geem, K.M., 2023. Beyond group additivity: Transfer learning for molecular thermochemistry prediction. Chemical Engineering Journal 472, 144874.

176. Vaghjiani, G.L., Ravishankara, A.R., 1991. New measurement of the rate coefficient for the reaction of OH with methane. Nature 350, 406–409. https://doi.org/10.1038/350406a0
177. Valera-Medina, A., Xiao, H., Owen-Jones, M., David, W.I.F., Bowen, P.J., 2018. Ammonia for power. Progress in Energy and Combustion Science 69, 63–102. https://doi.org/10.1016/j.pecs.2018.07.001
178. Valkó, É., Varga, T., Tomlin, A.S., Turányi, T., 2017. Investigation of the effect of correlated uncertain rate parameters on a model of hydrogen combustion using a generalized HDMR method. Proceedings of the Combustion Institute 36, 681–689. https://doi.org/10.1016/j.proci.2016.07.061
179. Van Der Laan, G. P. and A. A. C. M. Beenackers (1999). Kinetics and Selectivity of the Fischer–Tropsch Synthesis: A Literature Review. Catalysis Reviews 41(3-4): 255-318.
180. Van Geem, K. M., M.-F. Reyniers, G. B. Marin, J. Song, W. H. Green and D. M. Matheu (2006). Automatic reaction network generation using RMG for steam cracking of n-hexane. AIChE Journal 52(2): 718-730.
181. van Santen, R. A., A. J. Markvoort, I. A. W. Filot, M. M. Ghouri and E. J. M. Hensen (2013). Mechanism and microkinetics of the Fischer–Tropsch reaction. Physical Chemistry Chemical Physics 15(40): 17038-17063.
182. Vasudevan, V., Cook, R.D., Hanson, R.K., Bowman, C.T., Golden, D.M., 2008. High-temperature shock tube study of the reactions CH3 + OH → products and CH3OH + Ar → products. International Journal of Chemical Kinetics 40, 488–495. https://doi.org/10.1002/kin.20334
183. Vasudevan, V., Davidson, D.F., Hanson, R.K., 2005. Direct measurements of the reaction OH + CH2O → HCO + H2O at high temperatures. International Journal of Chemical Kinetics 37, 98–109. https://doi.org/10.1002/kin.20056
184. Venkatesh, P. K., A. Y. Chang, A. M. Dean, M. H. Cohen and R. W. Carr (1997). Parameterization of pressure- and temperature-dependent kinetics in multiple well reactions. AIChE Journal 43(5): 1331-1340.
185. Vereecken, L., Glowacki, D.R., Pilling, M.J., 2015. Theoretical Chemical Kinetics in Tropospheric Chemistry: Methodologies and Applications. Chem. Rev. 115, 4063–4114. https://doi.org/10.1021/cr500488p
186. vom Lehn, F., Cai, L., Pitsch, H., 2020. Investigating the impacts of thermochemical group additivity values on kinetic model predictions through sensitivity and uncertainty analyses. Combustion and Flame 213, 394–408. https://doi.org/10.1016/j.combustflame.2019.12.011
187. vom Lehn, F., Cai, L., Pitsch, H., 2019. Sensitivity analysis, uncertainty quantification, and optimization for thermochemical properties in chemical kinetic combustion models. Proceedings of the Combustion Institute 37, 771–779. https://doi.org/10.1016/j.proci.2018.06.188
188. vom Lehn, F., Cai, L., Tripathi, R., Broda, R., Pitsch, H., 2021. A property database of fuel compounds with emphasis on spark-ignition engine applications. Applications in Energy and Combustion Science 5, 100018. https://doi.org/10.1016/j.jaecs.2020.100018
189. Wagnon, S.W., Karwat, D.M.A., Wooldridge, M.S., Westbrook, C.K., 2014. Experimental and Modeling Study of Methyl trans-3-Hexenoate Autoignition. Energy Fuels 28, 7227–7234.
190. Wang, G., Li, Y., Yuan, W., Wang, Y., Zhou, Z., Liu, Y., Cai, J., 2018. Investigation on laminar flame propagation of n-butanol/air and n-butanol/O2/He mixtures at pressures up to 20 atm. Combustion and Flame 191, 368–380. https://doi.org/10.1016/j.combustflame.2018.01.025
191. Wang, S., Davidson, D.F., Hanson, R.K., 2017. Rate constants of long, branched, and unsaturated aldehydes with OH at elevated temperatures. Proceedings of the Combustion Institute 36, 151–160. https://doi.org/10.1016/j.proci.2016.06.017
192. Wayne, R.P., 1969. The Theory of the Kinetics of Elementary Gas Phase Reactions, in: Comprehensive Chemical Kinetics. Elsevier, pp. 189–301. https://doi.org/10.1016/B978-0-444-40674-3.50009-2

193. Warth, V., N. Stef, P. A. Glaude, F. Battin-Leclerc, G. Scacchi and G. M. Côme (1998). Computer-Aided Derivation of Gas-Phase Oxidation Mechanisms: Application to the Modeling of the Oxidation of n-Butane. Combustion and Flame 114(1): 81-102.
194. Westbrook, C. K., W. J. Pitz, O. Herbinet, H. J. Curran and E. J. Silke (2009). A comprehensive detailed chemical kinetic reaction mechanism for combustion of n-alkane hydrocarbons from n-octane to n-hexadecane. Combustion and Flame 156(1): 181-199.
195. Wollenhaupt, M., Carl, S.A., Horowitz, A., Crowley, J.N., 2000. Rate Coefficients for Reaction of OH with Acetone between 202 and 395 K. J. Phys. Chem. A 104, 2695–2705. https://doi.org/10.1021/jp993738f
196. Wu, C. K. and C. K. Law (1985). On the determination of laminar flame speeds from stretched flames. Symposium (International) on Combustion 20(1): 1941-1949.
197. Wu, T., Z. Huang, W.-g. Zhang, J.-h. Fang and Q. Yin (2007). Physical and Chemical Properties of GTL−Diesel Fuel Blends and Their Effects on Performance and Emissions of a Multicylinder DI Compression Ignition Engine. Energy & Fuels 21(4): 1908-1914.
198. Yang, B., Oßwald, P., Li, Y., Wang, J., Wei, L., Tian, Z., Qi, F., Kohse-Höinghaus, K., 2007. Identification of combustion intermediates in isomeric fuel-rich premixed butanol–oxygen flames at low pressure. Combustion and Flame 148, 198–209. https://doi.org/10.1016/j.combustflame.2006.12.001
199. Yang, S. Y., S. H. Chung and H. J. Kim (2003). Effect of pressure on effectiveness of quenching meshes in transmitting hydrogen combustion. Nuclear Engineering and Design 224(2): 199-206.
200. Yoneda, Y. (1979). A computer program for the analysis, creation and estimation of generalised reactions: GRACE, . Bulletin of the Chemical Society of Japan 52: 8-14.
Zádor, J., C. A. Taatjes and R. X. Fernandes (2011). Kinetics of elementary reactions in low-temperature autoignition chemistry. Progress in Energy and Combustion Science 37(4): 371-421.
201. Züttel, A., A. Remhof, A. Borgschulte and O. Friedrichs (2010). Hydrogen: the future energy carrier. Philosophical Transactions of the Royal Society A: Mathematical, Physical and Engineering Sciences 368(1923): 3329-3342.

Reports

- German Environment Agency (2016) Power-to-LiquidsPotentials and Perspectives for the Future Supply of Renewable Aviation Fuel, https://www.umweltbundesamt.de/sites/default/files/medien/377/publikationen/161005_uba_hintergrund_ptl_barrierrefrei.pdf
- Royal Academy of Engineering (2017) Sustainability of liquid biofuels: https://www.raeng.org.uk/publications/reports/biofuels

Books

- Atkins, P.., Julio de Paula, Atkins' Physical Chemistry, Oxford University Press, 2010.
- Battin-Leclerc, Frédérique, Simmie, John M., Blurock, Edward (Eds.), Cleaner Combustion, Developing Detailed Chemical Kinetic Models, Springer, 2013.
- Benson, S.W. Thermochemical Kinetics: Methods for the Estimation of Thermochemical Data and Rate Parameters, Wiley–Blackwell, 1976.
- Griffiths, J.F. , J.A. Barnard, Flame and Combustion, 3rd Edition, CRC Press, 1995.

- Hirschfelder, J. O., C. F. Curtiss, and R. B. Bird, Molecular Theory of Gases and Liquids, John Wiley and Sons, New York, 1954.
- Kundu, P., Ameen M.M., Som S. In: De S., Agarwal A., Chaudhuri S., Sen S. (eds) Modeling and Simulation of Turbulent Combustion. Energy, Environment, and Sustainability. Recent Progress in Turbulent Combustion Modeling of Spray Flames Using Flamelet Models. Springer, Singapore, 2018.
- Law, C.K., Combustion physics, Cambridge University Press: Cambridge, UK, 2006.
- Lewis, Bernard & Von Elbe, Guenthe. Combustion, Flames and Explosions of Gases, 1968.
- Pilling, Michael J., Paul W. Seakins, Reaction Kinetics, Oxford Science Publications, 1996.
- Semenov, N., Chemical kinetics and chain reactions, Thompson, Oxford, 1935.
- Semenov, N., Some Problems in Chemical Kinetics and Reactivity, now available from Princeton University Press, 1958.
- Turányi, Tamas, Tomlin, Alison S., Analysis of Kinetic Reaction Mechanisms, Springer, 2014.
- Turns, S.R., An Introduction to Combustion: Concepts and Applications, McGraw-Hill Education, 2011.
- Zabetakis, M.G., Flammability characteristics of combustible gases and vapors, US Bureau of Mines Bull, 1965.

清华大学燃烧能源中心

Center for Combustion Energy